Damage Identification of Belt Conveyors Using Periodic and Isolated Local Vibration Modes

周期的局部振動モードと孤立局部振動モードを利用した ベルトコンベアの損傷同定

Amin Honarbakhsh

A dissertation submitted to
The University of Tokyo
In partial fulfillment of the requirement for
The Degree of Doctor of Philosophy

Department of Civil Engineering
The University of Tokyo
Tokyo, Japan

September 2012

Abstract

Due to aging and corrosion, large number of belt conveyor support structures in industrial plants has degraded over the past decades. These structures are in damage condition and may cause human injury or death and economy impacts as several structural accidents of belt conveyors have been reported in Japan and overseas which caused the operation of factories to stop. Therefore, structural condition assessment of these structures is urgent.

To overcome the problems of global vibration modes in damage identification (i.e. need of before-and-after comparison, incapable to be applied for structures with large number of damaged elements, considering effects of non-structural elements and environmental conditions), new damage identification methods are proposed based on two specific local vibration modes named Periodic Local Vibration Modes (PLVM) and Isolated Local Vibration Modes (ILVM). These modes are distinguished from other types of local vibration modes. PLVM is a mode in which vibrations of one group of the identical secondary members are much larger than the other members. The idea in damage identification is when one of these identical members is damaged, this member no longer vibrates in PLVM, instead, it has ILVM in a lower frequency. Numerical and experimental results show that PLVM and ILVM are better observed when each secondary member is directly hit. As an alternative method to easily observe PLVM, one of the undamaged members in each identical members set can be hit. By hitting one of the undamaged members in each identical members set, damaged secondary members of the identical members set are localized and the relative severity of damage is identified by comparing PLVM amplitude in the corresponding PLVM range.

The existence of PLVM and ILVM in systems consisting of main and secondary members is investigated using mass-spring system. A 3-DOF system including coupler, main, and secondary members is considered and mode localization phenomenon is mathematically explained. Then, a more complicated lamped mass-spring system which has 21-DOF is compared with a finite element model of the support structure of a belt-conveyor to find a correspondence between these two models and the existence condition of PLVM and ILVM is numerically discussed. It is found that when main members are much stiffer than secondary members, PLVM and ILVM of secondary members exist and their frequencies are nearly the same as natural frequencies of the corresponding secondary members.

Next, the method based on global vibration modes and two damage identification methods based on PLVM and ILVM frequencies comparison and PLVM amplitude comparison are utilized to identify damaged members of a finite element model of the support structure of a typical belt conveyor. Then, based on the sensitivity analyses of frequencies of PLVM and ILVM which show that the appropriate parameters in damage quantification of secondary members are the local internal connections and the properties of the corresponding member, beam theory and its applicability on the quantification of damage degree are discussed and the stiffness of local boundary conditions and the stiffness reduction of damaged members are reliably identified.

Likewise, the two damage identification techniques based on PLVM and ILVM are examined for two laboratory models. One has continuous longitudinal members and the other has separated longitudinal members. The method is applicable for all secondary members (i.e. diagonal and lateral members) of the structure with continuous main members, and all damaged and undamaged members almost vibrate in their own natural frequencies; yet, these damage identification methods cannot identify the damaged lateral members of the structure with non-continuous main members since coupling of modes happens for these members. The reason is due to the fact that the stiffness of the main members is not much larger than the lateral members and no other secondary member is attached to one of the connections of each lateral member.

The existence of PLVM and ILVM of the secondary members of a planar full-scale model of a belt conveyor is investigated and the damaged members are identified using the method based on PLVM and ILVM frequencies comparison. Finally, using the method based on PLVM and ILVM frequencies comparison, damaged secondary members of a real belt-conveyor are correctly localized and using beam theory, the equivalent damage degree is quantified for each damaged member while each member is directly hit and the method is experimentally verified. Moreover, using the damage identification method based on PLVM amplitude comparison, the damaged secondary members are localized and the relative severity of the damage is correctly identified.

In conclusion, damage identification techniques to identify damages on belt conveyor support structures utilizing local vibration modes taking advantage of the non-contact measurement device have been proposed. These techniques are capable of identifying multiple damages on a structure without the need of before-and-after comparison. The Laser Doppler Vibrometer allows a quick assessment of damages. The applicability to belt conveyors is confirmed through numerical and experimental verifications. Further studies on criteria to distinguish local vibration modes and on the applicability to structures of other types such as truss bridges and towers are considered to advance the techniques toward their full-fledged use.

To my Family

Acknowledgement

All the praises are to my God, who is the most generous and merciful, Lord of mankind and the only One I always ask for help and guidance to find the correct way in my life.

I would like to express my deepest gratitude and sincere appreciation to my advisor, Associate Professor Tomonori Nagayama, for his invaluable advice and kind encouragement during the entire period of this study as well as my personal life. I have got incredible motivation after each discussion with him. No word seems to be enough to describe my respect and appreciation for his patient and tireless counsel. Without his help, this dissertation would not have been possible to finish. I will not forget all his help and guide in the rest of my life.

I am profoundly indebted to my co-advisor, Professor Yozo Fujino, for his great advice and support. I am honored and fortunate to work with him whose knowledge and encouragement always exist in all directions of my research. His invaluable idea in the field of my research would have remarkably helped me to improve my work. The intensity of my gratitude and respect to him will not be reduced even after several decades.

I honestly appreciate my committee members, Prof. Takeshi Ishihara, Prof. Tsuyoshi Takada, and Prof. Riki Honda, for all their valuable comments and ideas through which the quality of this work was enhanced.

I sincerely thank Dr. Su Di, Lecturer in the Bridge and Structure Laboratory, and Dr. Dionysius Manly Siringoringo, Assistant Professor in the Bridge and Structure Laboratory, for their great help to solve my research problems.

I would like to thank Associate Professor Mayuko Nishio and Assistant professor Takafumi Nishikawa, and Dr. Dinh Hung for all their support during the time we were together in the Bridge and Structure Laboratory.

I would like to thank Assistant Professor Atsushi Yamaguchi, Assistant Professor Tsukasa Mizutani, Dr. Muhammad Waheed Sarwar, Mr. Sun Zhen, Mr. Yuko Murata, Dr. Elisa Sorrivi, Mr. Takahiro Hida, Mr. Akihiko Urushima, Mr. Kosuke Takahashi, Ms. Juliette Marin, Ms. Jitboon Laomanit, Mr. Chondro Hidayat Tandian, Mr. Hisashi Yamasaki, Ms. XU Nan, Mr. Liu Zhenqing, Ms. Sho Oh, Ms. Yuka Kikuchi, Mr. Jun Tanemoto, Mr. Ken Kagaya, Mr. Toshihiko Kobayashi, Mr. Takuo Sato, Mr. Gotaro Takamoto, Mr. Akira Miyajima, Mr. Akihiko Miwa, Ms. Helene Huang, Mr. Umar Ahad Butt,

Mr. Zou Zilong, Mr. Masataka Kago, Mr. Yuuki Shimada, Mr. Tomoaki Takeda, Mr. Yuki Yokota, Mr. Niklas Kent Persson, Mr. Pineda Allen Juan Carlos, Mr. Tayyab Khalid, Mr. Syuuta Takada, and other members of the Bridge and Structure Laboratory to make me feel comfortable in this laboratory.

Also, I would like to appreciate Ms. Naomi Nakashima and Ms. Harumi Yokoyama for their support in all matters regarding the lab.

Special thanks to Associate Professor Masoud Soltani, Assistant Professor Esatas Gebreyouhannes, Dr. Benny Suryanto, Dr. Ahmed Mohammed Youssef, and Mr. Mahyarudin Dalimunthe for their help in and out of my research life.

I acknowledge the FSO staff, Ms. Toshiko Nakamura, Ms. Nami Hayashi, Ms. Miki Sembokuya, and Ms. Masumi Tonegawa for their help in my daily life. I also appreciate all civil office staff especially Ms. Junko Aoyama for their help during my stay in this department.

I would like to deeply appreciate steel research laboratory of Nippon Steel Corporation for their great cooperation in this study. Their comments and support significantly helped me to be more motivated in my research. A special thank goes to Dr. Tomonori Tominaga, Mr. Kazumasa Hisazumi, and Mr. Kenichiro Imafuku who kindly supported me to carry out my experimental works.

I also sincerely acknowledge the scholarship granted to me by the Ministry of Education, Science and Culture of the Japanese Government.

Finally and most importantly, I would like to express my deepest gratitude to my parents, brother and sisters for their unconditional support and continuous encouragement throughout my whole life. I could not have achieved anything without their help. I also cordially thank my grandmothers from the bottom of my heart.

Contents

List of Figures

List of Tables

Chapter 1

Introduction

1.1 Motivation and research objectives

Belt conveyors which carry materials using belts are widely used in the world. Some of them are small scale in a factory as shown in figure 1-1 while others are in a large size at a mining field, brick, asphalt, cement, concrete or steel factory shown in figure 1-2.

Figure 1-1 An indoor belt conveyor **[1]**

Figure 1-2 A belt conveyor at a steel factory

Large belt conveyors, as shown in figure 1-2, usually consist of machinery parts which are inside the structure, walkways located on the one or both sides of the conveyor belt, and the support structure including columns and main frames.

There are a huge number of belt conveyors all around the world built decades ago. According to the US Department of Labor Bureau of Labor Statistics' report (2010), more than 50 injuries and deaths involving belt conveyors occur every year. Some of these injuries and deaths are caused by a sudden collapse of the structures. The main reason is that, due to ageing, many members of the support structure of belt conveyors have corroded over decades as shown in figure 1-3. Moreover the economy impacts are serious and significant as several structural accidents of belt conveyors have been reported in Japan and overseas which caused the operation of factories to stop. Thus structural condition assessment of belt conveyors is urgent. Over the past decade, research has been conducted on the health monitoring of belts or machinery parts of belt conveyors such as Harrison **[2]**, Bozma and Yalcin **[3]** and Mazurkiewicz **[4].** Yet structural condition assessments of the support structure of belt conveyors have not been studied. This dissertation discusses the Structural Health Monitoring (SHM) of the support structures of belt conveyors, which are considered as space structures consisting of longitudinal, lateral, diagonal and vertical members connecting with each other.

Figure 1-3 A damaged belt conveyor

Vibration-based damage identifications which utilize the fact that the properties of vibration modes, i.e. frequencies, mode shapes or damping ratio, change as material deteriorations occur, have long been studied and are considered promising approach for damage identification of the support structure of belt conveyors. However, there are difficulties in applying the old techniques to the support structures due to the following characteristics of belt conveyors:

1. Since monitoring of belt conveyor support structures have not been usual in the past, there is no baseline to compare with the current situations.
2. A large number of damages exist in a single belt conveyor. Therefore, dynamic properties of the support structure are affected in a complicated manner by these multiple damages.

3. Non-structural members affect the vibration modes. For large structures such as bridges or large building, these effects can be negligible, yet, in case of belt conveyors, the contribution of non-structural members, such as walkways and machinery parts, are not so small as compared to structural members because their dimensions are not dispensable. In addition, these members are replaced more frequently than structural members. Numerical model without considering these members hardly reproduces the dynamic behavior accurately.

Therefore, application of vibration based-damage identification methods to detect damage of belt conveyors is difficult in practice.

To overcome these difficulties, the use of local vibration modes is proposed. Local vibration modes usually happen in a higher frequency range and have less power as compare to global modes. Therefore, it is difficult to observe these modes in reality. Another problem is their differentiation difficulties. There are many local vibration modes such as coupled local modes, partially chaotic local mode, Periodic Local Vibration Modes (PLVM) and Isolated Local Vibration Modes (ILVM). PLVM and ILVM are explained in detail in chapter 3. These modes have to be distinguished from the other modes if these modes are utilized in damage identification. Recently developed non-contact vibrometer is expected to enable observation and differentiation of local vibration modes in space structures efficiently. Laser Doppler Vibrometer (LDV), shown in figure 1-4, is a non-contact sensor and capable to measure small vibration with high resolutions in a wide frequency range.

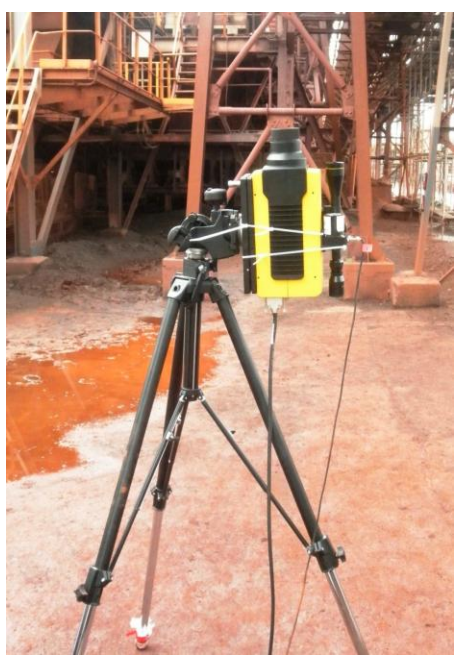

Figure 1-4 Laser Doppler Vibrometer

In this dissertation, damage identification of the support structure of belt conveyors is investigated. This research has mainly four objectives: first, clarification of dynamic characteristics of the main frame of the support structure of belt conveyors. Second, establishment of a damage localization method based on two

specific types of local vibration mode. Third, development of a damage severity identification method and finally experimental verification of the identification methods.

1-2 Dissertation outline

The contents of this thesis are arranged in eight chapters:

Chapter 1. This chapter generally presents motivation and objectives of this research. An overview of the thesis is also included in this chapter.

Chapter 2. This chapter presents the literature review of damage identification techniques based on vibration measurements applicable to space structures. The methods are classified according to necessary measurements and analysis approaches.

Chapter 3. In this chapter, to clarify dynamic characteristics of the support structure of belt conveyors, a finite element model of a typical frame of a belt conveyor support structure is generated. Then, the sensitivity of modal properties is examined in details with respect to stiffness changes of members. The applicability and advantages of using local vibration modes compared to global ones in damage identification of the support structure of belt conveyors are discussed as well.

Chapter 4. The existence of local vibration modes in systems consisting of main and secondary members is investigated in this chapter. First a 3-DOF system including coupler, main, and secondary members are considered and mode localization phenomenon is mathematically explained. Then, a more complicated lumped mass-spring system which has 21-DOF is compared with the FEM model of the support structure of a belt conveyor to find a correspondence between these two models and the existence condition of PLVM and ILVM are numerically discussed on the lumped mass-spring system and the results are verified on the finite element model.

Chapter 5. In this chapter, damage identification methods utilizing global vibration modes, PLVM and ILVM are proposed and applied to a finite element model of the support structure of a typical belt conveyor. Beam theory and its applicability on the quantification of damage degree are discussed.

Chapter 6. In this chapter, the damage identification techniques are applied to two scale-model space structures. Some of the secondary members of the frames are damaged and the locations of the damaged members are identified based on frequency changes of PLVM. Then the frequencies of PLVM and ILVM in the structures are compared with the natural frequencies of the corresponding simple beams to confirm whether frequencies of PLVM and ILVM are nearly the same as natural frequencies of the corresponding simple beam.

Chapter 7. The existence of PLVM and ILVM in the braces and lateral members of a planar full scale model of a belt conveyor are investigated in chapter 7. Meanwhile, the rotational stiffness of connections is estimated based on the special properties of PLVM and ILVM. Finally damaged secondary members of a real belt conveyor are localized and the damage degree is identified using PLVM and ILVM.

Chapter 8. Based on the discussion on the proposed methods conclusions are summarized. Limitations of this method and suggestions for future works are summarized as well.

Chapter 2

Literature review on vibration-based damage identification

2.1 Introduction

This chapter presents the literature review of Structural Health Monitoring (SHM) which is a process to identify the presence, location and severity of damage in structures and in its most ambitious case, contains evaluating the remaining service life of structures **[5]**. This literature review covers some domains of SHM which involve vibration-based damage identification techniques and are applicable to space structures. The methods are classified according to analysis approaches and necessary measurement. First, the methods based on frequency changes are introduced. Second, the methods based on changes in measured mode shapes or their curvature will be discussed. Third section will introduce methods that use updating modal properties of structures to detect damage. Next, this chapter briefly presents the methods involved using changes in measured flexibility coefficients to identify damage. Finally, some limitations of global vibration modes in damage identification of belt conveyor support structures are briefly cited.

2.2 Frequency changes

The idea that changes in structural properties would change the natural frequencies of structure is the major motivation to apply this method. One of the main problems of this method is the low sensitivity of frequency shifts to damage especially in frequencies of global modes requires either precise measurements **[6]** or large level of damage. Tests conducted on the I-40 bridge show that frequency shifts are not a good index for damage detection because they have small sensitivity to damage **[7]**. When the stiffness at the center of a main plate girder was reduced by 96.4%, no remarkable reductions in the natural frequencies were observed. Another main problem is that the frequencies cannot generally provide spatial information about structural change because frequencies are global properties of the structure and their shifts may not identify more than the mere existence of damage. However this problem might be solved using higher frequency ranges in which most members locally vibrate specially in space structures. Note that as explained in the later chapters, the need of precise device together with some special techniques to measure and excite these modes are indispensable. As an example Yoshioka, et al **[8]** conducted a hammer test on healthy and corroded diagonal members of a truss bridge shown in figure 2-1.

Figure 2-1 Hammer test on a truss bridge **[8]**

As shown in figure 2-2, the shift in frequencies of local modes is observed.

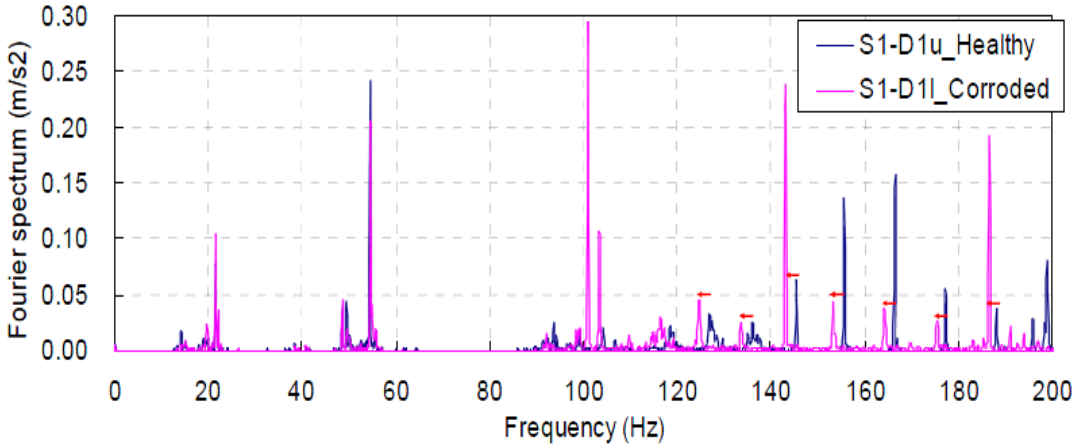

Figure 2-2 Shift of frequencies of local modes **[8]**

Frequency changes method can be categorized in two different parts named forward and inverse problems. The forward problems usually discuss about the presence of damage in the structure and the damage is modeled mathematically, then the measured natural frequencies are compared to the predicted ones to determine the damage. Cawaley and Adames **[9]** use this method to find a formula to identify damage in composite materials from frequency shifts. The inverse problems are usually dealt with the determination of the location of damage as well as quantification of the damage severity. This method consists of calculating the damage parameters, i.e. type of damage or location, from the frequency shifts. As an example of this method, Richardson and Mannan **[10]** introduced a method that assumes damage is limited to change in stiffness. In all of the research based on this method the information about the conditions of the undamaged structure is needed.

The application of these methods on belt conveyors is limited since, most of the time, for global modes, there is no available baseline to compare with the current results. For local modes, there is no evidence that shows the two comparing modes are relevant to each other and differentiation of these modes is difficult.

2.3 Mode shape changes

Mode shape is usually considered more sensitive to damage compared to frequency, as mentioned by Srinivasan and Kot **[11]**, However the accuracy of measured mode shapes are relatively less than frequencies and need to utilize precise devices. The most common criterion being used to compare mode shapes of damaged structure with either mode shapes of finite element model or undamaged structure is modal assurance criterion (MAC) defined as:

$$MAC(\phi_i, \phi_j) = \frac{\left|\{\phi_i\}^T\{\phi_j\}\right|^2}{\{\phi_i\}^T\{\phi_i\}\{\phi_j\}^T\{\phi_j\}} \tag{2.1}$$

where ϕ_i and ϕ_j are comparative eigenvectors.

Many researchers in the past used this criterion or its derivatives such as Partial MAC (PMAC) or coordinate MAC (COMAC). Kim, el al. **[12]** used COMAC and PMAC to detect the damage area of structure. Ko, et al **[13]** introduced a method that uses a combination of MAC and COMAC and sensitivity analysis to identify damage in steel frame structures. They used COMAC as an indicator of damage.

In some papers, authors used mode shapes together with frequencies to detect damage. Lim and Kashangaky **[14]** developed a method based on the use of the best achievable eigenvector in damage identification problem and applicable to large scale structures. This method requires measured frequencies as well as mode shapes. The damage is detected by computing the Euclidean distances between the measured mode shapes and the best achievable modal eigenvectors. This method is able to detect loss of both stiffness and mass properties. Later this method was developed by S. Ricci **[15]** using a limited number of low frequency measured modes. The distance between the measured mode shape and the best achievable modal eigenvector for each element can be computed using the Frobenious norm:

$$d_{kj} = \left\|\phi_{tj} - \phi_{tj}^{a}\right\|_F \tag{2.2}$$

Where ϕ_{tj} is the *j*-th measured mode shape and ϕ_{tj}^{a} is the best achievable eigenvector for the *j*-th mode and *k*-th element of the structure. Therefore, for a structure, having *m* potentially damaged elements and using *r* measured modes, the evaluation of $m \times r$ Frobenious norm of the Euclidean distances is needed. If the damage is located on the *k*-th element and influences the *j*-th mode, then the d_{kj} will be close to zero otherwise it will be significantly higher.

The author considered a tenbar structure shown in figure 2-3 and reduced the stiffness of member 2 by 10 percent and checked this method numerically.

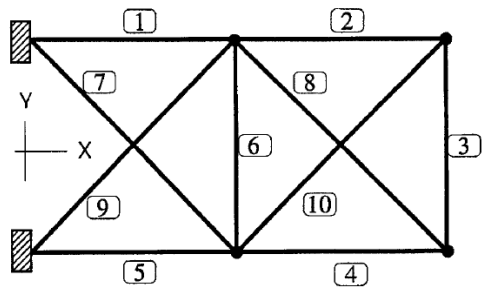

Figure 2-3 Tenbar structure **[15]**

Figure 2-4 shows a three-dimensional bar diagram representing the final Euclidean distances, in which the highest values have been truncated to simplify the representation. The Euclidean distance corresponding to element 2 is close to zero for all considered modes, so the localization method correctly identifies this element as the damaged one.

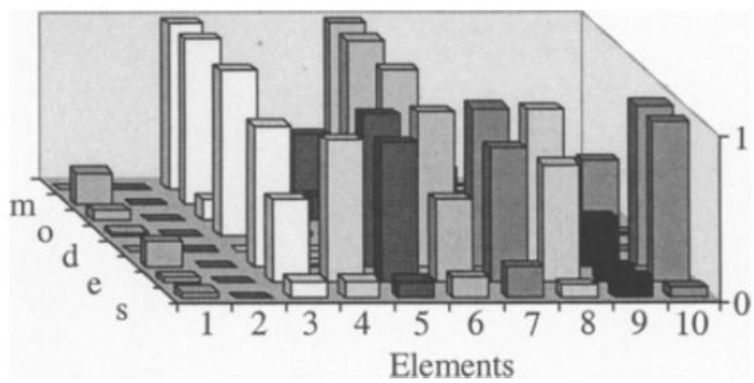

Figure 2-4 Three-dimensional bar diagram representing the final Euclidean distances **[15]**

The method correctly identified the damaged member in a 10-bay laboratory model as well. The disadvantage of this method is that a fine finite element model of the undamaged structure is required that might not be feasible due to the lack of measured modal information of the undamaged structure to update the finite element model.

There are some techniques which are often based on periodically monitoring the modal behavior in real service life conditions to detect and localize damage. The damage detection is formulated as an inverse problem, where the structural uncertainties are located on the real structure and the analytical model is considered as accurate. Kashangaki, et al. **[16]** and Firiswell, MI and Penny, J.E.T. **[17]** used these techniques as an efficient and reliable method for health monitoring of a complex system.

Some authors have used methods which are inferred from modal displacement. Carrasco, el al. **[18]** used a method based on modal strain energy to do modal tests of a space truss model and damage localization. Sooyong Park and Yeon-Bok Kim **[19]** introduced a nondestructive damage detection theory based on the fraction of the strain energy. They considered the following expression as a damage index:

$$\beta_j = \frac{\frac{1+\sum_{i=1}^{NM} f_{ij}^*}{1+\sum_{i=1}^{NM} f_{ij}}+1}{2} \tag{2.3}$$

where NM is the number of considered modes and f_{ij} and f_{ij}^* corresponds to the undamaged and damaged structures respectively and defined by:

$$f_{ij} = (\Delta_{ij})^2 / \sum_{i=1}^{NE} (\Delta_{ij})^2 \text{ and } f_{ij}^* = (\Delta_{ij}^*)^2 / \sum_{i=1}^{NE} (\Delta_{ij}^*)^2 \tag{2.4}$$

in which Δ_{ij} and Δ_{ij}^* represent the deformation of the *j*-th element in the *i*-th mode of the undamaged and damaged structures respectively.

Next, a criteria for damage localization based on statistical approaches were established by the assumption that β_j for each element can be considered as realization of a random variable. (An overview of statistical pattern recognition was provided by Anil. K, el al. **[20]**). The normalized damage indicator is given by:

$$Z_j = \frac{\beta_j - \mu_\beta}{\sigma_\beta} \tag{2.5}$$

where μ_β and σ_β represent mean and standard deviation of the damage index, β_j, respectively.

Then, they defined a threshold value equal to 3, based on the statistical pattern recognition techniques, which assigns a 99% significant level of damage. They developed a finite element model shown in figure 2-5 and considered different damage cases. As an example, once they reduced the stiffness of a member (member 46) by five percent and considered the first four modes of the truss, shown in figure 2-6, to localize the damaged member.

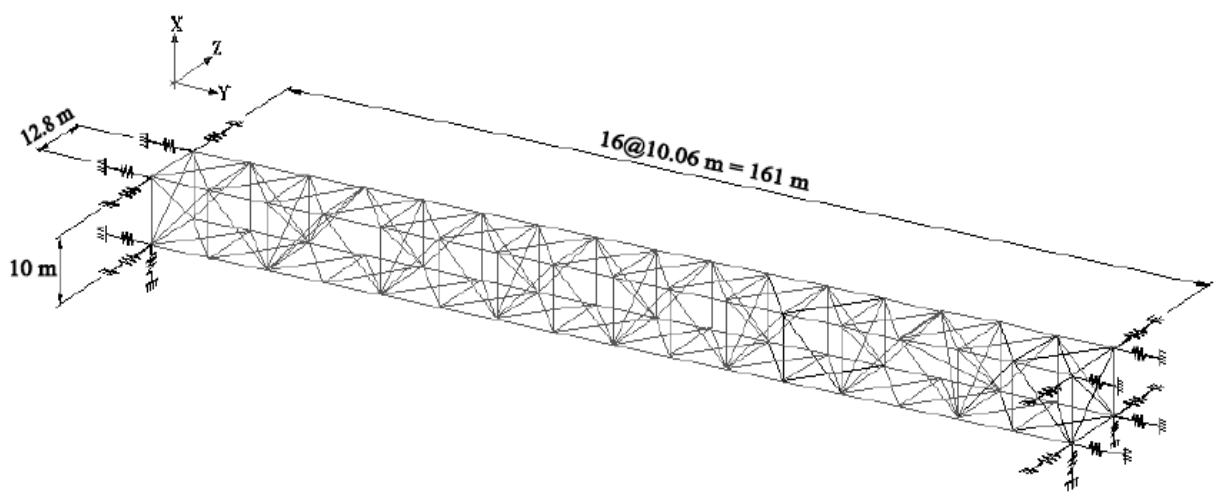

Figure 2-5 Schematic of the finite element model **[19]**

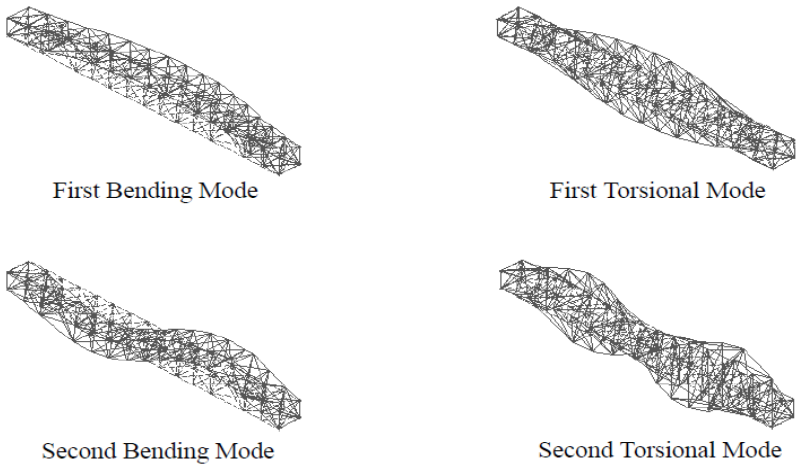

Figure 2-6- First four mode shapes of the truss **[19]**

As shown in figure 2-7, the method can correctly identify the damaged member especially when several modes are used simultaneously.

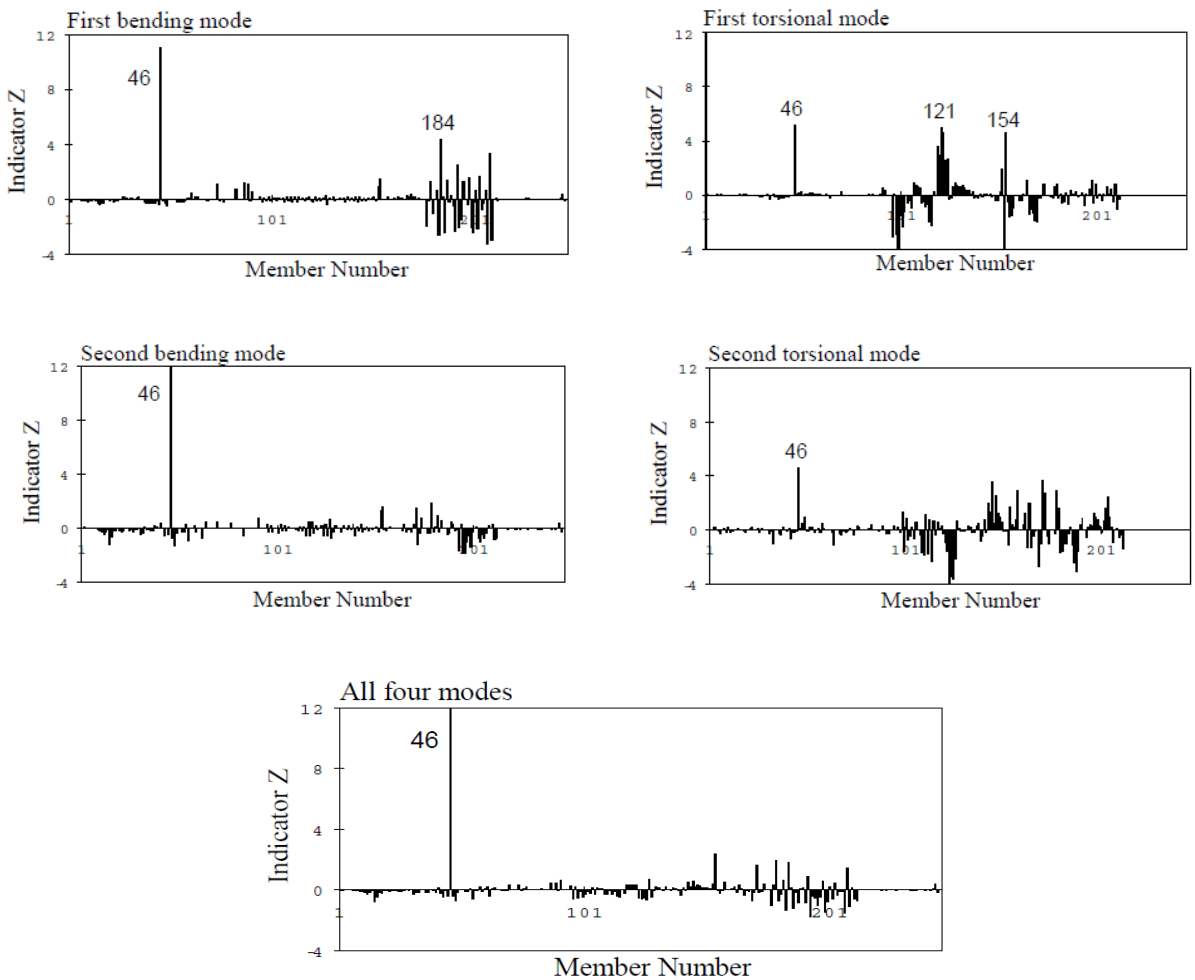

Figure 2-7 Damage localization results **[19]**

They also conducted a laboratory test on a truss model to experimentally validate the applicability of this method. The experimental study showed that the performance of the proposed method might be significantly impacted by the noise in the measurement data, especially when small amount of damage is introduced.

The methods presented here are based on global vibration modes. The application of these methods on belt conveyors is limited since, most of the time, there is no available baseline to compare with the current results. Moreover, large number of damaged members makes the use of this method difficult. Meanwhile, considering the effects of non-structural components is important but difficult in belt conveyors.

2.4 Mode shape curvature changes

An alternative to use mode shapes, to identify damage locations, is using the 2nd derivative of mode shapes (or curvatures) which are known more sensitive to damage than mode shapes. Pandey, el al. **[21]** expressed that damage of the FEM beam structures can be identified by considering the absolute changes in mode shape curvature. The curvature value of mode *i* and DOF *q* is computed by:

$$\phi''_{q,i} = \frac{\phi_{q-1,i} - 2\phi_{q,i} + \phi_{q+1,i}}{h^2} \tag{2.6}$$

where *h* is the length of each of the two elements between the DOF (*q-1*) and (*q+1*).

Salawu and Williams **[22]** used a mode shape curvature measure calculated by above equation and they compared the performance of mode shape curvature changes with mode shape changes. They emphasized that the most important factor is the selection of modes sensitive to damage. They found the curvature changes may not give a good indication of damage using experimental data. Chance, el al. **[23]** demonstrated that numerically computing curvature from mode shapes caused unacceptable errors. They tried to use measured strains instead of measured curvature and found that the results remarkably improved.

The methods presented here are based on global vibration modes. The application of these methods on belt conveyors is limited because of the reasons explained in the previous part.

2.5 Model updating

Model updating, at its most ambitious, is about correcting invalid or suspicious assumptions by comparing the model with measurement. There are some damage identification methods based on model updating techniques in which the structure model matrices such as mass, stiffness and damping are modified to as closely as possible reproduce the measured static or dynamic response of the data. Comparisons of the updated matrices to the corresponding original matrices provide an indication of damage and can be used to detect the location and quantify the damage degree. Updating methods can be categorized based on the differences in objective functions to be minimized, constraints in the updating problem and numerical schemes for the optimization process.

The basic formulations are based on the modal force error equation. As expressed by Ojalvo and Pilon **[24]**, the modal force error vector indicates the harmonic force excitation that is applied to the undamaged structure and given by:

$$((\lambda_i^d)^2[M^u] + (\lambda_i^d)[C^u] + [K^u])\{\phi^d\}_i = \{E\}_i \tag{2.7}$$

where $\{E\}_i$ is defined as the residual force or modal force error, for the i*th* mode of the damaged structure. $\lambda_i{}^d$ and $\{\phi^d\}_i$ are the measured i*th* eigenvalue and eigenvector of the damaged structure respectively. $\{M^u\}, \{C^u\}, \{K^u\}$ are the mass, damping and stiffness matrices of the undamaged structure. The eigenvalue equation for the undamaged structure is given by:

$$((\lambda_i^u)^2[M^u] + (\lambda_i^u)[C^u] + [K^u])\{\phi^u\}_i = \{0\} \tag{2.8}$$

where $\lambda_i{}^u$ and $\{\phi^u\}_i$ are the measured i*th* eigenvalue and eigenvector of the undamaged structure respectively. Likewise, the eigenvalue equation for the damaged structure is given as:

$$((\lambda_i^d)^2[M^d] + (\lambda_i^d)[C^d] + [K^d])\{\phi^d\}_i = \{0\} \tag{2.9}$$

where $\{M^d\}, \{C^d\}, \{K^d\}$ are the mass, damping and stiffness matrices of the damaged structure. It is obvious that the damaged modal matrices are defined as the modal matrices of the undamaged structure minus a perturbation:

$$\begin{aligned} [M^d] - [M^u] &= [\Delta M] \\ [C^d] - [C^u] &= [\Delta C] \\ [K^d] - [K^u] &= [\Delta K] \end{aligned} \tag{2.10}$$

Using the above equations and rearranging those yields:

$$((\lambda_i^d)^2[\Delta M] + (\lambda_i^d)[\Delta C] + [\Delta K])\{\phi^d\}_i = \{E\}_i \tag{2.11}$$

This equation can be solved to obtain the matrix perturbations. The modal force error is used as both an objective function and a constraint. The most common is the preservation of the property matrix symmetry that can be presented for each modal matrix:

$$\begin{aligned} [\Delta M] &= [\Delta M]^T \\ [\Delta C] &= [\Delta C]^T \\ [\Delta K] &= [\Delta K]^T \end{aligned} \tag{2.12}$$

Other constraints in the various methods can be preservation of the property matrix sparsity which is one way to preserve the allowable load paths of the structure in the updated model, and preservation of the property matrix positivity.

Some methods use a close-form, direct solution to compute the perturbation matrices called optimal matrix update methods or direct methods using modal data. A complete explanation of these methods has been published by Friswell and mottershead **[25].** Moreover, review of these methods was presented by Hemez **[26]**, Kaouk **[27]** and Zimmerman and smith **[28]**. Direct methods generally consist of Lagrange multiplier methods, Matrix mixing and methods from control theory (or eigenstructure assignment methods). The Lagrange multiplier method is simply a convenient means of minimizing a function subject to exact constraints on the independent variable which can be written as:

$$Min_{\Delta M,\Delta C,\Delta K}\{J(\Delta M,\Delta C,\Delta K)+\lambda R(\Delta M,\Delta C,\Delta K)\} \qquad (2.13)$$

Where J is the objective function, λ is the penalty constant or Lagrange multiplier and R is the constraint function.

Liu **[29]** presents an optimal update technique for computing the elemental stiffness and mass parameters for a truss structure from measured modal frequencies and mode shapes. They minimized the norm of the modal force error and detected a damaged member in a FEM of a truss using the first four measured modes. Berman and Nagy **[30]** and Kabe **[31]** used a common technique to minimize the Frobenius norm of global parameter matrix perturbations using zero modal force error as well as property matrix symmetry as constraints.

Yang, el al. **[32]** presented a new updating method that can refine the stiffness matrix of the model by using a subset vectors from the full set of acceleration frequency response functions (FRFs) that are extracted from test data and calculated from an updated finite element model. The perturbation matrix was computed from:

$$H_t(\omega)\ \Delta K = \omega^2(I - H_t(\omega)\ H_a(\omega)^{-1}) \qquad (2.14)$$

where ΔK is the stiffness perturbation matrix, ω is the exciting frequency and $H_a(\omega)$ and $H_t(\omega)$ are the matrix of acceleration FRF from the finite element and measured model respectively. It was assumed that the mass remains unchanged before and after damage and that the damping effect to the natural frequency is negligible. The method was experimentally verified using a space truss model shown in figure 2-8.

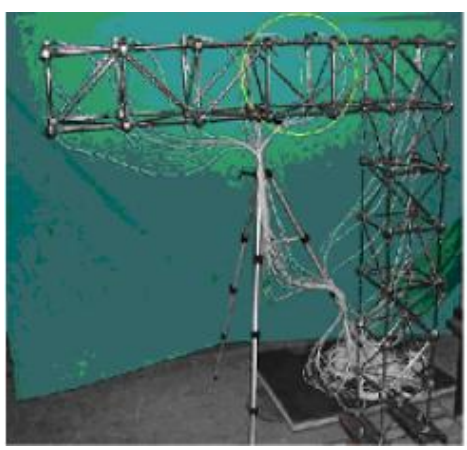

Figure 2-8 Space truss model **[31]**

Although the method could accurately identify the damage location, there was a large error in prediction of the damage degree. They mentioned that the possible reasons for this large error are: existence of the finite element modeling error, measurement noise and insufficient number of measured points. They counted some of the advantages of damage detection method based on FRF, namely, FRF is easy to measure, the process of computation is simple and the number of sampling points and frequency range are convenient to be controlled.

Some approaches to the optimal matrix update problem takes into account the minimization of the rank of the perturbation matrix instead of the norm of the perturbation matrix. The perturbation matrices are considered to be of small rank due to the observation that damage will tend to be concentrated in a few structural members, rather than distributed throughout a large number of structural members. This method has been published widely by Zimmerman and Kaouk **[33]**, Kaouk and Zimmerman **[34]** and Zimmerman, el al. **[35]**.

Doebling **[36]** computed a minimum-rank solution for the perturbation of the elemental stiffness parameter while constraining the connectivity of the global stiffness matrix. The matrix perturbation ΔK is a function of the diagonal elemental stiffness pretreated matrix ΔP as:

$$[\Delta K] = [A]\,[\Delta P][A]^T \tag{2.15}$$

where [A] is a sensitivity matrix relating the entries in the global stiffness matrix to the elemental stiffness parameters (stiffness connectivity matrix). .

The author detected single as well as multiple damaged members of an eight bay laboratory truss at NASA shown in figure 2-9 and found that the proposed method is better than a minimum-norm method in updating the data of the laboratory truss model. Like all minimum-rank methods, a limitation of this technique is that the rank of the perturbation is always equal to the number of modes used in the computation of the modal force error.

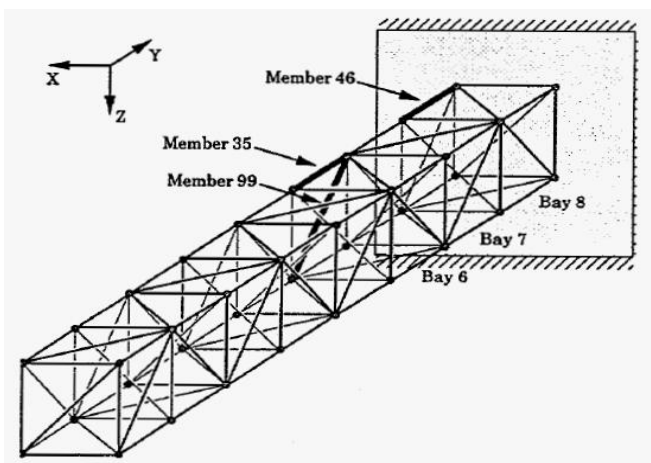

Figure 2-9 The NASA eight-bay truss **[36]**

Caesar **[37]** and Link, el al. **[38]** developed a method named matrix mixing approach. Since the number of measured modes is usually far fewer than the order of analytical model, the matrix mixing approach uses the data from the finite element model to fill in the gaps of the measured data. The updated matrices using this method are generally fully populated and so bear little relation to the physical connectivity in the structure. This method requires the calculation of all the high frequency modes and is not generally the best way to compute the updated matrices.

Another updating method is the eigenstructure assignment method from control theory. The method is based on the design of a faked controller which tries minimizing the modal force error to reproduce the measured modal data. The controller gains are interpreted as parameter matrix perturbations to the undamaged model. Lim **[39]** published an overview of this method. The best achievable eigenvector methods which already presented as a mode shape changes method fall into this method as well.

One important feature of the direct methods introduced here is that they exactly reproduce the measured data and they are not iterative, thus the possibilities of divergence and excessive computation are eliminated. On the other hand, a major drawback of the direct methods is that the updated modal matrices may have little physical meaning and cannot be related to the physical changes of the finite elements in the original model.

Some other model updating methods are known as sensitivity-based update method. These methods are usually based on the solution of the first-order Taylor series that minimize the error function of the matrix perturbation. A comprehensive list of sensitivity-based update approaches have been published by Hemez **[40]**. These methods are generally iterative and can be categorized to penalty function and minimum variance methods. Penalty function methods generally use a truncated Taylor series expansion of the modal data in terms of the unknown parameters. The expansion is usually limited to the first two terms in order to produce a linear approximation given by:

$$\delta Z = S_j \delta\theta \tag{2.16}$$

where: $\delta Z = Z_m - Z_j$ is the error in the measured output, $\delta\theta = \theta - \theta_j$ is the perturbation in the parameters and S_j is the sensitivity matrix.

There are two ways to deal with penalty function methods. First one is computing the updated parameter value by minimizing a penalty function and the second one is finding a general solution for the above equation with various weighting matrices. If $\mathcal{E} = \delta Z - S\delta\theta$ is the error in the predicted measurements based on the updated parameters, the ultimate equation is obtained by minimizing the weighted penalty function:

$$J(\delta\theta) = \mathcal{E}^T W_{\mathcal{E}\mathcal{E}} \mathcal{E} \quad , \quad J(\delta\theta) = \mathcal{E}^T W_{\theta\theta} \mathcal{E} \quad \text{or} \quad J(\delta\theta) = \mathcal{E}^T W_{\mathcal{E}\mathcal{E}} \mathcal{E} + \mathcal{E}^T W_{\theta\theta} \mathcal{E} \tag{2.17}$$

where $W_{\mathcal{E}\mathcal{E}}$ and $W_{\theta\theta}$ are a positive definite weighting matrix. The weighting matrix is often considered as a diagonal matrix whose elements are equal to the reciprocals of the variance of the corresponding measurements. Each weighting matrix can be used in different conditions depend on the number of measurement data or unknown parameters (over-determined and under-determined problems).

Minimum variance methods can be considered as penalty function methods in which the weighting matrices change in a particular way from one iteration to the next one. One of the advantages of this method is that a measure of the quality of the updated parameters is produced through their estimated variance. This method assumes that both the initial parameter estimates and the measured data have error that may be presented in terms of variance matrices. Then the updated parameters are found in a way that have minimum variance. This method, in its most progressive case, can consider a correlation matrix between each parameter estimate and the measurement noise. More explanation of iterative sensitivity-base update methods were provided by Friswell and Mottershead **[25]**.

Since the measured data is not always available in sufficient quantities to take unique parameters to be estimated, perturbed boundary condition testing is used to improve the numerical conditioning of the modal extraction method. This can be done by testing the structure with adding mass or stiffness or somehow measuring in slightly different configuration. Dinh, el al. **[41]**, Nalitolela, et al. **[42, 43, and 44]**, Li, el al. **[45]** and Dinh **[46]** used this method to increase the number of modal extraction data.

For complex structures, the presented methods are not always appropriate because the problem is ill-conditioned. Hybrid matrix update methods may be useful in damage identification of complex structures. Jung, el al**. [47]** proposed a new FE model updating method based on a hybrid optimization technique using a genetic algorithm and Nelder-Mead simplex method. They found this method can be used in a nonlinear problem with many local minima. Li and smith **[48, 49]** presented a hybrid model update method using a combination of the sensitivity and optimal update methods to identify damage. Kim and Bartkowicz **[50, 51]** proposed a two-step damage identification approach for large structures with limited instrumentation. They used optimal matrix update as a first step to detect the area of damage and, as a second step, utilized a sensitivity-based method to spot the specific damaged element of the structure.

The methods presented here are based on global vibration frequencies or modes. The application of these methods on belt conveyors is limited since inclusion of the finite element modeling of non-structural components is important but difficult. Moreover, large number of damaged members makes the use of this method difficult.

2.6 Dynamically measured flexibility matrix

Damage identification techniques based on dynamically measured flexibility matrix eliminate changes in the static behavior of the structure. Each column of the flexibility matrix represents the displacement of the structure associated with a unit force applied to the associated DOF.

$$\{\mathrm{u}\} = [\mathrm{G}]\{\mathrm{F}\} \tag{2.18}$$

The measured flexibility matrix can be estimated from the mass-normalized measured mode shapes and frequencies

$$[G] \approx [\phi][\Lambda]^{-1}[\phi]^{T} \tag{2.19}$$

To exactly calculate the flexibility matrix, the measurement of all of the frequencies and mode shapes are needed, however, many times this matrix can be approximated with high accuracy using the lower frequency modes. Comparing the flexibility matrix calculated by the frequencies and modes of the damaged structure to the flexibility matrix calculated by the frequencies and modes of the undamaged structure or fine FEM would identify damage. It should be noted that the measured flexibility matrix is most sensitive to changes in the lower frequency modes of the structure because of the inverse relationship to the square of the frequencies. Toksoy and Akan **[52]** calculated the measured flexibility of a bridge and examine the cross sectional deflection with and without a baseline data set. They mentioned that the damage can be identified even without a baseline data set due to the existence of anomalies in the deflection profile.

Lin **[53]** used a method based on the pseudo inverse relationship between the dynamically measured flexibility matrix and the structural stiffness matrix to the problem of damage identification. The error matrix is defined as:

$$[E] = [G^u][K^u] - [I] \tag{2.20}$$

He checked the error and defined a least square problem for the elemental stiffness changes in potentially damaged members. It should be noted that the elemental stiffness changes are consistent with the unity check error defined above.

The stiffness error matrix, as a function of the flexibility change in the structure and the undamaged stiffness matrix, is defined as:

$$[E] = [K^u][\Delta G][K^u] \tag{2.21}$$

in which

$$[\Delta G] = [G^d] - [G^u] \tag{2.22}$$

This matrix can be used as an indicator of errors between measured parameters and analytical stiffness matrix. He and Evins **[54]** used this matrix for the problem of damage detection.

Damage location vector method is a method based on dynamically measured flexibility matrix. This method first developed by Bernal **[55].** Since no stress is generated in the damaged elements while these loads are applied to the structure as static forces at the sensor locations, this method can be utilized to detect damage.

Distributed Computing Strategy (DCS) proposed by Gao and Spencer **[56]** and Stochastic Damage Locating Vector (SDLV) method introduced by Bernal **[57]** are two recent methods based on dynamically measured flexibility matrix which can be employed in damage identification. Extension of DSC with SDLV can be utilized to improve the procedure in damage detection. Nagayama and Spencer **[58]** implemented these methods to detect the damaged elements of a three-dimensional truss structure.

The methods presented here are based on global vibration frequencies and modes. The application of these methods on belt conveyors is difficult because, most of the time, there is no available baseline. Moreover, large number of damaged members, considering the effects of non-structural components and

need of precisely measuring mode shapes make application of these methods difficult on the belt conveyors.

2.7 Summary

There are different damage identification techniques applicable to civil engineering structures. Almost all of these methods are involved with global vibration modes. There are some limitations regarding the use of global vibration modes in damage identification of belt conveyor support structures that cause the use of these techniques to fail in these structures. The main limitations are as follows:

1. Before-and-after comparison is needed to identify the damage degree of structures and since monitoring of belt conveyor support structures have not been usually conducted in the past, there is no baseline to compare with the current situations.
2. Large number of damaged elements makes damage identification difficult. As explained, due to aging and corrosion many members of some belt conveyor support structures have been severely damaged.
3. Non-structural members affect the properties of global vibration modes. For large structures such as bridges or large building, these effects are negligible, yet, in case of belt conveyors, non- structural members, such as walkways and machinery parts, strongly affect global vibration modes. Moreover, these non-structural components are frequently replaced with other types of non-structural members that significantly affects the global vibration modes.

Moreover, as described in many papers **[59, 60, 61, 62 and 63]**, properties changes of global vibration modes are remarkably depend on environmental conditions such as temperature.

Therefore, in a real belt conveyor, using global vibration modes to identify damage of the support structure of belt conveyors is difficult. Nevertheless, simulating the support structure of belt conveyors and investigating about the effects of damage on the modal properties of global vibration modes would give an initial assessment about the characteristics of the support structure of belt conveyors.

To overcome these difficulties, local vibration-based approach is utilized and expected to be efficient in damage identification of the support structure of belt conveyors. In the following chapters, the applicability of some damage identification methods using global and local vibration modes to the support structures of belt conveyors is assessed through sensitivity and observibility analysis and then damage identification methods based on two specific local vibration modes, PLVM and ILVM, are proposed and mainly investigated.

Chapter 3

Dynamic characteristics of the support structure of belt conveyor

3.1 Introduction

In this chapter, at first, belt conveyors are described briefly. Then, a finite element model of a typical frame of a belt conveyor support structure is created. After that, sensitivity of global and local mode characteristics, i.e. frequencies, mode shapes and its derivatives, are examined in details with respect to the stiffness changes of members based on the finite element model. Finally observibality of two specific local vibration modes is investigated to figure out the conditions in which these local modes are excited. The applicability and advantages of using local vibration modes compared to global ones in damage identification are discussed in this chapter as well.

3.2 Finite element model of a belt conveyor

A design drawing of a typical belt conveyor is shown in figure 3-1. One representative span of this belt conveyor, shown in figure 3-1 and 3-2, is modeled in ABAQUS.

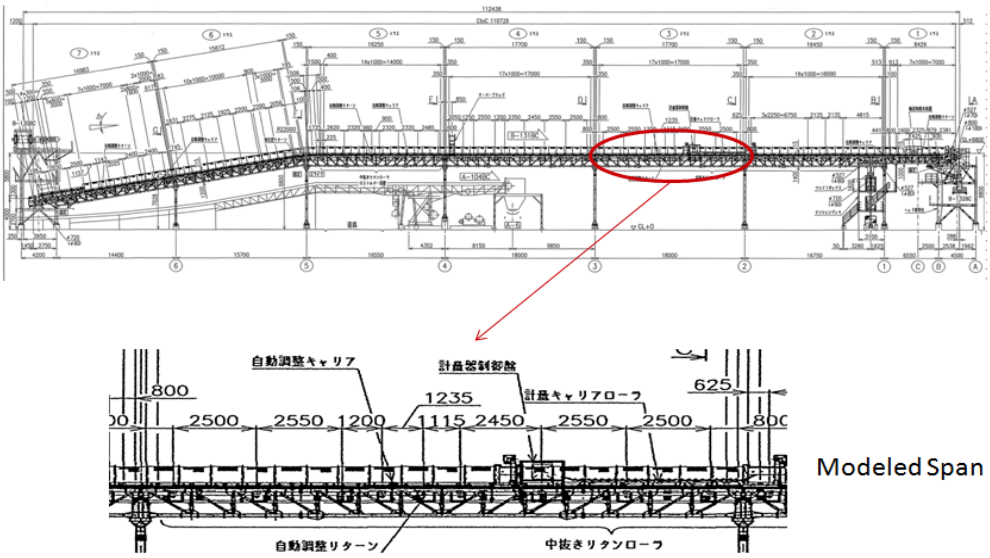

Figure 3-1 Design drawing of a typical belt conveyor

Figure 3-2 Modeled span

The main frame of belt conveyors consists of main and secondary parts. The main part includes continuous longitudinal members and the secondary part includes braces, lateral members, and vertical members connected to the longitudinal members. The boundary conditions of the whole structure, i.e. the connections between the columns and ground, and the connections between the main frame and columns are modeled as fixed. 3-D linear beam element has been used for all members in the model. Figure 3-3 shows the ABAQUS model of the representative span of the belt conveyor.

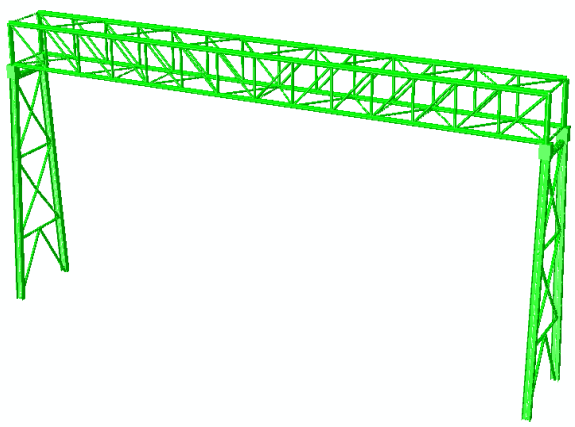

Figure 3-3 Finite element model of the representative span

Different vibration modes are identified through eigenvalue analysis of this model. Among all these vibration modes, some global and local vibration modes of the main frame are considered and the sensitivity of these modes with respect to the stiffness changes of different members is examined.

3.3 Global vibration modes

The eigenvalue analysis of the belt conveyor reveals global vibration modes. The 1st vertical bending, 1st torsional and 1st lateral bending modes are plotted in figures 3-4, 3-5 and 3-6 respectively.

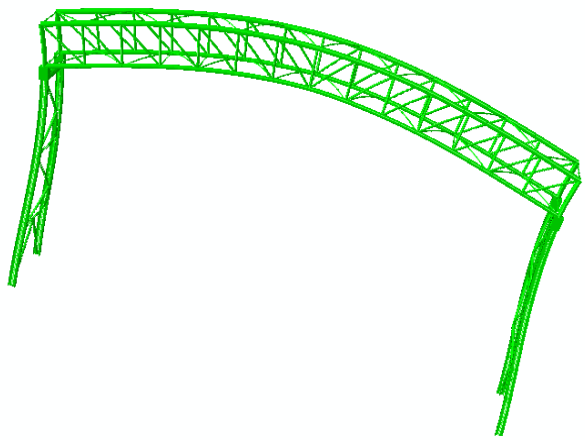

Figure 3-4 1st FEM vertical bending mode of the belt conveyor

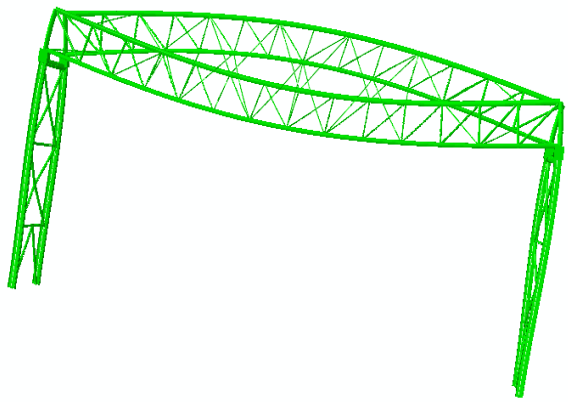

Figure 3-5 1st FEM torsional mode of the belt conveyor

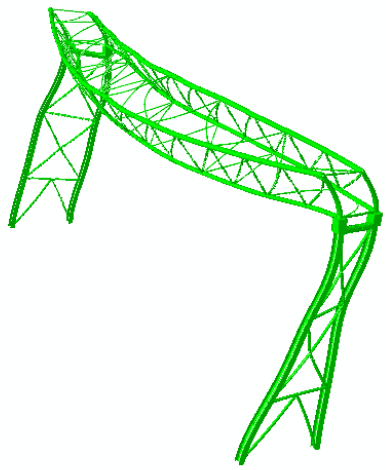

Figure 3-6 1st FEM lateral bending mode of the belt conveyor

Some of the FEM global vibration modes of the belt convertor and their vibration frequencies are listed in table 3-1.

Table 3-1 List of some global vibration modes

Type of mode	Frequency (Hz)
First sway	8.3486
First vertical bending	9.6322
First torsional	10.489
Second sway	14.834
First lateral bending	19.735
Second torsional	27.197
Second vertical bending	31.849

3.3.1 Frequency sensitivity analysis of global vibration modes of the belt conveyor with respect to stiffness changes

Modal properties sensitivity analysis is one of the important steps in vibration based-damage identification methods. In order to carry out frequency sensitivity analysis of global modes with respect to the stiffness changes of members, the young's modulus of different members, i.e. a longitudinal member, a brace of the bottom part, a lateral member, a brace of the side part and a vertical member, separately change and their influence on frequency changes of the 1st vertical bending, 1st lateral bending and 1st torsional modes are checked. First, the young's modulus of a longitudinal member, shown in figure 3-7, is reduced. The percentage variations of frequency in terms of the stiffness reduction of the longitudinal member for the 1st vertical bending, 1st lateral bending and 1st torsional modes are shown in figures 3-8, 3-9 and 3-10 respectively.

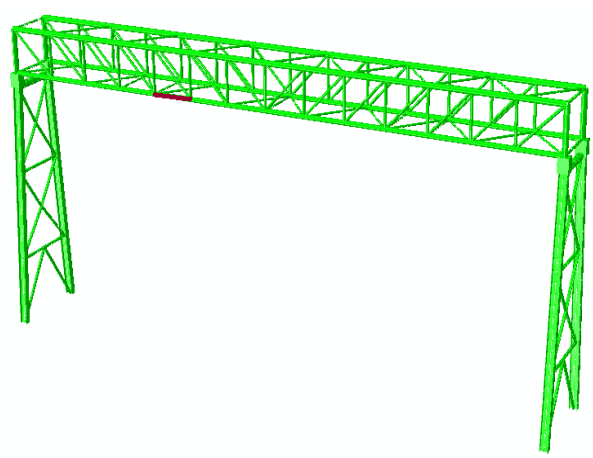

Figure 3-7 Location of the modified longitudinal member

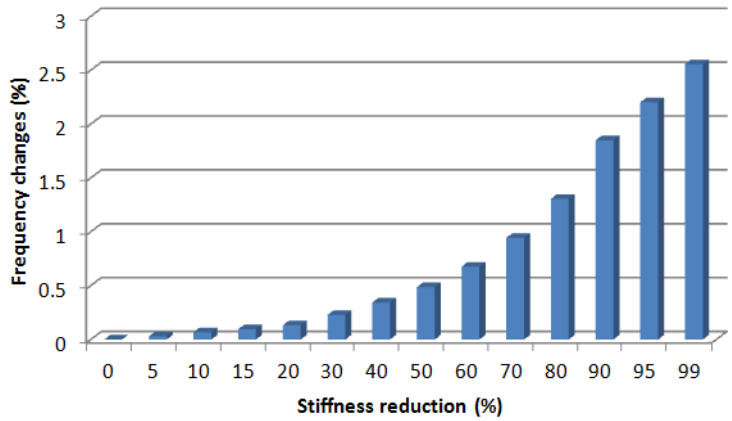

Figure 3-8 Variations of frequency for the 1st vertical bending mode (Longitudinal member)

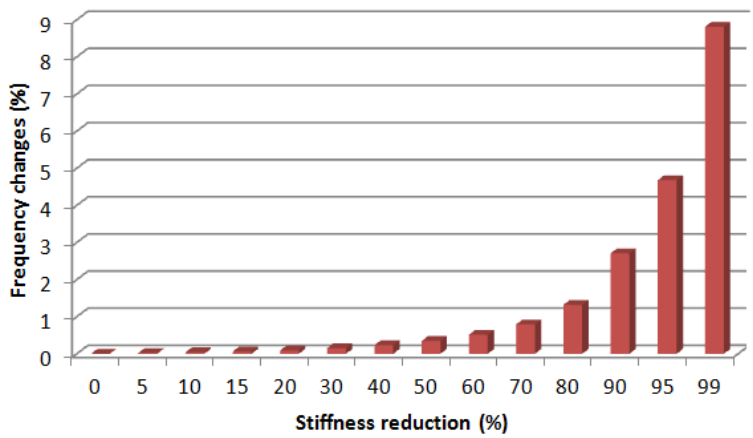

Figure 3-9 Variations of frequency for the 1st lateral bending mode (Longitudinal member)

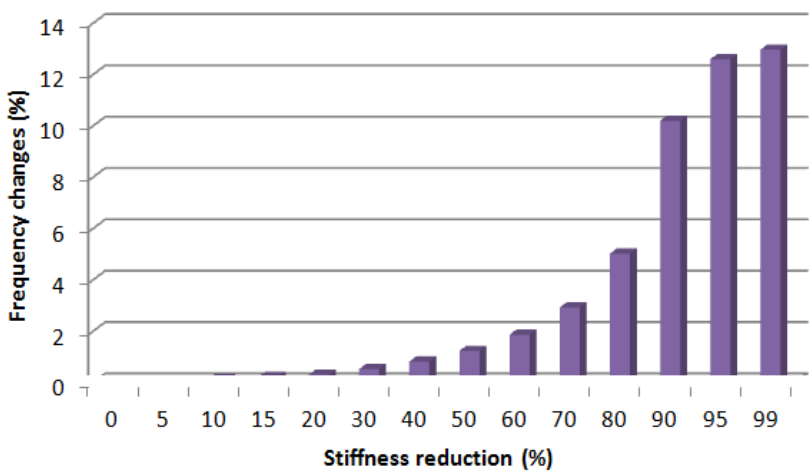

Figure 3-10 Variations of frequency for the 1st torsional mode (Longitudinal member)

As shown in the above figures, frequency of the 1st torsion mode is more sensitive than the 1st vertical bending mode as well as the 1st lateral bending mode with respect to the stiffness reduction of longitudinal members. However for the low degree of damage, even frequency of the 1st torsional mode

has a low sensitivity and is not a good indicator to judge about the presence of damage, As shown in figure 3-10, for 40% reduction in the stiffness of the longitudinal member, the frequency reduction is about 0.8%.

To check the sensitivity of the 1st vertical bending, 1st lateral bending and 1st torsional modes with respect to damage of braces in the bottom and top parts of the belt conveyor, the young's modulus of a bottom brace, shown in figure 3-11, is reduced.

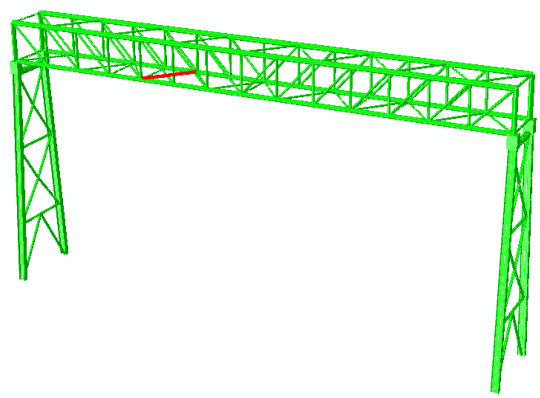

Figure 3-11 Location of the modified bottom brace

The percentage variations of frequency in terms of the stiffness reduction of the bottom brace for the 1st vertical bending, 1st lateral bending and 1st torsional modes are shown in figures 3-12, 3-13 and 3-14 respectively.

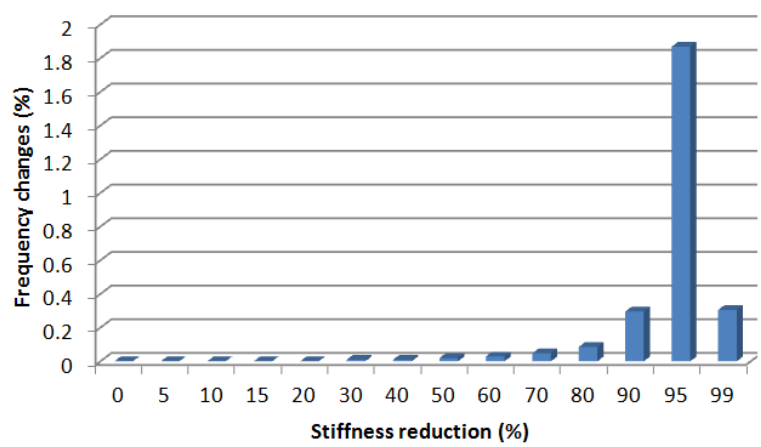

Figure 3-12 Variations of frequency for the 1st vertical bending mode (Bottom brace)

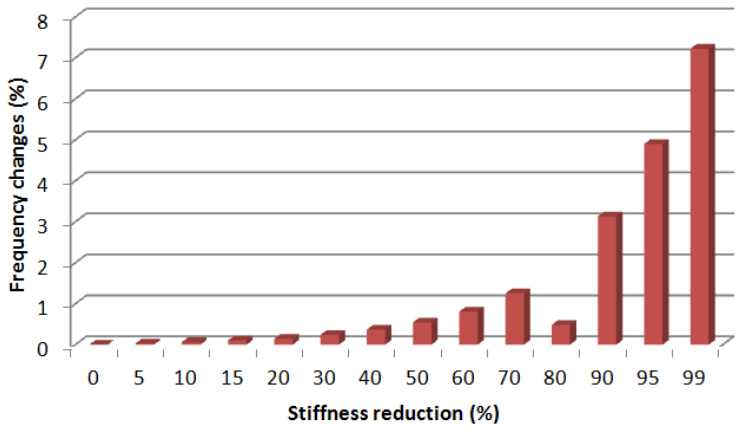

Figure 3-13 Variations of frequency for the 1st lateral bending mode (Bottom brace)

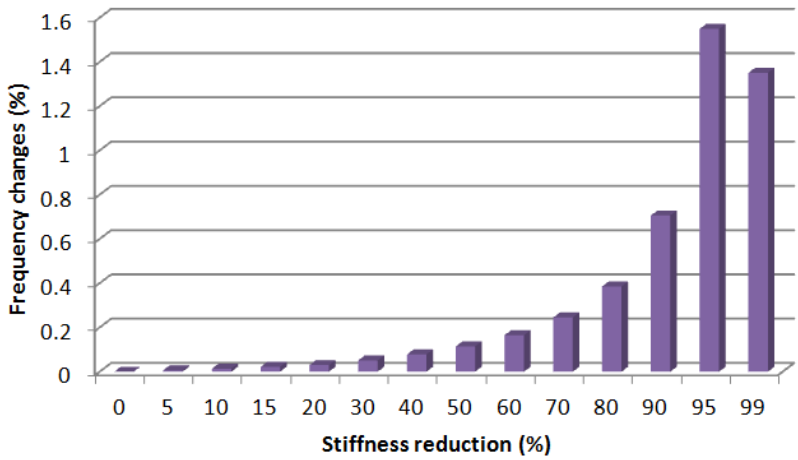

Figure 3-14 Variations of frequency for the 1st torsional mode (Bottom brace)

Frequency of the 1st lateral bending mode is more sensitive than the 1st vertical bending mode and 1st torsional mode with respect to the stiffness reduction of bottom or top braces. However the frequencies of global modes have a small sensitivity to the stiffness changes of these members and even for 60% reduction in the stiffness, the frequency change of the 1st lateral bending mode, which is the most sensitive one in this case, is 0.8%. The reason of the unexpected drop in frequency changes of the 1st lateral bending mode for 80% reduction in the stiffness of the bottom brace compared to 70% reduction, is that the frequencies of the 1st lateral bending mode of the belt conveyor and the local vibration mode of the damaged bottom brace are close to each other. Likewise, this unexpected drop happens in the 1st vertical bending and 1st torsion mode for 99% reduction in the stiffness of the bottom brace compared to 95% reduction due to the same reason as it is for the 1st lateral bending mode.

In order to examine the sensitivity of the 1st vertical bending, 1st lateral bending and 1st torsional modes with respect to the damage on lateral members of the belt conveyor, the young's modulus of a lateral member, shown in figure 3-15, is reduced.

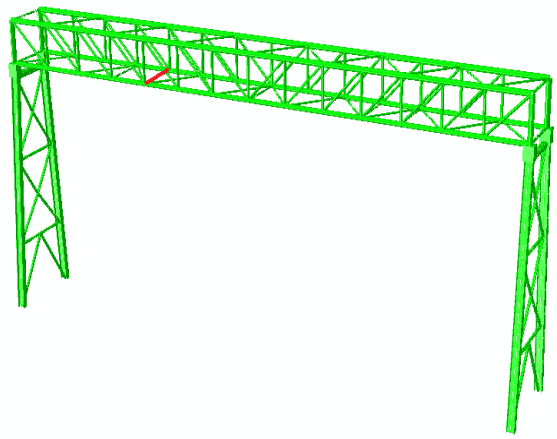

Figure 3-15 Location of the modified lateral member

The percentage variations of frequency in terms of the stiffness reduction of the lateral member, shown in the above figure, for the 1st vertical bending, 1st lateral bending and 1st torsional modes are illustrated in figures 3-16, 3-17 and 3-18 respectively.

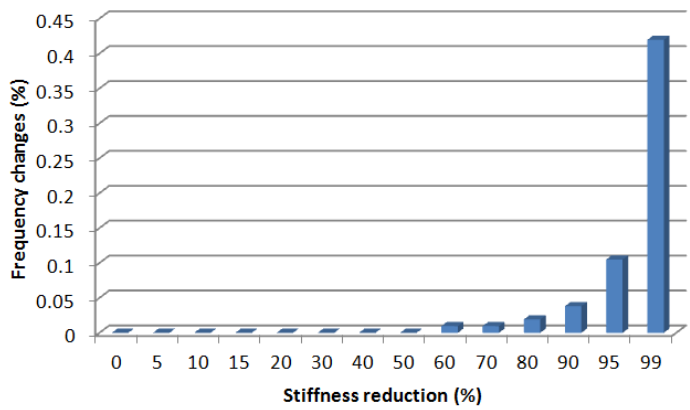

Figure 3-16 Variations of frequency for the 1st vertical bending mode (lateral member)

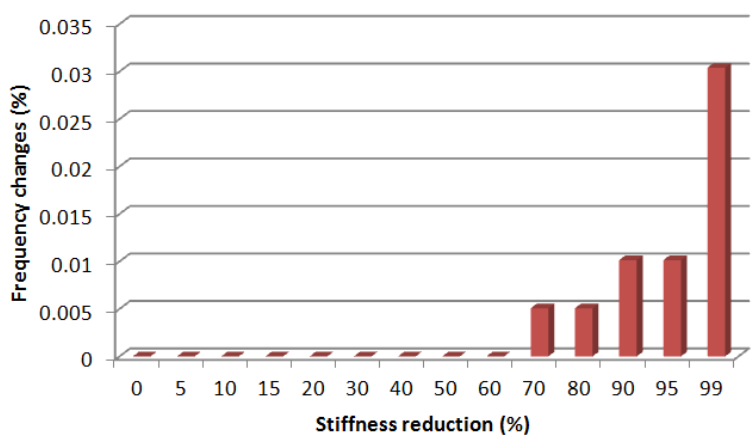

Figure 3-17 Variations of frequency for the 1st lateral bending (lateral member)

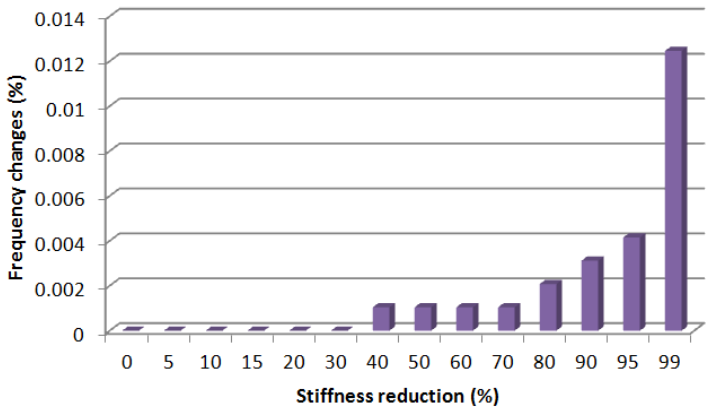

Figure 3-18 Variations of frequency for the 1st torsional mode (lateral member)

Frequencies of the 1st vertical bending, 1st vertical bending and 1st torsional modes have a negligible sensitivity with respect to the stiffness reduction of lateral members of the belt conveyor. As shown in the above figures, even for 99% reduction in the stiffness of the lateral member, the reduction in the frequency is 0.01%, 0.03% and 0.42% for the 1st torsional, 1st lateral bending and 1st vertical bending modes respectively. Thus, these global modes are not good indicators to even judge about the presence of damage in lateral members of the belt conveyor.

The sensitivity of the 1st vertical bending, 1st lateral bending and 1st torsional modes with respect to the damage on vertical members of the belt conveyor is checked by reducing the young's modulus of a vertical member shown in figure 3-19.

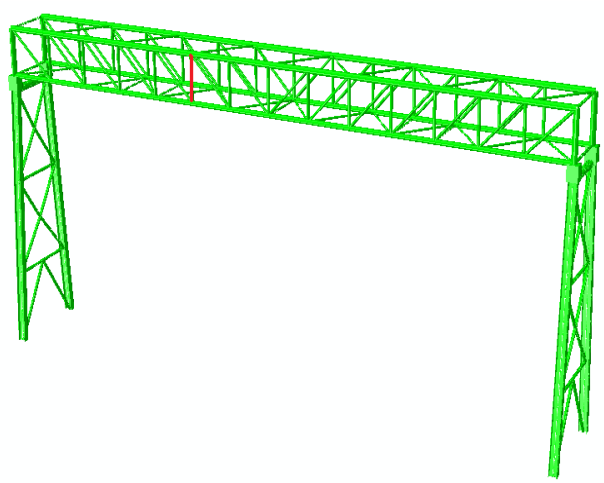

Figure 3-19 Location of the modified vertical member

The percentage changes of frequency with respect to the stiffness reduction of the vertical member for the 1st vertical bending, 1st lateral bending and 1st torsional modes are shown in figures 3-20, 3-21 and 3-22 respectively.

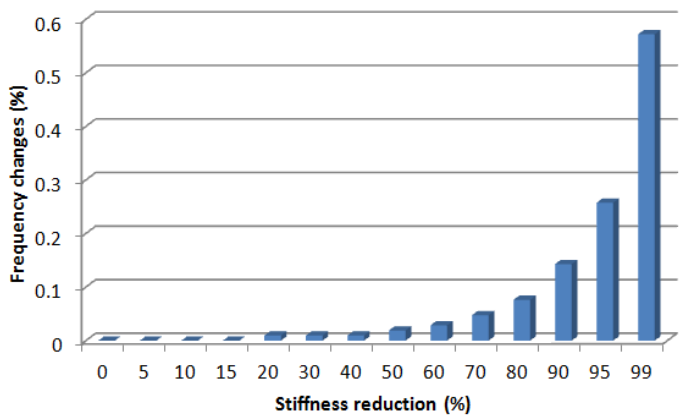

Figure 3-20 Variations of frequency for the 1st vertical bending mode (vertical member)

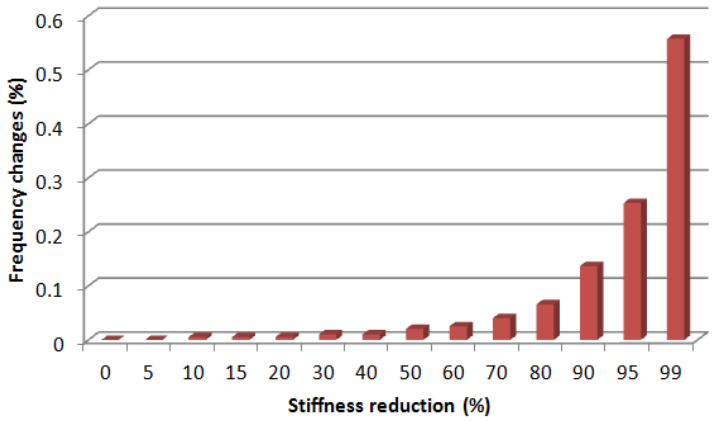

Figure 3-21 Variations of frequency for the 1st lateral bending mode (vertical member)

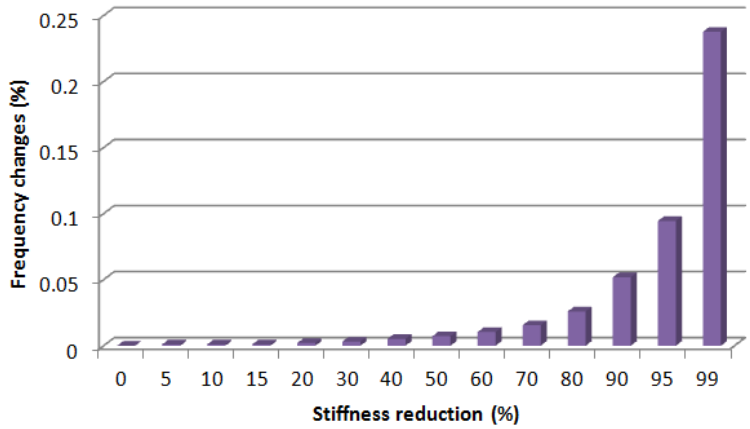

Figure 3-22 Variations of frequency for the 1st torsional mode (vertical member)

As shown in the above figures, frequencies of the 1st vertical bending, 1st vertical bending and 1st torsional modes have a small sensitivity with respect to the stiffness reduction of vertical members of the belt conveyor and even for 99% reduction in the stiffness of the vertical member, the reduction in the frequency is 0.57%, 0.56% and 0.24% for the 1st vertical bending, 1st vertical bending and 1st torsional

modes respectively. Therefore, these global modes are not appropriate indices in damage identification of vertical members of the belt conveyor even to judge about the presence of damage in these members.

The sensitivity of the 1st vertical bending, 1st lateral bending and 1st torsional modes with respect to the damage on side braces of the belt conveyor is examined by reducing the young's modulus of a side brace shown in figure 3-22.

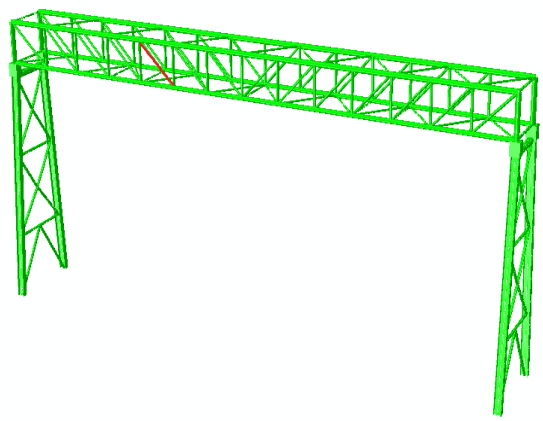

Figure 3-23 Location of the modified side brace

The percentage variations of frequency with respect to stiffness reduction of the side brace for the 1st vertical bending, 1st lateral bending and 1st torsional modes are illustrated in figures 3-24, 3-25 and 3-26 respectively.

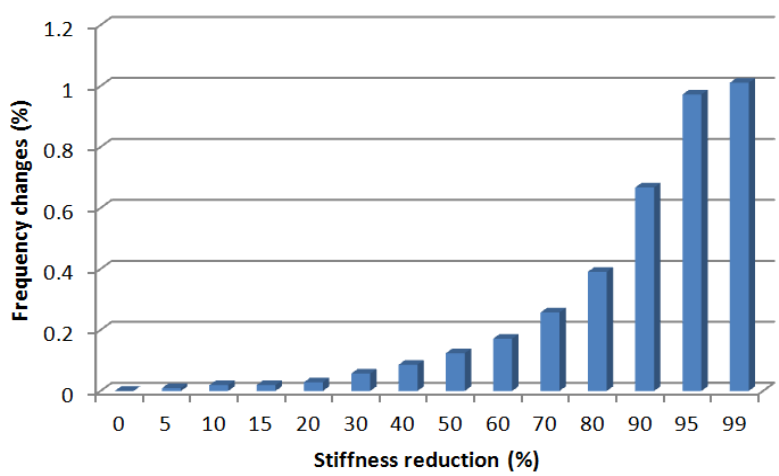

Figure 3-24 Variations of frequency for the 1st vertical bending mode (side brace)

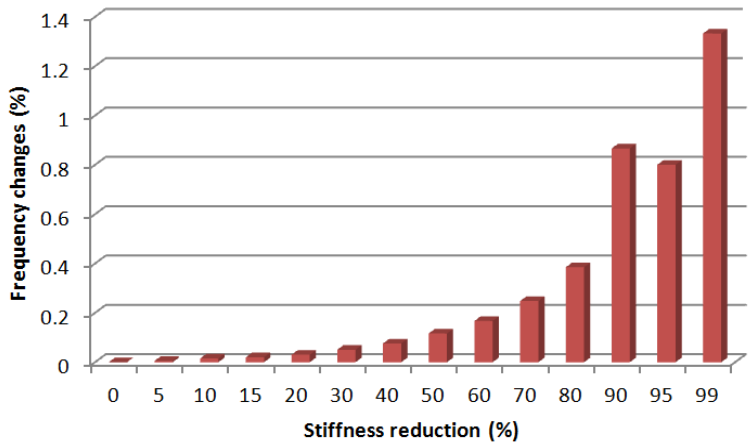

Figure 3-25 Variations of frequency for the 1st lateral bending mode (side brace)

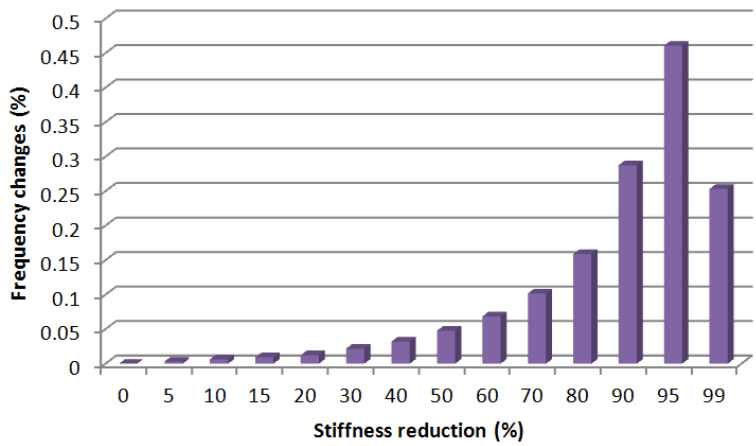

Figure 3-26 Variations of frequency for the 1st torsional mode (side brace)

It should be noted that the unexpected drops in frequency changes of the 1st lateral bending mode for 95% reduction in the stiffness of the bottom brace compared to 90% reduction and the 1st torsional mode for 99% reduction in the stiffness of the side brace compared to 95% reduction, have been caused by being nearly the same frequencies of the 1st lateral bending and 1st torsional modes of the belt conveyor with the frequency of local vibration mode of the damaged side brace. As shown in the above figures, frequencies of the 1st vertical bending, 1st lateral bending and 1st torsional modes have a small sensitivity with respect to the damage of side braces of the belt conveyor and the frequency changes are less than 0.4% for 80% stiffness reduction of the side brace in these three global vibration modes. Even for 99% reduction in the stiffness of the side brace, the frequency changes are always less than 1.34%. Therefore, these global modes are not appropriate indicators to even judge about the presence of damage in the side braces.

To have a better judgment about the effect of each member on different global vibration modes, the frequency variations of the 1st vertical bending, 1st lateral bending and 1st torsional modes with respect to the stiffness reduction of different members are plotted in figures 3-27, 3-28 and 3-29 respectively.

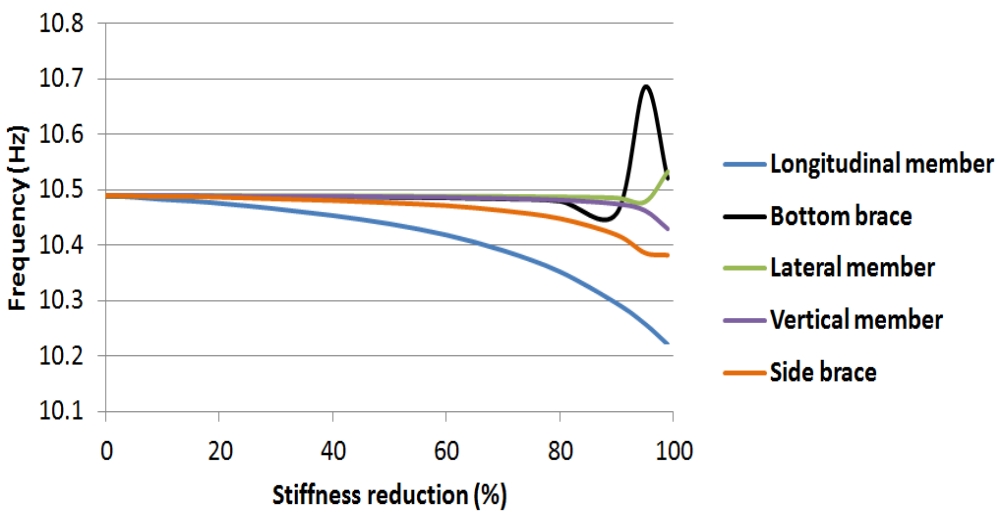

Figure 3-27 Frequency variation of the 1st vertical bending mode with respect to the stiffness reduction of different members

Frequency of the 1st vertical bending mode is relatively sensitive to the stiffness reduction of the longitudinal members; however, as shown in the above figure, this sensitivity to the longitudinal members is small (less than 2.5% for the 99% stiffness reduction of the member) and cannot be used as an indicator to judge about presence of the damage in the longitudinal members.

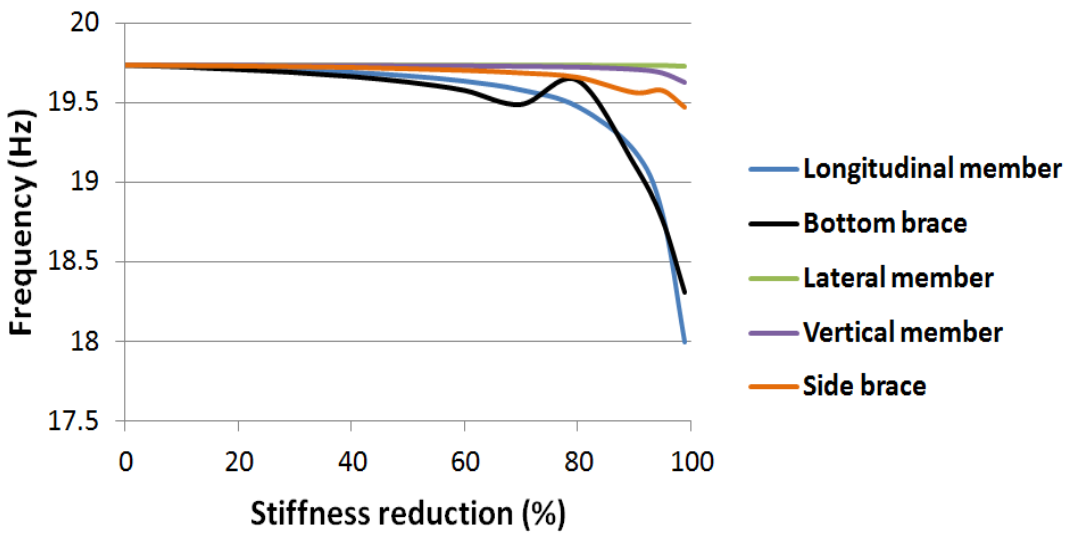

Figure 3-28 Frequency variation of the 1st lateral bending mode with respect to the stiffness reduction of different members

Frequency of the 1st lateral bending mode is much more sensitive to the stiffness reduction of the longitudinal members as well as bottom braces than the other members sets as shown in the above figure. Therefore, as long as the measurement results of the undamaged structure are available, a significant change in the frequency of this mode of the damage structure would indicate the presence of damage in either longitudinal members or bottom braces or both of these two members sets. This conclusion is valid

under the assumption that limited numbers of members in the belt conveyors are damaged since many damaged members of lateral members, side braces, or vertical members would cause a significant change in the frequency of the 1st lateral bending mode. Another assumption that should be noted is the ignorance of the effects of environmental conditions such as temperature and the effects of non- structural components such as walkways or conveyor belts on the frequencies of global vibration modes. Taking into account the effects of walkways, conveyor belts, boundary conditions and temperature leads to a complex problem in prediction of the presence of damage using the frequency changes of global vibration modes.

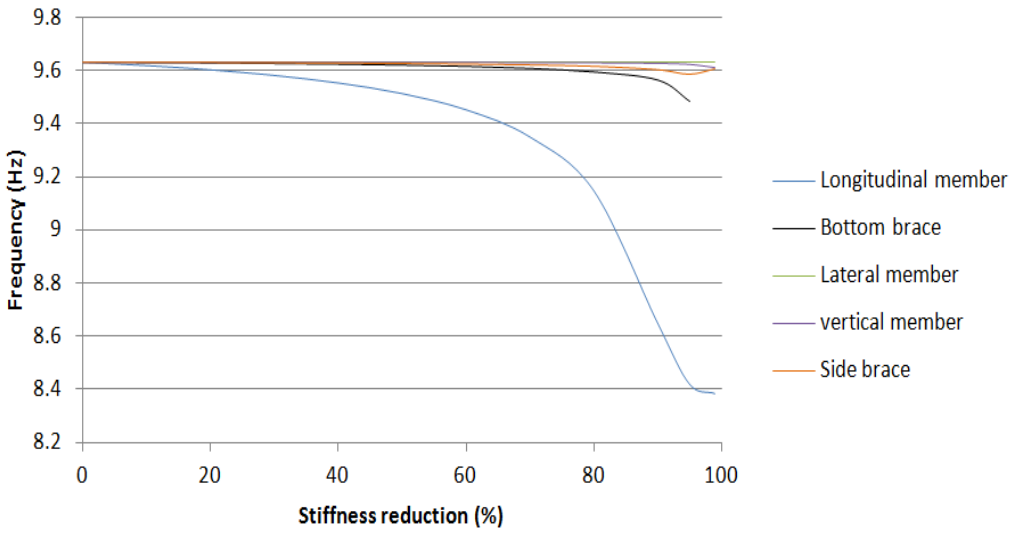

Figure 3-29 Frequency variation of the 1st torsional mode with respect to the stiffness reduction of different members

Frequency of the 1st torsional mode is much more sensitive to the stiffness reduction of the longitudinal members than the other members sets as shown in the above figure. Thus, under the mentioned assumptions, a significant change in the frequency of the 1st torsional mode would be an index to judge about the presence of damage in longitudinal members.

Even with the assumptions, this method is not able to identify the exact locations of damaged members, nor the severity of the damage. Existence of these limitations in using this approach makes it necessary to apply different methods to identify the presence, location and severity of damage in the support structure of belt conveyors. There are methods that use mode shapes of global vibration modes and their derivatives to identify the locations of damage in the structures.

3.3.2 Mode shape sensitivity of global vibration modes of the belt conveyor with respect to stiffness changes

Mode shapes and their derivatives are generally considered more sensitive to damage compared to frequencies of vibration modes **[64, 65]**. But the estimation error of mode shapes is usually larger than that of the corresponding frequencies **[25]**. In order to carry out a sensitivity analysis of the global

vibration mode shapes with respect to damage on members, the young's modulus of different members, i.e. a longitudinal member, a brace of the bottom part, a lateral member, a brace of the side part and a vertical member, separately changes and their influence on the shapes of the 1st vertical bending mode, 1st lateral bending mode and their 1st and 2nd derivative along different lines are checked. These lines are shown in figure 3-30.

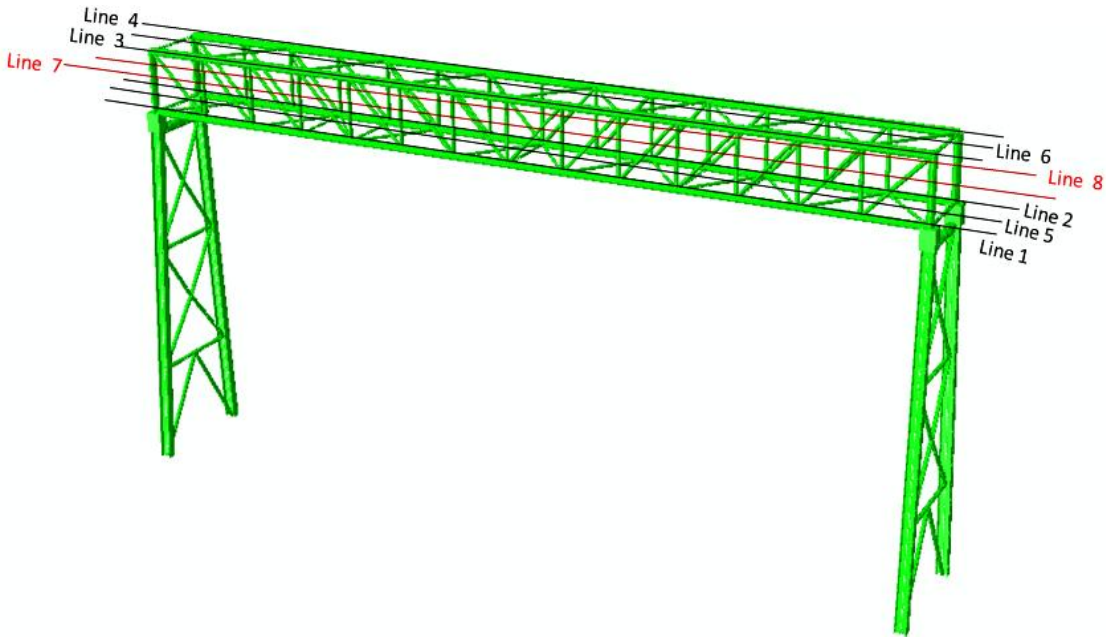

Figure 3-30 Locations of different lines where mode shapes are checked

In the above figure, line 1 to 8 are located at the front of the bottom part, back of the bottom part, middle of the bottom part, front of the top part, back of the top part, middle of the top part, middle of the front view and middle of the back view, respectively.

The Modal Assurance Criterion (MAC) is a common indicator to estimate the degree of correlation between two mode shape vectors. The MAC between a mode in undamaged condition ϕ_{Ui} and a mode in damage condition ϕ_{Dj} is defined as:

$$MAC_{ij} = \frac{|\phi_{Ui}^T \phi_{Dj}|^2}{(\phi_{Ui}^T \phi_{Ui})(\phi_{Dj}^T \phi_{Dj})} \tag{3.1}$$

The value of the MAC is between zero and one. A value of zero means that two comparative mode shape vectors are totally orthogonal and a value of one means that one mode shape vector is a multiple of the other or, in other words, they are identical.

3.3.2.1 Mode shape sensitivity of the 1st vertical bending mode of the belt conveyor with respect to stiffness changes of the longitudinal members

The young's modulus of the longitudinal member shown in figure 3-7 reduces by 10%, 20% and 40%. The MAC values between the 1st vertical bending mode shape vector of the undamaged structure and that

of the damaged structure along different lines for 10%, 20% and 40% stiffness reduction of the longitudinal member are shown in table 3-2.

Table 3-2 MAC values between the 1st vertical bending mode shape vectors of the undamaged and damaged structures (longitudinal member)

Stiffness reduction	Line 1	Line 2	Line 3	Line 4	Line 5	Line 6	Line 7	Line 8
10%	0.9999991	1	0.9999991	1	0.9999991	0.9999991	0.9999991	1
20%	0.9999954	0.9999999	0.9999956	0.9999999	0.9999958	0.9999956	0.9999957	0.9999999
40%	0.9999703	0.9999995	0.9999713	0.9999995	0.9999730	0.9999705	0.9999716	0.9999995

The MAC values for all cases is almost equal to 1 even for 40% damage; however it is relatively smaller along line 1 where the damaged member is located. MAC value is usually used to figure out the presence of the damage in structures. To have a more accurate judgment about the presence, or even location, of damage in the structure, normalized mode shapes of the damaged and undamaged structures are plotted along the eight lines and the graphs will be compared to each other. Equation 3.2 is used to normalize the mode vectors:

$$|\phi^T \phi| = 1 \tag{3.2}$$

The shapes of the 1st vertical bending mode along the eight lines for the undamaged and damaged structures with 10%, 20% and 40% reduction in the stiffness of the longitudinal member are compared before and after damage and the results of 40% are shown in figure 3-31.

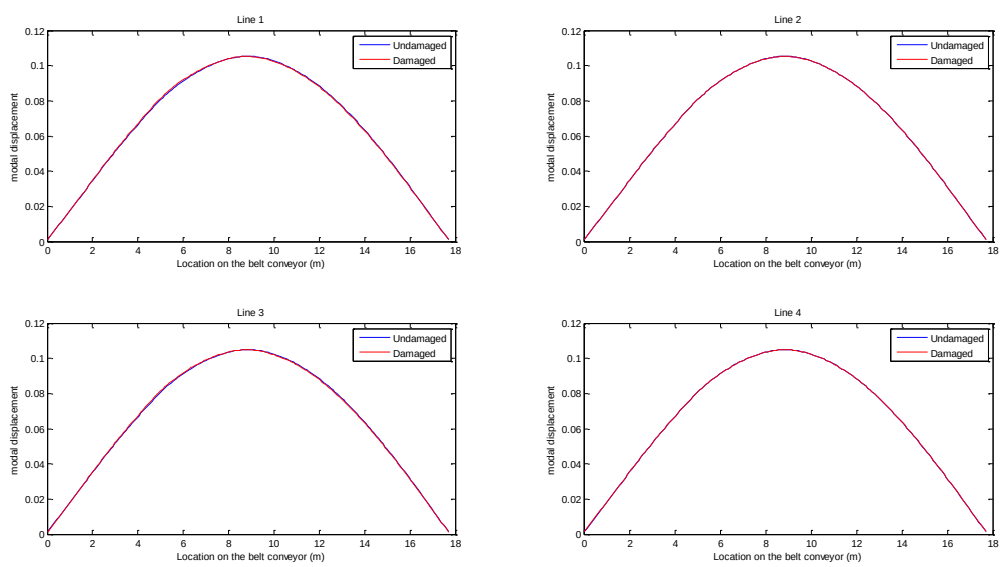

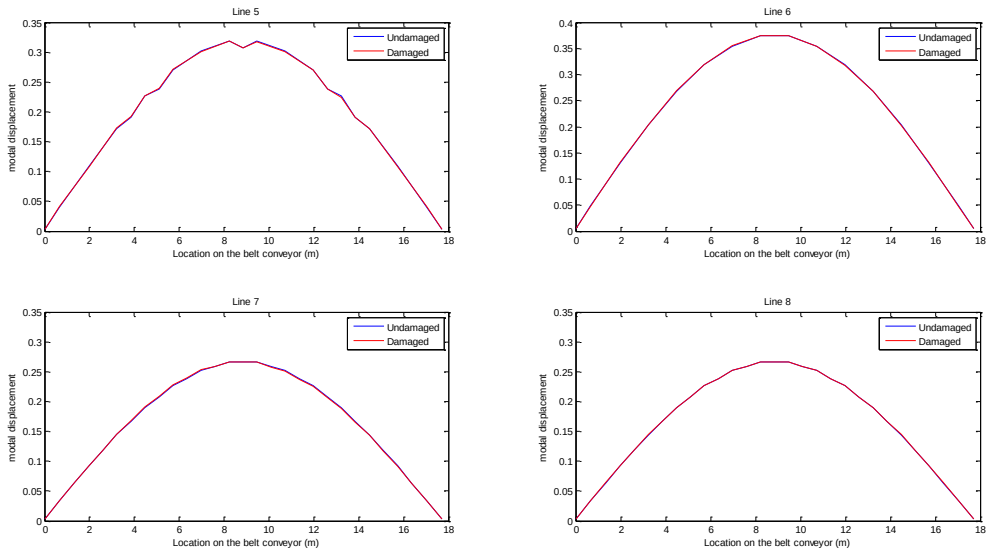

Figure 3-31st vertical bending mode shapes of the damaged and undamaged structures (40% stiffness reduction of the longitudinal member)

The mode shapes along all eight lines are overlapped. Though the degree of damage is remarkable, the damaged members are not detected. The corresponding 1st derivative curves along the eight lines with 10%, 20% and 40% reduction in the stiffness of the longitudinal member are compared before and after damage and the results of 40% are shown in figure 3-32. It should be noted that the derivatives of mode shapes are usually considered more sensitive to damage than the mode shapes. As for the lines 1, 2, 3 and 4, the interval between two successive points to calculate the derivatives is 0.1 m. For the lines 5, 6, 7 and 8, the considered points to calculate the derivatives are at the intersections of the lines and the members. Accordingly, for line 5 and 6, the intervals between two successive points are not always constant. The 1st and 2nd derivatives of mode i and point q are respectively calculated by:

$$\phi'_{q,i} = \frac{\phi_{q,i} - \phi_{q-1,i}}{h} \tag{3.3}$$

$$\phi''_{q,i} = \frac{\phi_{q-1,i} - 2\phi_{q,i} + \phi_{q+1,i}}{h^2} \tag{3.4}$$

where h is the interval between two successive points.

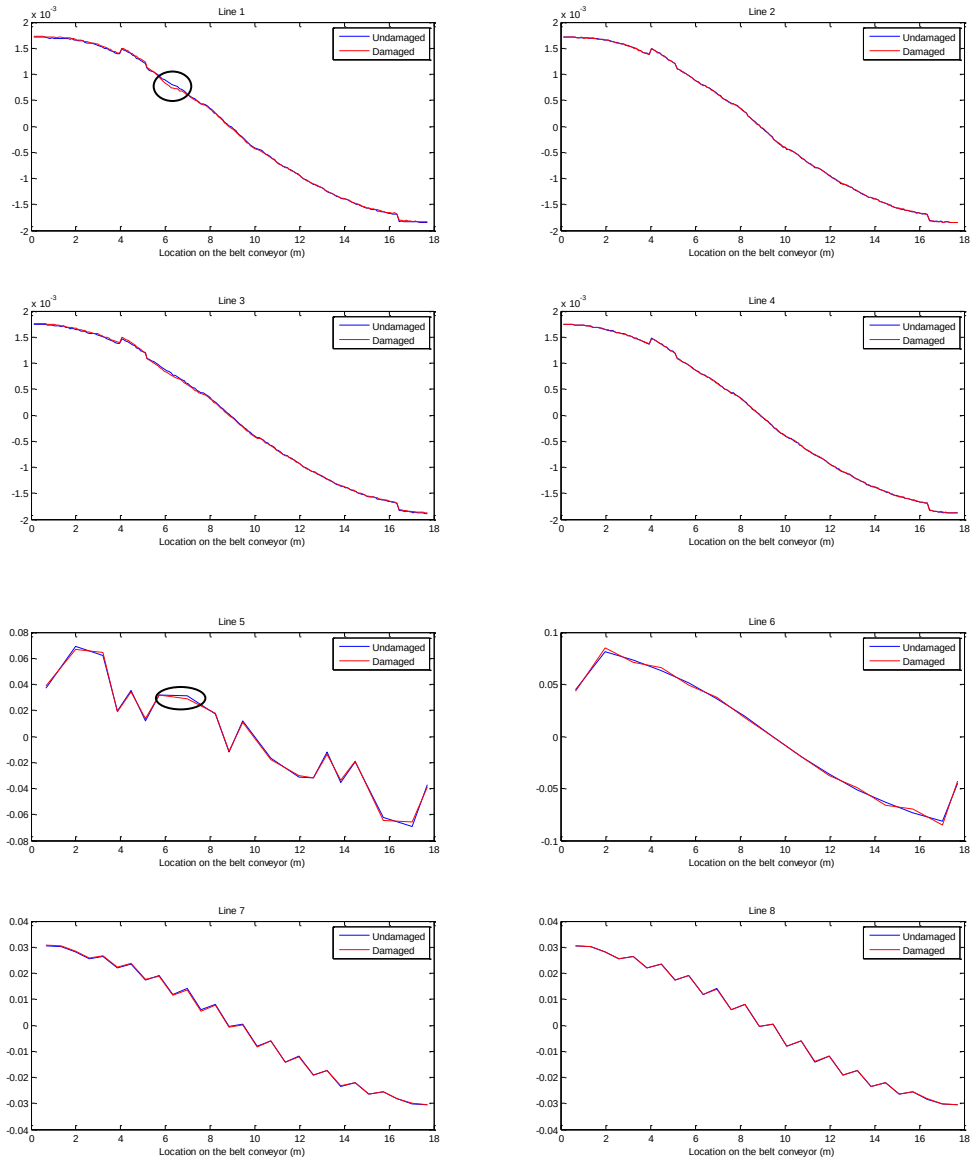

Figure 3-32 1st derivatives of the 1st vertical bending mode shapes of the damaged and undamaged structures (40% stiffness reduction of the longitudinal member)

The curves are almost overlapped. However at the exact location as the damaged member in line 1, the two curves are a little different. Moreover, in line 5 which corresponds to the secondary members at the bottom part of the belt conveyor, at the same area as the damaged longitudinal member, there is a very small mismatch between the two curves. The corresponding 2nd derivative along the eight lines with 10%, 20% and 40% reduction in the stiffness of the longitudinal member are compared before and after damage and the results of 40% are plotted in figure 3-33.

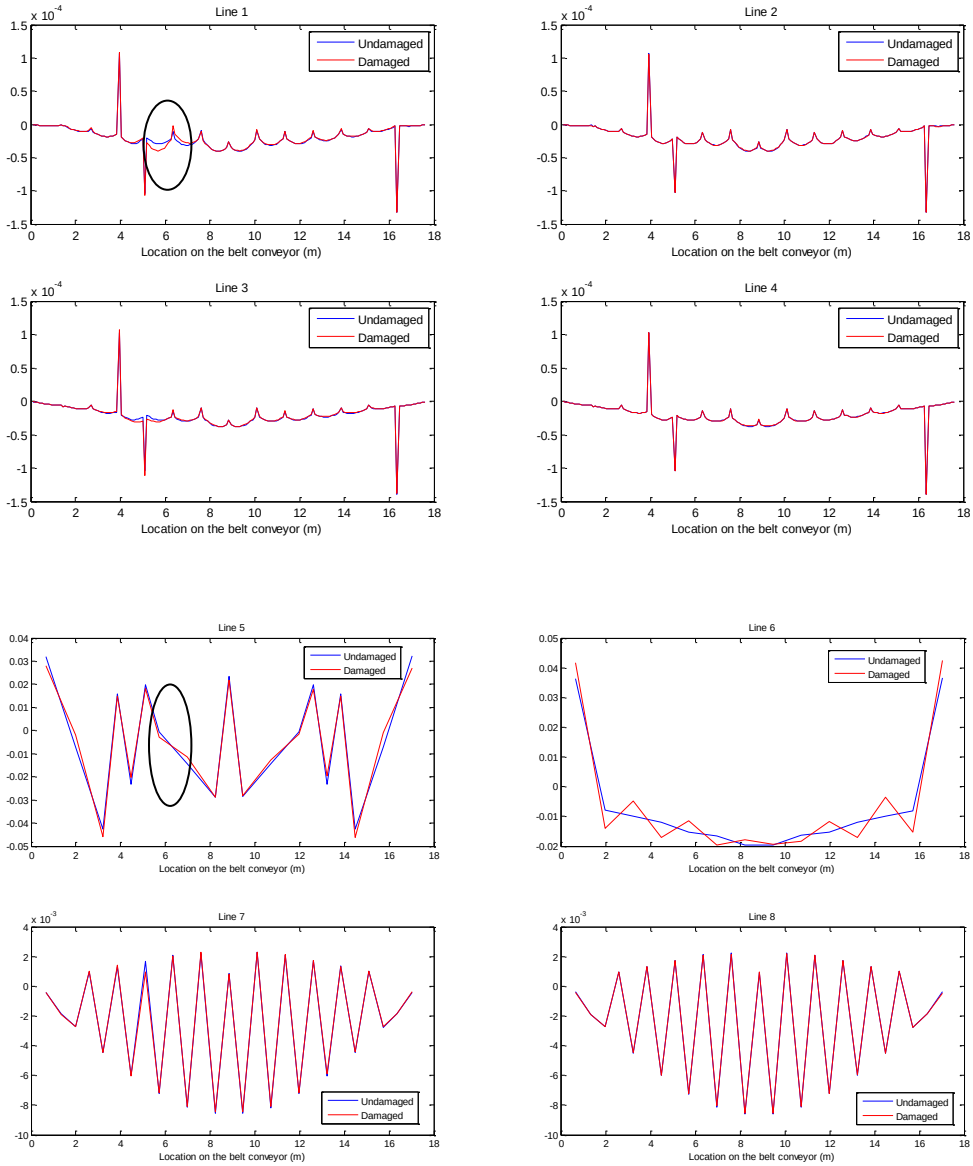

Figure 3-33 2nd derivatives of the 1st vertical bending mode shapes of the damaged and undamaged structures (40% stiffness reduction of the longitudinal member)

The difference between two curves along line 1 at the same location as the damaged longitudinal member is easily observable. Likewise, there is a mismatch between two curves along line 5 at the same area as the damaged longitudinal member. Along the other lines there is no clear sudden change that causes the curves nonsymmetrical.

The main conclusions of these analyses for 10%, 20% and 40% stiffness reduction of the longitudinal member, which corresponds to the 1st vertical bending mode, are firstly the 1st vertical bending mode shapes are not sensitive to damage on the longitudinal members and even with relatively high damage degree, there is no sudden change at the location of damaged longitudinal members. Secondly it has been

found that the 1st derivative of the mode shapes are more sensitive to the damage on the longitudinal members than the mode shapes and the 2nd derivative of the mode shapes are more sensitive than both the 1st derivative of mode shapes and the mode shapes themselves. The 1st and 2nd derivatives of the 1st vertical bending mode shape are sensitive to damage on the longitudinal members as long as the damage degree is relatively large. Fortunately the effects of damage on the longitudinal members mainly reflect only on the mode shapes along the line which damaged longitudinal members are placed and along the line passes the secondary members either on the bottom or the top part of the belt conveyor depends on damaged longitudinal members are located at the bottom or top parts of the belt conveyor. These conclusions can be expressed by difference rate, D, defined by:

$$D = \frac{\Delta d_{max}}{a_{max} - a_{min}} \tag{3.3}$$

Where $\Delta\ d_{max}$ is the maximum difference between curves of the damaged and undamaged structure and a_{max} and a_{min} are the maximum and minimum amplitudes of the two curves. Figures 3-34, 3-35 and 3-36 show the difference rate for the two curves of the damaged and undamaged structures with 10%, 20% and 40% of the stiffness reduction of the longitudinal member respectively. Note that the results are for the 1st vertical bending mode.

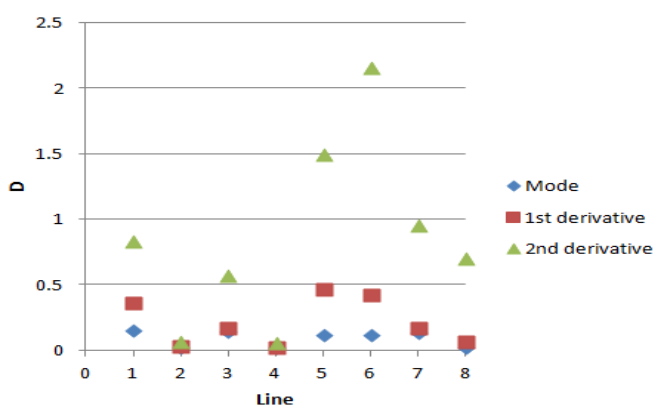

Figure 3-34 Difference rate of the eight lines for 10% stiffness reduction of the longitudinal member

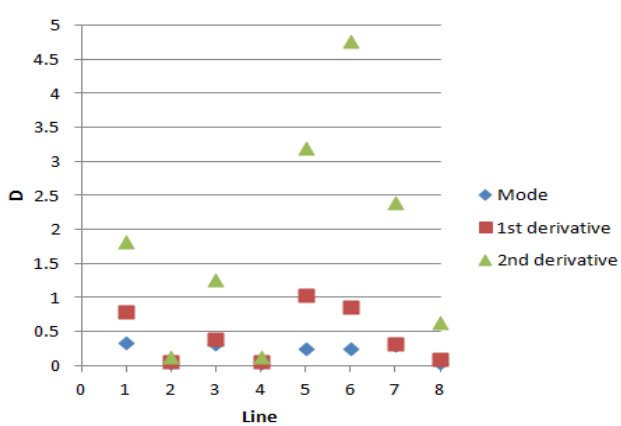

Figure 3-35 Difference rate of the eight lines for 20% stiffness reduction of the longitudinal member

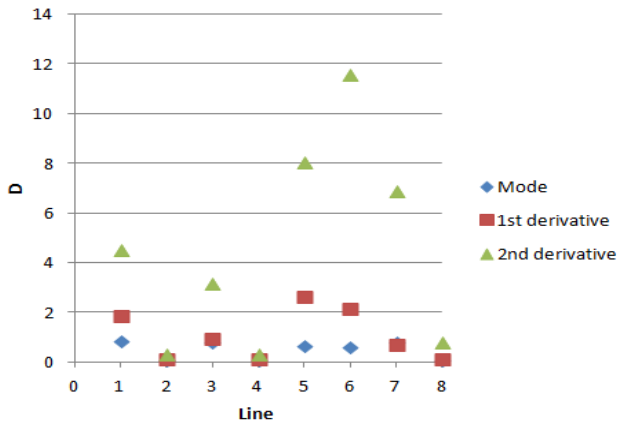

Figure 3-36 Difference rate of the eight lines for 40% stiffness reduction of the longitudinal member

3.3.2.2 Mode shape sensitivity of the 1st lateral bending mode of the belt conveyor with respect to stiffness changes of the longitudinal members

As another similar analysis, the 1st lateral bending mode of the belt conveyor is considered to check its sensitivity to damage on the longitudinal member shown in figure 3-7. The MAC values between the 1st lateral bending mode shape vector of the undamaged structure and that of the damaged structure along the different lines for 10%, 20% and 40% stiffness reduction of the longitudinal member are shown in table 3-3.

Table 3-3 MAC values between the 1st lateral bending mode shape vectors of the undamaged and damaged structures (longitudinal member)

Stiffness reduction	Line 1	Line 2	Line 3	Line 4	Line 5	Line 6	Line 7	Line 8
10%	0.9999932	0.9999951	0.9999951	0.9999950	0.9999951	0.9999953	0.9999971	0.9999987
20%	0.9999660	0.9999754	0.9999754	0.9999749	0.9999746	0.9999760	0.9999856	0.9999940
40%	0.9997644	0.9998284	0.9998278	0.9998238	0.9998217	0.9998332	0.9999029	0.9999596

The presence or location of the damage cannot be identified as the MAC values for all cases are close to one. However along line 1 where the damaged longitudinal member exists, MAC value is a little smaller. As another method to identify the location of the damaged members, the 1st normalized lateral mode shape and its 1st and 2nd derivatives along the eight lines, shown in figure 3-30, are compared in the damaged and undamaged structures. The shapes of the 1st lateral bending mode along the eight lines for the undamaged and damaged structures with 10%, 20% and 40% reduction in the stiffness of the longitudinal member are compared before and after damage and the results of 40% are illustrated in figure 3-37.

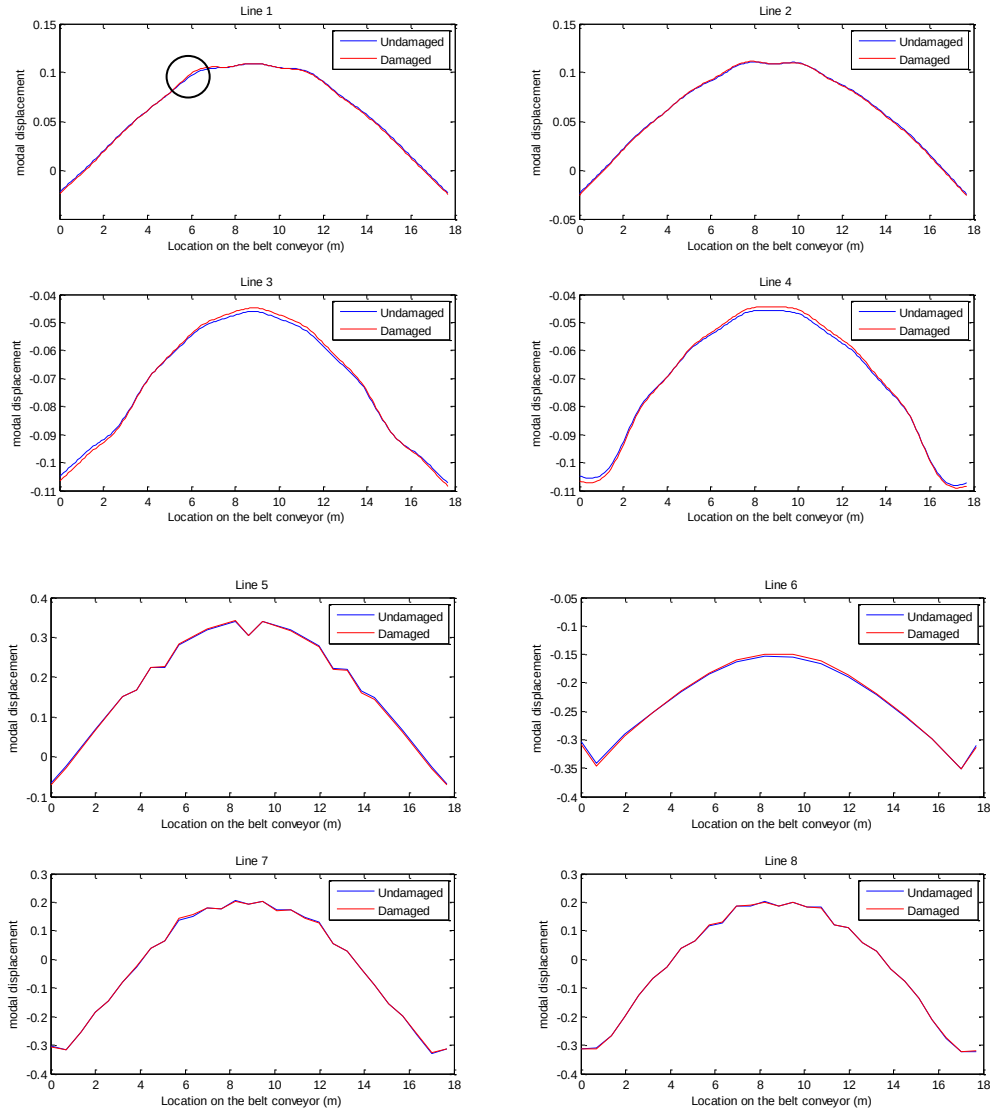

Figure 3-37 1st lateral bending mode shapes of the damaged and undamaged structures (40% stiffness reduction of the longitudinal member)

At the exact location as the damaged member in line 1, the two curves are a little different. Moreover, in line 7 which corresponds to the secondary members at the front side of the belt conveyor, at the same area as the damaged longitudinal member, there is a very small mismatch between the two curves. There is no any sudden change at any other parts of the lines. The 1st derivatives curves of the 1st lateral bending mode shapes along the eight lines are compared before and after damage in figure 3-38.

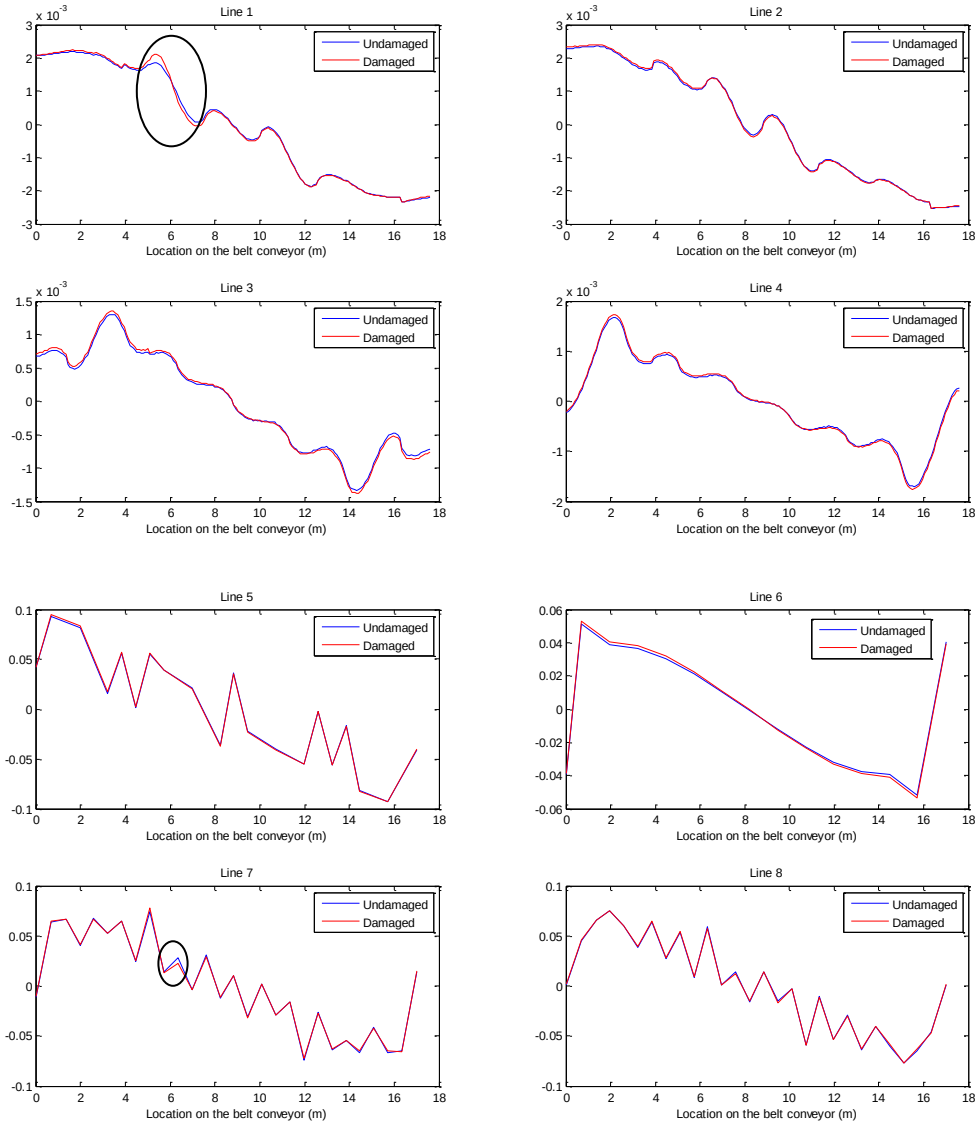

Figure 3-38 1st derivatives of the 1st lateral bending mode shapes of the damaged and undamaged structures (40% stiffness reduction of the longitudinal member)

As shown, the only sudden changes are along line 1 at the same location as the damaged longitudinal member and along line 7 at the same area as the damaged member. The corresponding 2nd derivative curves of the 1st lateral bending mode shapes along the eight lines before and after damage are plotted in figure 3-39.

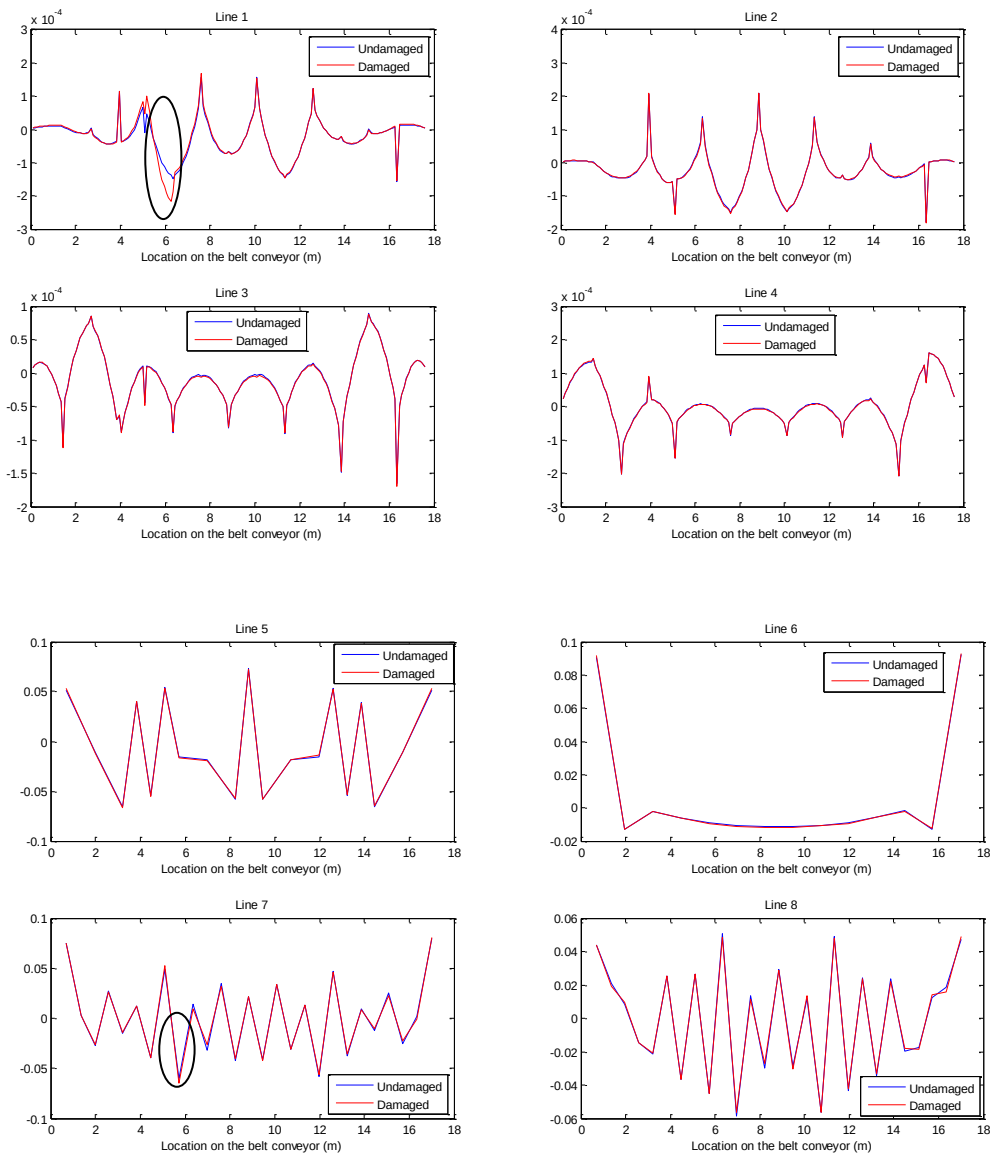

Figure 3-39 2nd derivatives of the 1st lateral bending mode shapes of the damaged and undamaged structures (40% stiffness reduction of the longitudinal member)

This time, the only sudden changes are along line 1 at the same location as the damaged longitudinal member and along line 7 at the same area as the damaged member. However, the change at line 7 is much smaller than that change at line 1 where the damaged longitudinal member is placed.

The main conclusions of these analyses for 10%, 20% and 40% stiffness reduction of the longitudinal member, which are corresponding to the 1st lateral bending mode, are firstly the 1st lateral bending mode shape has a very small sensitivity to damage on the longitudinal members and even with relatively high damage degree, there is a very small sudden change at the exact location of the damaged longitudinal members as well as the same area as the damaged members along the line passes the secondary members either on the front or back side of the belt conveyor depends on the damaged longitudinal members are

located at the front or back sides of the belt conveyor. Secondly it has been found that the 1st derivative of the mode shapes are more sensitive to the damage on the longitudinal member than the mode shapes and the 2nd derivative of the mode shapes are more sensitive than both the 1st derivative of the mode shapes and the mode shapes themselves. The 1st and 2nd derivatives of the 1st lateral bending mode cannot be identified the location of the damage when the damage is relatively small. If the damage is not small, the effects of damage on the longitudinal members mainly reflect only on the mode shape derivatives along the line which damaged longitudinal members are placed. However for large degree of damage these effects are observed on the mode shape derivatives along the secondary members at the same area as the damaged longitudinal members at either the front or back side of the belt conveyor depends on location of the damage members.

These conclusions can be expressed by the difference rate. Figures 3-40, 3-41 and 3-42 show the difference rate for the two curves of the damaged and undamaged structures with 10%, 20% and 40% of stiffness reduction of the longitudinal member respectively. Note that the results are for the 1st lateral bending mode.

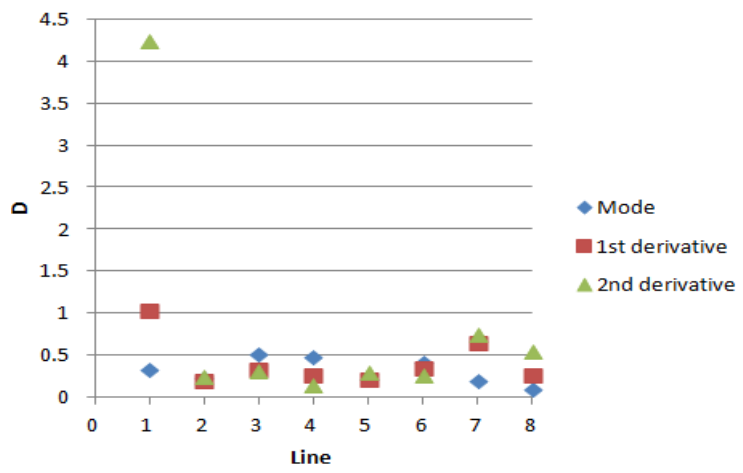

Figure 3-40 Difference rate of the eight lines for 10% stiffness reduction of the longitudinal member

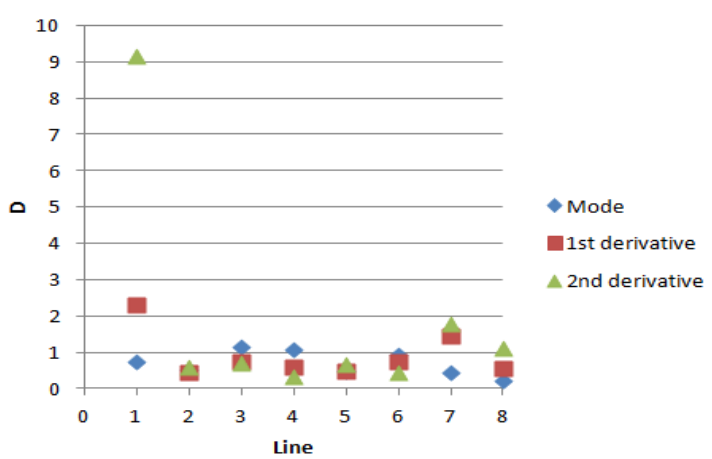

Figure 3-41 Difference rate of the eight lines for 20% stiffness reduction of the longitudinal member

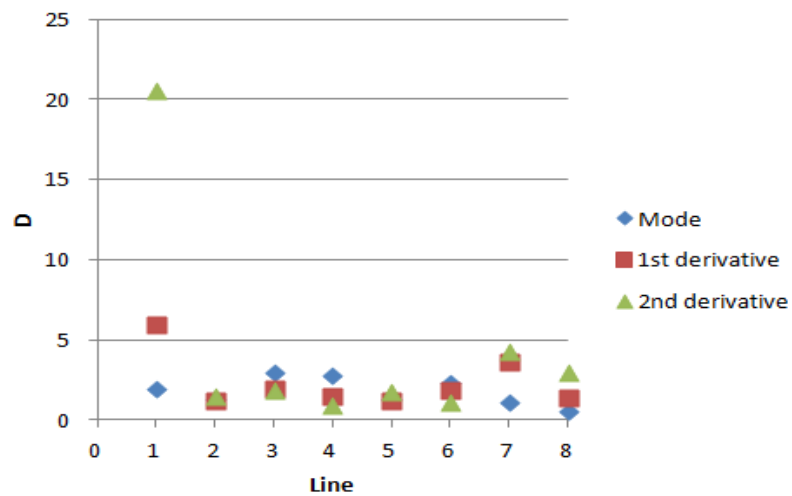

Figure 3-42 Difference rate of the eight lines for 40% stiffness reduction of the longitudinal member

Comparing the results of the 1st lateral bending and 1st vertical bending modes shows that the 1st lateral bending mode shape and its 1st and 2nd derivatives are more sensitive to damage on the longitudinal members than the 1st vertical bending mode shape and its 1st and 2nd derivatives.

3.3.2.3 Mode shape sensitivity of the 1st vertical bending mode of the belt conveyor with respect to stiffness changes of the bottom and top braces

In order to examine the sensitivity of the 1st vertical bending mode with respect to damage on the bottom and top braces, the young's modulus of a bottom brace, shown in figure 3-11, reduces by 10%, 20% and 40%. The MAC values between the 1st vertical bending mode shape vectors of the undamaged and damaged structures along the different lines for 10%, 20% and 40% stiffness reduction of the bottom brace are shown in table 3-4.

Table 3-4 MAC values between the 1st vertical bending mode shape vectors of the undamaged and damaged structures (bottom brace)

Stiffness reduction	Line 1	Line 2	Line 3	Line 4	Line 5	Line 6	Line 7	Line 8
10%	1	1	1	1	0.9999944	1	1	1
20%	1	1	1	1	0.9999712	1	1	1
40%	1	1	1	1	0.9997852	1	1	1

It is noted that the Mac has been calculated up to the seventh decimal digit. Even though the MAC values along line 5, where the damaged member is located, do not equal to 1 but it is still close to 1. Therefore, by using of this method, even presence of damage cannot be identified.

As another method, the 1st normalized vertical mode shape and its 1st and 2nd derivatives along the eight lines, shown in figure 3-30, are compared in the damaged and undamaged structures. The shape of the 1st vertical bending mode along the eight lines for the undamaged and damaged structures with 10%, 20%

and 40% reduction in the stiffness of the bottom brace are compared before and after damage and the results of 40% are shown in figure 3-43.

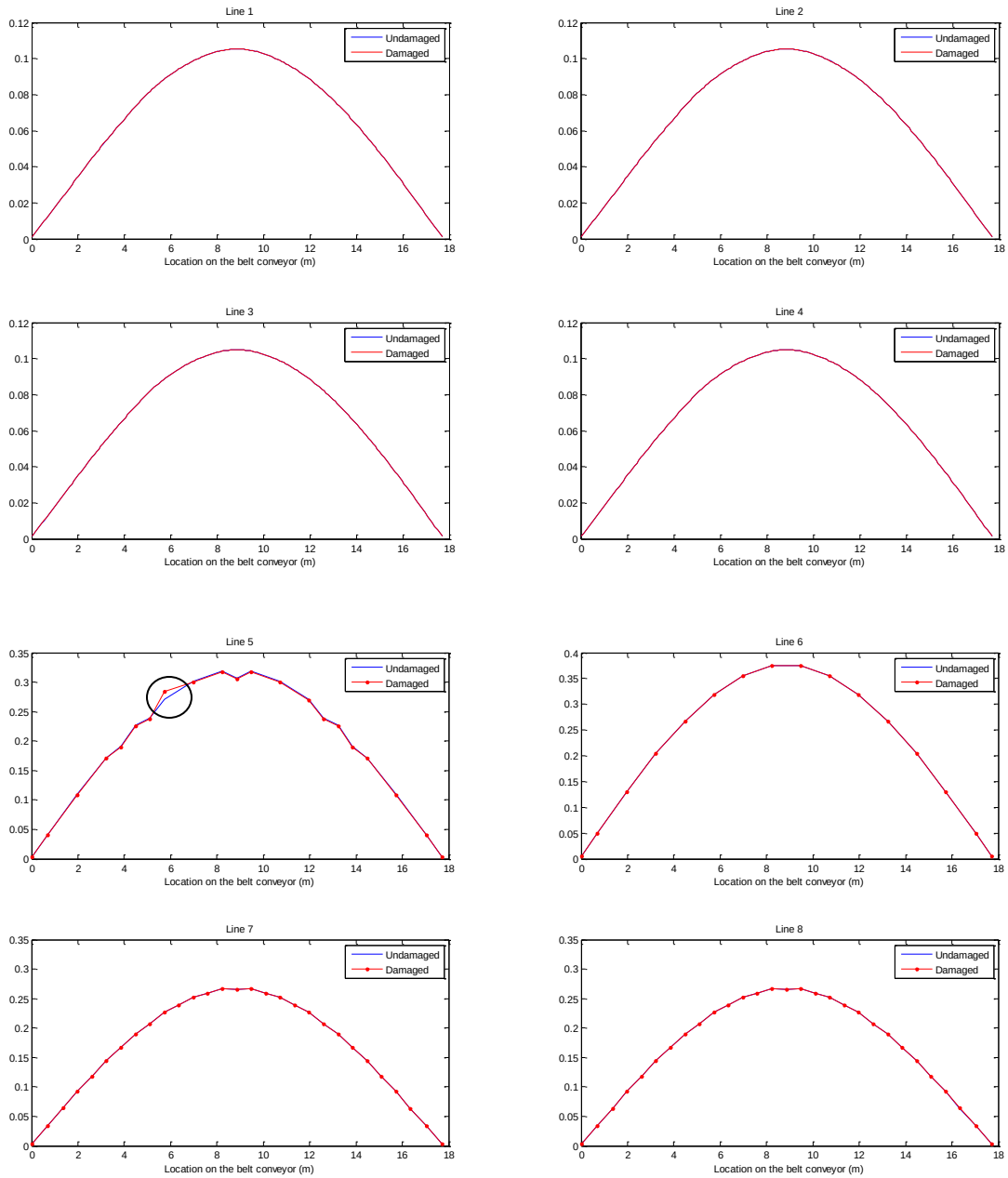

Figure 3-43 1st vertical bending mode shapes of the damaged and undamaged structures (40% stiffness reduction of the bottom brace)

With 40% stiffness reduction of the bottom brace, there is a small difference along line 5 between the damaged and undamaged structures and the other curves are almost overlapped. This small mismatch seems not to be sufficient to readily identify the damage location. The corresponding 1st derivative curves along the eight lines with 10%, 20% and 40% reduction in the stiffness of the bottom brace are compared before and after damage and the results of 40% are plotted in figure 3-44.

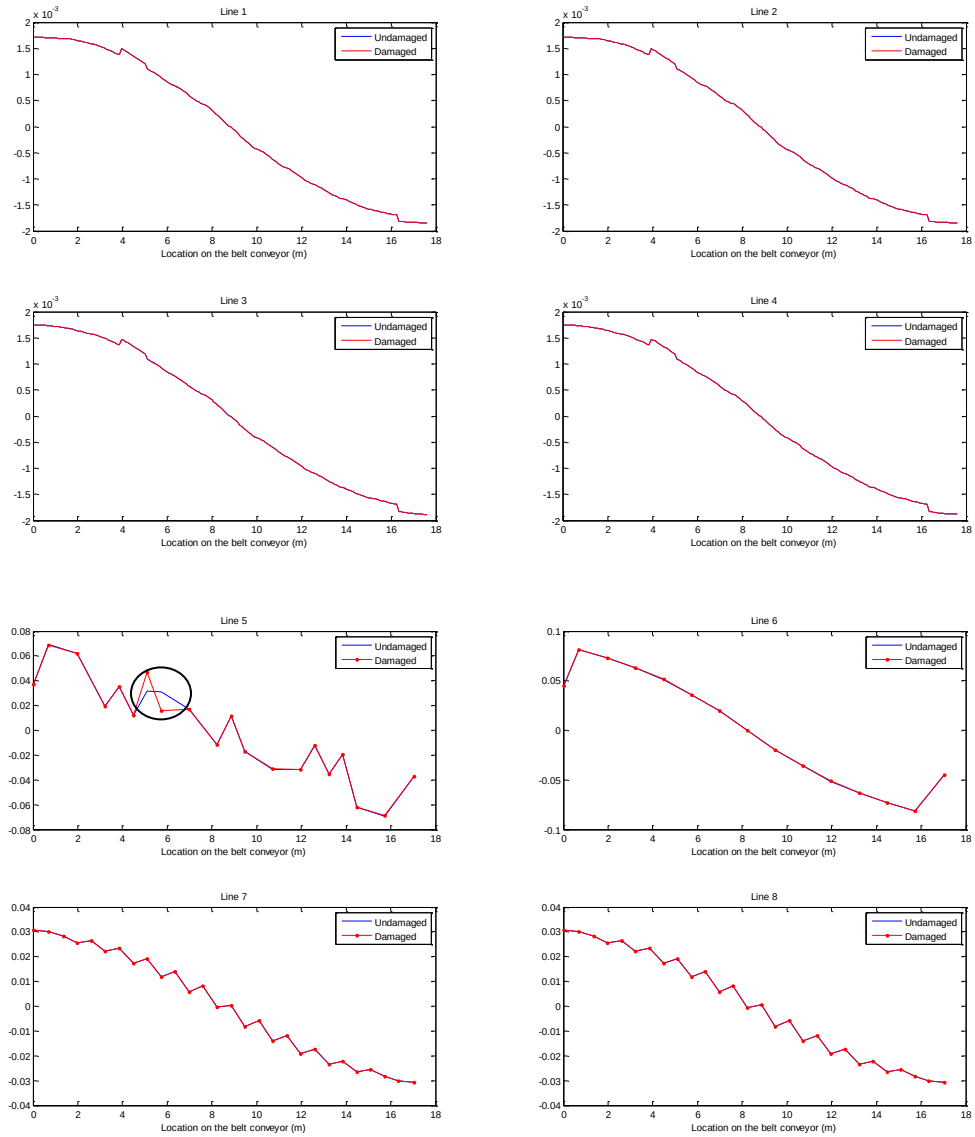

Figure 3-44 1st derivatives of the 1st vertical bending mode shapes of the damaged and undamaged structures (40% stiffness reduction of the bottom brace)

As shown in the above figure, exactly at the same location as the damaged member along line 5, there is an apparent mismatch between two carves and along the other lines, the two curves are almost overlapped. The corresponding 2nd derivative curves along the eight lines with 10%, 20% and 40% reduction in the stiffness of the bottom brace are compared before and after damage and the results of 40% are shown in figure 3-45.

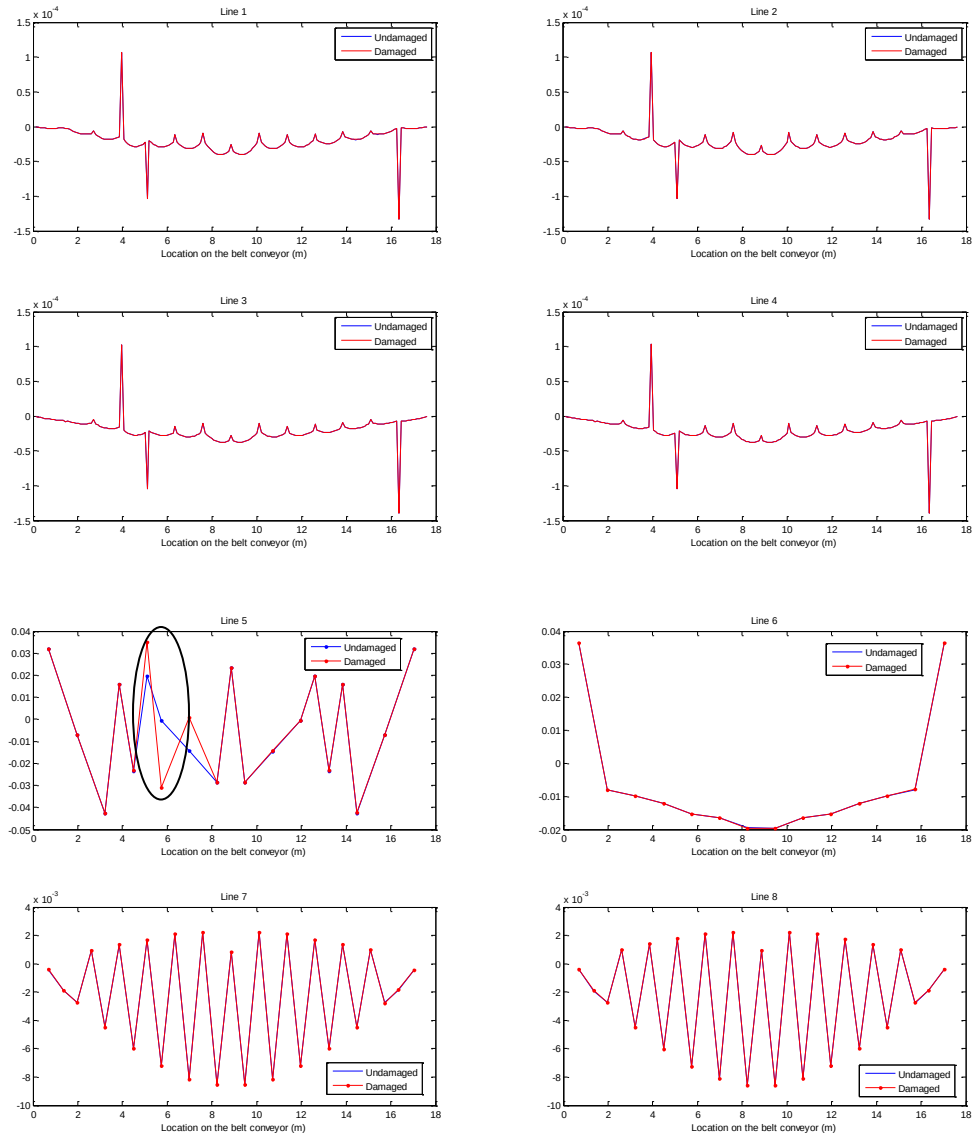

Figure 3-45 2nd derivatives of the 1st vertical bending mode shapes of the damaged and undamaged structures (40% stiffness reduction of the bottom brace)

A significant mismatch only happened at the same location as the damaged brace along line 5.

The main conclusions of these analyses for 10%, 20% and 40% stiffness reduction of the bottom brace, which corresponds to the 1st vertical bending mode, are that the damaged bottom or top braces are not be identified by comparison of the mode shapes when the damage is not severe. However, even with high damage severity, i.e. 40% reduction in the stiffness, damaged braces cannot be readily detected. Using the 1st and especially 2nd derivatives of the mode shape, damaged bottom or top braces can be readily identified so long as the severity of damage is not small. However, damaged braces with relatively small damage severity are hardly detected, i.e. 10% reduction in stiffness, using the 2nd derivative of the 1st vertical bending mode shape.

These conclusions can be expressed by the difference rate. Figures 3-46, 3-47 and 3-48 show the difference rate for the two curves of the damaged and undamaged structures with 10%, 20% and 40% stiffness reduction of the bottom brace respectively. Note that the results are for the 1st vertical bending mode.

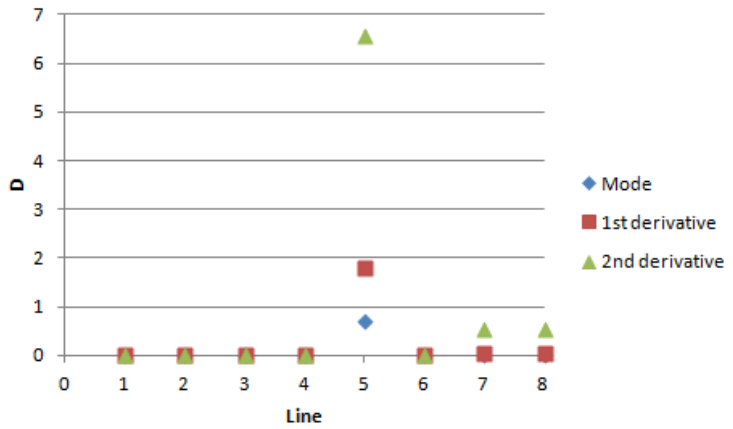

Figure 3-46 Difference rate of the eight lines for 10% stiffness reduction of the bottom brace

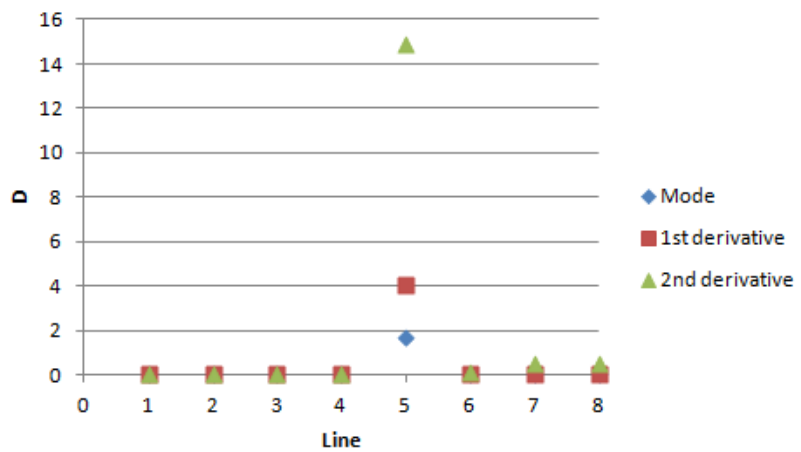

Figure 3-47 Difference rate of the eight lines for 20% stiffness reduction of the bottom brace

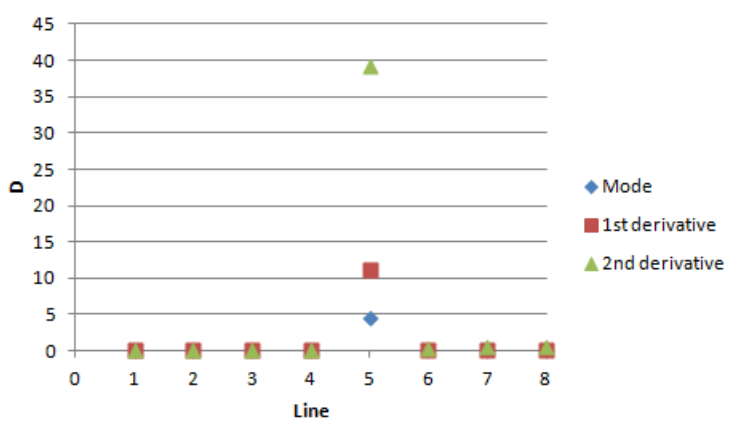

Figure 3-48 Difference rate of the eight lines for 40% stiffness reduction of the bottom brace

3.3.2.4 Mode shape sensitivity of the 1st lateral bending mode of the belt conveyor with respect to stiffness changes of the bottom and top braces

Similar analysis as carried out for the 1st vertical bending mode is performed for the 1st lateral bending mode. The MAC values between the 1st lateral bending mode shape vectors of the undamaged and damaged structures along the different lines for 10%, 20% and 40% stiffness reduction of the bottom brace are shown in table 3-5.

Table 3-5 MAC values between the 1st lateral bending mode shape vectors of the undamaged and damaged structures (bottom brace)

Stiffness reduction	Line 1	Line 2	Line 3	Line 4	Line 5	Line 6	Line 7	Line 8
10%	0.9999872	0.9999858	0.9999979	0.9999979	0.9999672	0.9999979	0.9999912	0.9999881
20%	0.9999360	0.9999294	0.9999898	0.9999898	0.9998292	0.9999895	0.9999561	0.9999414
40%	0.9995647	0.9995226	0.9999326	0.9999326	0.9986068	0.9999303	0.9997037	0.9996085

The MAC has been calculated up to the seventh decimal digit. Even though the MAC values along line 5, where the damaged member is placed, are smaller than they are along the other lines, it is still close to 1. Therefore, by using this method, even presence of damage cannot be identified.

As another method, the 1st normalized lateral mode shape and its 1st and 2nd derivatives along the eight lines, shown in figure 3-30, are compared in the damaged and undamaged structures. The 1st lateral bending mode shapes along the eight lines for the undamaged and damaged structures with 10%, 20% and 40% stiffness reduction of the bottom brace are compared before and after damage and the results of 40% are shown in figure 3-49.

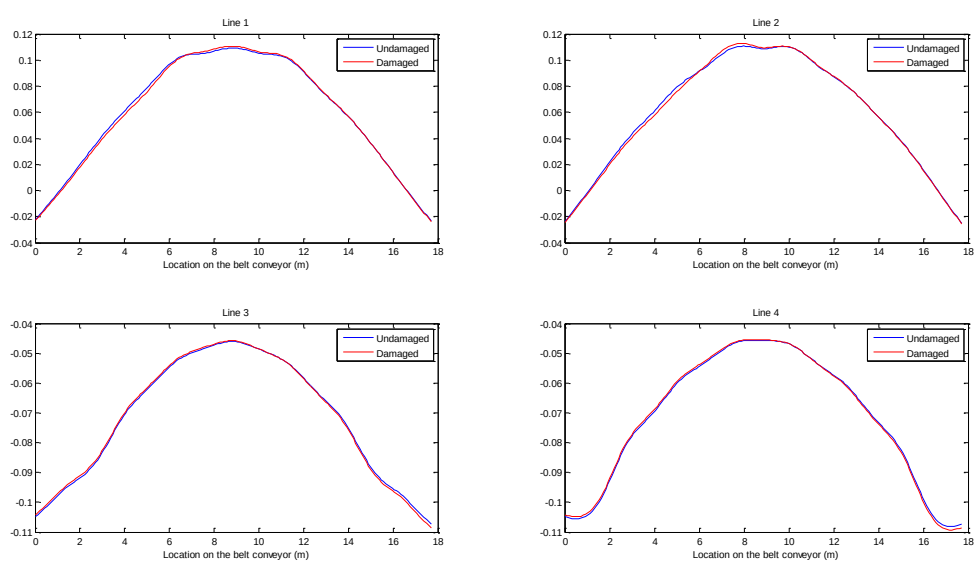

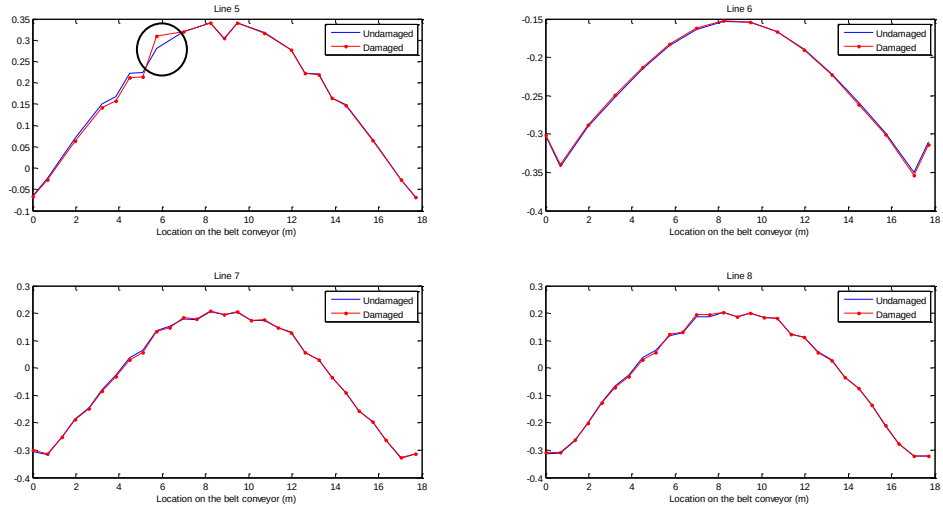

Figure 3-49 1st lateral bending mode shapes of the damaged and undamaged structures (40% stiffness reduction of the bottom brace)

As shown, the two curves are almost overlapped along all lines except line 5 at the same location as the damaged member. Therefore, the damage location is correctly identified. The corresponding 1st derivatives along the eight lines with 10%, 20% and 40% stiffness reduction of the bottom brace are compared before and after damage and the results of 40% are shown in figure 3-50.

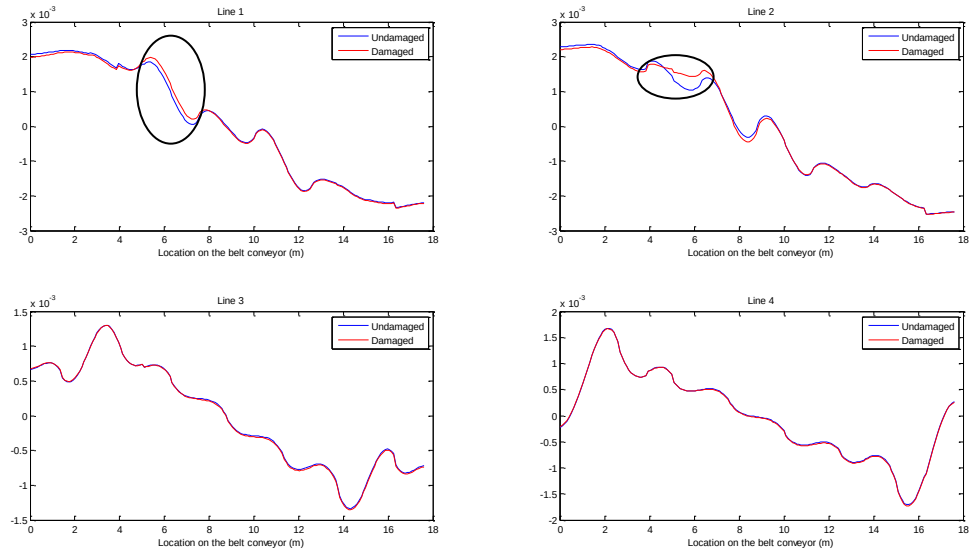

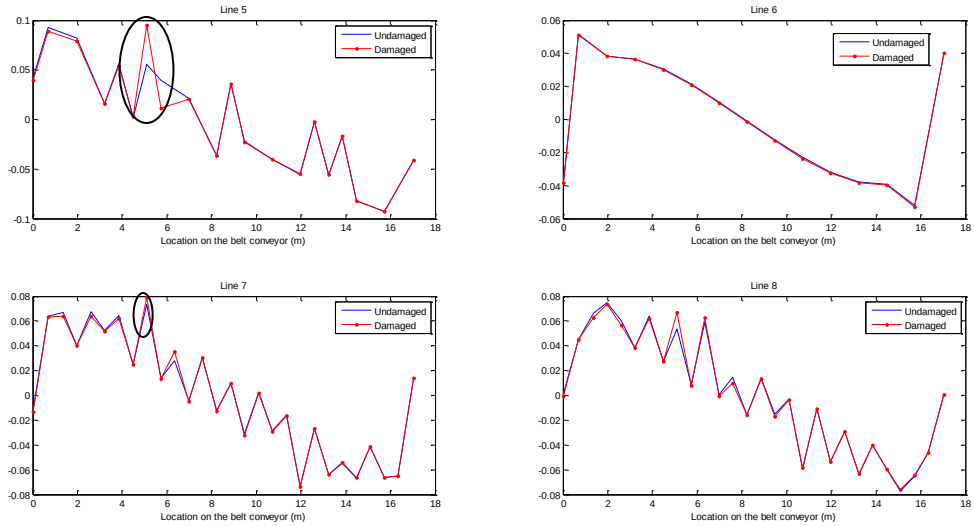

Figure 3-50 1st derivatives of the 1st lateral bending mode shapes of the damaged and undamaged structures (40% stiffness reduction of the bottom brace)

In the above figure, the two curves are not overlapped at the damage location along line 5 and at the same area as the damaged member along line 2. Moreover, there are a little difference at the same area as the damaged member along line 1 and 7. Carefully looking at the above figure shows that along some lines, i.e. line 1, 2, 5, 7 and 8, there are several other mismatches which are not at the same area as the damaged member. The corresponding 2nd derivatives along the eight lines with 10%, 20% and 40% reduction in the stiffness of the bottom brace are compared before and after damage and the results of 40% are shown in figure 3-51.

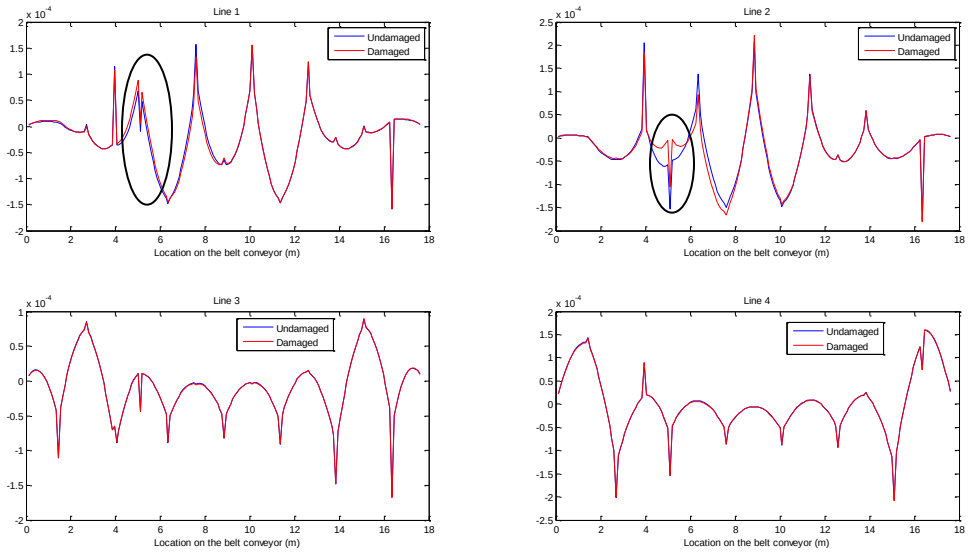

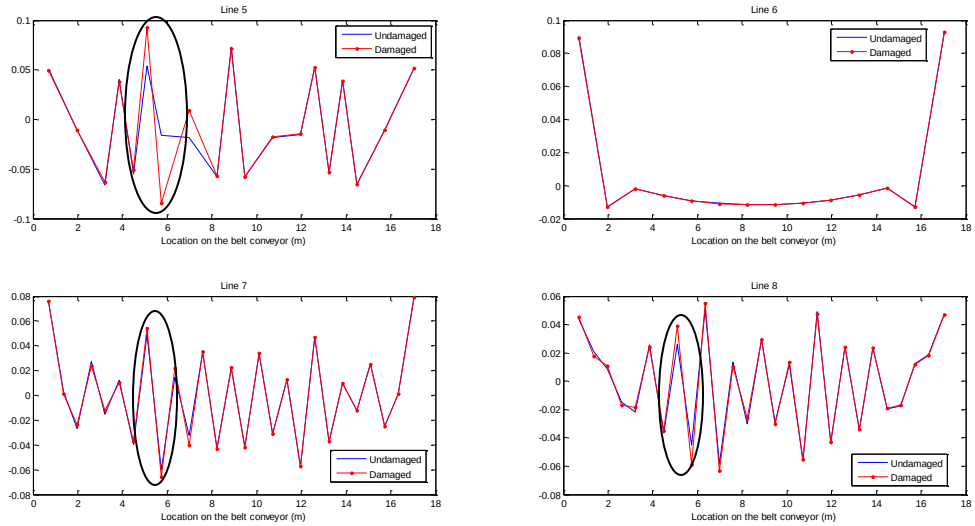

Figure 3-51 2nd derivatives of the 1st lateral bending mode shapes of the damaged and undamaged structures (40% stiffness reduction of the bottom brace)

There are remarkable differences at the same location as the damaged member along line 5 and at the same area as the damaged member along line 2. Moreover, a small difference is appeared at the same area as the damaged member along line 1, 7 and 8. Carefully looking at the above figure shows that along some lines, i.e. line 1, 2 and 8, there are some other mismatches which are not exactly at the same area as the damaged brace.

The main conclusions of these analyses for 10%, 20% and 40% stiffness reduction of the bottom brace, which corresponds to the 1st lateral bending mode, are that damaged bottom or top braces are not be identified by comparison of the mode shapes when the damage severity is small. But with high severity of damage, i.e. 40% stiffness reduction, the location of damaged braces can be detected. Using the 1st and especially 2nd derivatives of the 1st lateral bending mode, the effects of damage only reflect along line 5 at the same location as the damaged member and line 2 at the same area as the damaged member as long as the damage is not severe. For severe damage, i.e. 40% reduction in the stiffness, using the 1st and 2nd derivatives of the 1st lateral bending mode, although the effects of damage reflect at the same location as the damaged member along line 5 and the same area as the damaged member along line 2, but they also reflect to some other area along these two lines as well as some other lines and makes it difficult to identify the damage member.

These conclusions can be expressed by the difference rate. Figures 3-52, 3-53 and 3-54 show the difference rate for the two curves of the damaged and undamaged structures with 10%, 20% and 40% of the stiffness reduction of the bottom brace respectively. Note that the results are for the 1st lateral bending mode.

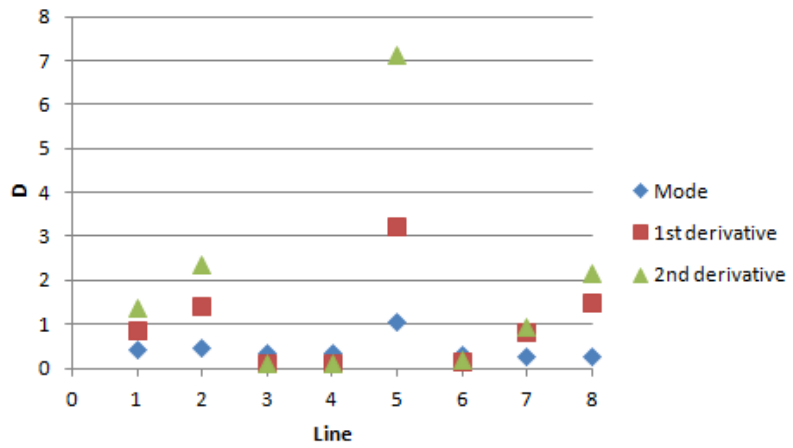

Figure 3-52 Difference rate of the eight lines for 10% stiffness reduction of the bottom brace

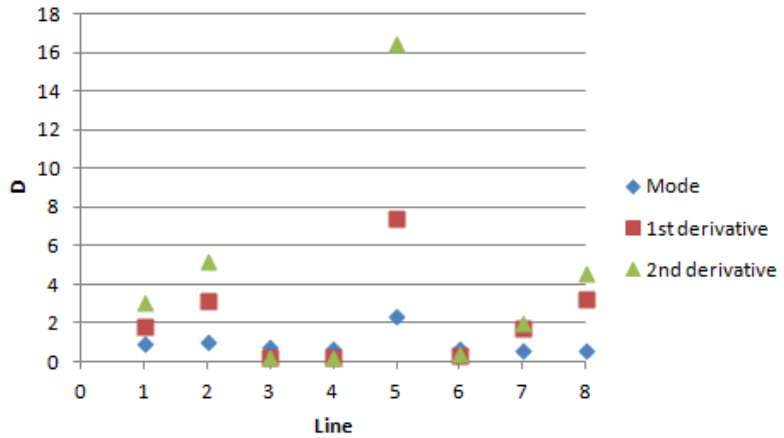

Figure 3-53 Difference rate of the eight lines for 20% stiffness reduction of the bottom brace

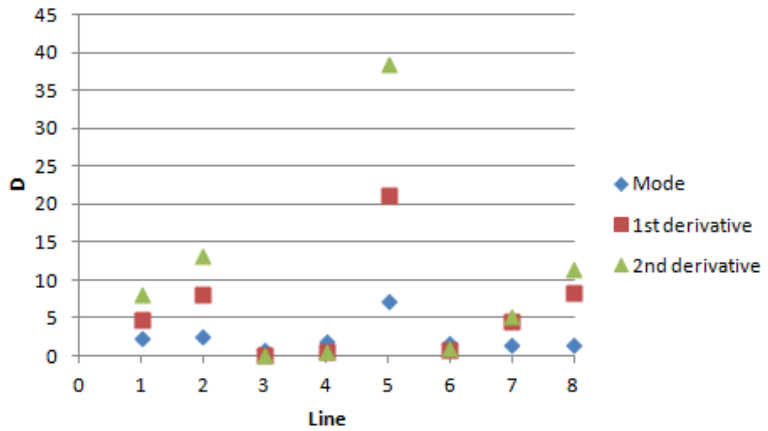

Figure 3-54 Difference rate of the eight lines for 40% stiffness reduction of the bottom brace

Comparing the results of the 1st lateral bending and 1st vertical bending modes shows that the 1st lateral bending mode shape and its 1st and 2nd derivatives are more sensitive to damage on bottom and top braces than the 1st vertical bending mode shape and its 1st and 2nd derivatives, however, as already described,

damaged bottom and top braces are more accurately identified using the derivatives of the 1st vertical bending modes.

3.3.2.5 Mode shape sensitivity of the 1st vertical bending mode of the belt conveyor with respect to stiffness changes of the lateral members

In order to examine the sensitivity of the 1st vertical bending mode with respect to damage on the lateral members, the young's modulus of a lateral member shown in figure 3-15 reduces by 10%, 20% and 40%. The MAC values between the 1st vertical bending mode shape vectors of the undamaged and damaged structures along the different lines for 10%, 20% and 40% stiffness reduction of the lateral member are shown in table 3-6.

Table 3-6 MAC values between the 1st vertical bending mode shape vectors of the undamaged and damaged structures (lateral member)

Stiffness reduction	Line 1	Line 2	Line 3	Line 4	Line 5	Line 6	Line 7	Line 8
10%	1	1	1	1	0.9999995	1	1	1
20%	1	1	1	1	0.9999973	1	1	1
40%	1	1	1	1	0.9999807	1	1	1

The MAC has been calculated up to the seventh decimal digit. Even though the MAC values along line 5, where the damaged member is placed, do not equal to 1 but it is still close to 1. Therefore, by using this method, even presence of damage cannot be identified.

As another method, the 1st normalized vertical mode shape and its 1st and 2nd derivatives along the eight lines, shown in figure 3-30, are compared in the damaged and undamaged structures. The 1st vertical bending mode shapes along the eight lines for the undamaged and damaged structures with 10%, 20% and 40% stiffness reduction of the lateral member are compared before and after damage and the results of 40% are shown in figure 3-55.

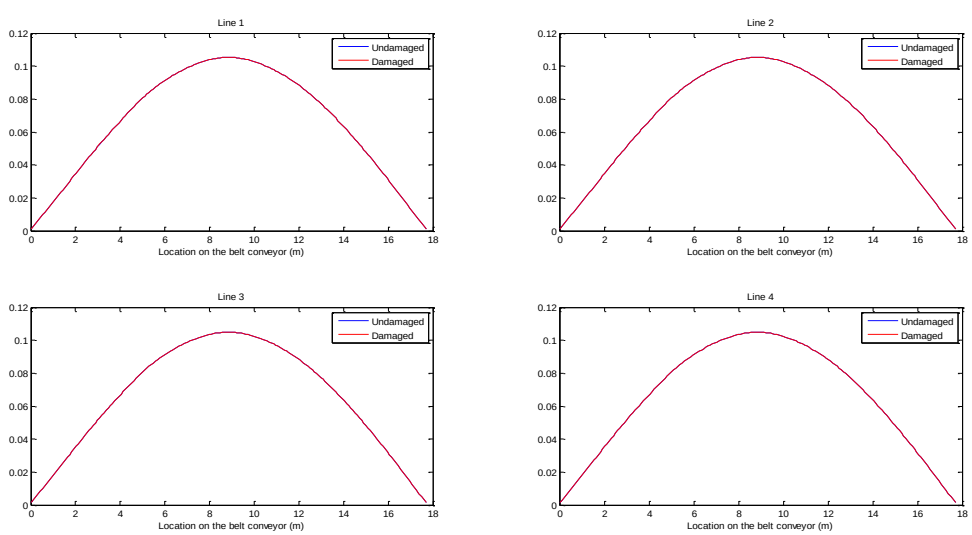

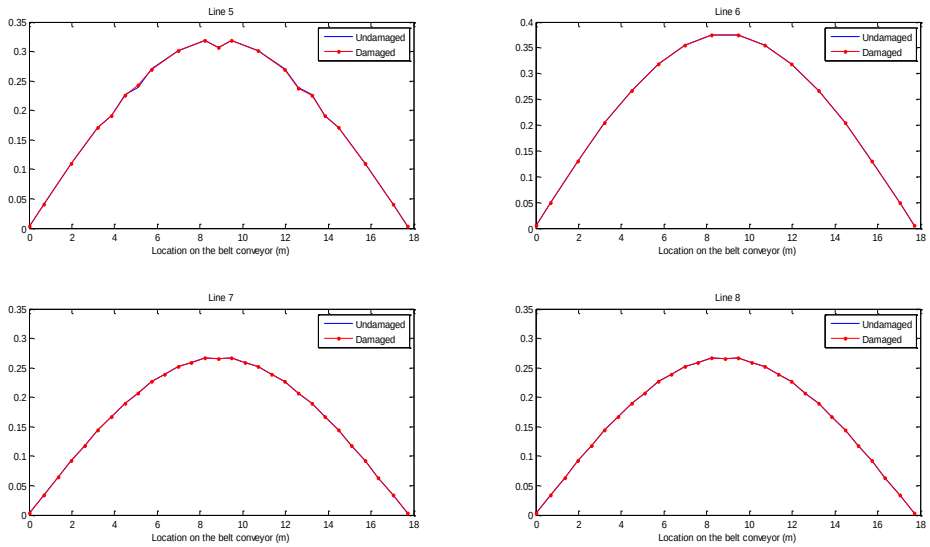

Figure 3-55 1st vertical bending mode shapes of the damaged and undamaged structures (40% stiffness reduction of the lateral member)

As shown, even with 40% stiffness reduction of the lateral member, the damaged member cannot be identified since the two curves along all lines are almost overlapped. The corresponding 1st derivative curves along the eight lines with 10%, 20% and 40% reduction in the stiffness of the lateral member are compared before and after damage and the results of 40% are shown in figure 3-56.

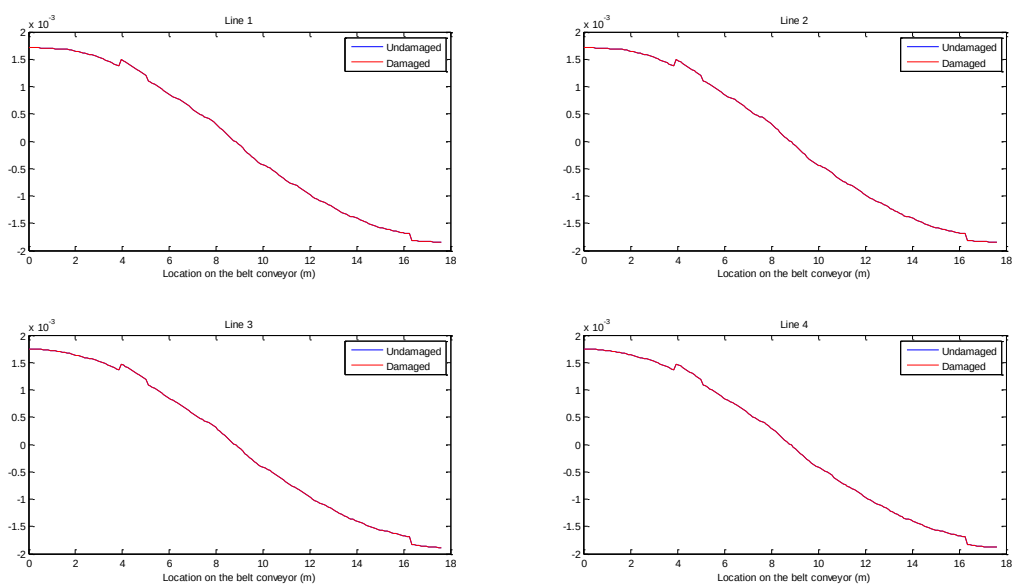

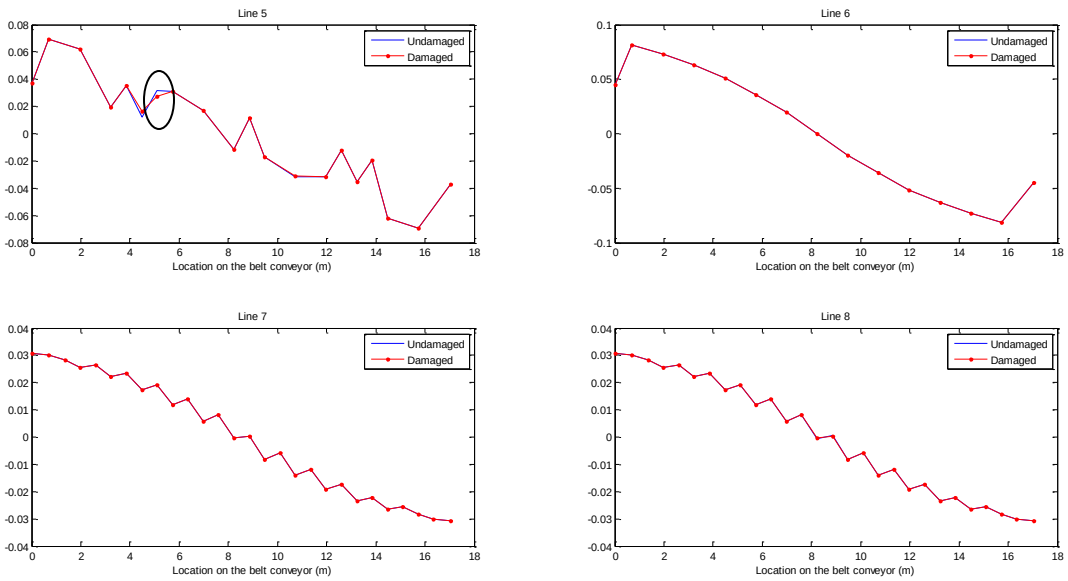

Figure 3-56 1st derivatives of the 1st vertical bending mode shapes of the damaged and undamaged structures (40% stiffness reduction of the lateral member)

The two curves along line 5 at the same location as the damaged member are mismatched. It means that the damaged member is correctly identified since along the other line there is no difference between the two curves corresponding to the damaged and undamaged structures. The corresponding 2nd derivative curves along the eight lines with 10%, 20% and 40% stiffness reduction of the lateral member are compared before and after damage and the results of 40% are plotted in figure 3-57.

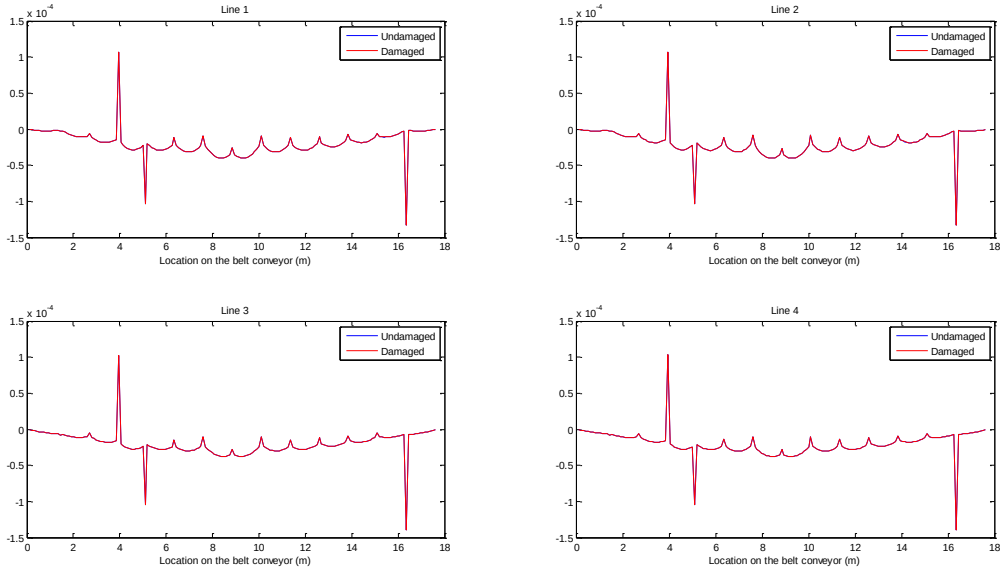

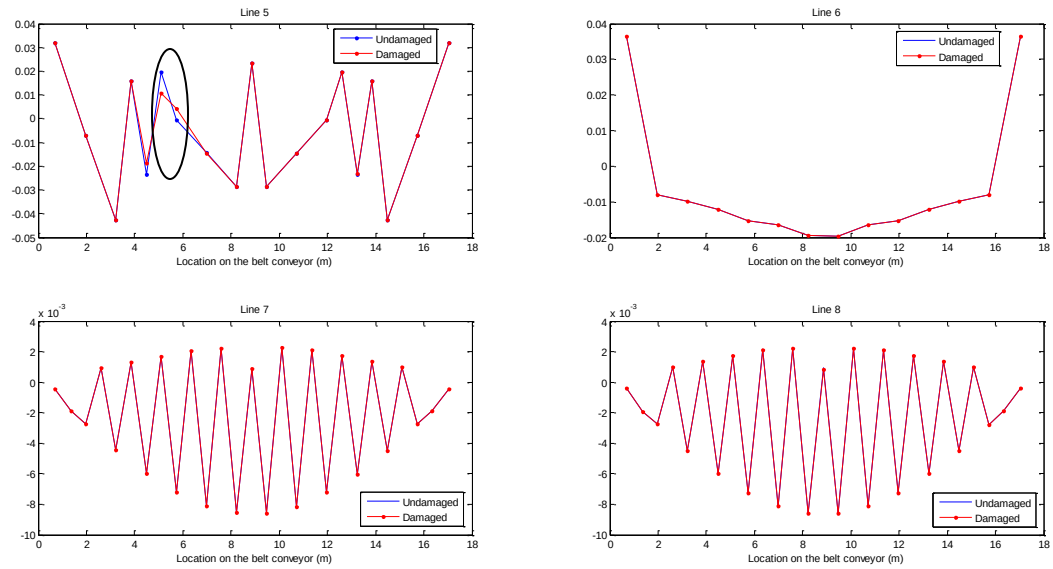

Figure 3-57 2nd derivatives of the 1st vertical bending mode shapes of the damaged and undamaged structures (40% stiffness reduction of the lateral brace)

The damage location is correctly identified since the only difference between the two curves is along line 5 at the same location as the damaged member.

The main conclusions of these analyses for 10%, 20% and 40% stiffness reduction of the lateral member, which corresponds to the 1st vertical bending mode, are that the damaged lateral are not identified by comparing the mode shapes. Using the 1st and especially 2nd derivatives of the mode shape, damaged lateral members can be identified provided the damage is severe, i.e. for 40% stiffness reduction. Damaged lateral members are hardly identified with even 20% reduction in the stiffness, using the 2nd derivative of the 1st vertical bending mode shape.

These conclusions can be expressed by the difference rate. Figure 3-58, 3-59 and 3-60 show the difference rate for the two curves of the damaged and undamaged structures with 10%, 20% and 40% of the stiffness reduction of the lateral member respectively. Note that the results are for the 1st vertical bending mode.

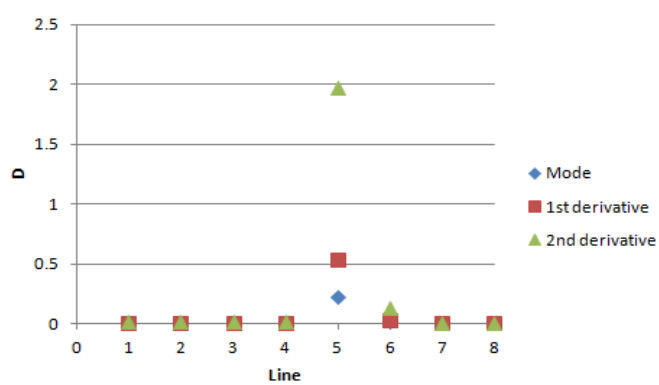

Figure 3-58 Difference rate of the eight lines for 10% stiffness reduction of the lateral member

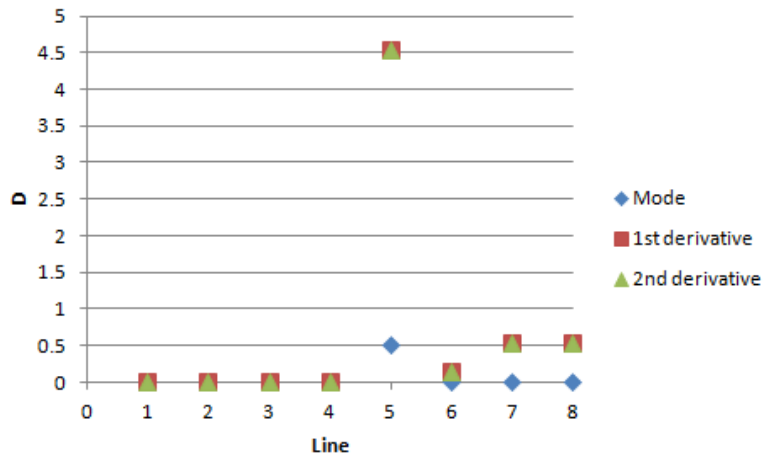

Figure 3-59 Difference rate of the eight lines for 20% stiffness reduction of the lateral member

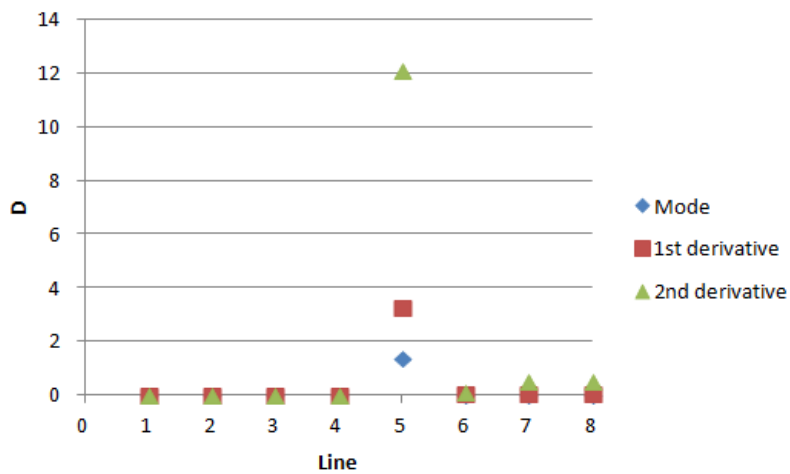

Figure 3-60 Difference rate of the eight lines for 40% stiffness reduction of the lateral member

3.3.2.6 Mode shape sensitivity of the 1st lateral bending mode of the belt conveyor with respect to stiffness changes of the lateral members

Similar analysis as performed for the 1st vertical bending mode is carried out for the 1st lateral bending mode. The MAC values between the 1st lateral bending mode shape vectors of the undamaged and damaged structures along the different lines for 10%, 20% and 40% stiffness reduction of the lateral member are shown in table 3-7.

Table 3-7 MAC values between the 1st lateral bending mode shape vectors of the undamaged and damaged structures (lateral member)

Stiffness reduction	Line 1	Line 2	Line 3	Line 4	Line 5	Line 6	Line 7	Line 8
10%	1	1	1	1	1	1	1	1
20%	1	1	1	1	1	1	1	0.9999999
40%	1	0.9999997	1	1	0.9999999	1	1	0.9999995

The MAC has been calculated up to the seventh decimal digit. As shown, the MAC values are almost equal to 1 even along line 5 where the damaged lateral member is placed. Therefore, using this method, even presence of damage cannot be identified.

As another method, the 1st normalized lateral mode shape and its 1st and 2nd derivatives along the eight lines, shown in figure 3-30, are compared in the damaged and undamaged structures. The shape of the 1st lateral bending mode along the eight lines for the undamaged and damaged structures with 10%, 20% and 40% reduction in the stiffness of the lateral member are compared before and after damage and the results of 40% are shown in figure 3-61.

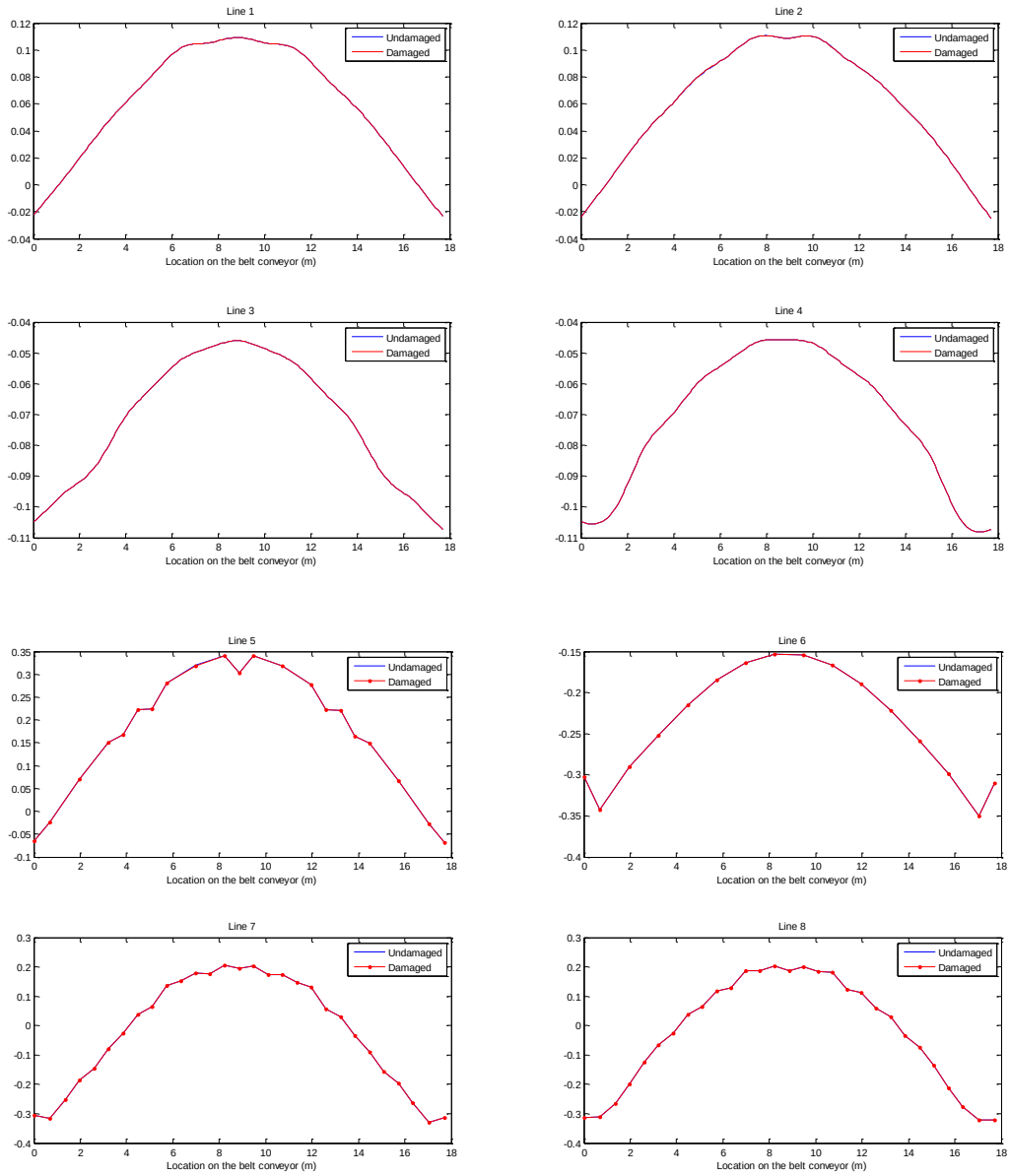

Figure 3-61 1st lateral bending mode shapes of the damaged and undamaged structures (40% stiffness reduction of the lateral member)

The two curves corresponding to the damaged and undamaged structure are overlapped along the eight lines even for 40% stiffness reduction of the lateral member. The corresponding 1st derivative curves along the eight lines with 10%, 20% and 40% stiffness reduction of the lateral member are compared before and after damage and the results of 40% are shown in figure 3-62.

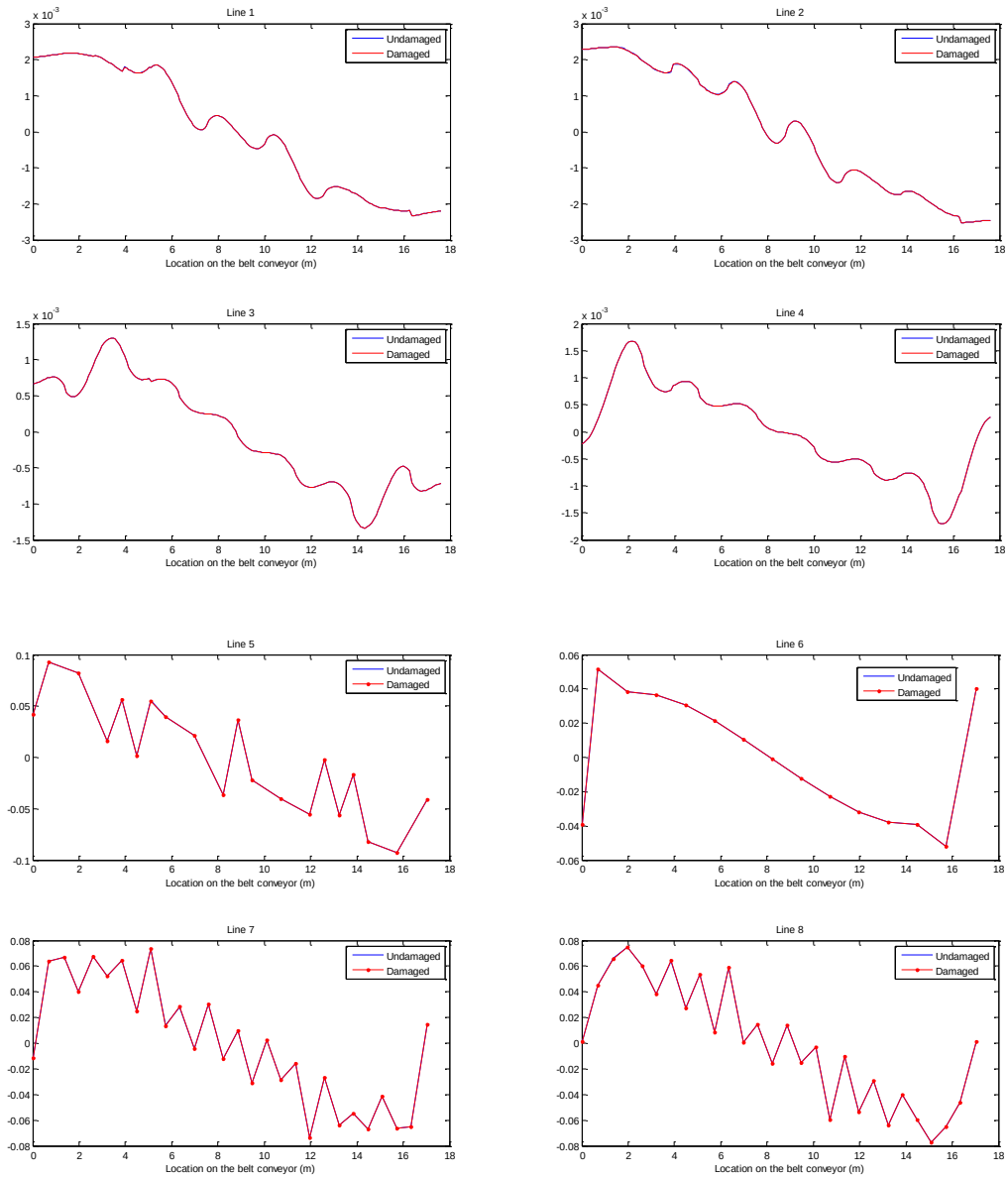

Figure 3-62 1st derivatives of the 1st lateral bending mode shapes of the damaged and undamaged structures (40% stiffness reduction of the lateral member)

As shown in the above figure, the damaged member cannot be identified since the two curves along all lines are overlapped. The corresponding 2nd derivative curves along the eight lines with 10%, 20% and 40% reduction in the stiffness of the lateral member are compared before and after damage and the results of 40% are shown in figure 3-63.

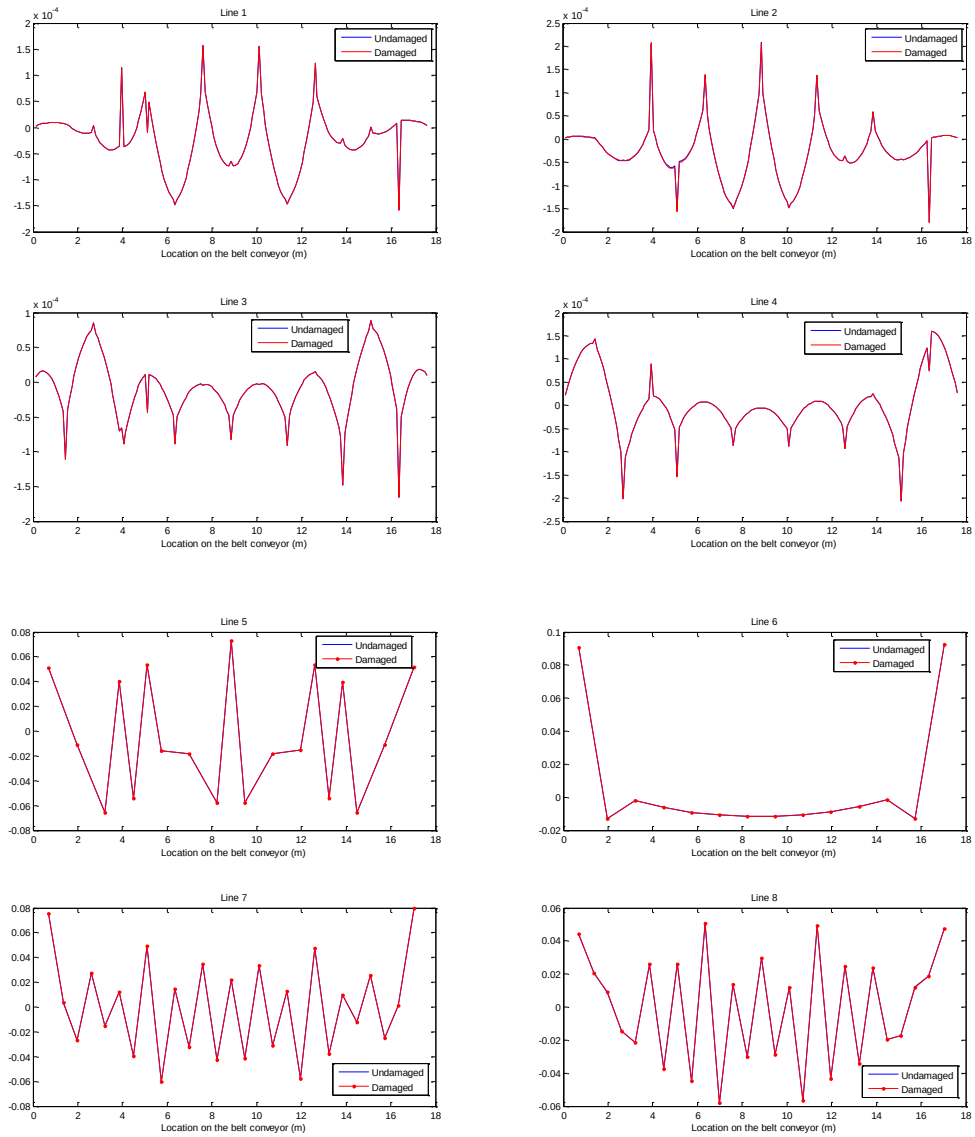

Figure 3-63 2nd derivatives of the 1st lateral bending mode shapes of the damaged and undamaged structures (40% stiffness reduction of the lateral member)

There is almost no difference between the two curves along all lines even line 5 where the damaged member is placed. Therefore, even with 40% stiffness reduction of the lateral member, the damage location cannot be identified.

The main conclusions of these analyses for 10%, 20% and 40% stiffness reduction of the lateral member, which corresponds to the 1st lateral bending mode, are that damaged lateral members are not identified by comparison of the mode shapes and their 1st and 2nd derivatives even with 40% stiffness reduction of lateral members which is relatively severe.

These conclusions can be expressed by the difference rate. Figure 3-64, 3-65 and 3-66 show the difference rate for the two curves of the damaged and undamaged structures for 10%, 20% and 40% stiffness reduction of the lateral member respectively. Note that the result is for the 1st lateral bending mode.

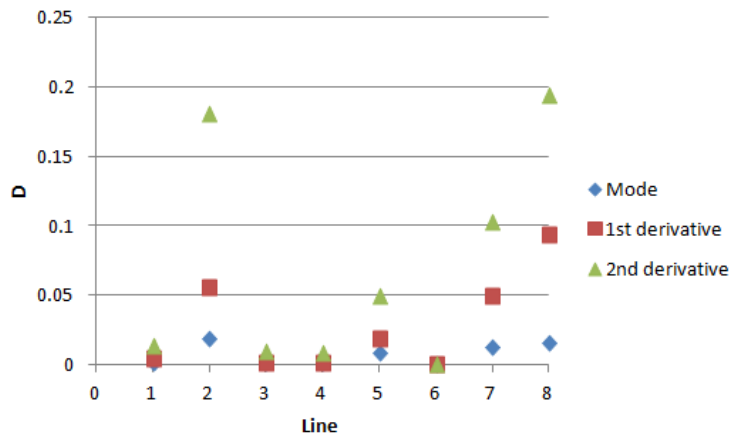

Figure 3-64 Difference rate of the eight lines for 10% stiffness reduction of the lateral member

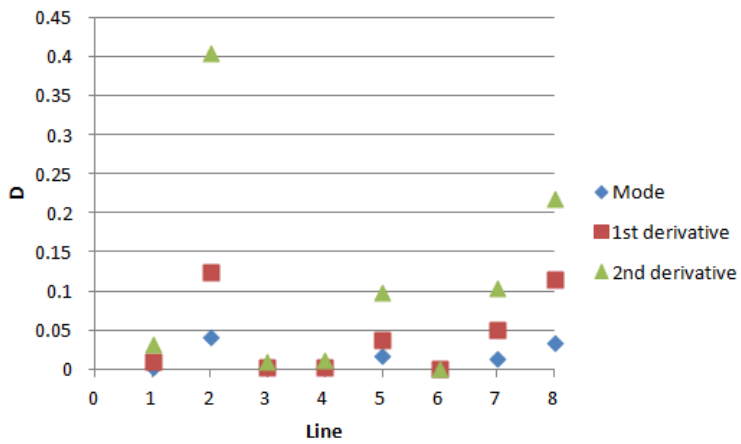

Figure 3-65 Difference rate of the eight lines for 20% stiffness reduction of the lateral member

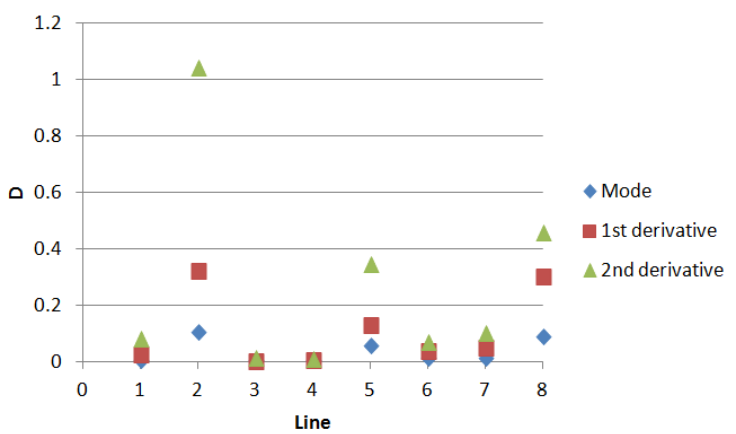

Figure 3-66 Difference rate of the eight lines for 40% stiffness reduction of the lateral member

Comparing the results of the 1st lateral bending and 1st vertical bending modes shows that generally the 1st vertical bending mode shape and especially its 1st and 2nd derivatives are more sensitive to damage on lateral members compared to the 1st lateral bending mode and its 1st and 2nd derivatives, however, even using the 2nd derivative of the 1st vertical bending mode, the location of damaged lateral members cannot be identified when the damage is not severe.

3.3.2.7 Mode shape sensitivity of the 1st vertical bending mode of the belt conveyor with respect to stiffness changes of the vertical members

In order to examine the sensitivity of the 1st vertical bending mode with respect to damage on the vertical members, the young's modulus of a vertical member, shown in figure 3-19, reduces by 10%, 20% and 40%. The MAC values between the 1st vertical bending mode shape vectors of the undamaged and damaged structures along the different lines for 10%, 20% and 40% stiffness reduction of the vertical member are shown in table 3-8.

Table 3-8 MAC values between the 1st vertical bending mode shape vectors of the undamaged and damaged structures (vertical member)

Stiffness reduction	Line 1	Line 2	Line 3	Line 4	Line 5	Line 6	Line 7	Line 8
10%	1	1	1	1	1	1	1	1
20%	0.9999999	1	0.9999999	1	1	1	0.9999999	1
40%	0.9999994	1	0.9999996	1	0.9999998	0.9999999	0.9999995	1

Note that the MAC has been calculated up to the seventh decimal digit. The MAC values along line 7, where the damaged member is placed, are close to 1. Therefore, by using of this method, even presence of damage cannot be identified.

As another approach, the 1st normalized vertical mode shape and its 1st and 2nd derivatives along the eight lines, shown in figure 3-30, are compared in the damaged and undamaged structures. The 1st vertical bending mode shapes along the eight lines for the undamaged and damaged structures with 10%, 20% and 40% reduction in the stiffness of the vertical member are compared before and after damage and the results of 40% are shown in figure 3-67.

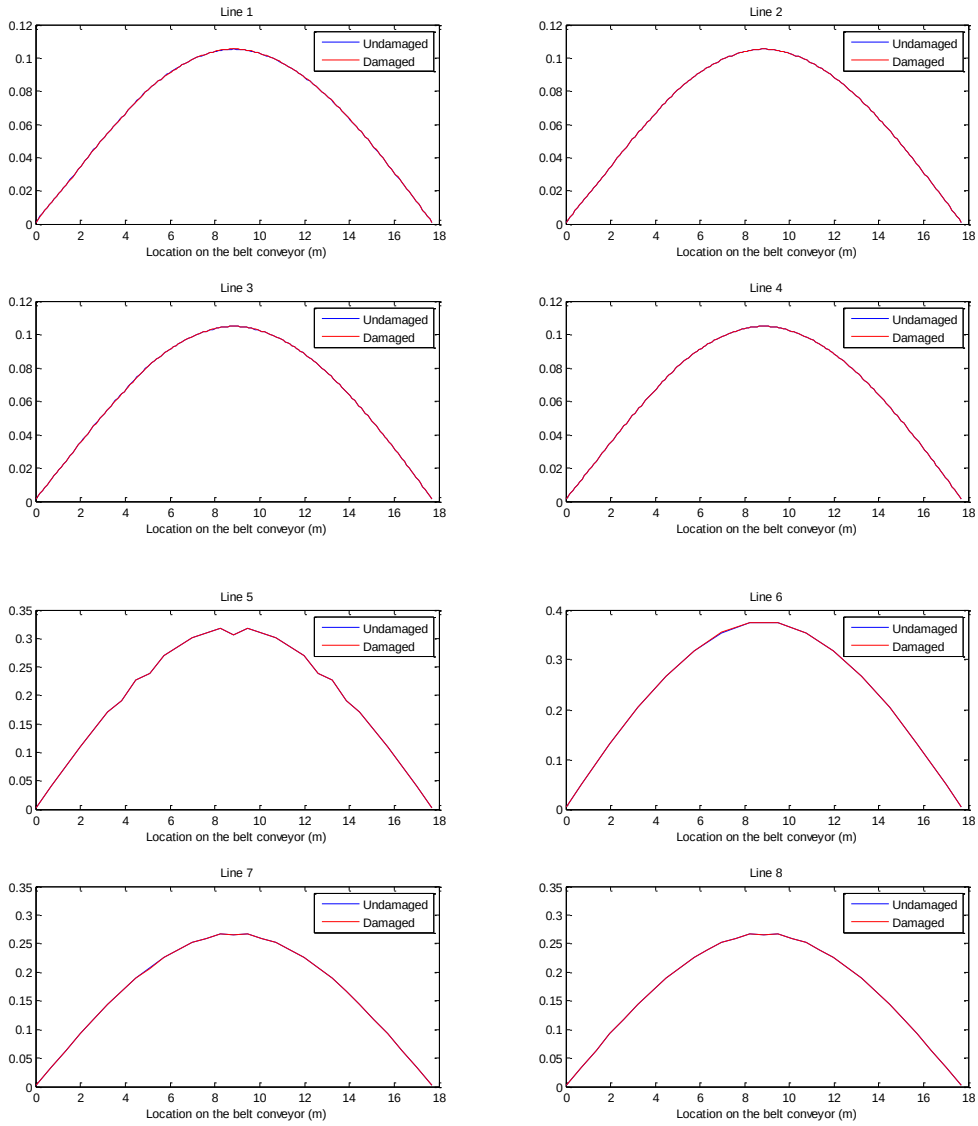

Figure 3-67 1st vertical bending mode shapes of the damaged and undamaged structures (40% stiffness reduction of the vertical member)

The two curves corresponding to the damaged and undamaged structures are overlapped along the eight lines even for 40% stiffness reduction of the vertical member. The corresponding 1st derivative curves along the eight lines with 10%, 20% and 40% stiffness reduction of the vertical member are compared before and after damage and the results of 40% are plotted in figure 3-68.

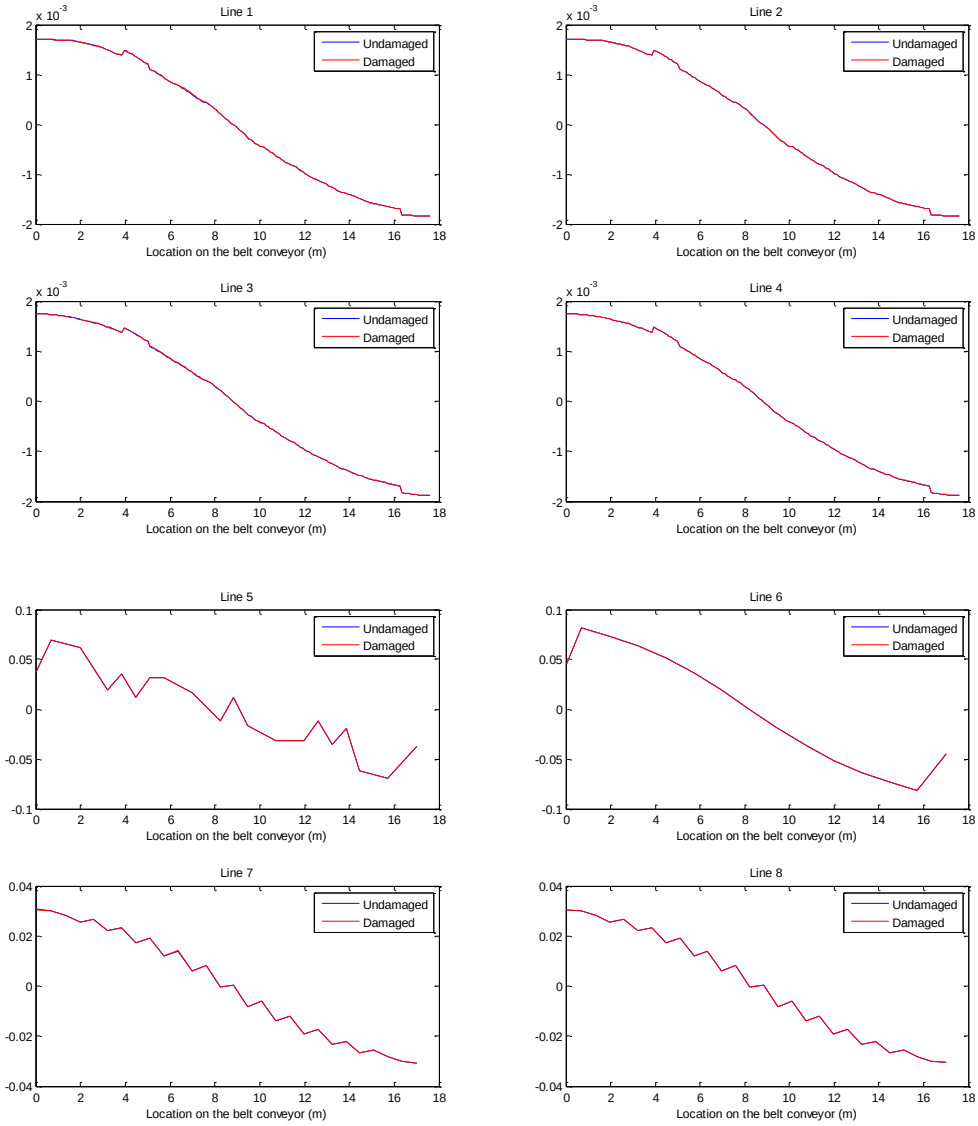

Figure 3-68 1st derivatives of the 1st vertical bending mode shapes of the damaged and undamaged structures (40% stiffness reduction of the vertical member)

It is found that the curves along the eight lines are almost overlapped and the damage location cannot be identified by comparison of these curves. The corresponding 2nd derivative curves along the eight lines with 10%, 20% and 40% stiffness reduction of the vertical member are compared before and after damage and the results of 40% are shown in figure 3-69.

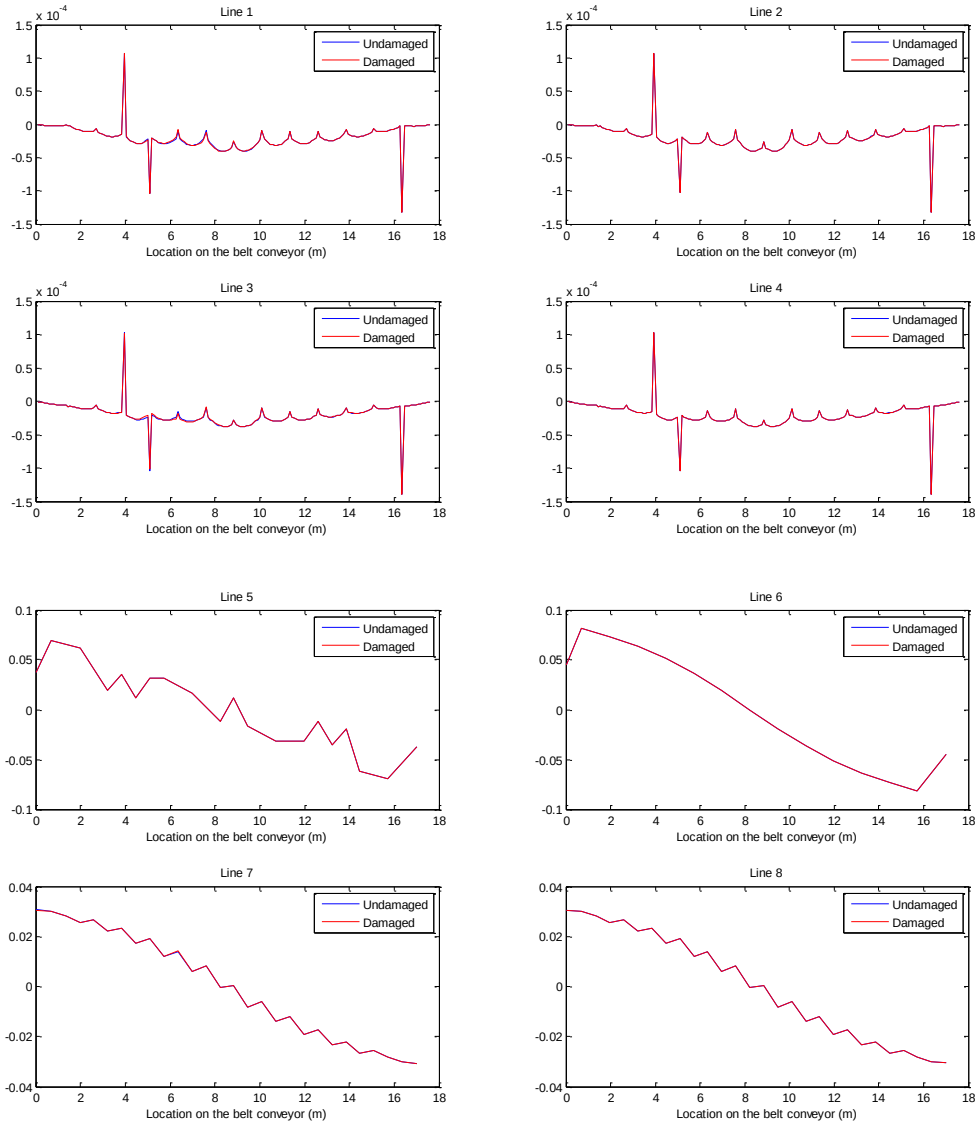

Figure 3-69 2nd derivatives of the 1st vertical bending mode shapes of the damaged and undamaged structures (40% stiffness reduction of the vertical member)

As shown, even using the 2nd derivative, for 40% stiffness reduction of the vertical member, the two curves are almost overlapped along the eight lines and the damaged members cannot be detected.

The main conclusions of these analyses for 10%, 20% and 40% stiffness reduction of the vertical member, which corresponds to the 1st vertical bending mode, are that damaged vertical members are not identified by comparing the mode shape and the corresponding 1st and 2nd derivatives even with high severity reduction, i.e. 40%, in the stiffness of vertical members.

These conclusions can be expressed by the difference rate. Figure 3-70, 3-71 and 3-72 show the difference rate for the two curves of the damaged and undamaged structures with 10%, 20% and 40% of

stiffness reduction of the vertical member respectively. Note that the results are for the 1st vertical bending mode.

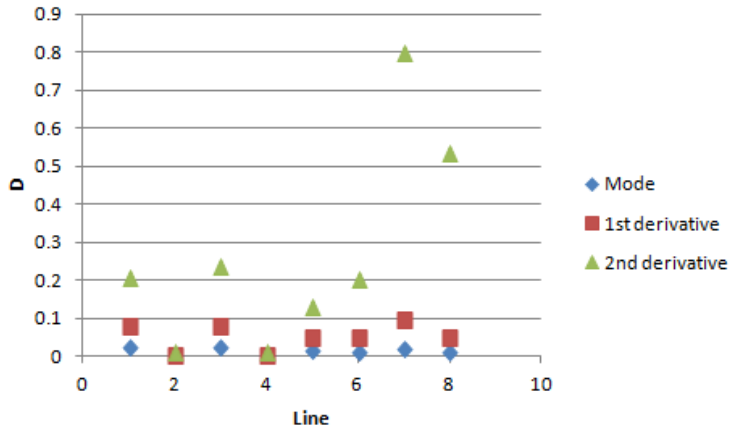

Figure 3-70 Difference rate of the eight lines for 10% stiffness reduction of the vertical member

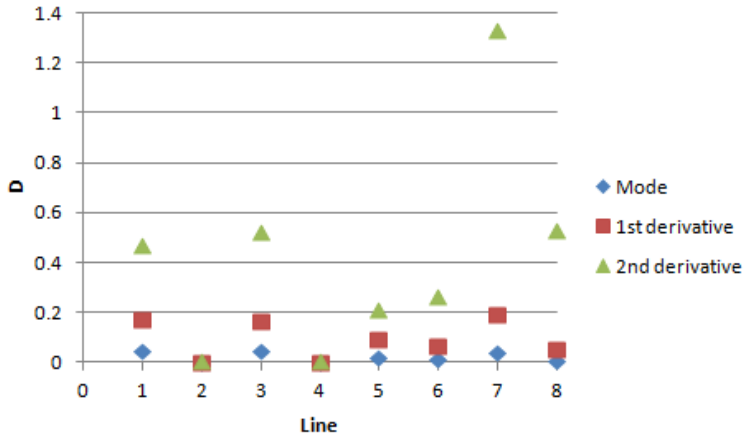

Figure 3-71 Difference rate of the eight lines for 20% stiffness reduction of the vertical member

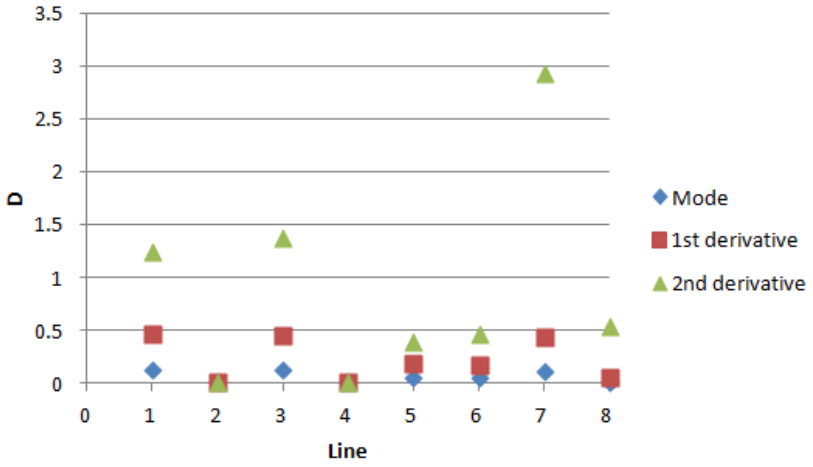

Figure 3-72 Difference rate of the eight lines for 40% stiffness reduction of the vertical member

3.3.2.8 Mode shape sensitivity of the 1st lateral bending mode of the belt conveyor with respect to stiffness changes of the vertical members

Similar analysis as performed for the 1st vertical bending mode is carried out for the 1st lateral bending mode. The MAC values between the 1st lateral bending mode shape vectors of the undamaged and damaged structures along the different lines for 10%, 20% and 40% stiffness reduction of the lateral member are shown in table 3-9.

Table 3-9 MAC values between the 1st lateral bending mode shape vectors of the undamaged and damaged structures (vertical member)

Stiffness reduction	Line 1	Line 2	Line 3	Line 4	Line 5	Line 6	Line 7	Line 8
10%	1	1	1	1	1	1	0.9999999	1
20%	1	1	1	1	1	1	0.9999994	1
40%	0.9999999	0.9999999	0.9999998	0.9999998	0.9999999	0.9999998	0.9999958	0.9999998

The MAC has been calculated up to the seventh decimal digit. Although the MAC values along line 7, where the damaged vertical member is located, is relatively smaller but it is close to 1. Therefore, using this approach, even presence of damage is difficult to be identified.

As another method, the 1st normalized lateral mode shape and its 1st and 2nd derivatives along the eight lines, shown in figure 3-30, are compared in the damaged and undamaged structures. The shape of the 1st lateral bending mode along the eight lines for the undamaged and damaged structures with 10%, 20% and 40% stiffness reduction of the vertical member are compared before and after damage and the results of 40% are plotted in figure 3-73.

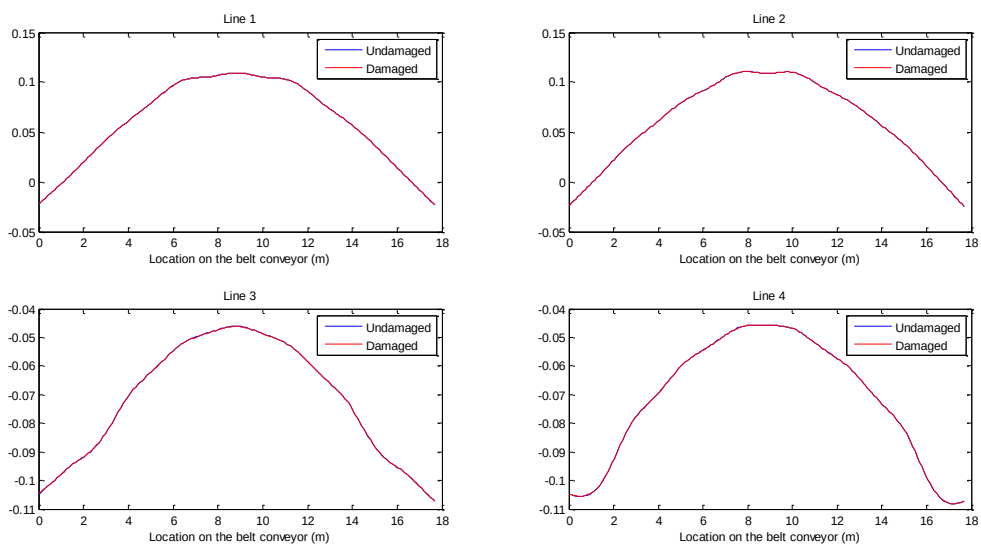

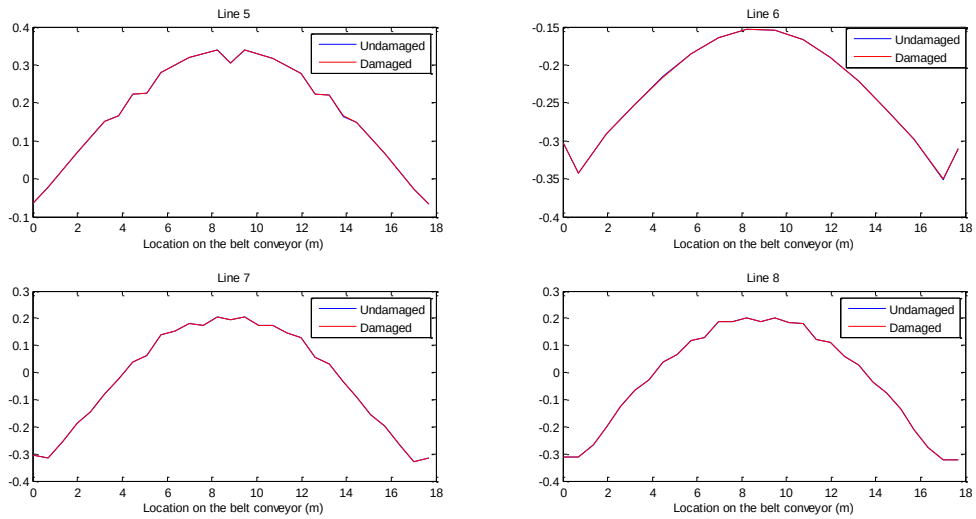

Figure 3-73 1st lateral bending mode shapes of the damaged and undamaged structures (40% stiffness reduction of the vertical member)

The two curves corresponding to the damaged and undamaged structures are overlapped along the eight lines. Therefore, the damaged member cannot be identified even with 40% stiffness reduction of the vertical member. The corresponding 1st derivative curves along the eight lines with 10%, 20% and 40% reduction in the stiffness of the vertical member are compared before and after damage and the results of 40% are shown in figure 3-74.

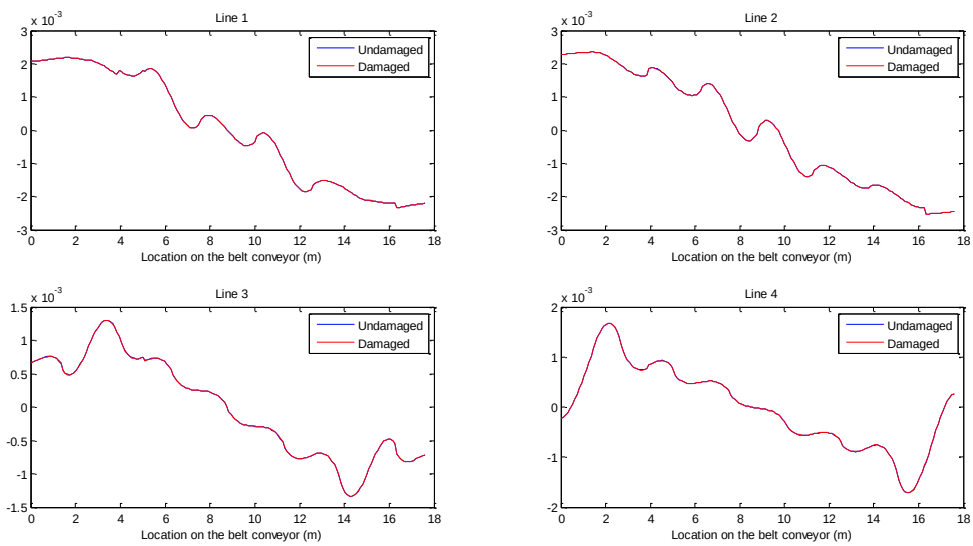

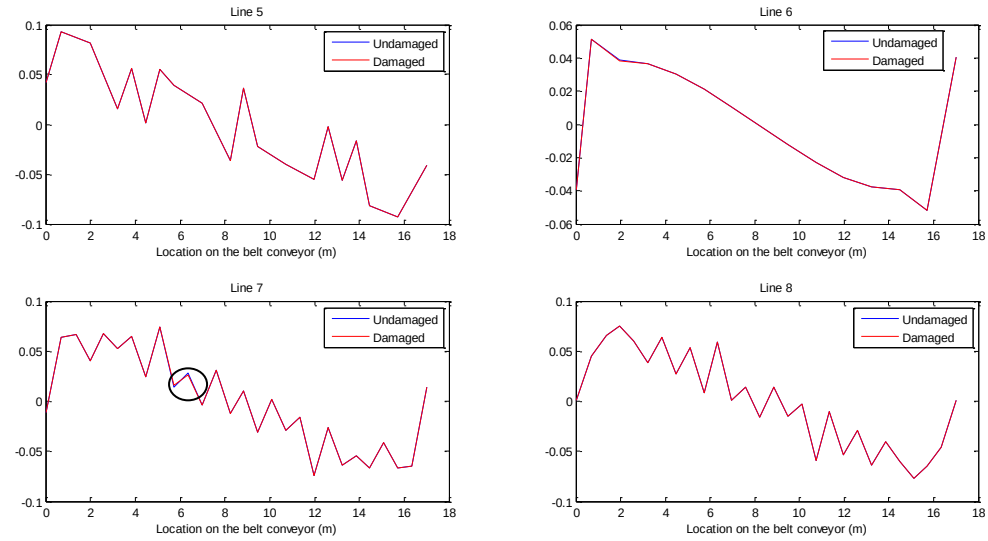

Figure 3-74 1st derivatives of the 1st lateral bending mode shapes of the damaged and undamaged structures (40% stiffness reduction of the vertical member)

With 40% stiffness reduction, the two curves are almost overlapped. However, at the same location as the damaged member along line 7, there is a very small mismatch between two curves is being observed. But with this difference, identification of the damage location is almost impossible. The corresponding 2nd derivative curves along the eight lines with 10%, 20% and 40% stiffness reduction of the vertical member are compared before and after damage and the results of 40% are shown in figure 3-75.

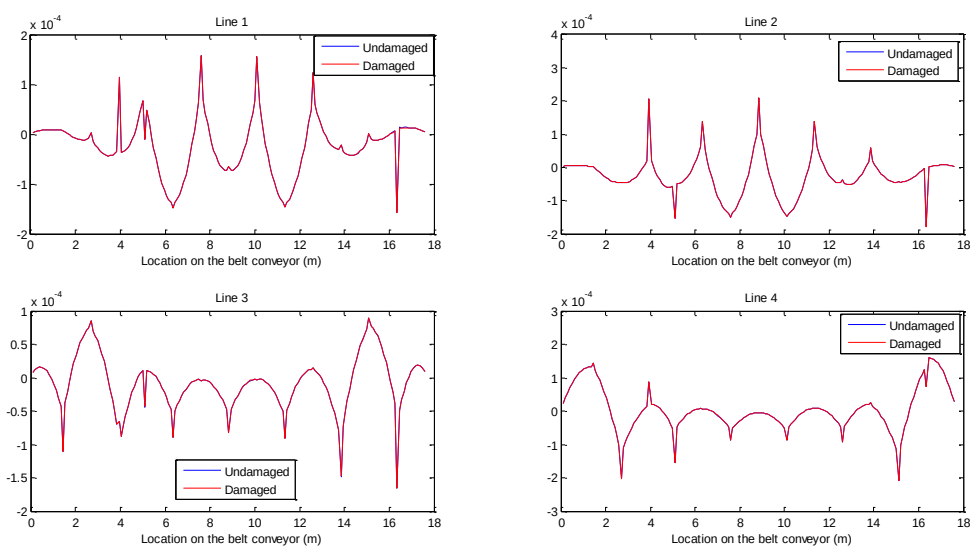

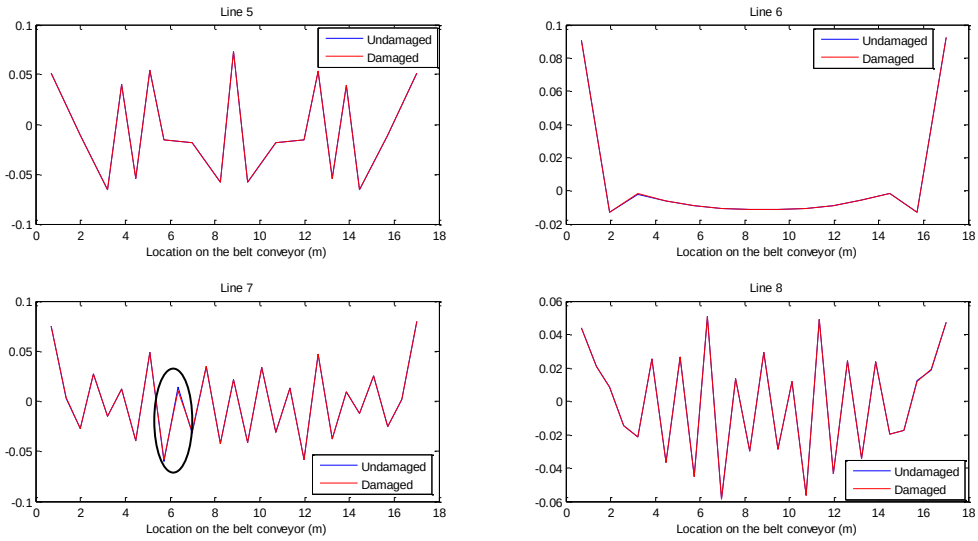

Figure 3-75 2nd derivatives of the 1st lateral bending mode shapes of the damaged and undamaged structures (40% stiffness reduction of the vertical member)

As shown, the only mismatch between two curves is along line 7 at the same location as the damaged vertical member. However, this mismatch is very small to confidently judge about the damage location.

The main conclusions of these analyses for 10%, 20% and 40% stiffness reduction of the vertical member, which corresponds to the 1st lateral bending mode, are that damaged vertical members are not identified by comparison of the 1st lateral mode shape. Using the corresponding 1st and 2nd derivatives of the 1st lateral bending mode shape, damaged vertical members are not identified when the damage is not severe. Even if the damage is severe, i.e. 40%, the damage location is not confidently identified since the mismatch between two curves before and after damage is pretty small.

These conclusions can be expressed by the difference rate. Figure 3-76, 3-77 and 3-78 show the difference rate for the two curves of the damaged and undamaged structures for 10%, 20% and 40% stiffness reduction of the vertical member respectively. Note that the results are for the 1st lateral bending mode.

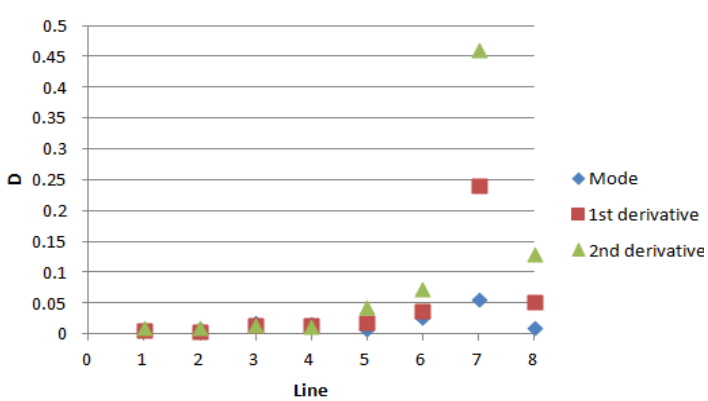

Figure 3-76 Difference rate of the eight lines for 10% stiffness reduction of the vertical member

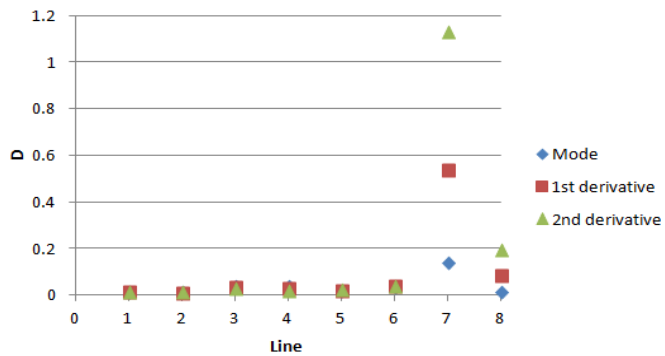

Figure 3-77 Difference rate of the eight lines for 20% stiffness reduction of the vertical member

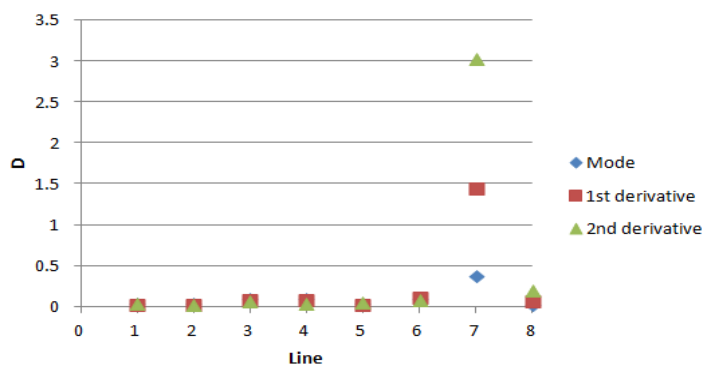

Figure 3-78 Difference rate of the eight lines for 40% stiffness reduction of the vertical member

Comparing the results of the 1st lateral bending and 1st vertical bending modes shows that generally the 1st and 2nd derivatives of the 1st lateral bending mode shape are more sensitive to damage on vertical members compared to the 1st vertical bending mode and its 1st and 2nd derivatives, however, even using the 1st and 2nd derivatives of the 1st lateral bending mode for severe damage on vertical members, damaged vertical members are not confidently identified.

3.3.2.9 Mode shape sensitivity of the 1st vertical bending mode of the belt conveyor with respect to stiffness changes of the side braces

In order to examine the sensitivity of the 1st vertical bending modes with respect to damage on the side braces, the young's modulus of a side brace shown in figure 3-23 reduces by 10%, 20% and 40%. The MAC values between the 1st vertical bending mode shape vectors of the undamaged and damaged structures along the different lines, shown in figure 3-30, for 10%, 20% and 40% stiffness reduction of the side brace are shown in table 3-10.

Table 3-10 MAC values between the 1st vertical bending mode shape vectors of the undamaged and damaged structures (side brace)

Stiffness reduction	Line 1	Line 2	Line 3	Line 4	Line 5	Line 6	Line 7	Line 8
10%	0.9999997	1	0.9999997	1	0.9999999	0.9999994	0.9999996	1
20%	0.9999983	1	0.9999983	1	0.9999995	0.9999996	0.9999979	1
40%	0.9999890	1	0.9999890	1	0.9999966	0.9999974	0.9999857	1

Note that the MAC has been calculated up to seventh decimal digit. Although the MAC values along line 7, where the damaged member is placed, are smaller than those of the other lines but they are close to 1. Therefore, using of this method, even presence of damage cannot be identified.

As another method, the 1st normalized vertical mode shape and its 1st and 2nd derivatives along the eight lines, shown in figure 3-30, are compared in the damaged and undamaged structures. The 1st vertical bending mode shapes along the eight lines for the undamaged and damaged structures with 10%, 20% and 40% stiffness reduction of the side brace are compared before and after damage and the results of 40% are shown in figure 3-79.

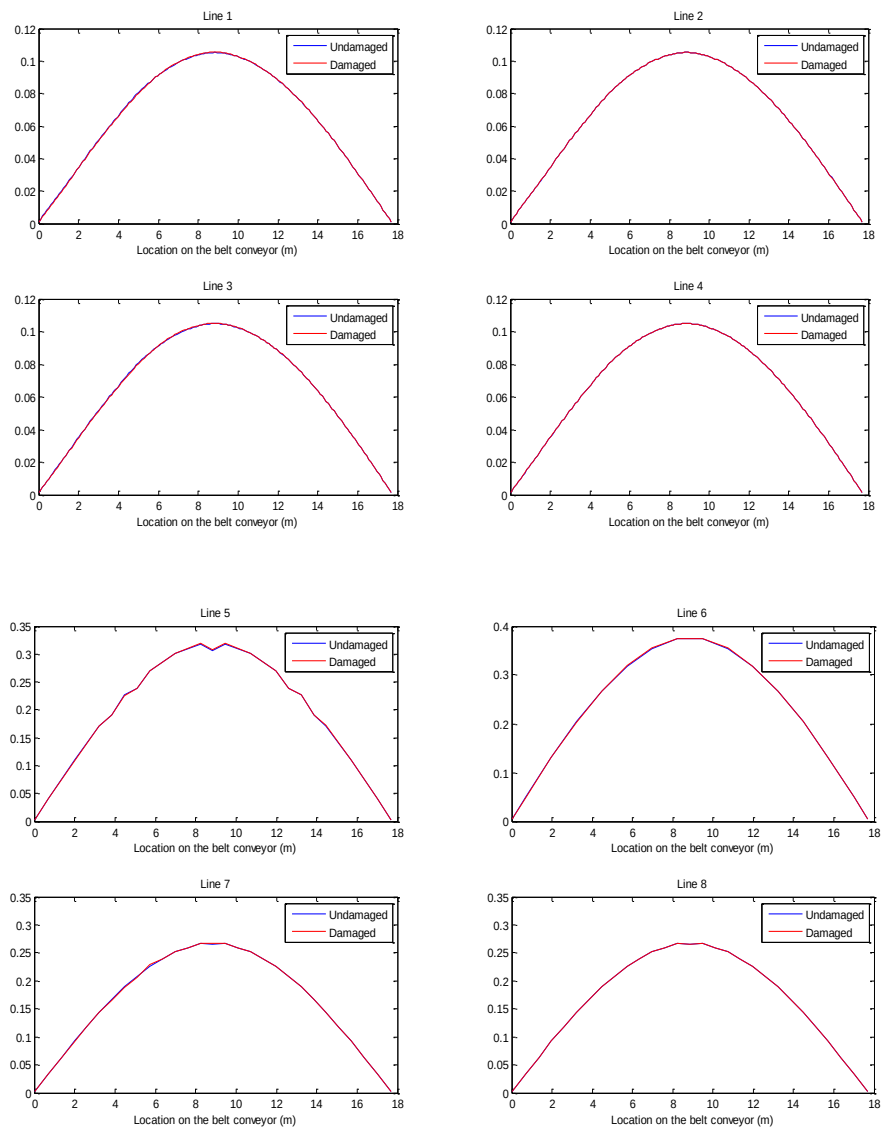

Figure 3-79 1st vertical bending mode shapes of the damaged and undamaged structures (40% stiffness reduction of the side brace)

The two curves corresponding to the damaged and undamaged structures are almost overlapped along the eight lines even for 40% stiffness reduction of the side brace. The corresponding 1st derivative curves along the eight lines for 10%, 20% and 40% stiffness reduction of the side brace are compared before and after damage and the results of 40% are shown in figure 3-80.

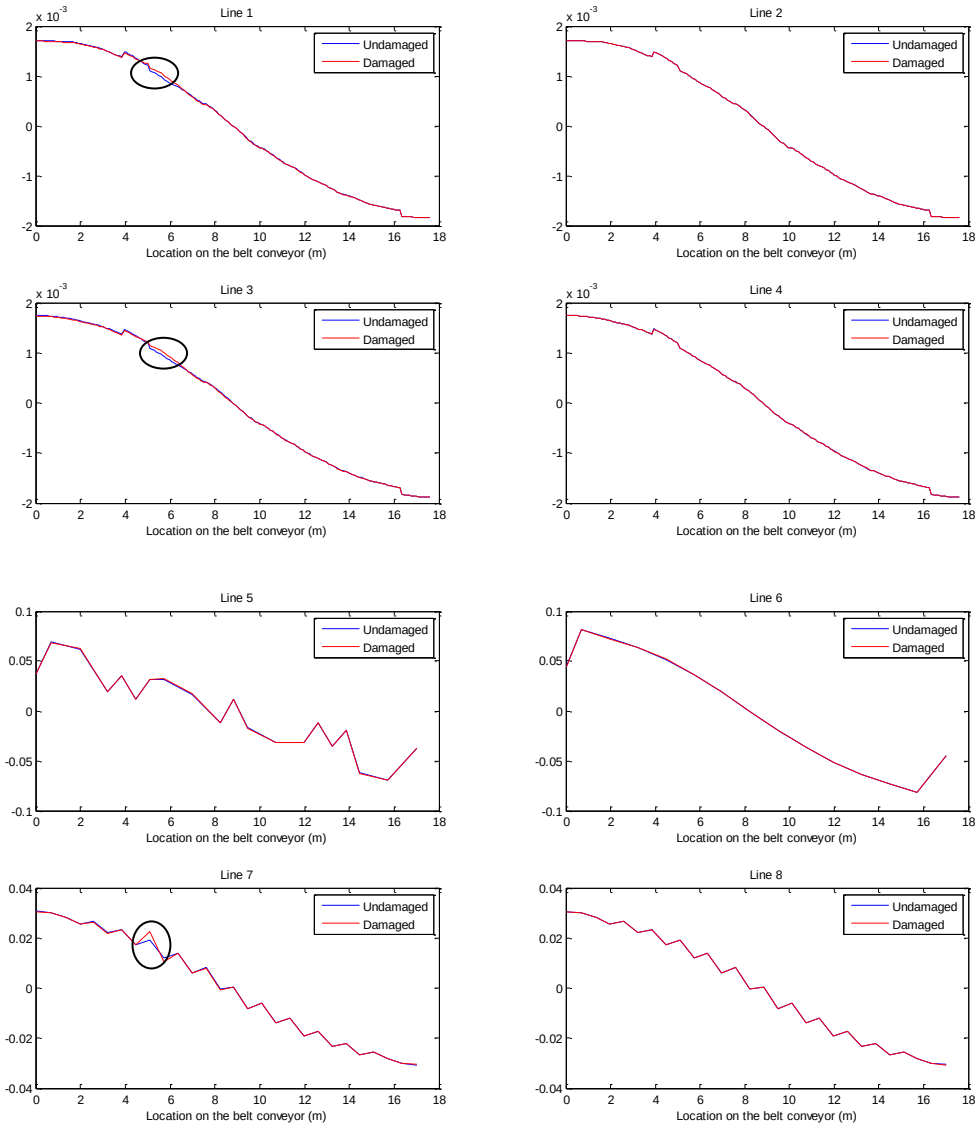

Figure 3-80 1st derivatives of the 1st vertical bending mode shapes of the damaged and undamaged structures (40% stiffness reduction of the side brace)

As shown, there are small differences between two curves along line 1 and line 3 at the same area as the damaged brace and there is a mismatch along line 7 at the same location as the damaged brace. The other lines are almost overlapped. The corresponding 2nd derivative curves along the eight lines for 10%, 20% and 40% stiffness reduction of the side brace are compared before and after damage and the results of 40% are plotted in figure 3-81.

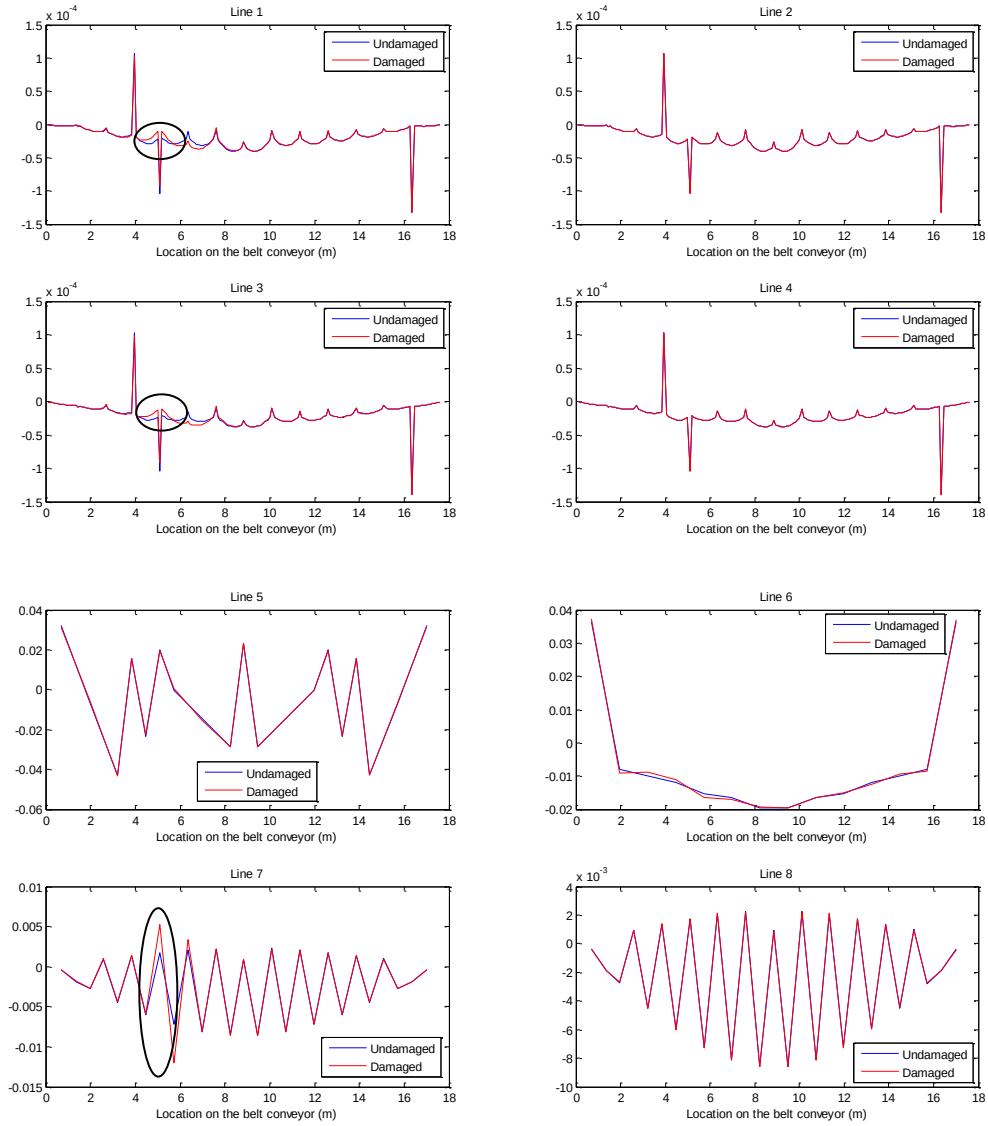

Figure 3-81 2nd derivatives of the 1st vertical bending mode shapes of the damaged and undamaged structures (20% stiffness reduction of the side brace)

There are sudden mismatches between two cures corresponding to the damaged and undamaged structures along line 1 and line 3 at the same area as the damaged side brace as well as along line 7 at the same location as the damaged brace. Along the other lines there is no sudden difference between two curves.

The main conclusions of these analyses for 10%, 20% and 40% stiffness reduction of the side brace, which corresponds to the 1st vertical bending mode, are that damaged vertical members are not identified by comparing the mode shape of undamaged and damaged structures. Using the corresponding 1st and especially 2nd derivative curves, the effects of damage mostly reflect along line 7 where damaged side members are placed provided damage is not severe, i.e. 10% and 20% stiffness reduction of side braces. For severe damage, i.e. 40% stiffness reduction of side braces, the effects of damage reflect along line 1

and 3 at the same area as damaged side braces as well as line 7 at the same locations as damaged side braces. Although mismatches between two curves along line 7, where damaged members are located, are more severe than those of line 1 and line 3, but identifying the exact locations of damaged members are difficult using only this comparison.

These conclusions can be expressed by the difference rate. Figure 3-82, 3-83 and 3-84 show the difference rate for the two curves of the damaged and undamaged structures with 10%, 20% and 40% stiffness reduction of the side brace respectively. Note that the results are for the 1st vertical bending mode.

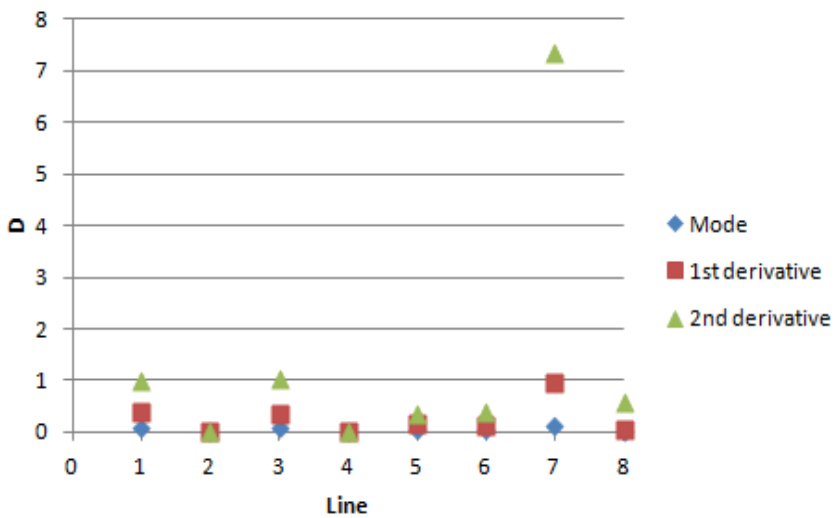

Figure 3-82 Difference rate of the eight lines for 10% stiffness reduction of the side brace

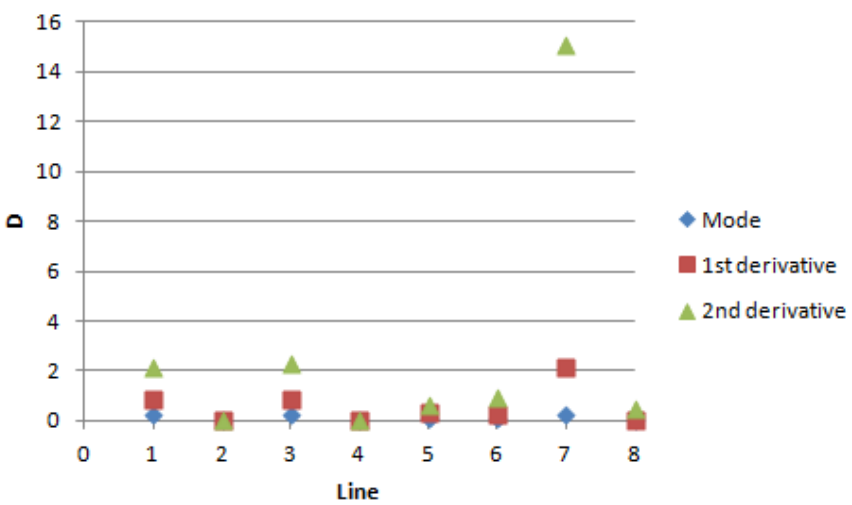

Figure 3-83 Difference rate of the eight lines for 20% stiffness reduction of the side brace

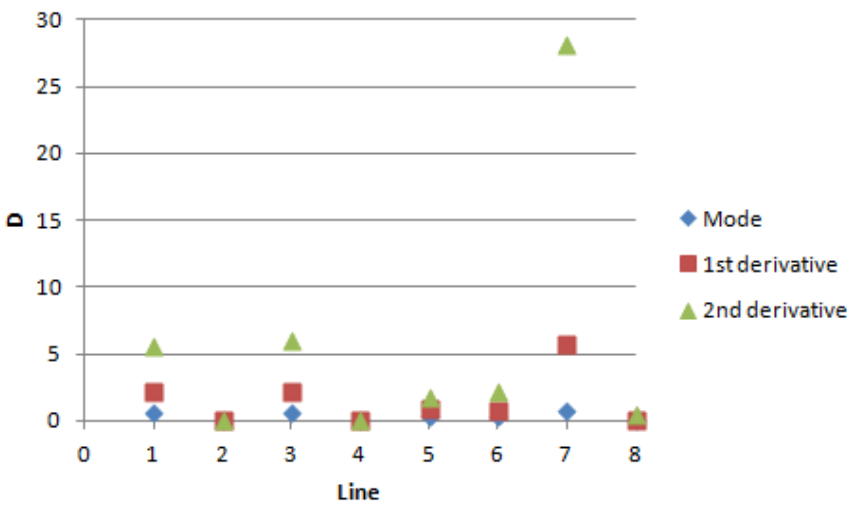

Figure 3-84 Difference rate of the eight lines for 40% stiffness reduction of the side brace

3.3.2.10 Mode shape sensitivity of the 1st lateral bending mode of the belt conveyor with respect to stiffness changes of the side braces

Similar analysis as carried out for the 1st vertical bending mode is performed for the 1st lateral bending mode. The MAC values between the 1st lateral bending mode shape vectors of the undamaged and damaged structures along the different lines for 10%, 20% and 40% stiffness reduction of the side brace are presented in table 3-11.

Table 3-11 MAC values between the 1st lateral bending mode shape vectors of the undamaged and damaged structures (side brace)

Stiffness reduction	Line 1	Line 2	Line 3	Line 4	Line 5	Line 6	Line 7	Line 8
10%	0.9999999	0.9999999	0.9999997	0.9999997	0.9999999	0.9999997	0.9999968	0.9999999
20%	0.9999995	0.9999995	0.9999984	0.9999984	0.9999994	0.9999985	0.9999833	0.9999993
40%	0.9999964	0.9999967	0.9999896	0.9999891	0.9999963	0.9999902	0.9998735	0.9999955

The MAC has been calculated up to the seventh decimal digit. Although the MAC values along line 7, where the damaged side brace is placed, are smaller than the other lines but they are close to 1. Therefore, by using this method, even presence of damage is difficult to be identified.

As another approach, the 1st normalized lateral mode shape and its 1st and 2nd derivatives along the eight lines, shown in figure 3-30, are compared in the damaged and undamaged structures. The 1st lateral bending mode shapes along the eight lines for the undamaged and damaged structures with 10%, 20% and 40% reduction in the stiffness of the side brace are compared before and after damage and the results of 40% are plotted in figure 3-85.

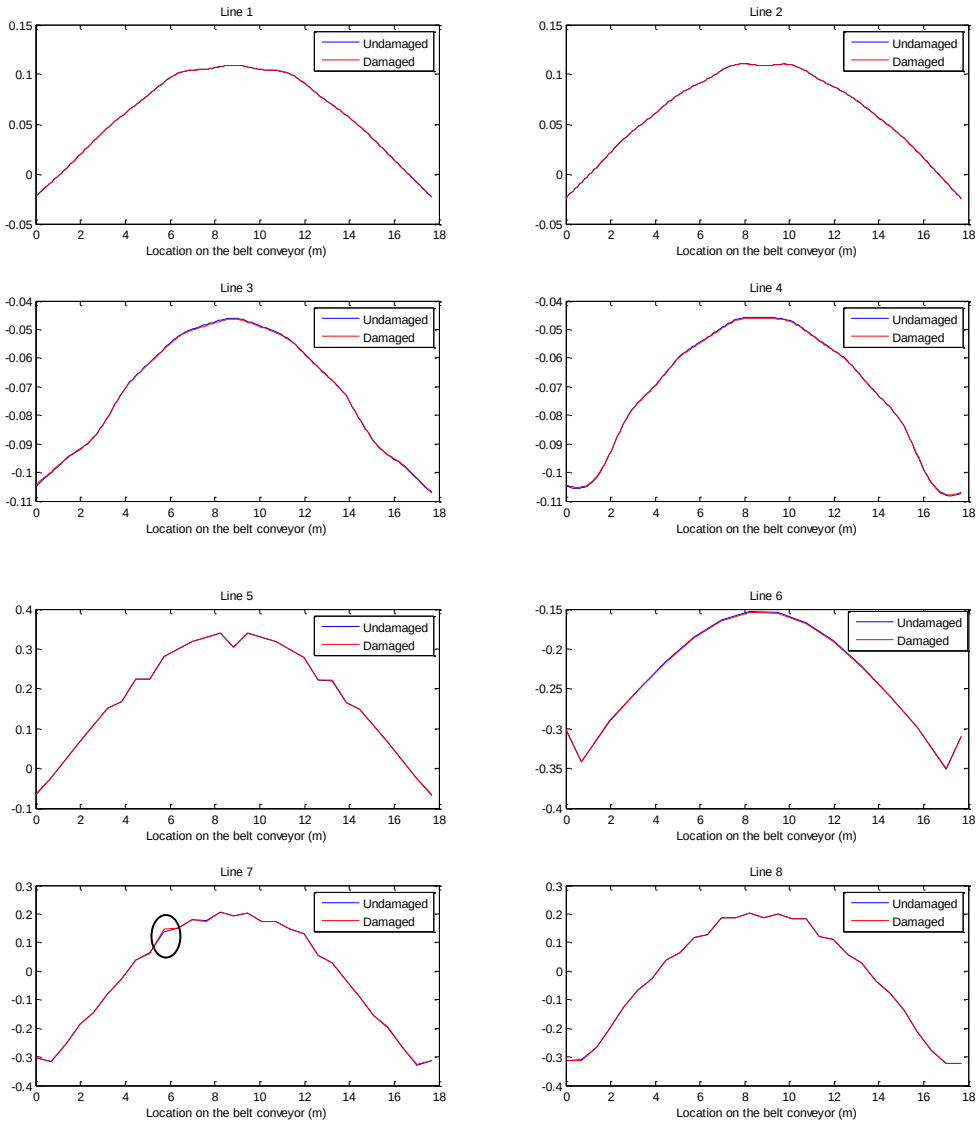

Figure 3-85 1st lateral bending mode shapes of the damaged and undamaged structures (40% stiffness reduction of the side brace)

The only sudden mismatch in the above figure is along line 7 at the same location as the damaged side brace but this difference between two curves is very small and identifying the damage location is difficult with this comparison. The corresponding 1st derivative curves along the eight lines with 10%, 20% and 40% stiffness reduction of the side brace are compared before and after damage and the results of 40% are shown in figure 3-86.

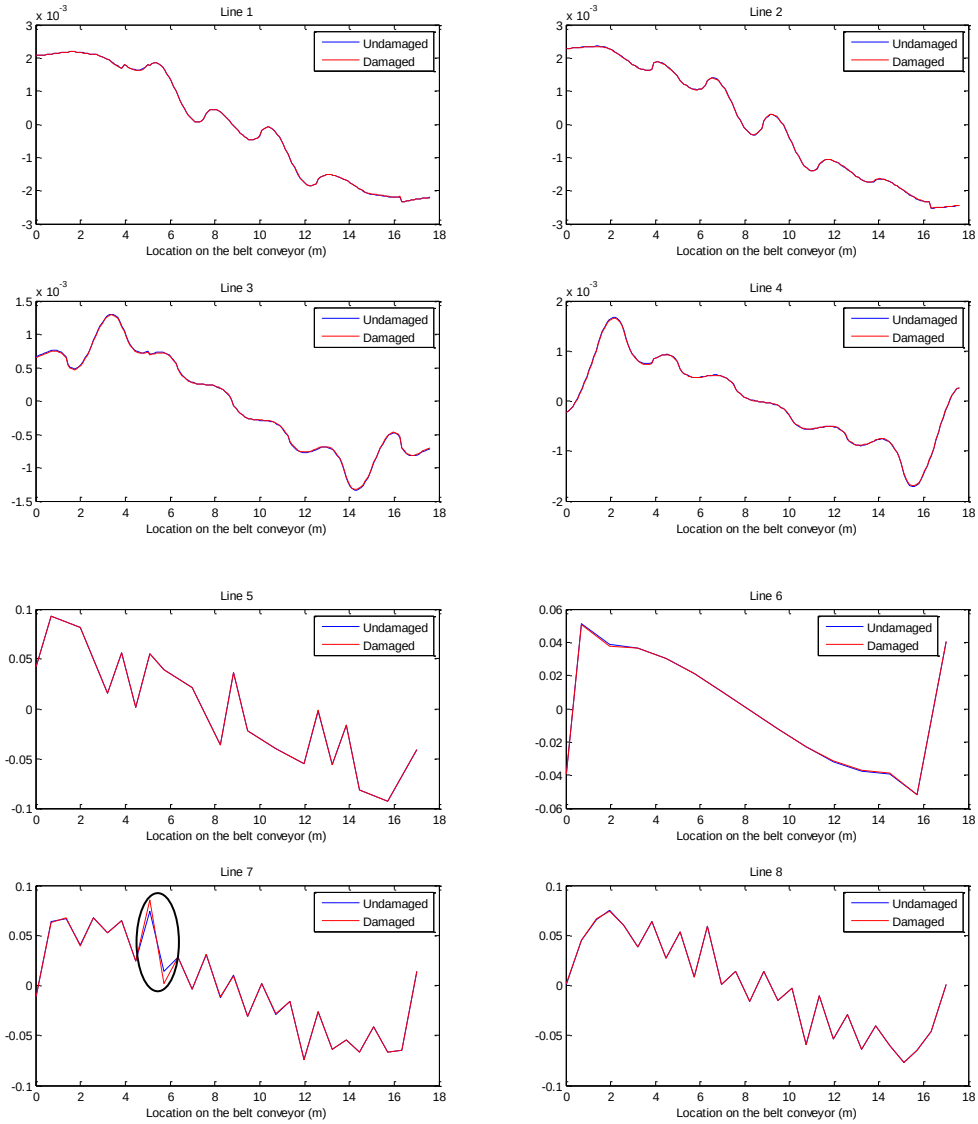

Figure 3-86 1st derivatives of the 1st lateral bending mode shapes of the damaged and undamaged structures (40% stiffness reduction of the side brace)

As shown, there is a mismatch along line 7 at the same location as the damaged member. The two curves along the other lines are almost overlapped. Therefore, the damage location is correctly identified. The corresponding 2nd derivative curves along the eight lines with 10%, 20% and 40% stiffness reduction of the side brace are compared before and after damage and the results of 40% are shown in figure 3-87.

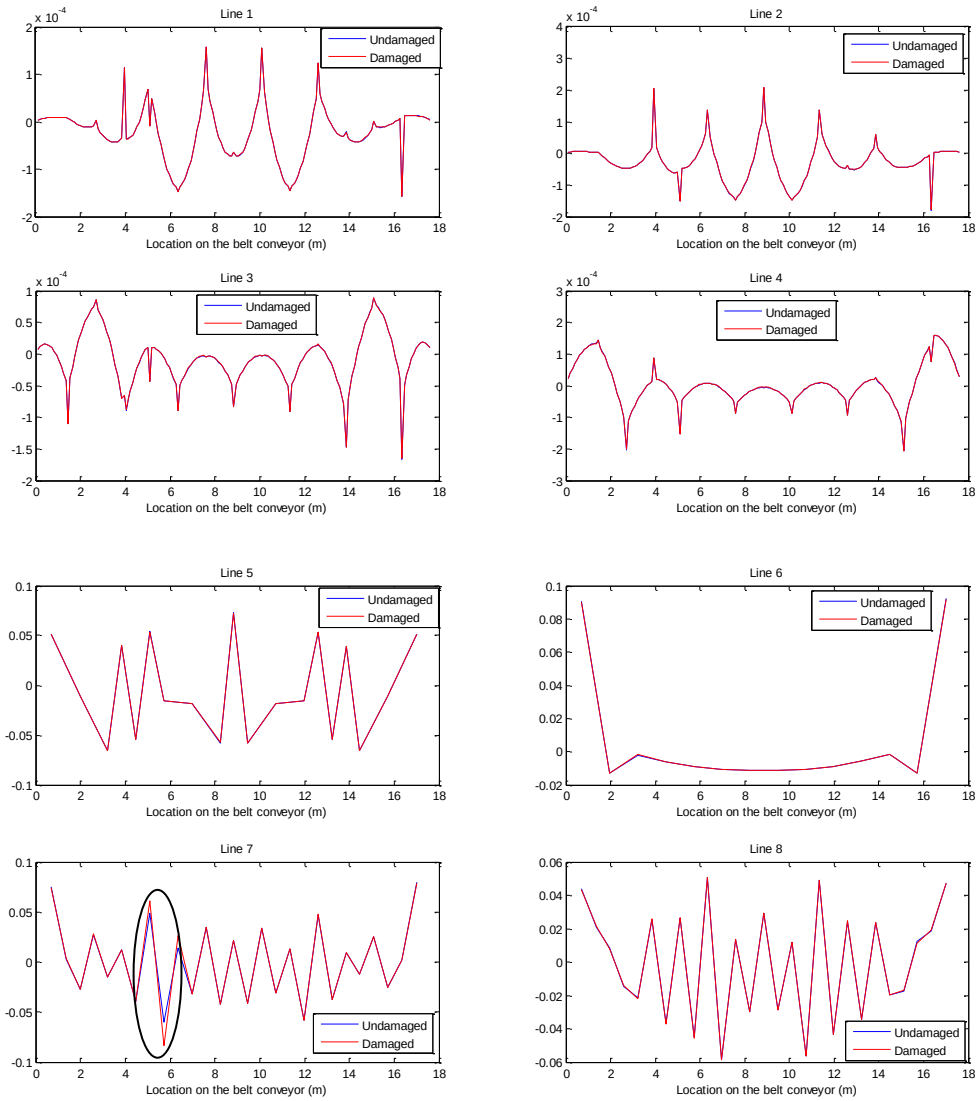

Figure 3-87 2nd derivatives of the 1st lateral bending mode shapes of the damaged and undamaged structures (40% stiffness reduction of the side brace)

Once again, the only mismatch between two curves corresponding to the damaged and undamaged structures is along line 7 at the same location as the damaged side brace. It means that the damage location is correctly identified.

The main conclusions of these analyses for 10%, 20% and 40% stiffness reduction of the side brace, which corresponds to the 1st lateral bending mode, are that damaged side braces are not identified by comparison of the 1st lateral mode shape. However, if damage is severe, i.e. 40% stiffness reduction of side braces, there are very small differences on the mode shape at the same locations as damaged members and identification of damage locations is difficult. Using the corresponding 1st and 2nd derivatives of the 1st lateral mode shape, damaged side braces are not identified when damage is not severe, i.e. 10% or 20% reduction in the stiffness of side braces. However, for 20% stiffness reduction of side braces, there are small mismatches between the curves corresponding to the damaged and

undamaged structures, but it is still difficult to identify damage locations. If damage is severe, i.e. 40% stiffness reduction of the side braces, damage locations are correctly identified.

These conclusions can be expressed by the difference rate. Figure 3-88, 3-89 and 3-90 show the difference rate for the two curves of the damaged and undamaged structures with 10%, 20% and 40% stiffness reduction of the side brace respectively. Note that the results are for the 1st lateral bending mode.

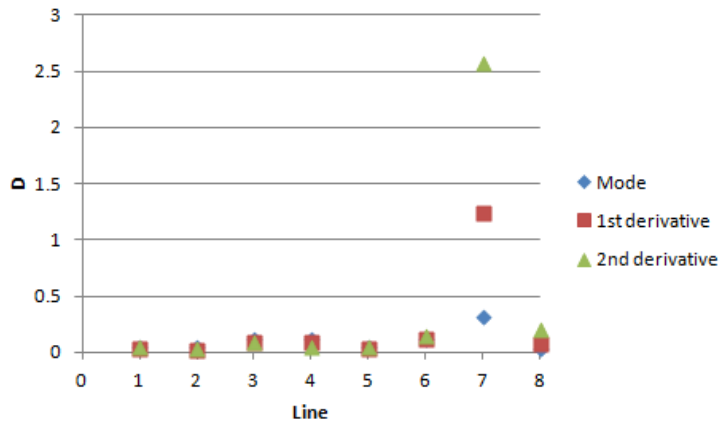

Figure 3-88 Difference rate of the eight lines for 10% stiffness reduction of the side brace

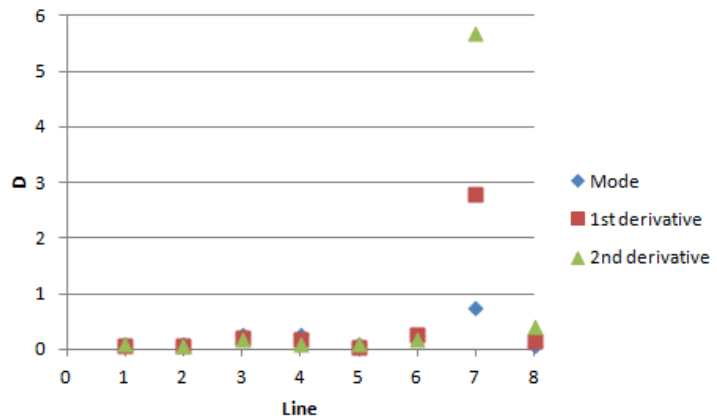

Figure 3-89 Difference rate of the eight lines for 20% stiffness reduction of the side brace

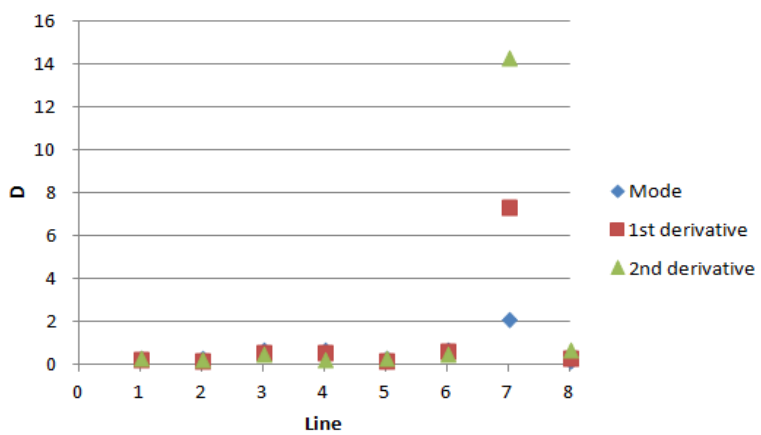

Figure 3-90 Difference rate of the eight lines for 40% stiffness reduction of the side brace

3.3.2.11 Conclusions of global modes sensitivity analysis

Comparison of the results of the 1st lateral bending and 1st vertical bending modes shows that generally the 1st and 2nd derivatives of the 1st vertical bending mode shape are more sensitive to damage on side braces compared to the 1st and 2nd derivatives of the 1st vertical bending mode. Using the 1st and 2nd derivatives of the 1st vertical bending mode for severe damage on side braces, the effects of damage are reflected not only at the exact locations of damaged members but at the same area as damage which might contain many members. Therefore, damaged members might not be confidently detected. Using the 1st and 2nd derivatives of the 1st lateral bending mode for severe damage on the side braces, damage locations are correctly identified. Using the 1st and 2nd derivatives of the 1st vertical and lateral bending modes for non-severe damage, 10% and 20% reduction in the stiffness, mismatches between the curves of before and after damage are small. Therefore, it is difficult to identify damage locations. Damaged side braces cannot be identified using only the 1st lateral and vertical bending mode shapes of the damaged and undamaged structures.

Comparing all the results of the 1st lateral bending mode shows that:

1. Any significant changes of the mode shape and its 1st and 2nd derivatives along line 1, 2, 3, and 4 are caused by stiffness changes of the corresponding longitudinal members, or connected bottom or top braces. However, this change is much larger for stiffness changes of the longitudinal members.

2. Any significant changes of the mode shape and its 1st and 2nd derivatives along line 5 and 6 are caused by stiffness changes of the corresponding bottom or top braces.

3. Any significant changes of the mode shape and its 1st and 2nd derivatives along line 7 and 8 are caused by stiffness changes of the corresponding side braces, vertical members, bottom or top braces, or longitudinal members. However, this change is much larger for stiffness changes of the side braces.

Comparing all the results of the 1st vertical bending mode shows that:

1. Any significant changes of the mode shape and its 1st and 2nd derivatives along line 1, 2, 3, and 4 are caused by stiffness changes of the corresponding longitudinal members, connected vertical members, or side braces. However, this change is smaller for stiffness changes of the connected vertical members.

2. Any significant changes of the mode shape and its 1st and 2nd derivatives along line 5 and 6 are caused by stiffness changes of the corresponding bottom or top braces, longitudinal member, or lateral members. However, this change is much larger for stiffness changes of the bottom or top braces.

3. Any significant changes of the mode shape and its 1st and 2nd derivatives along line 7 and 8 are caused by stiffness changes of the corresponding longitudinal members, side braces, or vertical members. However, this change is much larger for stiffness changes of the side braces.

It should be noted that, in general, the changes are the least for the shapes of the 1st lateral and vertical bending modes. The changes of the 2nd derivative of the 1st lateral and vertical bending modes with

respect to stiffness changes of the members are larger than the relevant 1st derivative and mode shapes. In general, the changes are relatively small and need precise measurement at many points.

1.4 Local vibration modes

The eigenvalue analysis of the belt conveyor reveals different local vibration modes of members.

3.4.1 Identical members

First, identical members sets in belt conveyors are introduced. The main frame of belt conveyors contains main and secondary members. Main members of belt conveyors are continuous along longitudinal direction. Secondary members are braces of the bottom and top parts, braces of the side parts, vertical members and lateral members. Since the main frame of belt conveyors contains same bays along the longitudinal direction and each bay has several members, as shown in figure 3-3, there are some groups of identical members repeated along the belt conveyor as shown in figure 3-91. These members having the same cross sections, lengths, and local boundary conditions are defined as identical members.

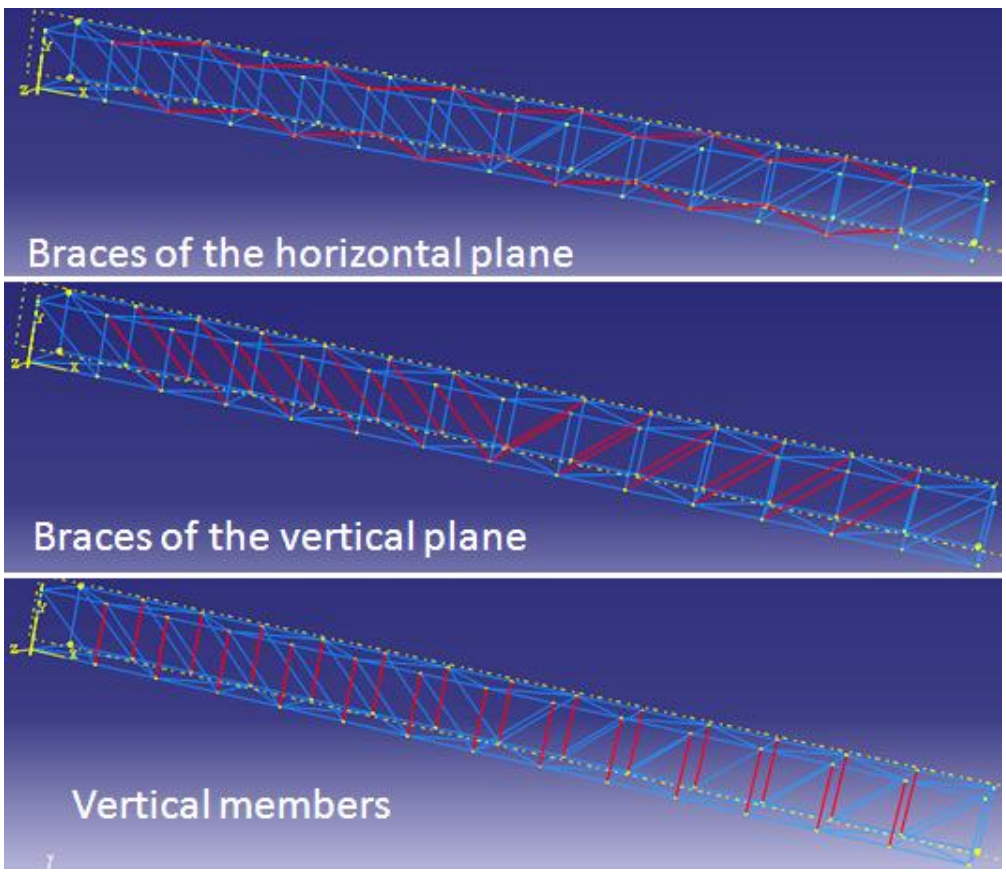

Figure 3-91 Identical members sets in the main frame of the belt conveyor

3.4.2 Classification of local vibration modes

Some local modes are combined with global vibration modes. Two sample of these coupled global-local vibration modes are shown in figure 3-92. The left figure is combination of the 3rd vertical bending mode

and some local vibration modes while the right one is combination of the 4th torsional mode and some local vibration modes.

3rd vertical bending mode with local modes

4th torsion mode with local modes

Figure 3-92 Combination of global and local vibration modes

In general, local vibration modes can be classified into three main categories: and named here by:

1. Coupled local vibration modes
2. Partially chaotic local vibration modes
3. Periodic and isolated local vibration modes

Coupled local vibration mode is a mode in which two or more different groups of identical members vibrate together. Note that in each group of members, all members are identical. Figure 3-93 shows two samples of these modes in the belt conveyor. In the left figure, lateral members, and bottom and top braces vibrate together. In the right one, side braces vibrate together with lateral members.

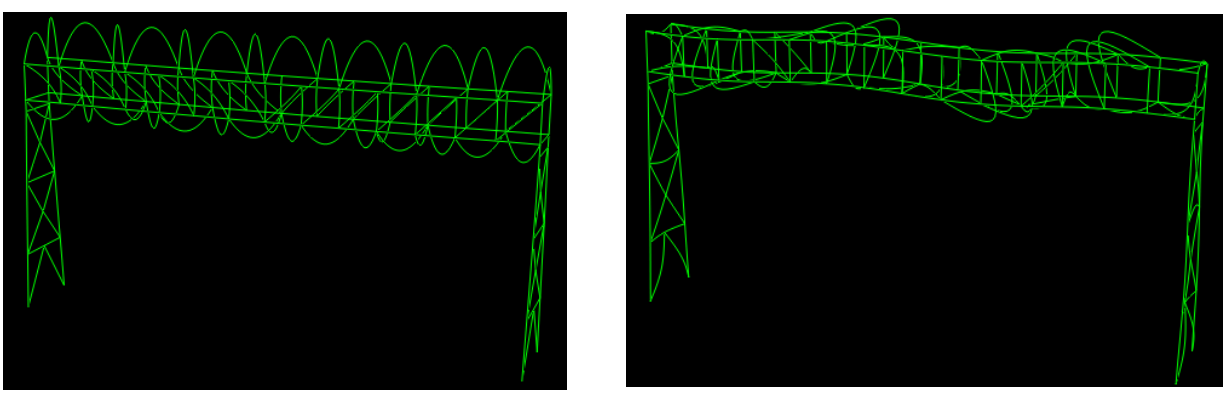

Figure 3-93 Coupled local vibration modes

Partially chaotic local vibration mode is a mode in which members of one part or more than one parts of the structure disorderly vibrate. Note that these members can be non-identical. Figure 3-94 shows two samples of these modes in the belt conveyor. In the right figure, members at the left and right sides of the main frame vibrate together. In the right one, Members of the front side of the main frame vibrate together.

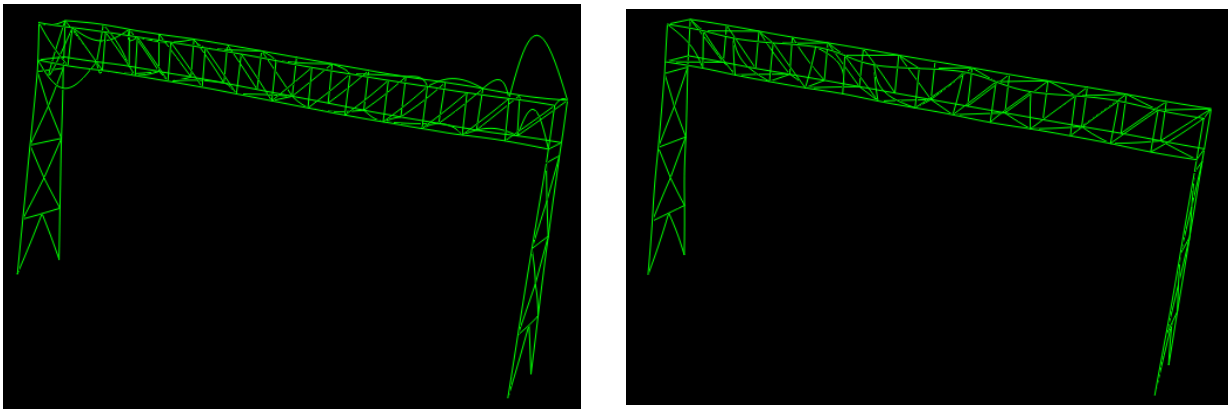

Figure 3-94 Partially chaotic local vibration mode

Periodic Local Vibration Mode (PLVM) is a mode where all identical members locally vibrate at the same frequency. Note that there is no PLVM for the main members because they are continuous. The 1st PLVM of the different identical members sets of the belt conveyor are shown in figure 3-95. Note that there are several 1st PLVM corresponding to each identical members set vibrating in a short frequency range. Other than these PLVM, there are higher PLVM, i.e. the 2nd PLVM, the 3rd PLVM and so on, vibrating in higher frequency range.

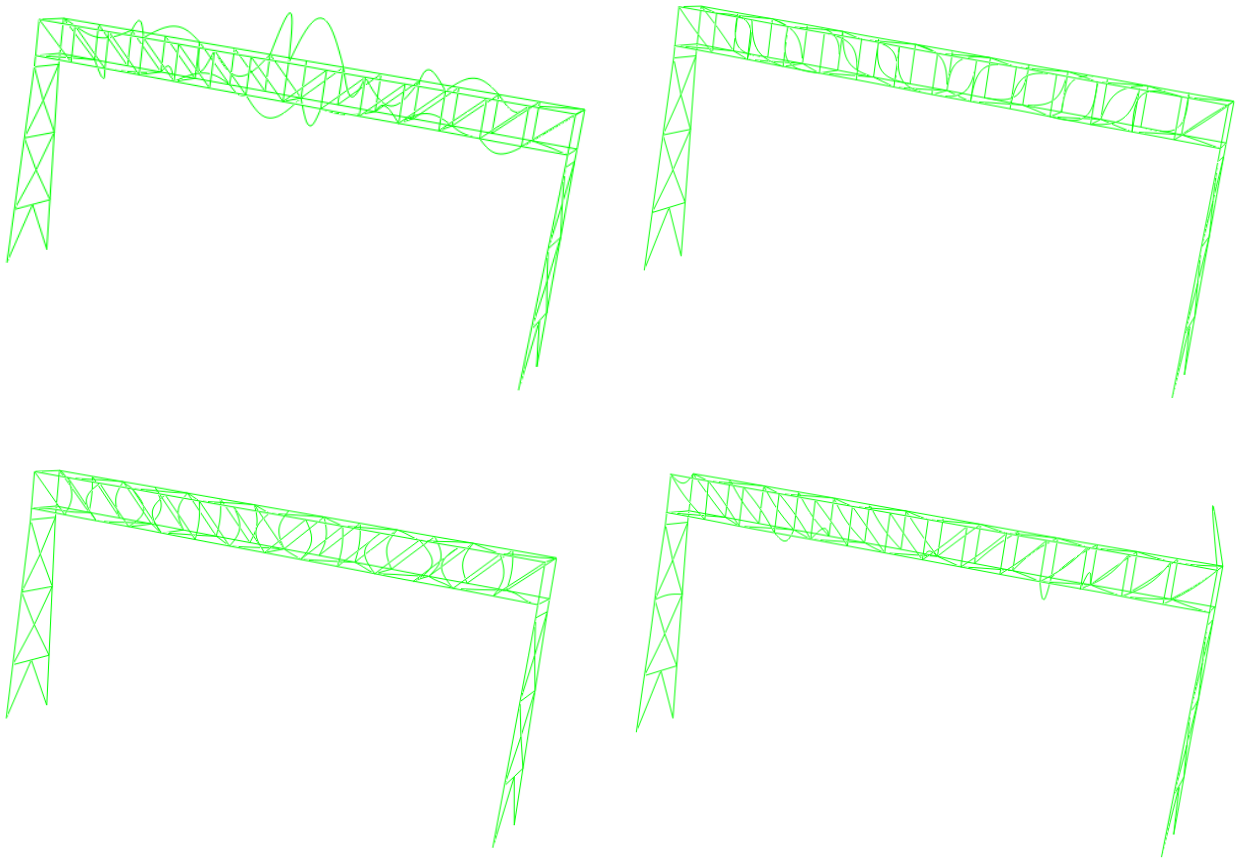

Figure 3-95 1st PLVM of the different identical members sets in the belt conveyor

If one of the identical members damages, the member is no longer identical with the other members set. Therefore, the damaged member alone locally vibrates in lower frequencies than PLVM of the identical members of the set. These local modes are Isolated Local Vibration Mode (ILVM). In other words, in a damaged structure, there are PLVM of the undamaged identical members sets with the same frequencies as the PLVM of the identical members sets of the undamaged structure, and ILVM corresponding to the damaged members vibrating in lower frequencies than those of PLVM. For example, 24 identical braces of the main frame of the belt conveyor are considered. These members are shown in figure 3-96.

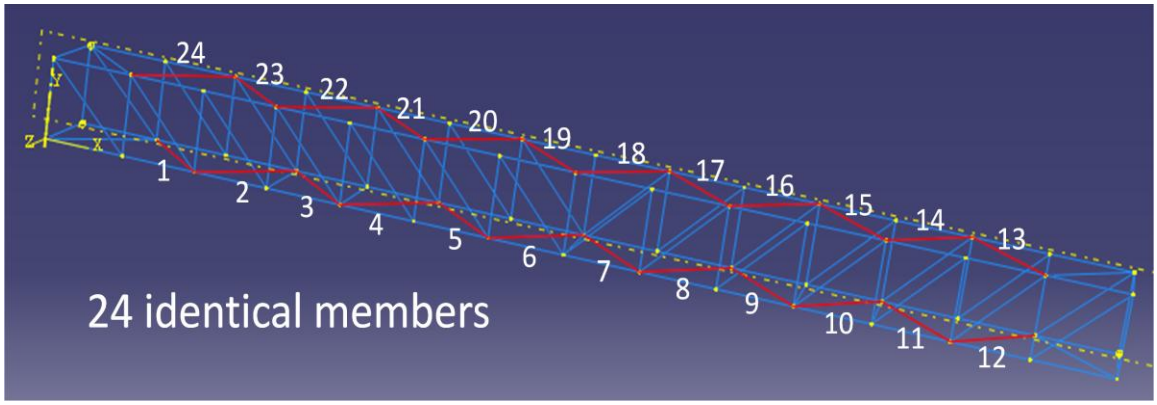

Figure 3-96 Identical braces at the bottom and top parts of the main frame

The eigenvalue analysis shows several PLVM around 42 Hz. One of those PLVM is shown in figure 3-97. The stiffness of member 4 in figure 3-96 is reduced by 20%. The eigenvalue analysis of the damaged structure shows PLVM at the nearly same frequency as PLVM of the undamaged structure shown in figure 3-98 and an ILVM corresponding to the damaged member illustrated in figure 3-99.

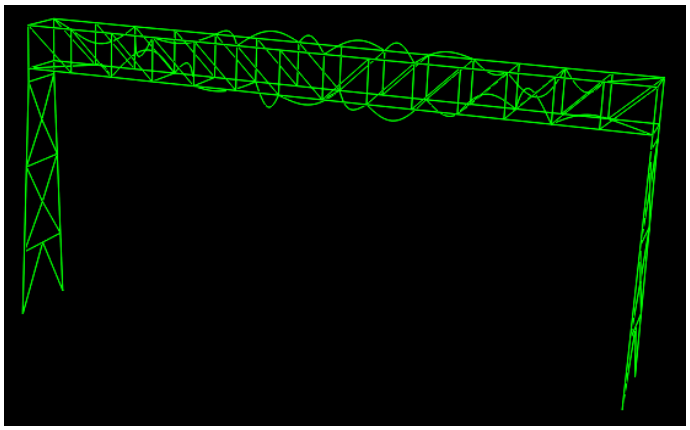

Figure 3-97 PLVM of the undamaged structure (Fr=42.136 Hz)

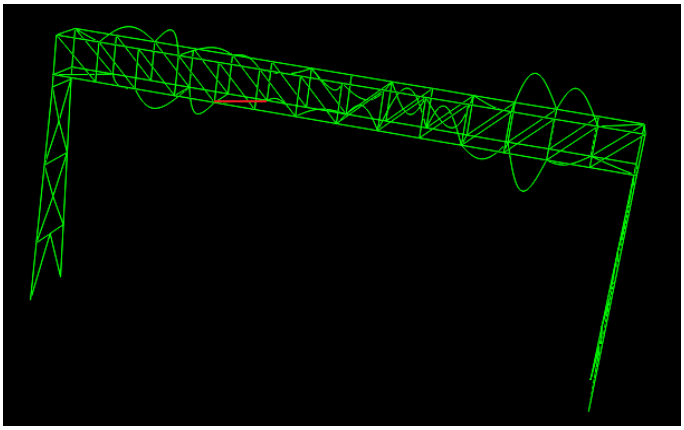

Figure 3-98 PLVM of the damaged structure (Fr=42.136 Hz)

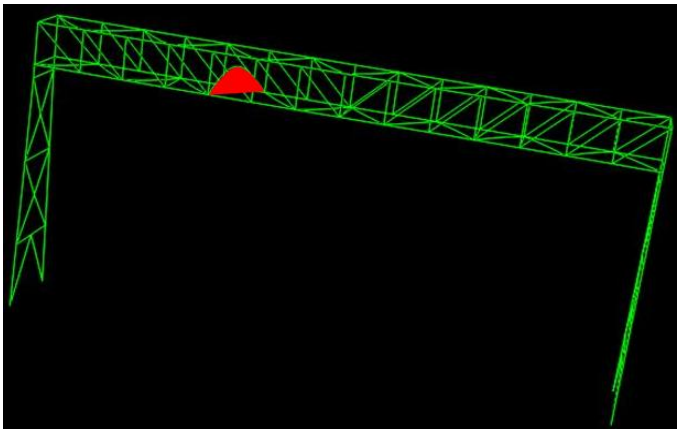

Figure 3-99 ILVM of the damaged member (Fr= 37.94 Hz)

As shown in the above figures, all 24 braces of the undamaged structure are vibrating at a frequency equals to 42.136 Hz. After applying damage to member 4, this member is not identical with the other braces anymore. Therefore, in the PLVM of the damaged structure, 23 identical members vibrate at a frequency equals to 42.136 Hz which is a PLVM and member 4 vibrates with a frequency equals to 37.94 Hz which is an ILVM.

3.4.3 Sensitivity of the frequencies of PLVM and ILVM

Using the finite element model, sensitivity of the frequencies of PLVM and ILVM are investigated in detail.

3.4.3.1 Sensitivity with respect to Stiffness reduction of the secondary members

At first, ILVM of three different members are examined. The stiffness of members 4, 7, and 17 are progressively reduced. In addition, the 1st ILVM frequency of member 4 when member 2 has 50% stiffness reduction is examined. The frequencies of the corresponding ILVM of each stiffness reduction for the different members are presented in table 3-12.

Table 3-12 Frequencies of ILVM for the different stiffness reduction of various members

Stiffness reduction (%)	Member 4	Member 7	Member 17	Member 4 + Member 2 (50%)
1%	41.917	41.942	41.969	41.918
2%	41.66	41.711	41.653	41.69
3%	41.511	41.598	41.519	41.535
4%	41.331	41.447	41.355	41.355
5%	41.143	41.304	41.189	41.172
7%	40.682	40.551	40.615	40.689
10%	40.126	39.923	39.997	40.132
15%	39.021	38.878	38.952	39.03
20%	37.937	37.819	37.821	37.951
30%	35.578	35.381	35.519	35.597
40%	32.971	32.824	32.972	32.972
50%	29.895	29.996	29.972	29.907
60%	26.764	26.836	26.853	26.762
70%	23.291	23.356	23.333	23.291
80%	19.173	19.212	19.214	19.173
90%	13.789	13.813	13.813	13.789
99%	5.2919	5.2906	5.2902	5.2919

The frequencies of ILVM with respect to the stiffness reduction of the members are plotted in figure 3-100.

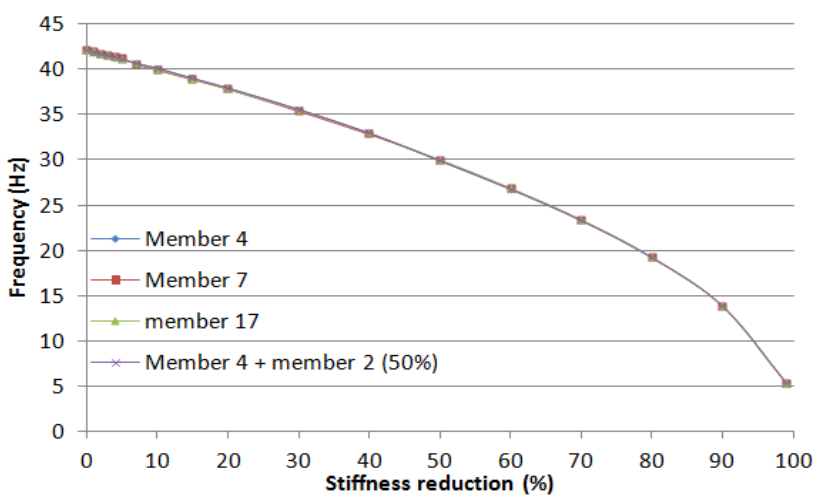

Figure 3-100 Frequencies of ILVM

The four curves plotted in the above figure are nearly overlapped. It means this phenomenon is almost independent from the damage locations. The percentage changes of the frequency of ILVM for different members with respect to the stiffness reduction of each member are drawn in figure 3-101.

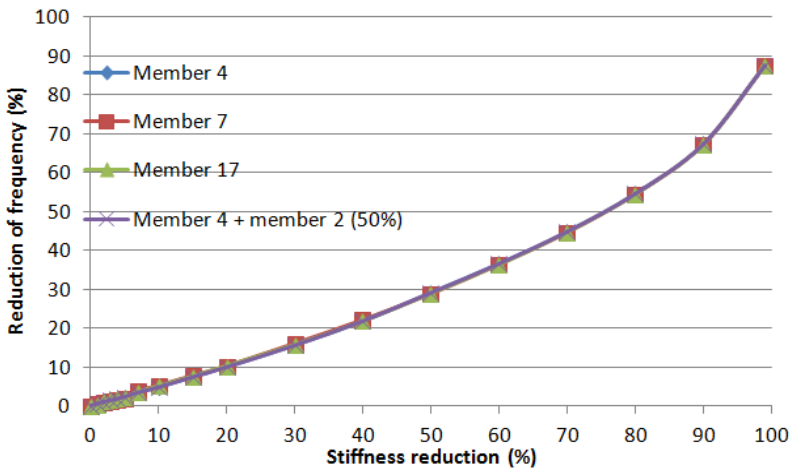

Figure 3-101 Percentage changes of the frequency of ILVM

It is found from the above figure that the frequency of ILVM of the members has a large sensitivity with respect to damage on the members. As an example, for 50% stiffness reduction of each member, the corresponding ILVM reduces by about 30%.

In order to verify that this phenomenon is independent from the number of damaged members that have the same severity of damage, first, the stiffness of members 3, 5, 9, 10, 14, 20 and 24, shown in figure 3-96, is reduced by 50%. The eigenvalue analysis of the damaged structure shows PLVM nearly at the same frequencies as PLVM of the undamaged structure (shown in figure 3-97) in which all members vibrate except the seven damaged members. In other words, only undamaged members vibrate with about 42 Hz. One of these modes is shown in figure 3-102.

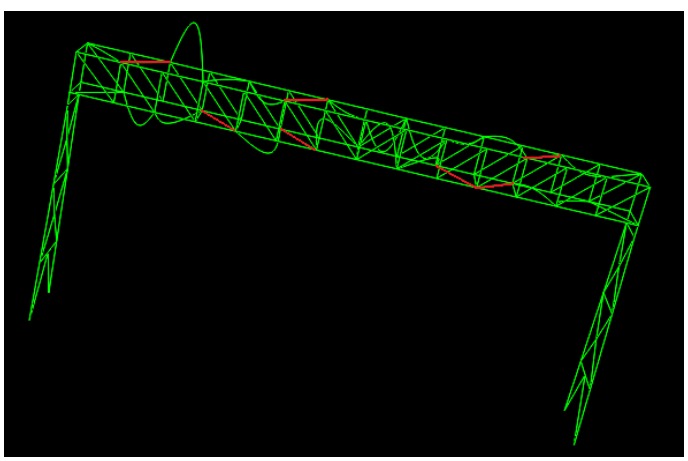

Figure 3-102 PLVM corresponding to the undamaged members (Fr=42.136 Hz)

Since there are more than one damaged member with the same damage degree, there are more than one ILVM with nearly the same frequency, and more than one damaged member vibrates in ILVM. One of the corresponding ILVM of the damaged members is shown in figure 3-103. The frequency of this mode is about 30 Hz.

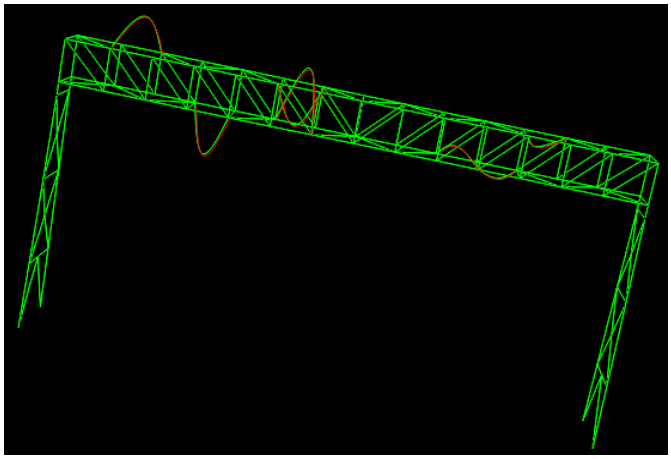

Figure 3-103 Local vibration mode of the seven damaged members (Fr=29.65)

Next, the young's modulus of members 3, 5, 9, 10, 14, 20 and 24, shown in figure 3-96, is progressively reduced. It is found that the seven damaged members vibrate together and do not vibrate with the undamaged members in the PLVM (Fr=42.13 Hz). Figure 3-104 shows the frequencies of ILVM and their percentage changes with respect to the stiffness reduction of the seven members.

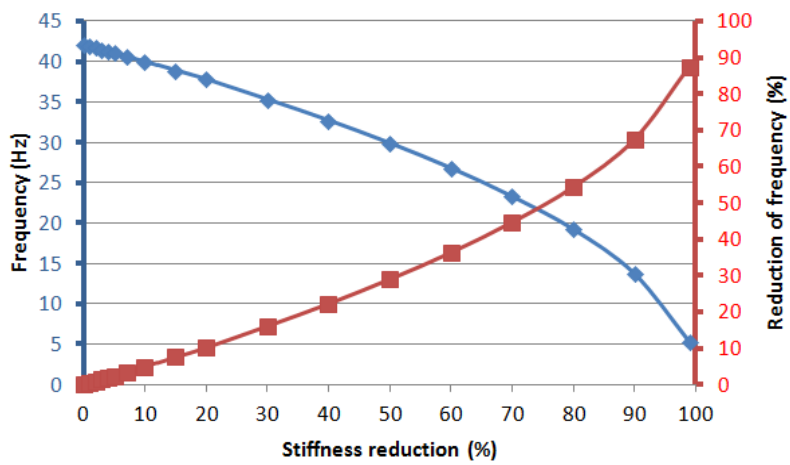

Figure 3-104 Frequencies of ILVM and their percentage changes for the seven damaged members

Comparison of the above graphs with figures 3-100 and 3-101 vividly shows that this phenomenon is almost independent from the number of damaged members.

To quantify the degree of isolated local vibration modes (ILVM) of the secondary members, a measure of the degree of mode localization (DML) is defined as **[66]**:

$$DML = \frac{m - m_{co}}{m - 1} \tag{3.4}$$

Where m is the number of identical members. m_{co} is an indicator for mode confinement, and always $1 \leq m_{co} \leq m$, computed by:

$$m_{co} = \frac{(\sum_{i=1}^{m} y_i)^2}{\sum_{i=1}^{m} y_i^2} \tag{3.5}$$

In which y_i is the maximum of absolute modal amplitude of the identical members. $DML = 0$, if the mode is not localized at all and $DML = 1$, if the mode is completely localized.

The degree of mode localization (DML) is calculated for different stiffness reductions of members 4 and 17. These members have been already specified in figure 3-96. The results are shown in figure 3-105.

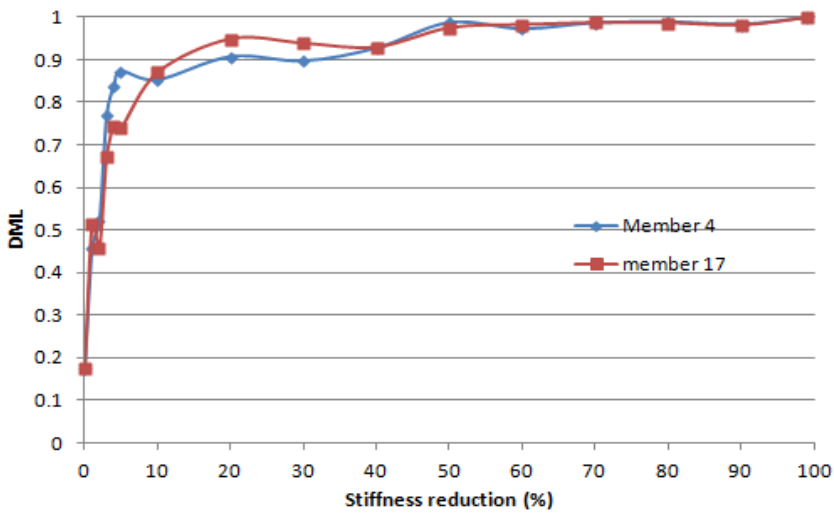

Figure 3-105 DML variations with respect to stiffness reduction changes of the members

The general shape of the curves in the above figure show that the ILVM of the damaged members tend to be more localized as the damage severity is enhanced. The exceptions in the above figure correspond to the cases where the ILVM are combined with the other modes, so that the undamaged members slightly vibrate.

In order to confirm that the relative severity of several damaged members can be reflected to the frequencies without interfering with each other, the stiffness of members 6, 7, 13 and 21, shown in figure 3-96, are respectively reduced by 2%, 5%, 10% and 20% at the same time. Figure 3-106 shows one of the PLVM (Freq. = 42.13 Hz) corresponding to the undamaged identical braces at the bottom and top parts of the belt conveyor.

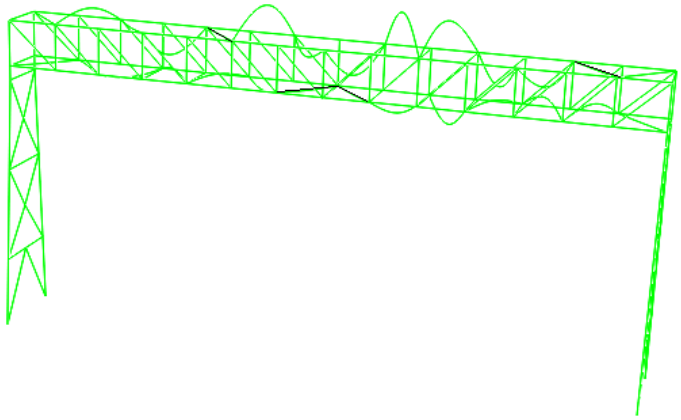

Figure 3-106 PLVM of the undamaged identical bottom and top braces

As shown in the above figure, the damaged members, shown in black, do not vibrate in this mode. Instead, they have their own ILVM. The ILVM corresponding to members 6, 7, 13 and 21 are shown in figure 3-107.

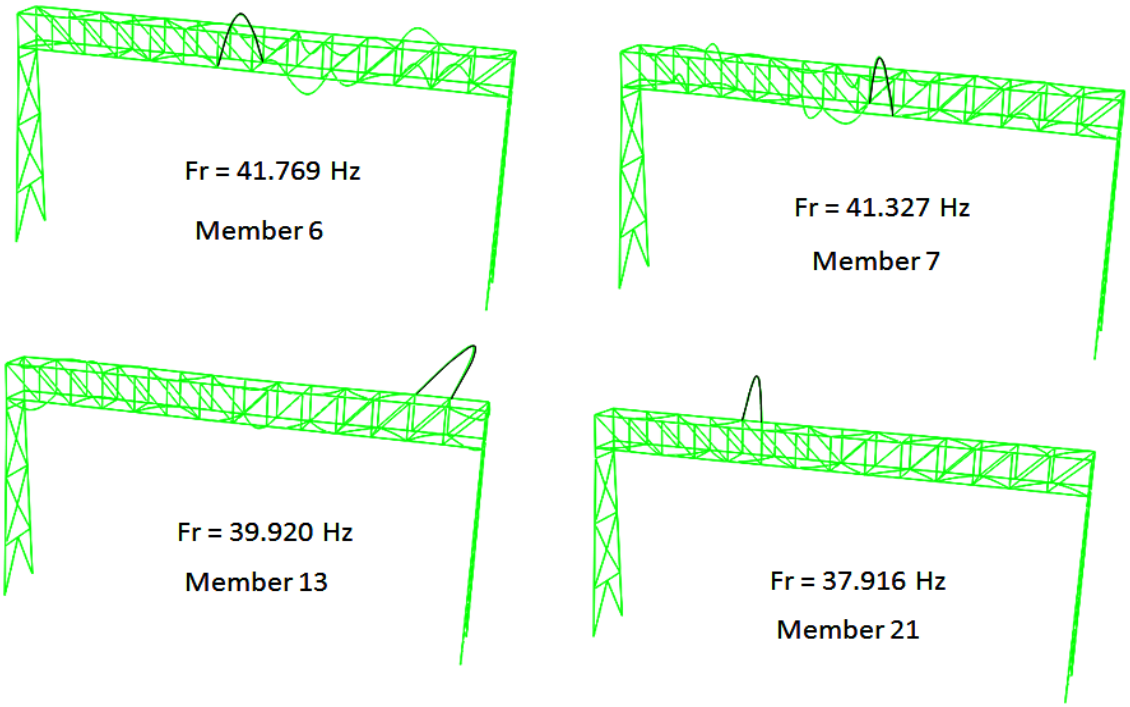

Figure 3-107 ILVM of the damaged members

In the above figure, vibrations of the damaged members are much larger than the other members. The frequencies of PLVM and ILVM corresponding to the 24 braces are shown in figure 3-108.

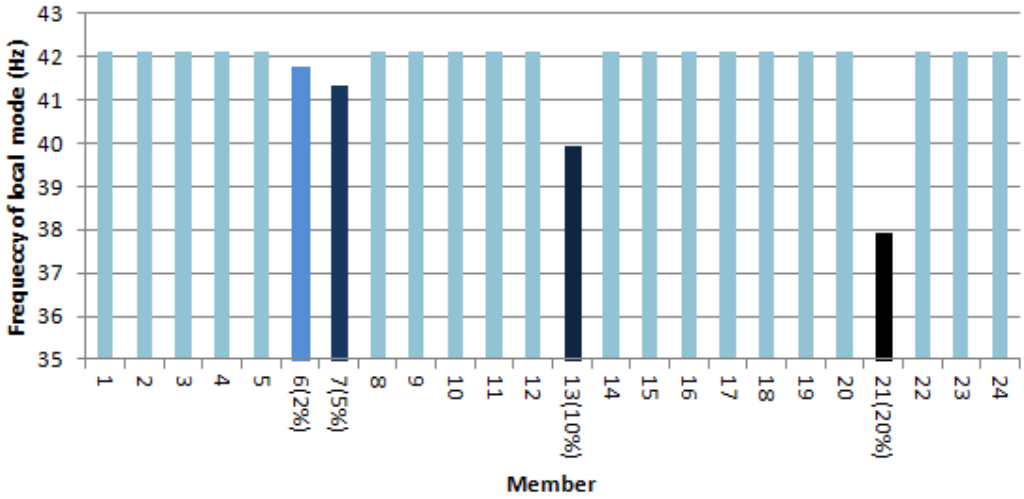

Figure 3-108 Frequencies of PLVM and ILVM

This figure shows the damaged members as well as the relative severity of the damage. As shown, the frequencies of ILVM corresponding to the damaged members are less than the frequencies of PLVM of

the undamaged braces and among the damaged members, the frequency of ILVM decreases as the degree of damage increases.

The other secondary identical members sets of the belt conveyor have their own PLVM. The eigenvalue analysis of the structure shows the same results as the bottom and top braces for the other secondary identical members sets. Figure 3-109, 3-110 and 3-111 show PLVM and ILVM for 20% damage of representative members of the lateral members set, side braces set and vertical members set respectively.

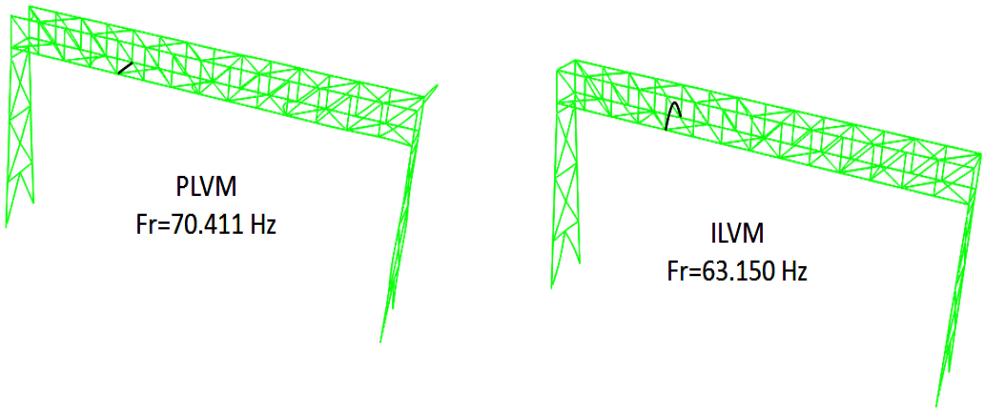

Figure 3-109 PLVM and ILVM of the lateral members set

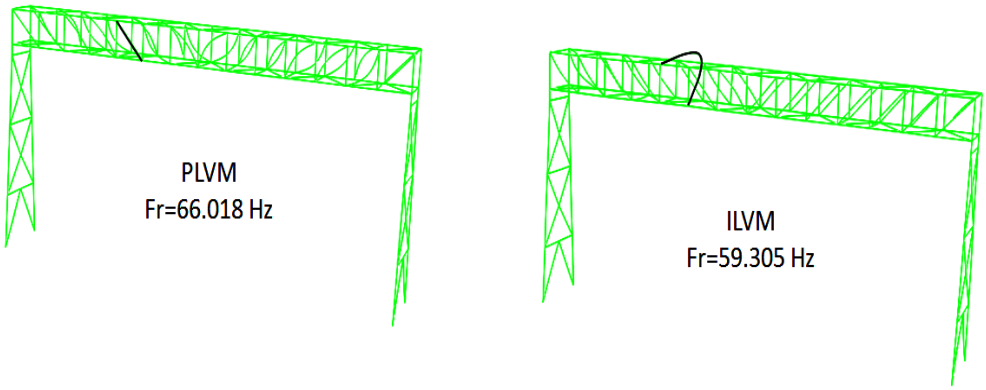

Figure 3-110 PLVM and ILVM of the side braces set

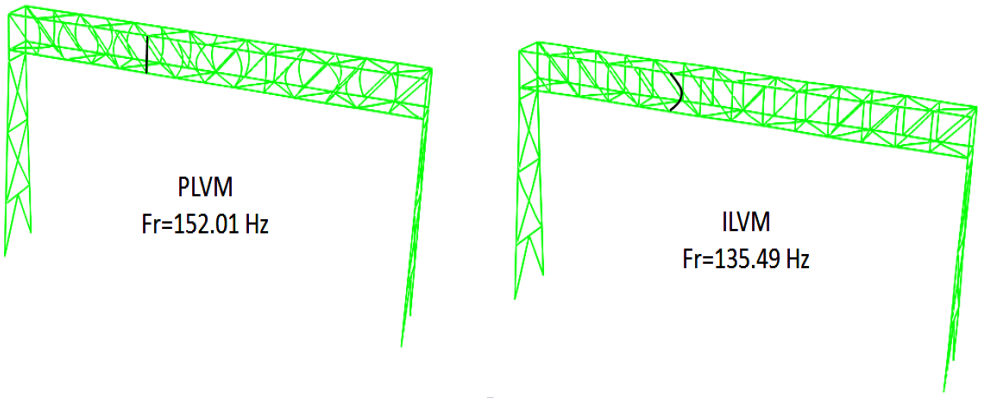

Figure 3-111 PLVM and ILVM of the vertical members set

As shown in the above figures, the damaged members in each members set locally vibrate in lower frequencies than the frequencies of PLVM in which the undamaged members vibrate.

It should be noted that sometimes, in the spectrum, there are more than one peak near ILVM of a damaged member. This phenomenon may happen even without existence of more than one damaged member with the same damage degree. To explain about existence of several peaks for ILVM, the fifth bottom brace, shown in figure 3-96, is damaged by 35% stiffness reduction of the Young's modulus. The velocity time history data of different members are simulated through dynamic implicit analysis while hitting the first bottom brace by 500 N and their power spectral density is examined. Figure 3-112 shows the power spectral density diagrams of the damaged brace, three undamaged bottom braces, the right most bottom brace and one of the lateral members.

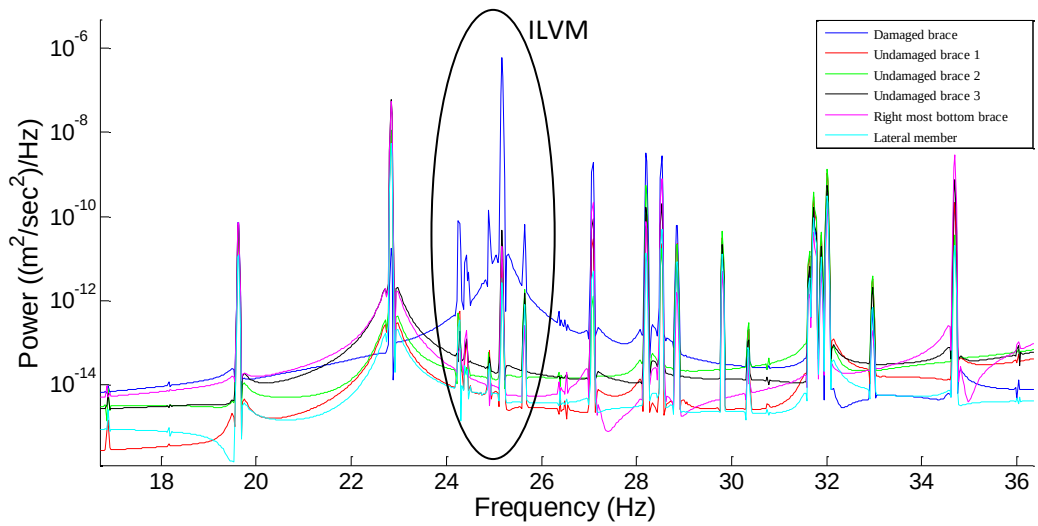

Figure 3-112 PSD diagrams of some members

The amplitude of the damaged brace is much larger than the other members in some peaks circled in the above figure and this damaged member seems locally vibrate in those modes. In fact only one of these peaks in the above figure corresponds to the ILVM of member 5; however, because the frequency of ILVM is at the vicinity of the frequencies of other modes in the structure, the damaged brace has much larger amplitude than the other identical bottom and top braces. Therefore, when many peaks exist, the mean value of the frequencies of these peaks is considered as the frequency of ILVM since these peaks are always close to each other. Figure 3-112 is zoomed on the corresponding range and shown in figure 3-113.

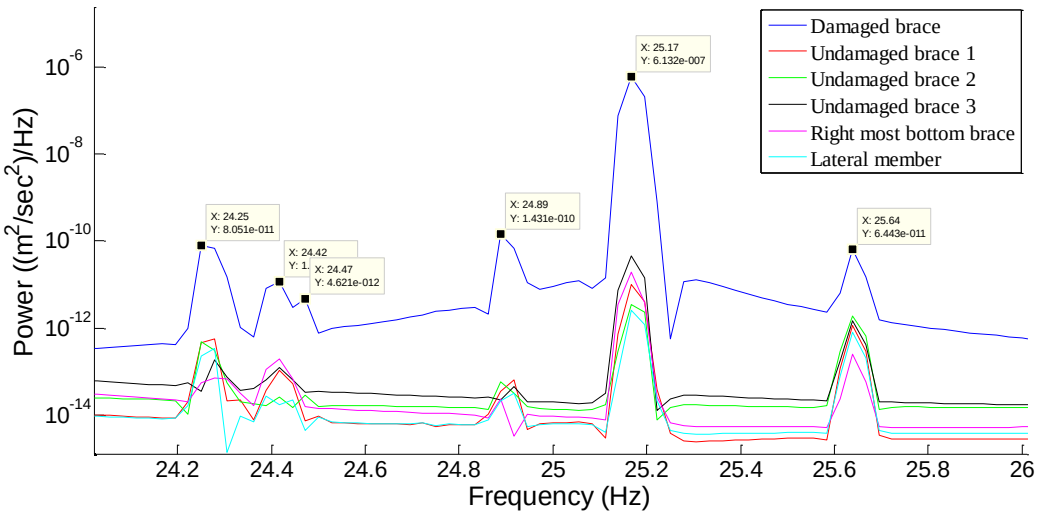

Figure 3-113 PSD diagrams of some members (Near ILVM of the damaged bottom brace)

Figure 3-114 shows the mode shapes of the corresponding peaks obtained through eigenvalue analysis.

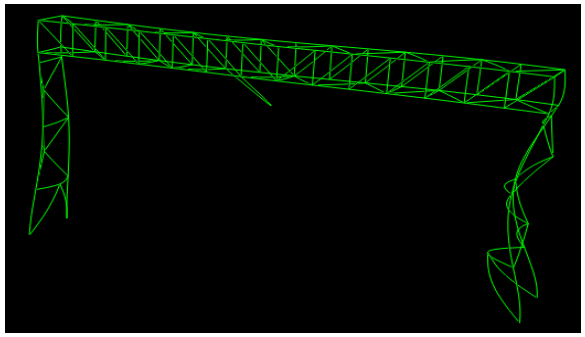

Freq= 24.267 Hz

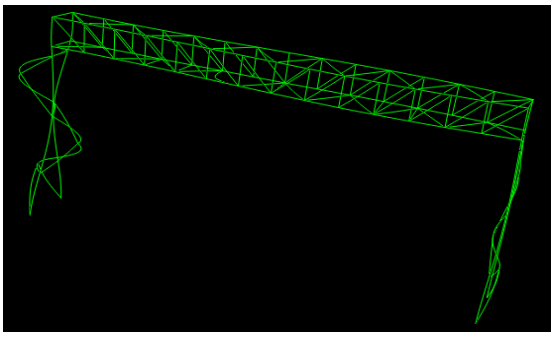

Freq= 24.419 Hz

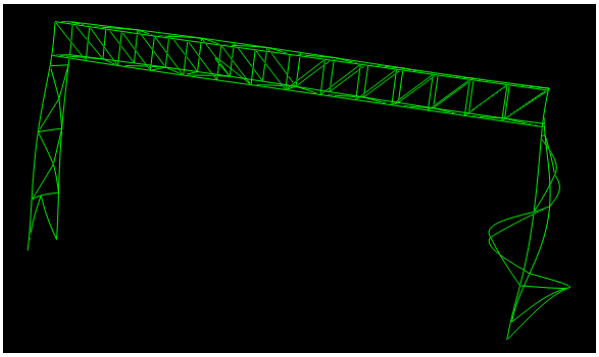

Freq = 24.467Hz

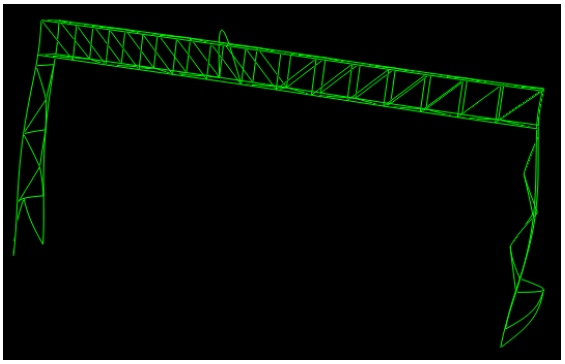

Freq = 24.903 Hz

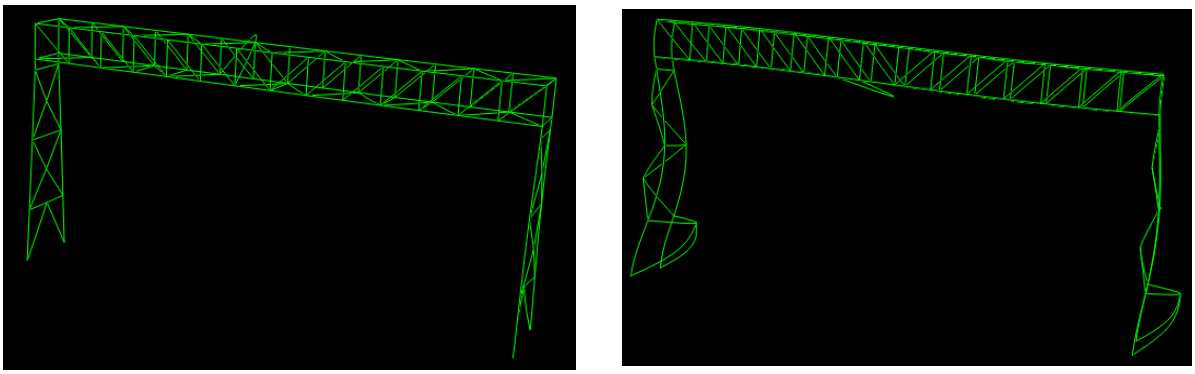

Freq = 25.178 Hz (Real ILVM) Freq = 25.645 Hz

Figure 3-114 Mode shapes of the peaks near ILVM of the fifth bottom brace

It is found that only the mode with 25.178 Hz is ILVM since only the damaged member is strongly vibrating. Figure 3-115 shows the power spectral density diagrams of the fifth bottom brace before damage, three undamaged bottom braces, the right most bottom brace and one of the lateral members while the first bottom brace is hit by 500 N.

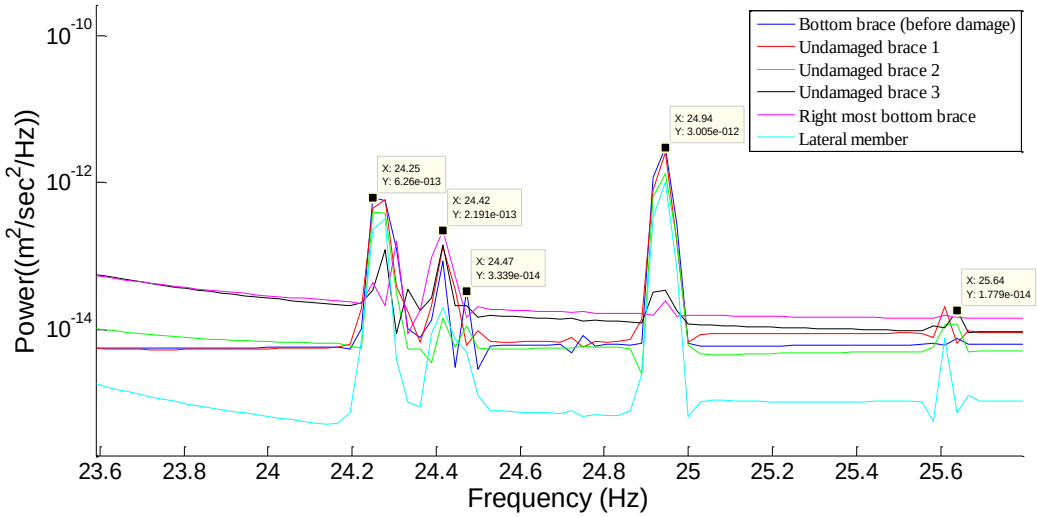

Figure 3-115 PSD diagrams of some members before damage

By comparing figures 3-115 and 3-113, it is found that the peak corresponding to the real ILVM (Freq = 25.178 Hz) appears only after damage.

3.4.3.2 Sensitivity with respect to the stiffness reduction of main members, global and local boundary conditions

In this section, sensitivity analysis of frequencies of PLVM and ILVM is conducted with respect to different parameters. The parameters to be checked are properties of the relevant secondary member, local boundary conditions of the relevant secondary members (stiffness of rotational springs), properties of the longitudinal members and global boundary conditions of the main frame (properties of the columns).

To carry out a sensitivity analysis of the frequencies of PLVM and ILVM of secondary members with respect to the stiffness of rotational springs at their ends, the stiffness of rotational springs at the ends of the bottom braces, as a representative secondary member shown in figure 3-11, changes for different reductions percentage of the stiffness of the member and the frequencies of PLVM and ILVM are calculated through eigenvalue analysis. Figure 3-116 shows the frequencies changes of PLVM and ILVM versus the changes of the stiffness of the rotational spring for the representative secondary member.

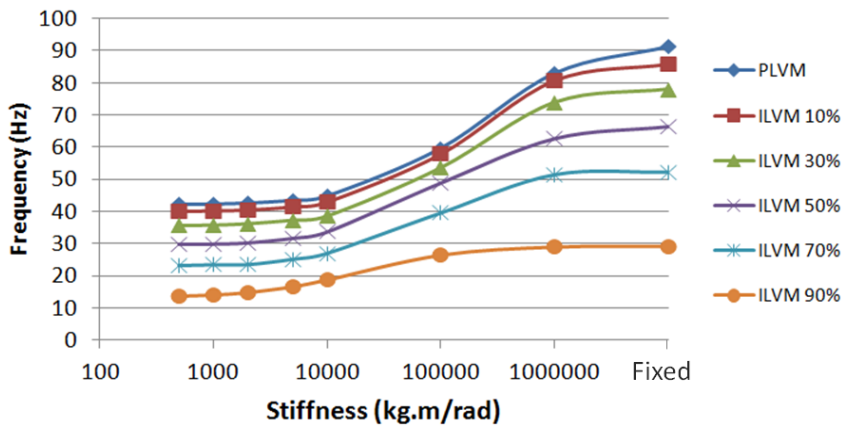

Figure 3-116 Frequencies of PLVM and ILVM changes versus changes of the stiffness of the rotational springs

As shown in the above figure, the frequencies of PLVM and ILVM significantly change as the stiffness of the rotational springs changes from 500 N.m/rad (soft spring) to infinity (fixed local boundary conditions).

In order to examine the sensitivity of the frequencies of PLVM and ILVM of secondary members with respect to the stiffness of main longitudinal members, the stiffness of the main longitudinal members reduces by 20%, 50% and 80% and the frequencies of PLVM and ILVM (for different degree of damage) of the bottom brace, as a representative secondary member shown in figure 3-11, are calculated through eigenvalue analysis. Figure 3-117, 3-118 and 3-119 show the relative changes of the frequencies of PLVM and ILVM while the stiffness of the main longitudinal members reduces by 20%, 50% and 80% respectively. In addition, in these figures the relative changes of frequencies of some global vibration modes are shown to compare with the relative changes of the frequencies of PLVM and ILVM.

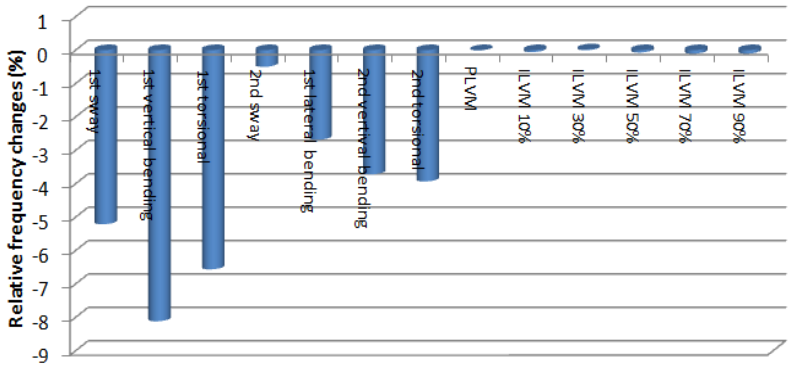

Figure 3-117 Relative frequencies changes of some global modes, PLVM and ILVM (20% stiffness reduction of the main longitudinal members)

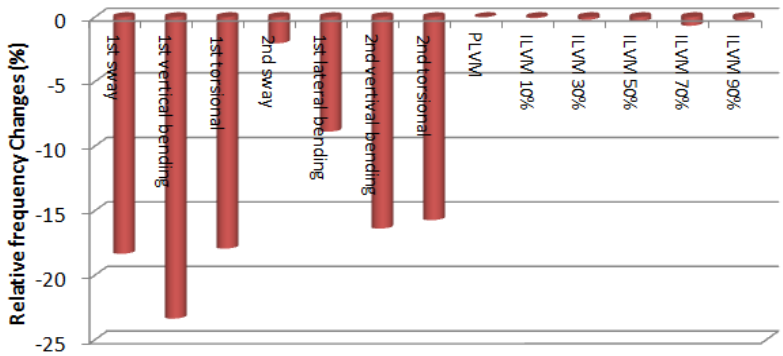

Figure 3-118 Relative frequencies changes of some global modes, PLVM and ILVM (50% stiffness reduction of the main longitudinal members)

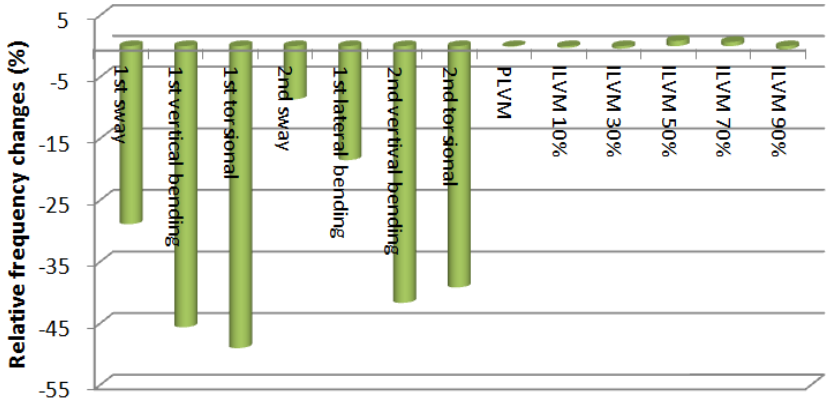

Figure 3-119 Relative frequencies changes of some global modes, PLVM and ILVM (80% stiffness reduction of the main longitudinal members)

It is shown in the above figures that the relative frequencies changes of PLVM and ILVM are small and always less than 0.8% even with 80% reduction of the main members' stiffness. As for global vibration modes, it is seen that the frequencies of global vibration modes are much more sensitive with respect to the properties of the main longitudinal members than frequencies of PLVM and ILVM.

To examine the sensitivity analysis of the frequencies of PLVM and ILVM of secondary members with respect to the global boundary conditions of the main frame, the stiffness of all of the column members are reduced by 20%, 50% and 80% and the frequencies of PLVM and ILVM (for different degree of damage) of the bottom brace, as a representative secondary member shown in figure 3-11, are calculated through eigenvalue analysis. Figure 3-120, 3-121 and 3-122 show the relative changes of the frequencies of PLVM and ILVM while the stiffness of the two columns reduce by 20%, 50% and 80% respectively. In addition, in these figures the relative changes of frequencies of some global vibration modes are shown to compare with the relative changes of the frequencies of PLVM and ILVM.

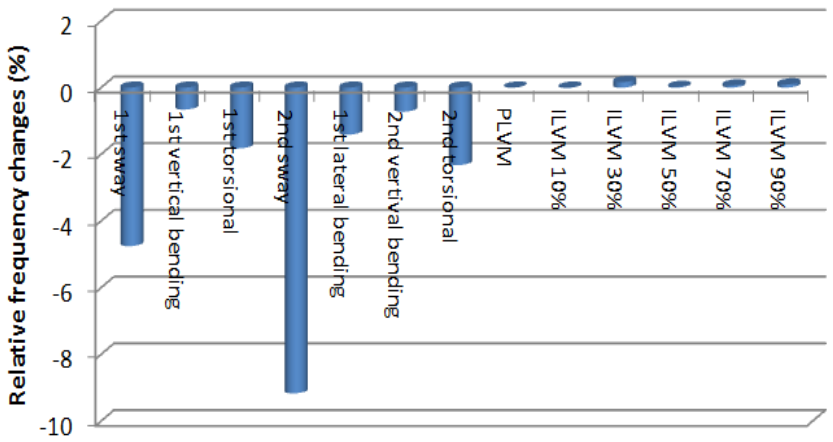

Figure 3-120 Relative frequencies changes of some global modes, PLVM and ILVM (20% stiffness reduction of the two columns)

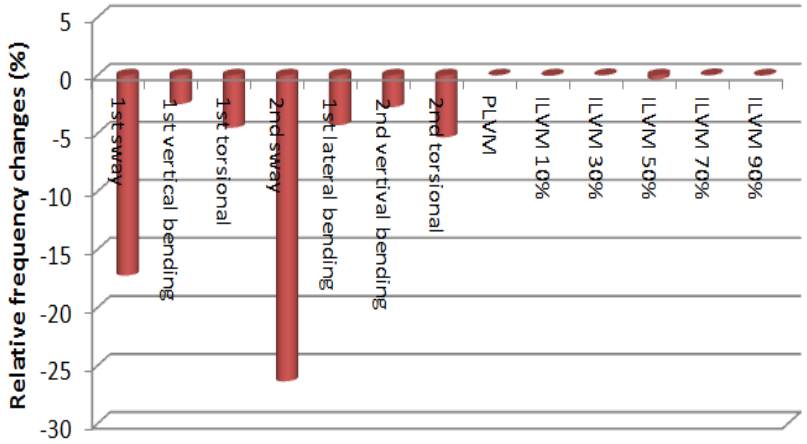

Figure 3-121 Relative frequencies changes of some global modes, PLVM and ILVM (50% stiffness reduction of the two columns)

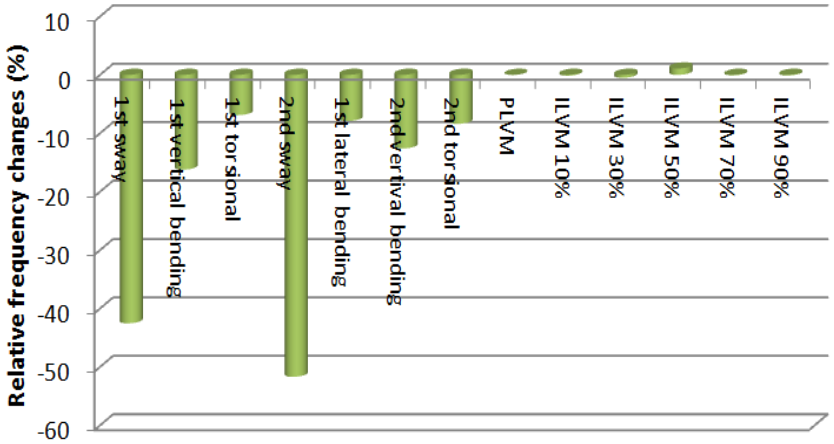

Figure 3-122 Relative frequencies changes of some global modes, PLVM and ILVM (80% stiffness reduction of the two columns)

The relative frequencies changes of PLVM and ILVM are small and always less than 1% even with 80% stiffness reduction of the two columns. As compared to global vibration modes, it is seen that the frequencies of global vibration modes are much more sensitive with respect to the properties of the two columns than the frequencies of PLVM and ILVM.

The conclusion of the above sensitivity analyses is that frequencies of PLVM and ILVM are sensitive to the local internal connections as well as the properties of the corresponding member, but they have a small sensitivity to the global boundary conditions of the main frame as well as the properties of the main longitudinal members. Therefore, the proper parameters in damage quantification based on updating procedures are local internal connections and the properties of the corresponding member. The effects of global boundary conditions of the main frame and the properties of the main longitudinal members on the frequencies of PLVM and ILVM are negligible. The change in frequencies of these modes is used for damage identification. The details of damage identification techniques using PLVM and ILVM are explained in chapter 5.

3.5 Observability analysis of vibration modes

Application of local vibration modes in damage identification of space structures has not been well studied. The reasons include:

- The observability problem using common sensors. Vibration is small and attaching contact type sensors may affect local vibration characteristics.
- The differentiation problem. Distinguishing the type of local vibration modes is difficult.

However, using recent precise sensors such as Laser Doppler Vibrometer (LDV), these modes may be observed and by utilizing accurate analysis, these modes may be distinguished from each others.

During field measurement, global vibration modes are usually observed by analyzing the time history data, such as displacement, velocity or acceleration. Yet, the observability of local vibration modes such as PLVM or ILVM is not well known since they are usually excited by high frequency components which have small power. Consider the members shown in figure 3-123.

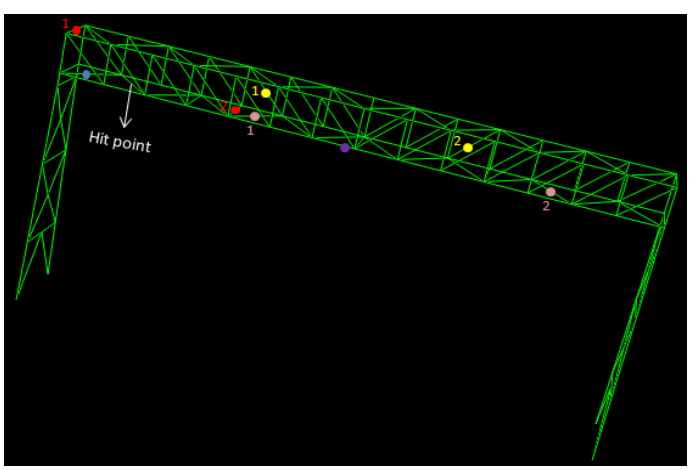

Figure 3-123 Different members of the main frame

The velocity time histories of the members are simulated through dynamic implicit analysis while hitting the bottom brace by 500 N. Then, power spectral density (PSD) of the simulated data is examined. The sampling frequency is 5000 Hz. Figure 3-124 shows the power spectral density diagrams of the members below 80 Hz.

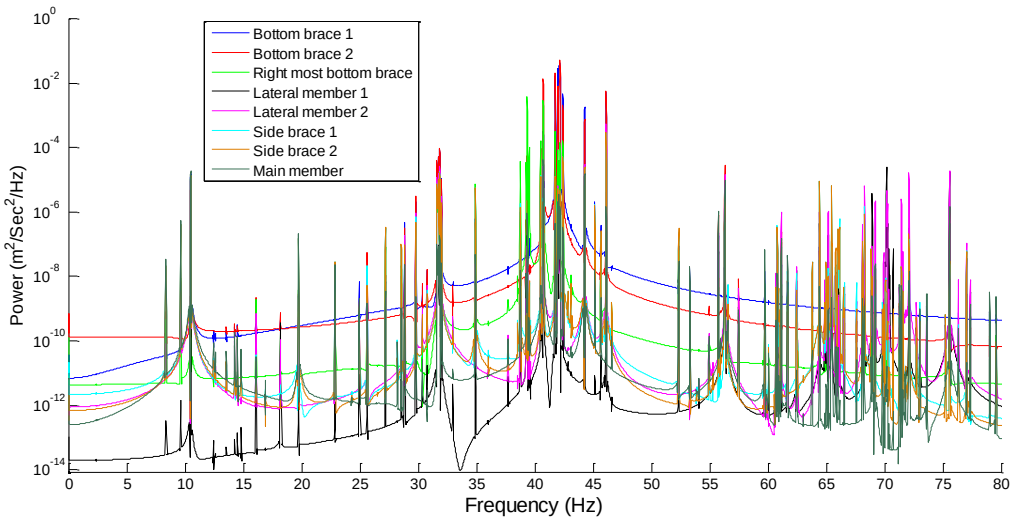

Figure 3-124 Power spectral density diagrams of some members below 80 Hz

As shown in the above figure, there are many peaks corresponding to different vibration modes observed below 80 Hz and distinguishing the type of these modes can be difficult. As examples, the first 20 largest peaks are chosen and the corresponding mode shapes, extracted through eigenvalue analysis, are shown in figures 3-125, 3-126, 3-127, 3-128, 3-129 and 3-130.

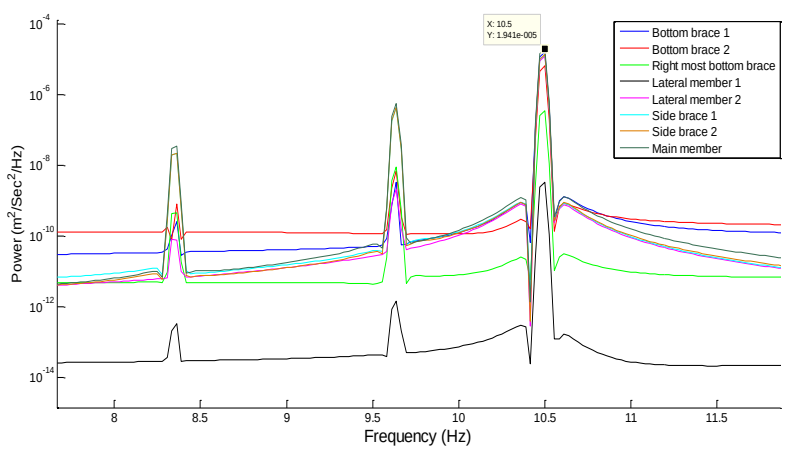

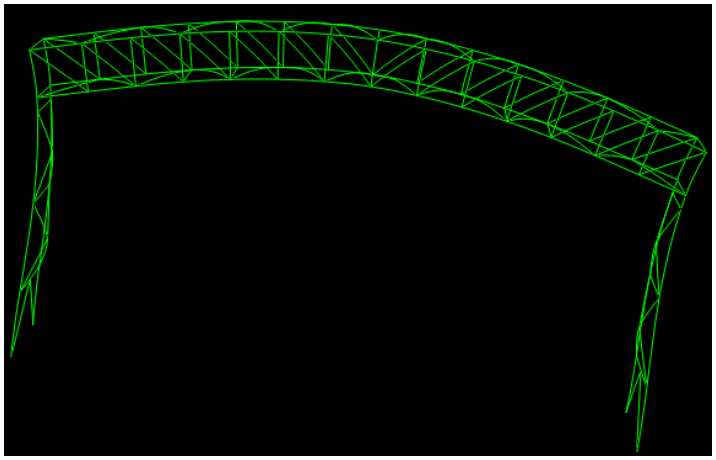

Freq = 10.489 Hz (global mode)

Figure 3-125 A peak in PSD diagrams and the corresponding mode shape (8 Hz-12 Hz)

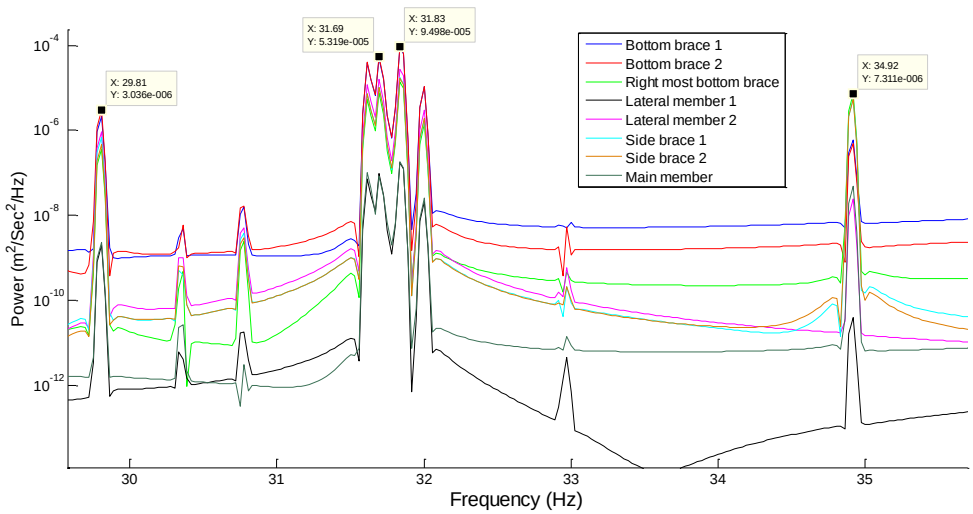

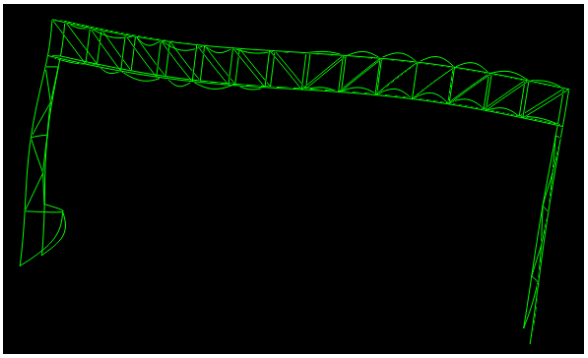

Freq = 29.803 Hz (coupled global-local mode)

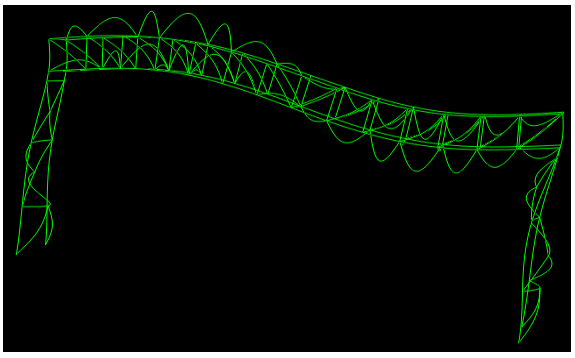

Freq = 31.701 Hz (coupled global-local mode)

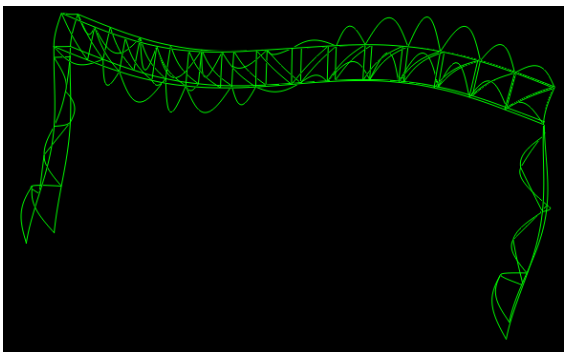

Freq = 31.849 Hz (coupled global-local mode)

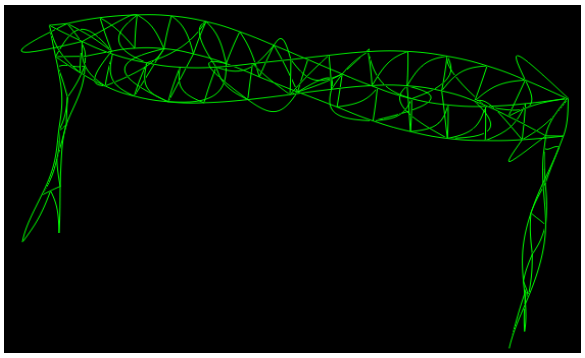

Freq = 34.917 Hz (coupled global-local mode)

Figure 3-126 Peaks in PSD diagrams and the corresponding mode shapes (29 Hz-35 Hz)

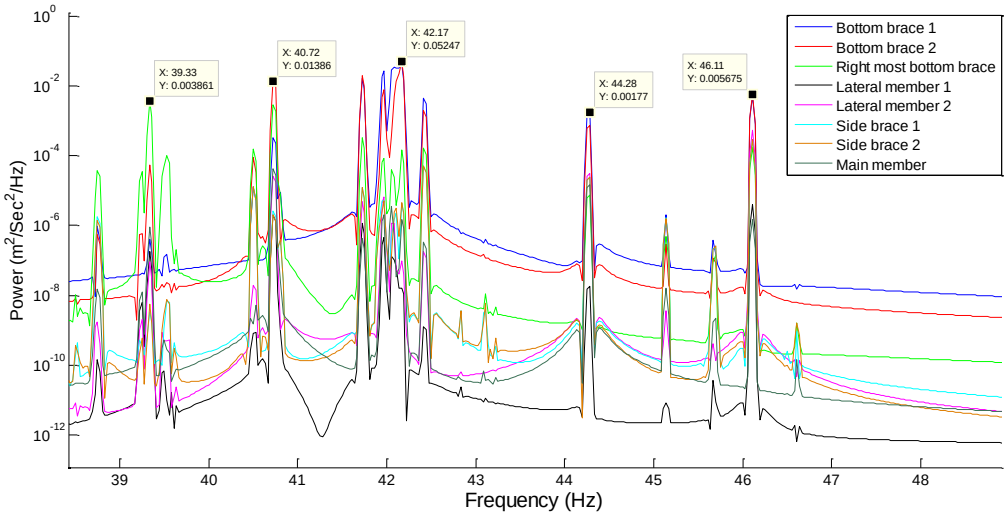

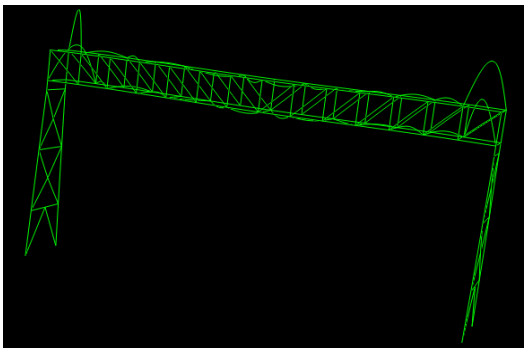

Freq = 39.346 Hz (Coupled local mode)

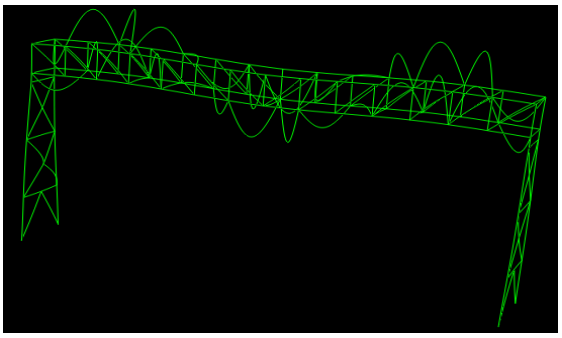

Freq = 40.742 Hz (Coupled local mode)

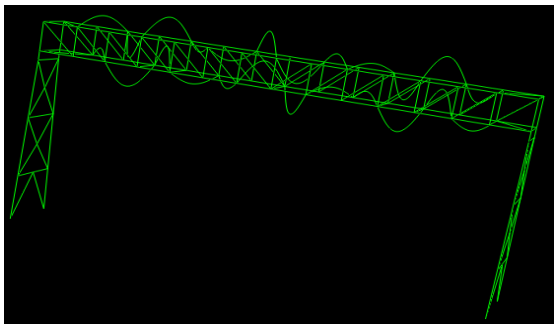

Freq = 42.188 Hz (PLVM of the bottom and top braces)

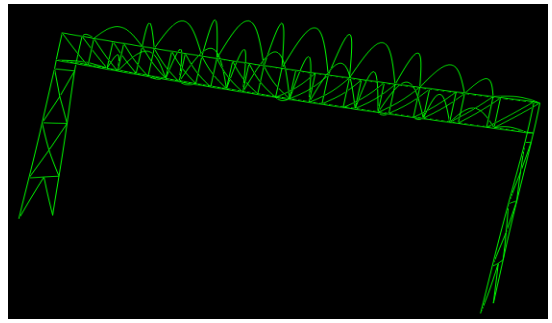

Freq = 44.277 Hz (Coupled local mode)

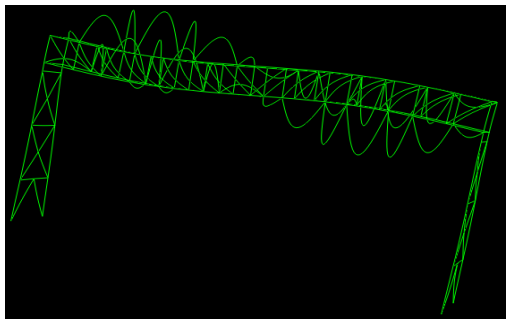

Freq = 46.123 Hz (Coupled global-local mode)

Figure 3-127 Peaks in PSD and the corresponding mode shapes (38 Hz-48 Hz)

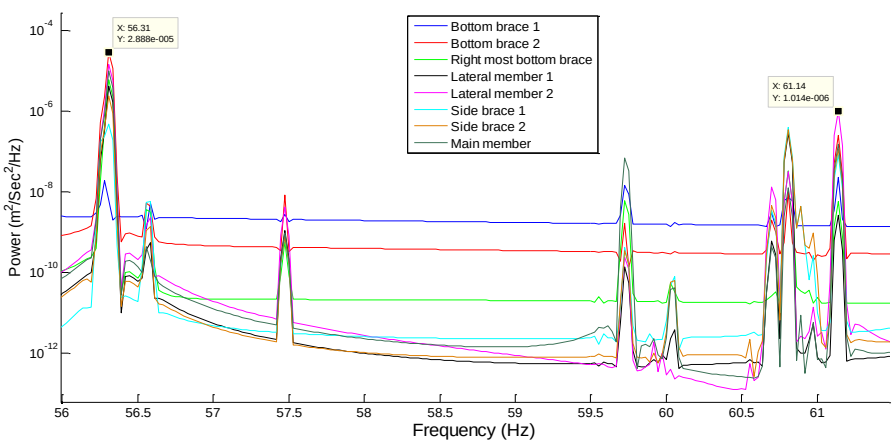

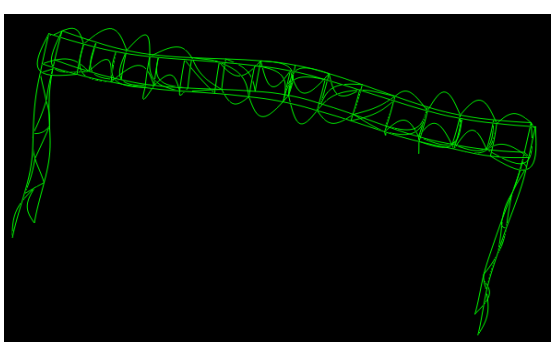

Freq = 56.336 Hz (Coupled global-local mode)

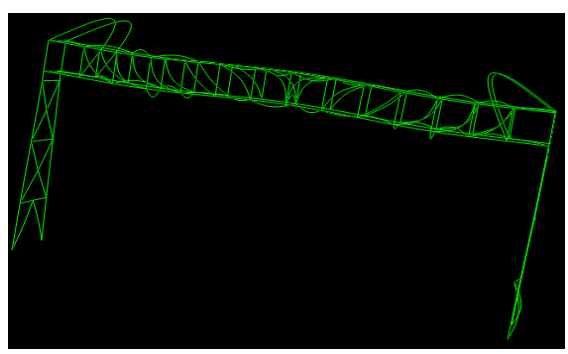

Freq = 61.168 Hz (Coupled local mode)

Figure 3-128 Peaks in PSD and the corresponding mode shapes (56 Hz-62 Hz)

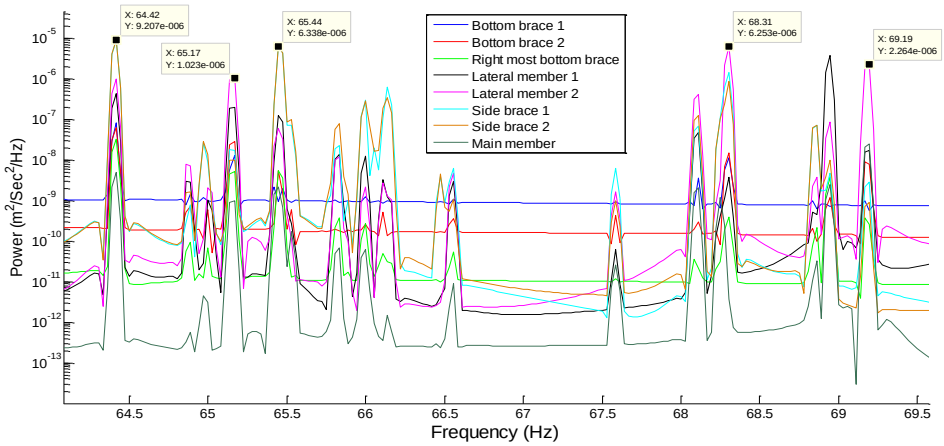

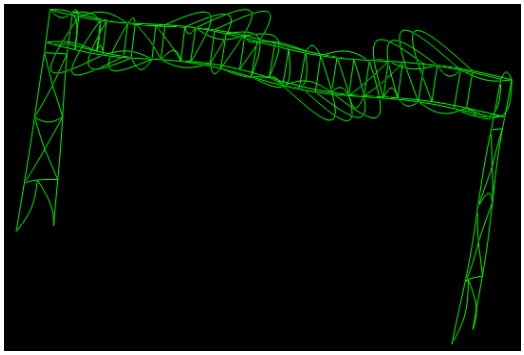

Freq = 64.446 Hz (Coupled global-local mode)

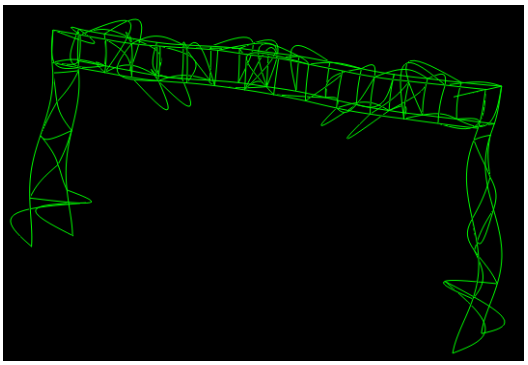

Freq = 65.191 Hz (partially chaotic local mode)

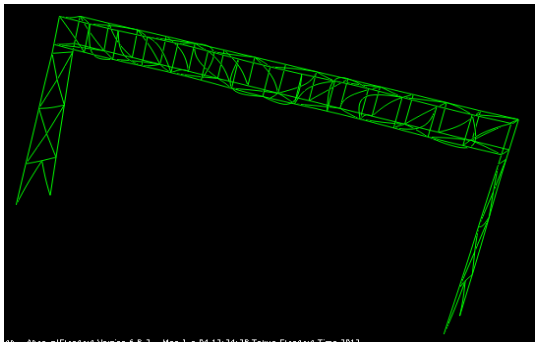

Freq = 65.670 Hz (Coupled local mode)

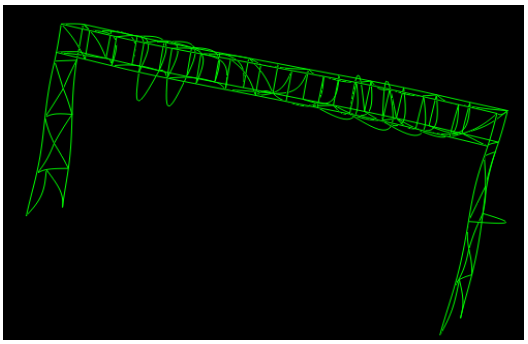

Freq = 68.344 Hz (Coupled local mode)

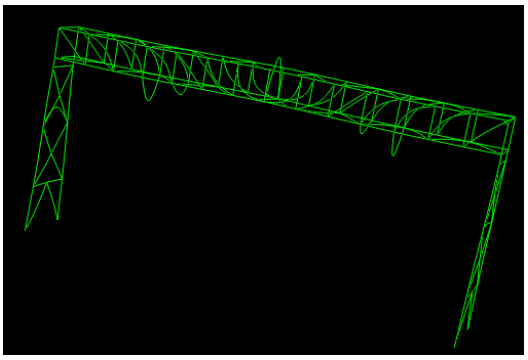

Freq = 69.227 Hz (Coupled local mode)

Figure 3-129 Peaks in PSD and the corresponding mode shapes (64 Hz-70 Hz)

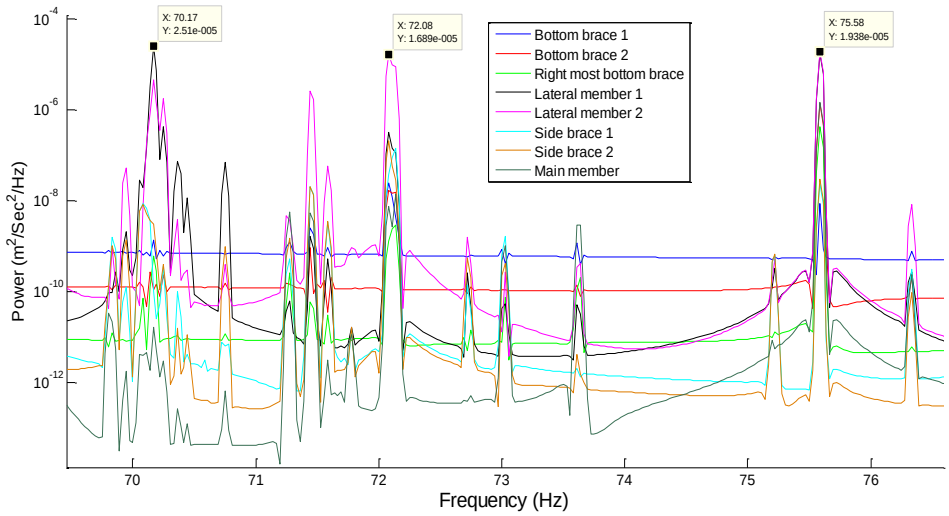

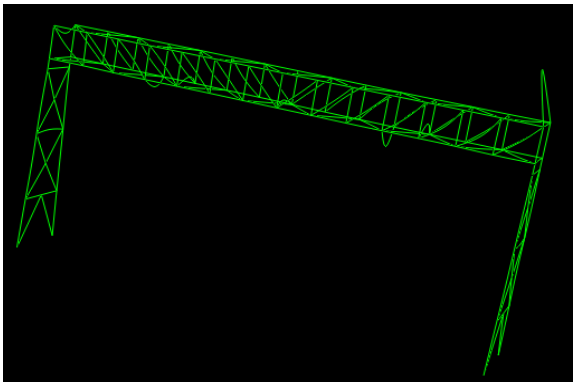

Freq = 70.168 Hz (PLVM of the lateral members)

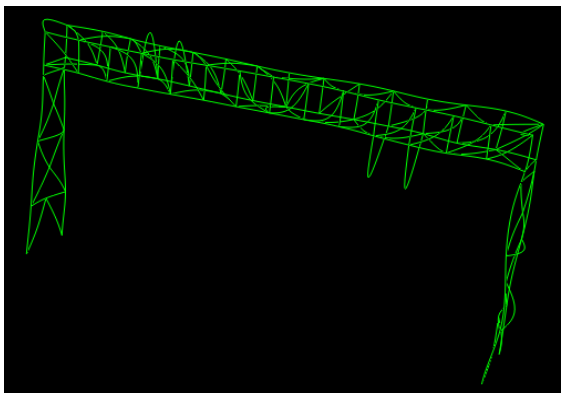

Freq = 72.129 Hz (Coupled local mode)

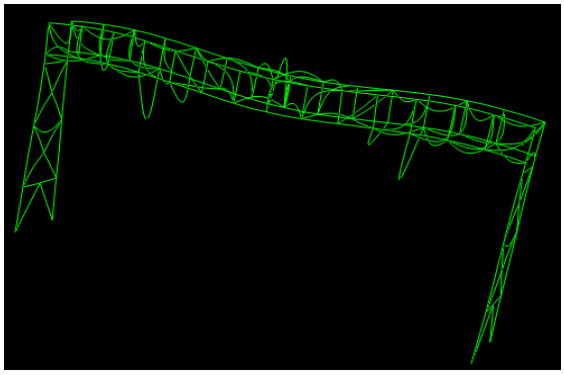

Freq = 75.647Hz (Coupled global-local mode)

Figure 3-130 Peaks in PSD and the corresponding mode shapes (70 Hz-77 Hz)

Distinguishing the type of these modes, in particular PLVM and ILVM, can be difficult only using power spectral density diagrams of few members and needs to have measurement data of various members from different parts of the structure.

In order to find a better vibration test to observe PLVM in the belt conveyor, the velocity time history of different members of the main frame is simulated in the finite element model while bottom parts of the

columns are hit as well as hitting one of the secondary members. Then, Fourier spectrum of the simulated velocity time data is examined. Comparison of the Fourier amplitudes of the peaks corresponding to the global vibration modes and PLVM of the secondary members specify the situations in which PLVM are feasible to observe since, in reality, lower global vibration modes are usually observable.

3.5.1 Amplitude comparison of vibration modes (hit at the bottom of the columns)

First, the bottom parts of columns are hit and the velocity time history of different members of the main frame is simulated in finite element model. The hit points are shown in figure 3-124. To make sure which peaks correspond to PLVM, the data for some identical members together with some different members are examined. If there are peaks in which the amplitude of identical members is much larger than the other members, the peaks are PLVM corresponding to those identical members. As an example, the vertical velocity time history of the middle point of members 2, 4, 12, 16, 22 and 23, shown in figure 3-131, is used to examine their Fourier spectrums.

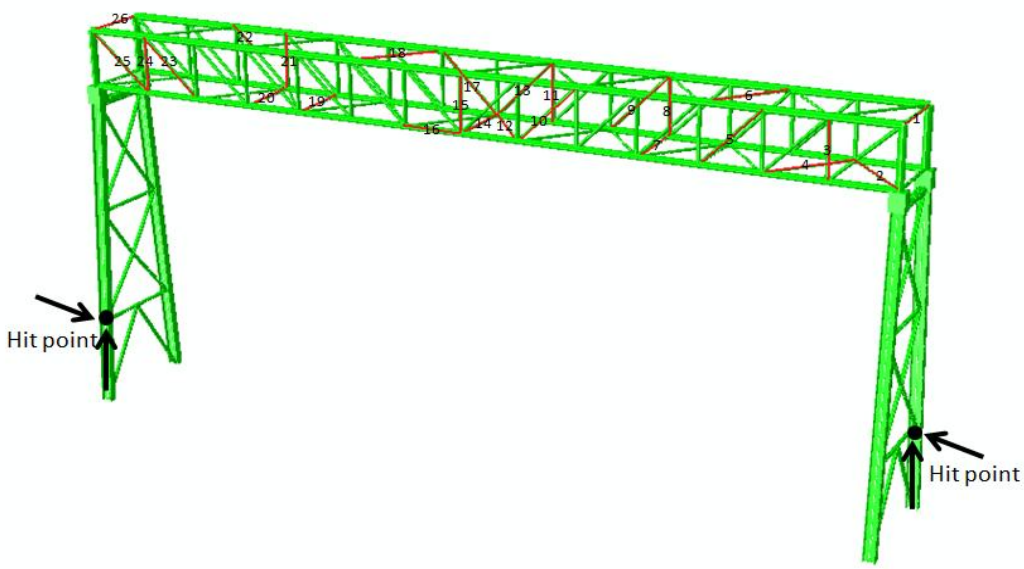

Figure 3-131 Some members of the main frame and hit points

The Fourier spectrums are plotted in figure 3-132. It should be noted that members 4, 12 and 22 are identical.

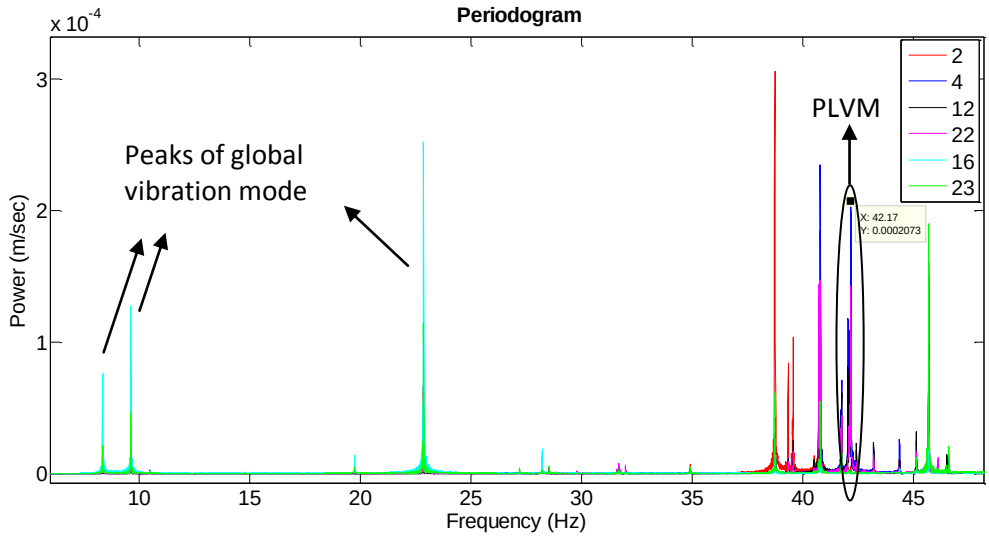

Figure 3-132 Fourier spectrums of some members (PLVM of the bottom and top braces)

As shown in the above figure, the power of PLVM exceeds the power of some global vibration modes. Therefore, in a real measurement, if those global vibration modes are observed, which is usually the case, the PLVM is observable. To confirm that the amplitudes of the identical braces are much larger than the other members in the PLVM range, the corresponding part of figure 3-132 is zoomed in and shown in figure 3-133.

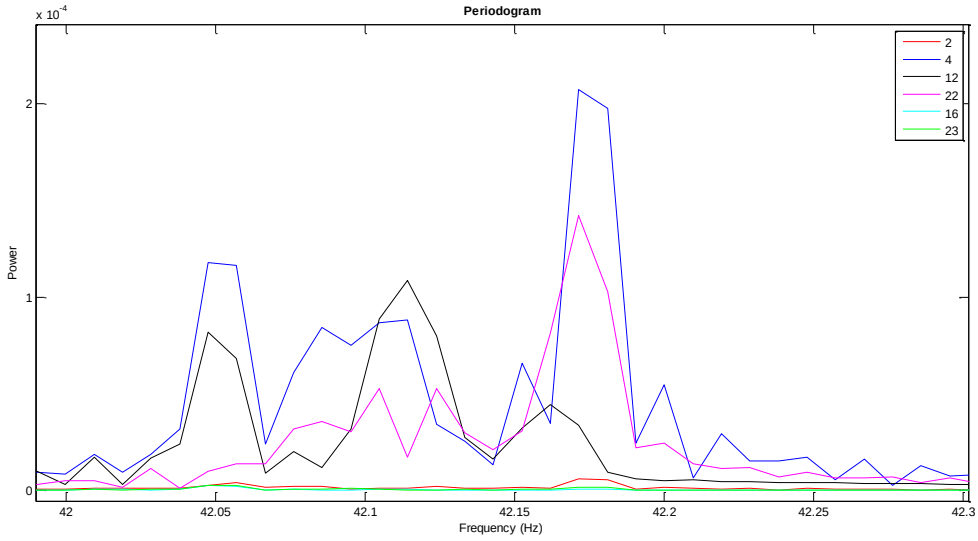

Figure 3-133 Fourier spectrums of some members in the range of 42 to 42.3 Hz

As shown in the above figure, the amplitudes of the identical braces are much larger than the other members at the PLVM range.

As another example, the vertical velocity time history of the middle point of members 1, 7, 14, 19, 20, 26 and 16, shown in figure 3-131, is used to examine their Fourier spectrums. The Fourier spectrums are plotted in figure 3-134. It should be noted that members 1, 7, 14, 19, 20, 26 are identical lateral members.

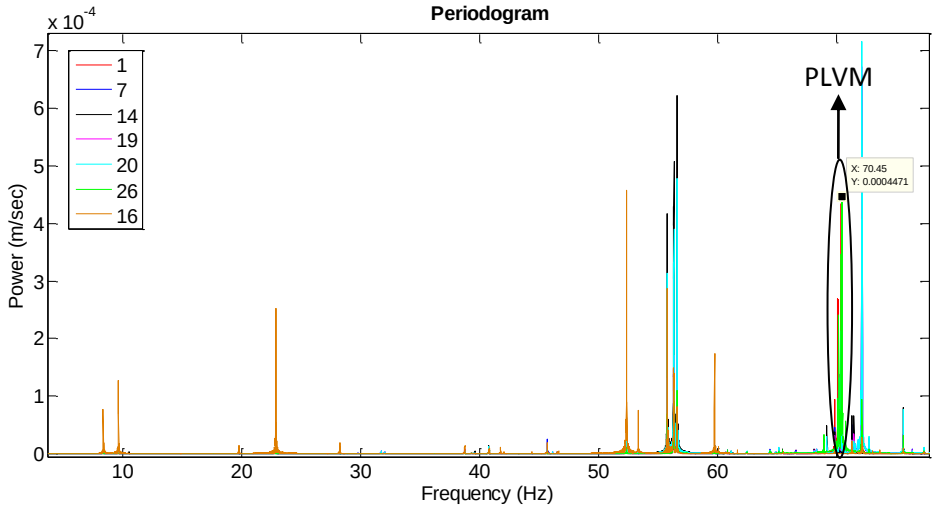

Figure 3-134 Fourier spectrums of some members (the PLVM of the lateral members)

Only the peaks around 70 Hz are PLVM corresponding to the lateral members because their power for the lateral members are much larger than member 16 which is a longitudinal member. Moreover, the power of PLVM exceeds the power of global vibration modes. Therefore, if the global vibration modes can be observed, which is usually the case, the PLVM is observable. To confirm that the amplitudes of the identical lateral members at the PLVM range are much larger than the amplitude of member 16 which is a longitudinal member, the corresponding part of figure 3-134 is zoomed in and shown in figure 3-135.

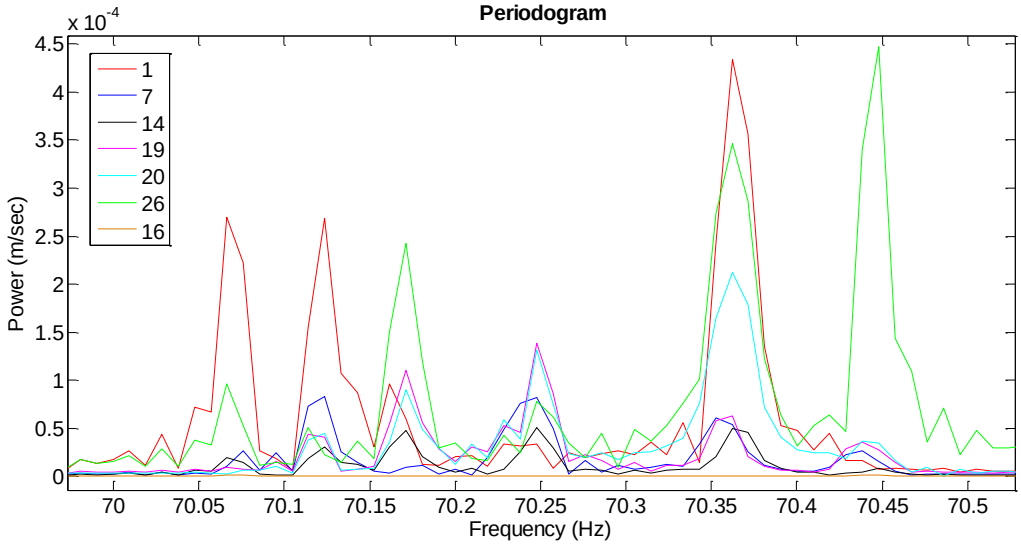

Figure 3-135 Fourier spectrums of some members in the range of 70 to 70.5 Hz

As shown in the above figure, at the PLVM range, the amplitudes of the identical lateral members are much larger than the amplitude of member 16.

In order to check the observabality of PLVM corresponding to the vertical members in the structure, the simulated velocity time history along the longitudinal direction at the middle point of members 3, 8, 11, 15, 21, 5 and 25, shown in figure 3-131, is used to examine their Fourier spectrums. The Fourier spectrums are plotted in figure 3-136. It should be noted that members 3, 8, 11, 15, 21 are identical vertical members.

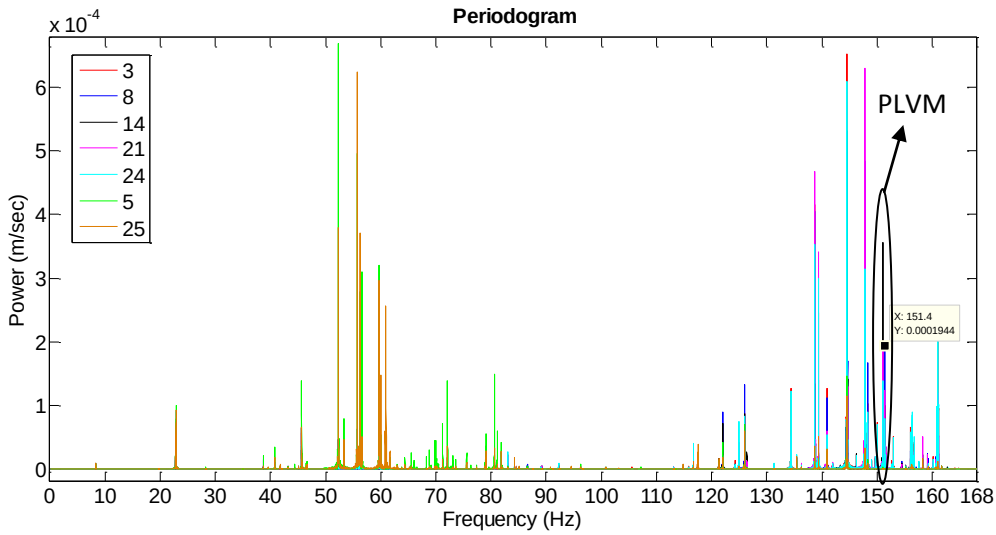

Figure 3-136 Fourier spectrums of some members (PLVM of the vertical members)

Only the specified peaks in the above figure are PLVM corresponding to the vertical members because their power for the vertical members are much larger than members 5 and 25 which are side braces. Moreover, the power of PLVM exceeds the power of global vibration modes. Therefore, if the global vibration modes can be measured, which is usually the case in real measurements, the PLVM is observable. In order to confirm that the amplitudes of the identical vertical members are much larger than the amplitudes of members 5 and 25 at the PLVM range, the corresponding part of figure 3-136 is zoomed in and shown in figure 3-137.

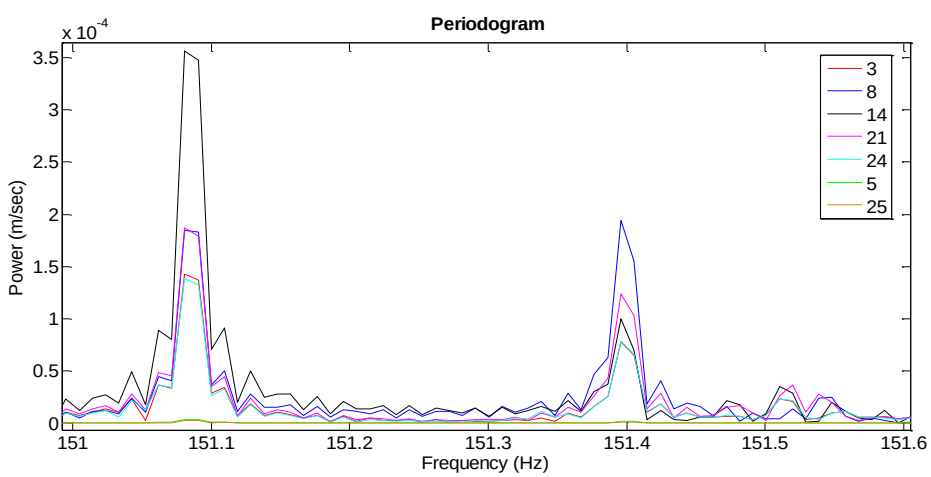

Figure 3-137 Fourier spectrums of some members in the range of 151 to 151.6 Hz

As shown in the above figure, at the PLVM range, the amplitudes of the identical vertical members are much larger than the amplitudes of members 5 and 25 which are side braces.

To check the observabality of PLVM corresponding to the identical side braces in the belt conveyor, the vertical velocity time history of the middle point of members 5, 9, 13, 17, 23, 25 and 6, shown in figure 3-131, is used to examine their Fourier spectrums. The Fourier spectrums are plotted in figure 3-138. It should be noted that members 5, 9, 12, 23 are identical side braces.

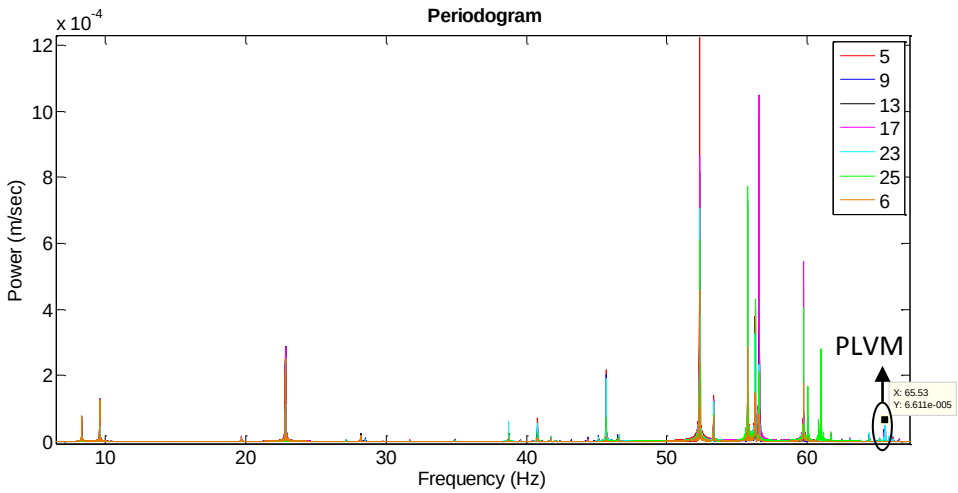

Figure 3-138 Fourier spectrums of some members (PLVM of the side braces)

Only the specified peaks in the above figure are PLVM corresponding to the side braces because their power for the side braces are much larger than members 25 and 6 which are not identical with the side braces. Yet, the power of PLVM does not exceed the power of global vibration modes. Therefore, the observability of these PLVM cannot be judged from the observability of the global vibration modes. In order to confirm that the amplitudes of the identical side braces are much larger than the amplitudes of members 25 and 6 at the PLVM range, the corresponding part of figure 3-138 is zoomed in and shown in figure 3-139.

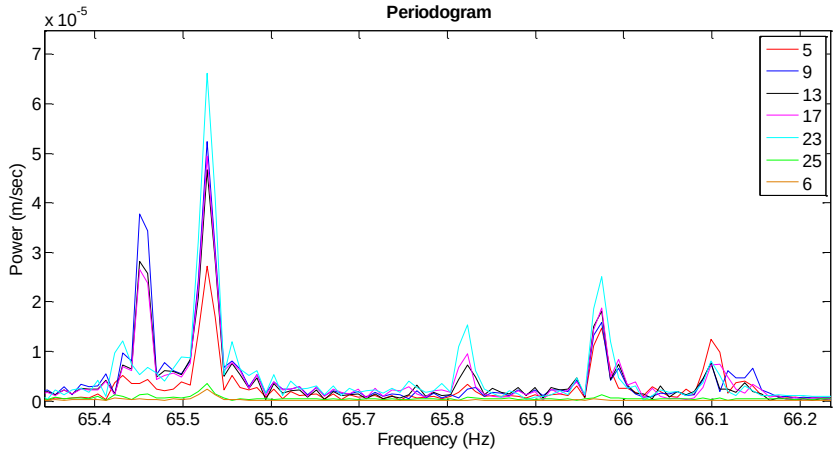

Figure 3-139 Fourier spectrums of some members in the range of 65.4 to 66.2 Hz

As shown in the above figure, at the PLVM range, the amplitudes of the identical side braces are much larger than the amplitudes of members 2 and 25 which are not identical with the side braces.

It is found from the above analyses, which corresponds to the case that the bottom parts of the columns are hit, that the PLVM of the bottom and top braces, lateral members and vertical members are most likely observable since their power exceeds than the power of some global vibration modes. Yet, since the power of the PLVM corresponding to the side braces does not exceed the power of any global vibration modes, the observability of these PLVM cannot be judged from the observability of global vibration modes. However, in reality, the excitation force which includes ambient vibrations may be different from the case presented here and the Fourier spectrum amplitudes of global vibration modes may be larger than those of PLVM corresponding to the secondary members.

3.5.2 PLVM amplitude comparison (hit at a secondary member)

This time, the middle of brace 1, shown in figure 3-96, is hit by 500 N along the vertical direction. The velocity time history of the middle point of the secondary members is simulated and their Fourier spectrums are examined. Then, the Fourier spectrum amplitude at PLVM of each secondary member is compared with the one in the previous part where the bottom parts of the columns were hit. Figures 3-140, 3-141 and 3-142 respectively show the maximum amplitude of Fourier spectrum of each bottom and top brace, lateral member and side brace in their own PLVM range.

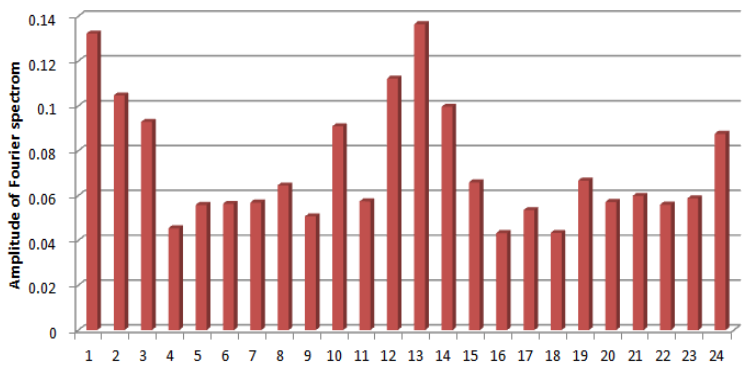

Figure 3-140 Maximum amplitude of Fourier spectrum of each bottom and top brace in their PLVM range

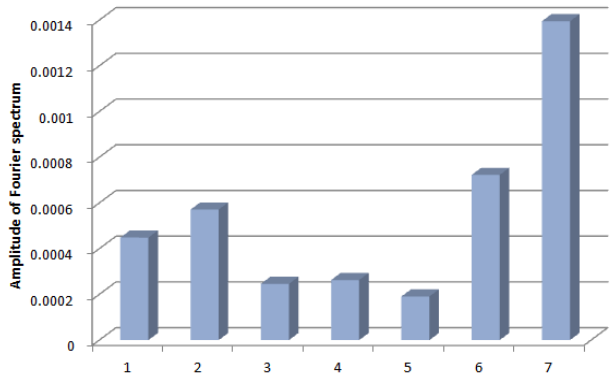

Figure 3-141 Maximum amplitude of Fourier spectrum of each lateral member in their PLVM range

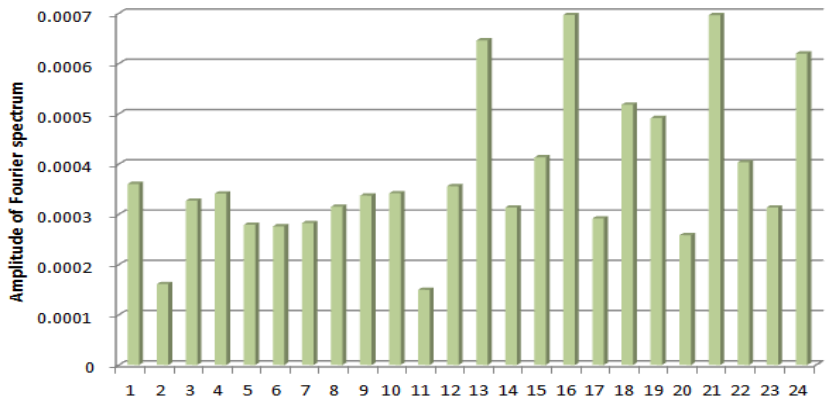

Figure 3-142 Maximum amplitude of Fourier spectrum of each side brace in their PLVM range

In the above figures, the amplitudes of Fourier spectrum are much larger in all the bottom and top braces compared to the lateral members and the side braces in their PLVM range when brace 1 is hit. Figures 3-143, 3-144 and 3-145 respectively show the relative amplitude of Fourier spectrum for each bottom and top brace, lateral member and side brace in their PLVM range when brace 1 and the bottom parts of the columns are hit.

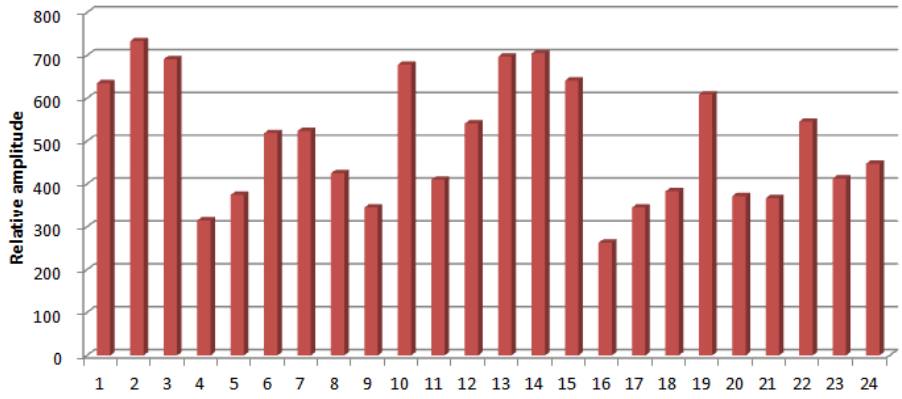

Figure 3-143 Relative amplitude of Fourier spectrum of each bottom and top brace in their PLVM range

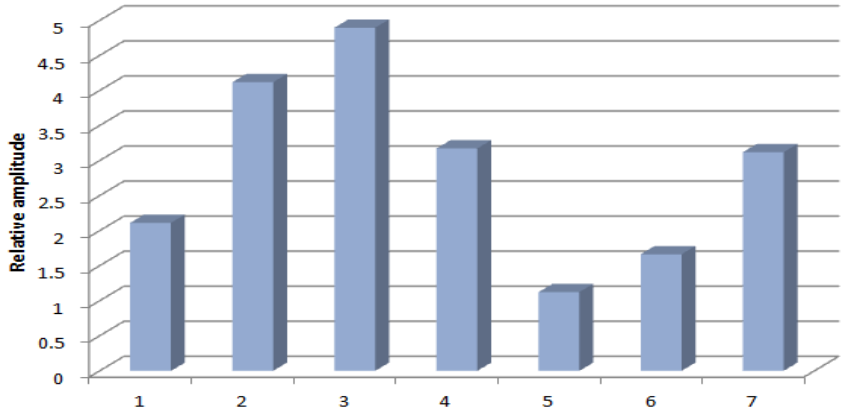

Figure 3-144 Relative amplitude of Fourier spectrum of each lateral member in their PLVM range

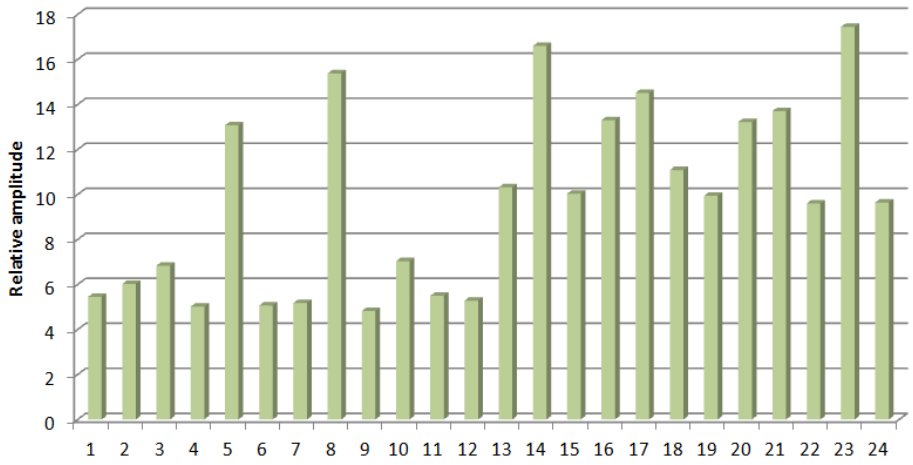

Figure 3-145 Relative amplitude of Fourier spectrum of each side brace in their PLVM range

The relative amplitude of all the bottom and top braces is significantly larger than the other secondary members in their PLVM range. Note that although the hitting point is only on the first brace, the amplitude of the other identical members (bottom and top braces) remarkably increases. Same results are obtained when another bottom and top brace is hit. Therefore, by hitting one of the identical bottom and top braces, PLVM of the other identical bottom and top braces are significantly excited.

Next, the middle of one of the lateral members at the bottom part of the main frame is hit by 500 N along the vertical direction. The velocity time history of the points at the middle of the secondary members is simulated and their Fourier spectrums are examined. Figures 3-146, 3-147 and 3-148 respectively show the maximum amplitude of Fourier spectrum of each bottom and top brace, lateral member and side brace in their own PLVM range.

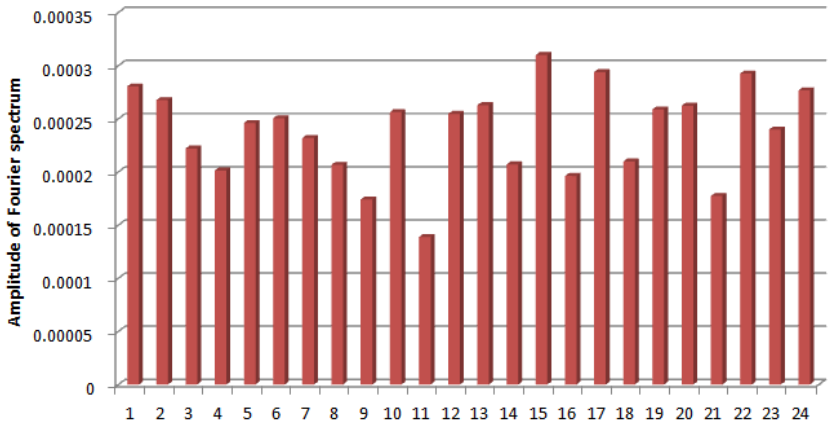

Figure 3-146 Maximum amplitude of Fourier spectrum of each bottom and top brace in their PLVM range

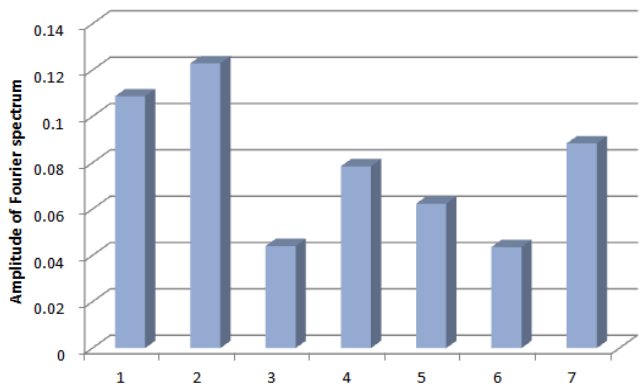

Figure 3-147 Maximum amplitude of Fourier spectrum of each lateral member in their PLVM range

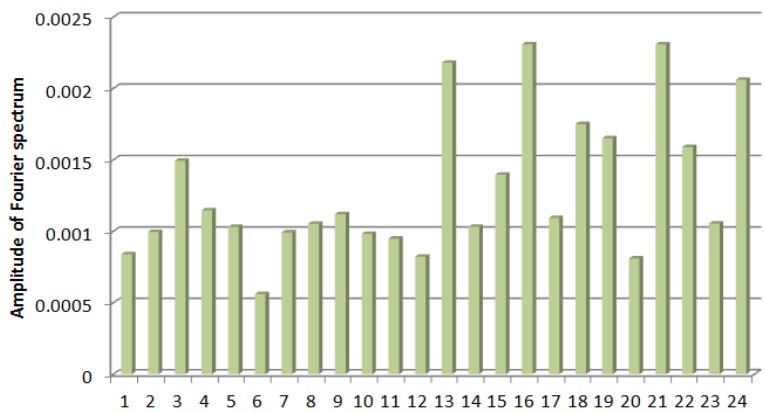

Figure 3-148 Maximum amplitude of Fourier spectrum of each side brace in their PLVM range

As shown in the above figures, the amplitude of Fourier spectrum is much larger in all the lateral members compared to the bottom, top and side braces in their PLVM range when only one of the lateral members (No 1) is hit. Figures 3-149, 3-150 and 3-151 respectively show the relative amplitude of Fourier spectrum for each bottom and top brace, lateral member and side brace in their PLVM range when one of the lateral members and the bottom parts of the columns are hit.

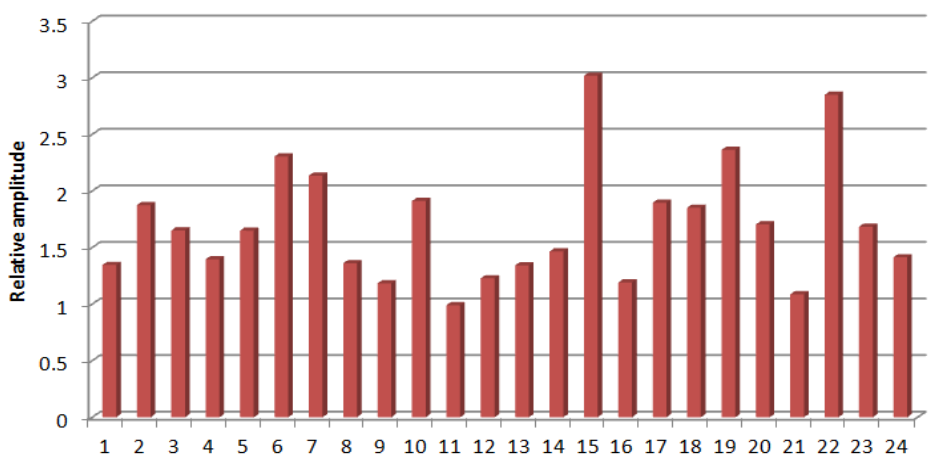

Figure 3-149 Relative amplitude of Fourier spectrum of each bottom and top brace in their PLVM range

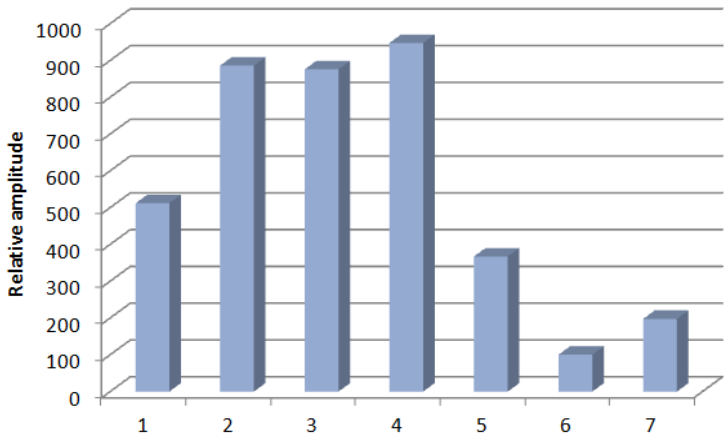

Figure 3-150 Relative amplitude of Fourier spectrum of each lateral member in their PLVM range

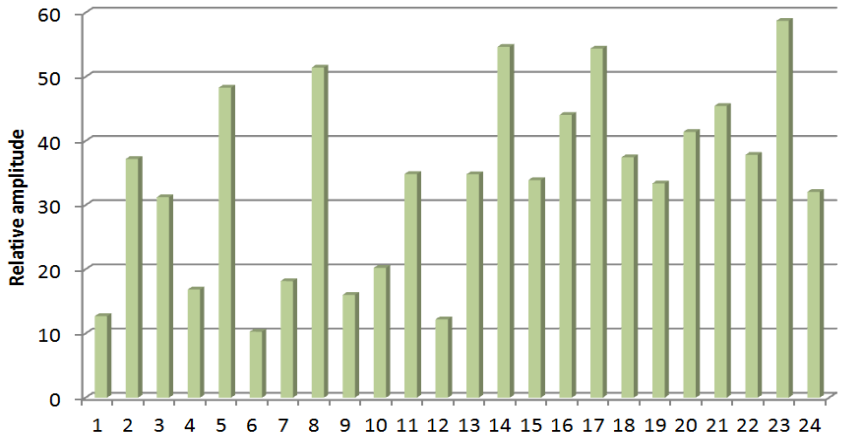

Figure 3-151 Relative amplitude of Fourier spectrum of each side brace in their PLVM range

The relative amplitude of all the bottom and top braces is significantly larger than the other secondary members in their PLVM range. Note that although the hitting point is only on the lateral member 1, the amplitude of the other identical lateral members significantly increases. Same results are obtained when another lateral identical member is hit. Therefore, by hitting one of the identical lateral members, PLVM of the other identical lateral members are remarkably excited. It should be noted that the relative amplitude of Fourier spectrum of the side braces is larger than the bottom and top braces while hitting one of the lateral members because the frequency of PLVM of the side braces and the lateral members are close to each other. Same results are obtained when one of the side braces or vertical members is hit.

The main conclusion of this part is that PLVM corresponding to each secondary members set are easily observed while one of the identical members of the corresponding set is hit. This is appropriate since, in reality, we may not be able to access all members to directly hit. In a real measurement, it might be even better than directly hitting each member since the output may be over ranged while each member is directly hit; yet, by hitting one of the identical members with the same impact force as hitting directly, we may solve the problem of over ranging and significantly excite PLVM of the corresponding identical members set.

3.6 Summary

This chapter mainly discusses sensitivity of vibration modes to damage of the members of a finite element model. Sensitivity of frequencies of the 1st lateral bending, 1st torsional and 1st vertical bending modes are examined with respect to the stiffness changes of different members in the support structure of a typical belt conveyor. The results show, generally, these frequencies do not change so much but can be used to predict the presence of damage in the structure provided there is a baseline. Damaged members cannot be localized using this method.

Sensitivity analysis of the 1st lateral and vertical bending mode shapes and their 1st and 2nd derivatives with respect to the stiffness changes of different members in the support structure of a typical belt conveyor shows using mode shapes and especially their 2nd derivatives along different lines, some damaged members may be localized provided the number of damaged members is small and damage is severe; Moreover, considering the 1st lateral and vertical bending modes at the same time along many lines is necessary. Most of the time, existence of a baseline is needed to correctly localize damage, however even without a baseline, due to the existence of anomalies in the shapes of the modes and their derivatives, damaged parts may be identified.

Among different types of local vibration modes, Periodic Local Vibration Modes (PLVM) and Isolated Local Vibration Modes (ILVM) are explained in detail. These modes are for the secondary members of the support structure of belt conveyors. PLVM is a mode in which vibrations of identical members set are much larger than the other members. ILVM is a mode in which vibration of a member is much larger than the other members. The eigenvalue analysis shows that for a damaged member, there are no PLVM, instead, the damaged member has ILVM with lower frequencies than PLVM. The Degree of Mode Localization (DML) is enhanced as the damage level is increased. Sensitivity analysis shows that frequencies of PLVM and ILVM are sensitive to the local internal connections as well as the properties of the corresponding member, but they have a small sensitivity to the global boundary conditions of the main frame as well as the properties of the main longitudinal members. The change in frequencies of these modes is used for damage identification. The details of damage identification techniques using PLVM and ILVM are explained in chapter 5

Application of local vibration modes in damage identification of space structures has not been well studied. To distinguish PLVM and ILVM from the other vibration modes, using a precise device such as Laser Doppler Vibrometer (LDV) that can measure higher frequencies is needed. In addition, many points from different parts of the structure have to be measured to compare with each other. The observability analysis of PLVM shows that these modes are more easily observed when each secondary member is hit or at least, one of the undamaged identical members of the corresponding identical members set is directly hit.

Chapter 4

Mode localization in structures consisting of main and secondary members

4.1 Introduction

There has been some research about mode localization in the past **[67, 68 and 69]**. In this chapter, the existence of local vibration modes (PLVM and ILVM) in systems which consist of main and secondary members are investigated. At the beginning, using a 3-DOF system including coupler, main, and secondary members, mode localization is mathematically explained and the corresponding frequencies are theoretically calculated. Then, a more complicated 21-DOF lamped mass-spring system is introduced to clarify the existence condition of PLVM and ILVM numerically and parametrically. Finally the existence condition is confirmed on the finite element model.

4.2 Theoretical analysis for the existence condition of local vibration mode

In order to examine the existence condition of mode localization in a simple spring-mass system, a 3DOF system including coupler, main, and secondary members, shown in figure 4-1, is considered.

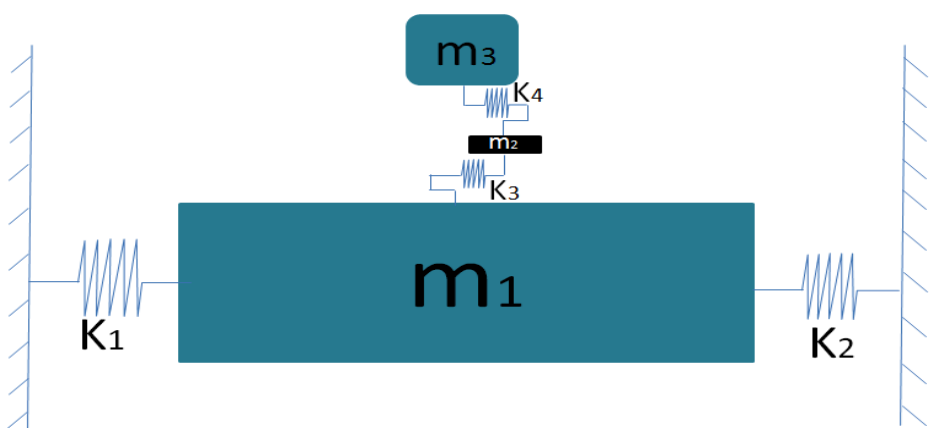

Figure 4-1 A 3DOF spring-mass system

The eigenvalue problem for free vibration of structures is:

$$[K - M\omega^2]\{X\} = \{0\} \tag{4.1}$$

This problem for the above simple system is written as:

$$\begin{bmatrix} k_1+k_2+k_3-\lambda m_1 & -k_3 & 0 \\ -k_3 & k_3+k_4-\lambda m_2 & -k_4 \\ 0 & -k_4 & k_4-\lambda m_3 \end{bmatrix} \begin{Bmatrix} x_1 \\ x_2 \\ x_3 \end{Bmatrix} = \begin{Bmatrix} 0 \\ 0 \\ 0 \end{Bmatrix} \tag{4.2}$$

where λ is eigenvalue or the square of circular natural frequency (ω^2) of the structure. This matrix equation consists of 3 linear homogenous equations. To discuss about mode localization, a ratio of the free vibration of the main and secondary members should be calculated by eliminating the displacement of the coupler (x_2). First from the second equation of 4.2, x_2 is written in terms of x_1 and x_3:

$$x_2 = \frac{k_3}{k_3+k_4-\lambda m_2} x_1 + \frac{k_4}{k_3+k_4-\lambda m_2} x_3 \tag{4.3}$$

Substituting x_2 with the right hand side of this equation in the first and third equations of 4.2, the following matrix equation is obtained:

$$\begin{bmatrix} k_1+k_2+k_3-\lambda m_1-\frac{{k_3}^2}{k_3+k_4-\lambda m_2} & -\frac{k_3k_4}{k_3+k_4-\lambda m_2} \\ -\frac{k_4k_3}{k_3+k_4-\lambda m_2} & k_4-\lambda m_3-\frac{{k_4}^2}{k_3+k_4-\lambda m_2} \end{bmatrix} \begin{Bmatrix} x_1 \\ x_3 \end{Bmatrix} = \begin{Bmatrix} 0 \\ 0 \end{Bmatrix} \tag{4.4}$$

This matrix equation can be written as:

$$k_1+k_2+k_3-\lambda m_1-\frac{{k_3}^2}{k_3+k_4-\lambda m_2} = \frac{k_3k_4}{k_3+k_4-\lambda m_2}\frac{x_3}{x_1} \tag{4.5.a}$$

$$k_4-\lambda m_3-\frac{{k_4}^2}{k_3+k_4-\lambda m_2} = \frac{k_4k_3}{k_3+k_4-\lambda m_2}\frac{x_1}{x_3} \tag{4.5.b}$$

Note that the eigenvalue of the main member, coupler and secondary member shown in figure 4-1, are respectively denoted by λ_1 , λ_2 and λ_3:

$$\lambda_1 = \frac{k_1+k_2+k_3}{m_1} \tag{4.6.a}$$

$$\lambda_2 = \frac{k_3+k_4}{m_2} \tag{4.6.b}$$

$$\lambda_3 = \frac{k_4}{m_3} \tag{4.6.c}$$

Subtracting equation (4.5.b) from (4.5.a) and multiplying each side by $\frac{x_3}{x_1}$ and using the definition of the eigenvalue of the main and secondary members and rearranging gives:

$$\left(\frac{x_3}{x_1}\right)^2 + \left(\frac{k_3}{k_4} - \frac{m_1}{m_3}\frac{k_4}{k_3}\right)\frac{x_3}{x_1} - \frac{m_1}{m_3} = \frac{m_1}{k_3k_4}\left(k_3+k_4-\lambda m_2\right)\left(\lambda_1-\lambda_3\right)\frac{x_3}{x_1} \tag{4.7}$$

This equation can be formed as:

$$(r - s_1)(r - s_2) = \alpha r \tag{4.8}$$

where:

$$s_1 = -\frac{k_3}{k_4} \tag{4.9.a}$$

$$s_2 = \frac{m_1}{m_3}\frac{k_4}{k_3} \tag{4.9.b}$$

$$r = \frac{x_3}{x_1} \tag{4.9.c}$$

$$\alpha = \frac{m_1}{k_3 k_4}(k_3 + k_4 - \lambda m_2)(\lambda_1 - \lambda_3) \tag{4.9.d}$$

Equation (4.8) can be used to discuss about the existence condition of mode localization in this system. The right hand side of this equation is a linear function with a slope equals to α and the left hand side is a parabolic function as shown in figure 4.2.

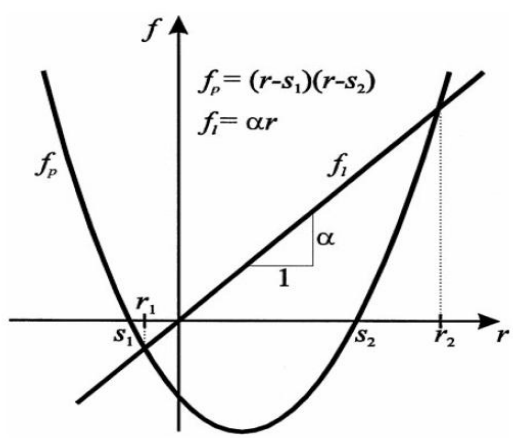

Figure 4-2 The linear and parabolic curves **[66]**

The horizontal axis of the above figure is the modal displacement ratio of the secondary member to the main member. Significant mode localization happens when r_1 or r_2 goes to infinity. Therefore, it seems the absolute value of the slope of the line α needs to become large and goes to infinity to have significant mode localization. In other words, the larger absolute value of α seems to cause the stronger mode localization in the system. Thus, to examine the existence condition of local vibration mode in the system, variations of α should be considered.

Assuming that the mass of coupler is small and negligible, as it is the case in most real structures, equation (4.9.d) becomes:

$$\alpha \sim \frac{m_1}{k_3 k_4}(k_3 + k_4)(\lambda_1 - \lambda_3) = \frac{k_1 + k_2 + k_3}{k_4} - \frac{m_1}{m_3} + \frac{k_1 + k_2 + k_3 - \frac{m_1}{m_3}k_4}{k_3} \tag{4.10}$$

It is found from the above equation that a significant difference between the eigenvalue of the substructures would cause a large value of α. This difference between eigenvalue of the main and secondary members is caused by all parameters involved in the definition of the two eigenvalues.

To examine the effect of k_3 on variations of α, the derivative of α with respect to k_3 is calculated:

$$\frac{d\alpha}{dk_3} = \frac{1}{k_4} - \frac{k_1+k_2-\frac{m_1}{m_3}k_4}{{k_3}^2} \tag{4.11}$$

The limit of this differentiation is calculated when k_3 goes to infinity:

$$\lim_{k_3\to\infty} \frac{d\alpha}{dk_3} = \frac{1}{k_4} > 0 \tag{4.12}$$

It means when k_3 has large values, α is an ascending function and seems to result in a drastic occurrence of local vibration modes. However, the parabolic curve in figure 4-2 shifts to the left as k_3 increases and accordingly a large value of k_3 does not necessarily grantee the occurrence of mode localization. The route of equation 4.8, as k_3 goes to infinity, are:

$$r_{1,2} = \frac{1-\frac{m_1}{m_3}+\frac{k_1+k_2}{k_4}\pm[(\frac{m_1}{m_3}-1-\frac{k_1+k_2}{k_4})^2+4\frac{m_1}{m_3}]^{0.5}}{2} \tag{4.13}$$

Extending equation (4-13) yields:

$$r_{1,2} = \frac{1-\frac{m_1}{m_3}+\frac{k_1+k_2}{k_4}\pm[(\frac{m_1}{m_3})^2+2\left(1-\frac{k_1+k_2}{k_4}\right)\frac{m_1}{m_3}+(1+\frac{k_1+k_2}{k_4})^2]^{0.5}}{2} \tag{4-14}$$

It is found, if $k_1 + k_2 \neq k_4$, r_2 have a large absolute value when m_1 has a large value. In other words the secondary member locally vibrates. To find the corresponding frequency of the local vibration mode, the modal displacement ratio of the secondary member to the main member is calculated. The two sides of the first linear equation of the matrix equation (4.2) is multiplied by $-\frac{k_4}{k_3}$ and then sum with the third linear equation of the matrix equation (4.2). The modal displacement ratio of the secondary member to the main member is:

$$\frac{x_3}{x_1} = \frac{k_1+k_2+k_3-\lambda m_1}{\frac{k_3}{k_4}(k_4-\lambda m_3)} \tag{4.15}$$

The limit of this equation is calculated when k_3 goes to infinity:

$$\lim_{k_3\to\infty} \frac{k_1+k_2+k_3-\lambda m_1}{\frac{k_3}{k_4}(k_4-\lambda m_3)} = \frac{k_4}{(k_4-\lambda m_3)} \tag{4.16}$$

As already shown, $\frac{x_3}{x_1}$ has a large positive value when k_3 has a large value and m_1 is large. Therefore, the denominator of $\frac{k_4}{(k_4-\lambda m_3)}$ is close to zero yields:

$$\lambda \simeq \frac{k_4}{m_3} \tag{4.17}$$

It means that one of the eigenvalue of the system equals to the eigenvalue of the secondary member in which the secondary member locally vibrates. Likewise, a large value of the stiffness of the secondary member would cause the structure has an eigenvalue equals to the eigenvalue of the main member in which the main member locally vibrates.

Although a large value of the other parameters involved in (4.13) may cause the occurrence of mode localization, but the corresponding eigenvalue of these local vibration modes does not equal to any of the eigenvalue of the substructures and have no physical definition.

To verify the theoretical analysis, a numerical analysis is conducted on the system shown in figure 4-1. Assume that $m_1 = 1000$ (relativelty large), $m_2 = 0.1$, $m_3 = 10$ and $k_1 = k_2 = 600$, $k_4 = 300$ and k_3 changes from 1 to 100000. Therefore, the eigenvalue of the secondary member is $\lambda_3 = \frac{k_4}{m_3} = 30$. The results, corresponding to one eigenvalue of the structure, are shown in figure 4-3.

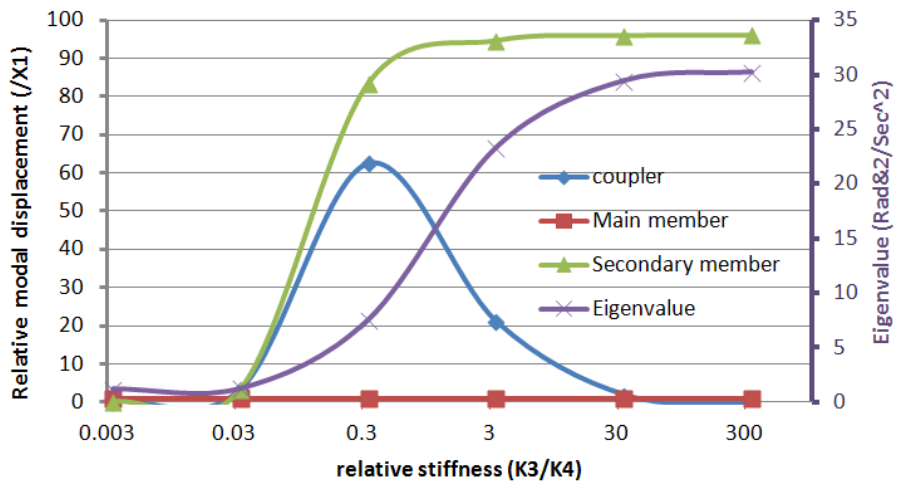

Figure 4-3 Relative modal amplitude and the corresponding eigenvalue

As shown in the above figure, only the modal displacement of the secondary member always enhances as the relative stiffness increases. In other words, the corresponding mode is getting much more localized while the stiffness of the main member becomes much larger than the secondary member. Moreover, one of the eigenvalue of the whole system becomes close to the eiganvalue of the secondary member as the stiffness of the main member becomes much larger than the secondary member. Meanwhile, one of the eigenvalue of the system is close to the eigenvalue of the main member ($\frac{k_1+k_2+k_3}{m_1} = 1.5$) when the stiffness of the main member (k_3) becomes much smaller than the stiffness of the secondary member (k_4). This is shown in figure 4-4. This figure is exactly the same as figure 4-3 which zoomed in the low relative modal displacements.

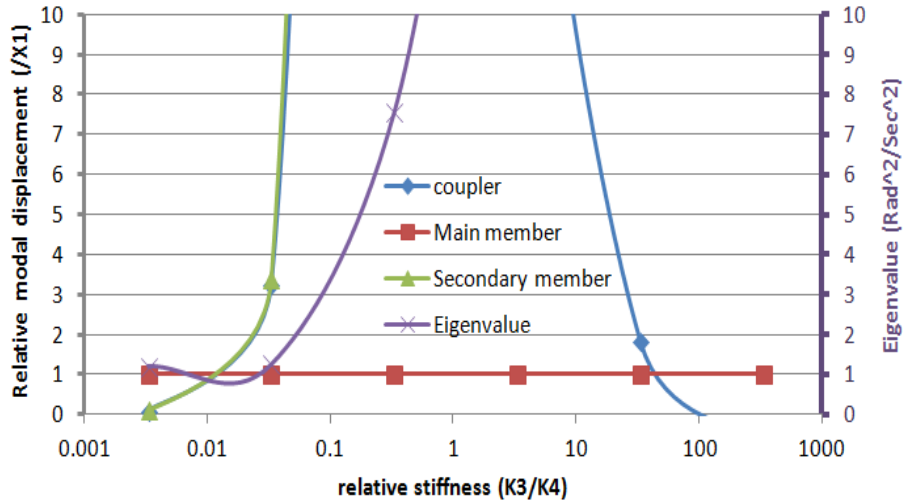

Figure 4-4 Relative modal amplitude and the corresponding eigenvalue (zoomed in the low relative modal displacements)

4.3 Numerical analysis for the existence condition of local vibration mode in spring-mass systems

In this part, the existence condition of local vibration modes, i.e. PLVM and ILVM, in 21DOF spring-mass system, are numerically examined. The correspondence between the lamped mass-spring system, shown in figure 4-5, and the belt conveyor model, shown in figure 4-6, is described in table 4-1.

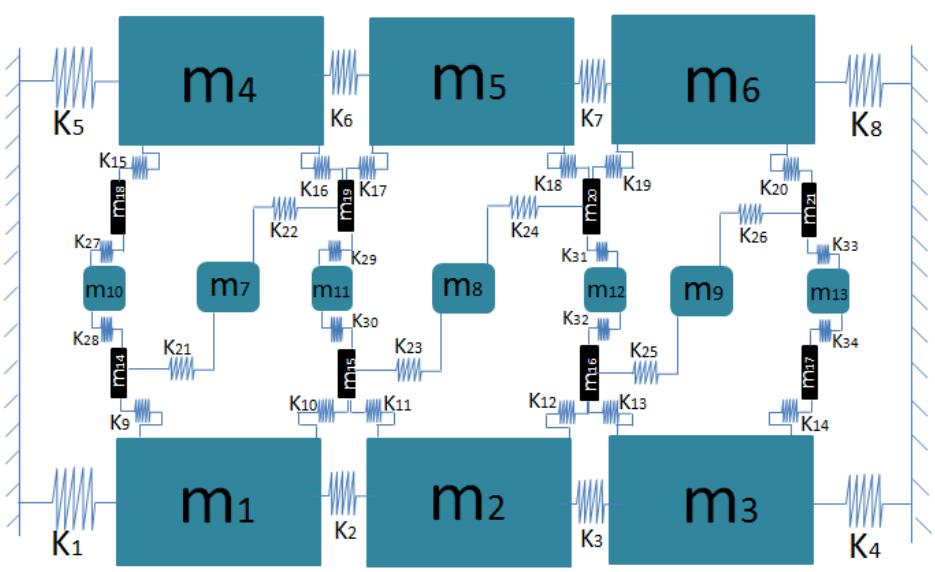

Figure 4-5 21-DOF mass-spring system

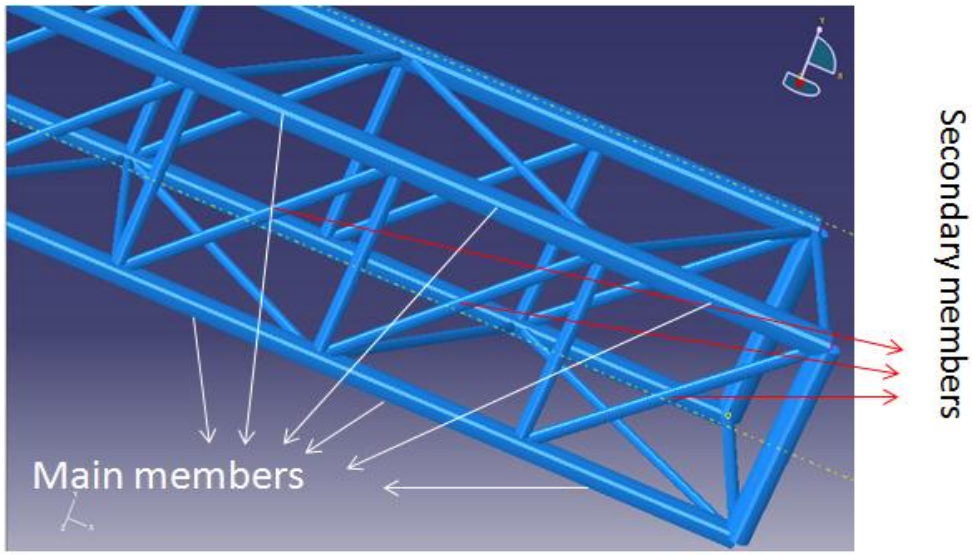

Figure 4-6 Abaqus model

Table 4-1 Correspondence between the spring-mass system and belt conveyor model

Spring-mass system	Belt conveyor model
m1,m2,m3,m4,m5,m6	Mass of main members
m7,m8,m9	Mass of secondary members
K1,k4,k5,k8	Stiffness of the external connections
K2,k3,k6,k7	Stiffness of the connections between main members
K9+K10,K11+K12,K13+K14,K15+K16,K17+K18,K19+K20	Stiffness of a main member including its connections (with couplers) and member itself
K21+K22,K23+K24,K25+k26	Stiffness of a secondary member including its connections and member itself

Note that although only one representative secondary members set is examined in this section, there is another secondary members set corresponding to m_{10} , m_{11} , m_{12} , m_{13} in figure 4-5 which has the same behavior as the considered secondary members set.

Two different structures are considered. In the first structure, the main members are separated from each other. It means that K2, k3, k6 and k7 equal to zero. The second structure has continuous main members. It means that K2, k3, k6 and k7 have large values.

4.3.1 Structure with separated main members

In order to conduct a numerical eigenvalue analysis for the existence condition of local vibration modes in the structure with seprated main members, representative values of different parameters in the structure are considered as they are listed in table 4-2.

Table 4-2 Values of different parameters in the system

descriptions	Parameters	Values
Main members	M1,M2,M3,M4,M5,M6	100
braces	M7,M8,M9	10
Vertical members	M10,M11,M12,M13	7
couplers	M14,M15,M16,M17,M18,M19,M20,M21	0.1
External stiffness components	K1,K4,K5,K8	1000
Internal stiffness components between the main members	K2,K3,K6,K7	0
Stiffness components of the undamaged braces	K21,K22,K23,K24	250
Stiffness components of damaged brace	K25,K26	150
Stiffness components of the undamaged vertical members	K27,K28,K31,K32,K33,K34	700
Stiffness components of the damaged vertical member	K29,K30	630
Stiffness components of the main members	K9,K10,K11,K12,K13,K14K15,K16,K17,K18,K19,K20,K21	10 to 1000000

Table 4-3 shows the properties of each members set based on the assigned values of the parameters.

Table 4-3 Properties of each member set in the spring-mass system

properties	value
Mass of main members	100
Stiffness of main members	20 to 2000000
Eigenvalue of main members	0.2 to 20000
Mass of couplers	0.1
Mass of vertical members	7
Stiffness of the undamaged vertical members	1400
Stiffness of the damaged vertical member	1260
Eigenvalue of the undamaged vertical members	200
Eigenvalue of the damaged vertical member	180
Mass of braces	10
Stiffness of the undamaged braces	500
Stiffness of the damaged braces	300
Eigenvalue of the undamaged braces	50
Eigenvalue of the damaged brace	30

As presented in the above table, the stiffness of the main members changes to find its effect on the existence of local vibration modes and confirm the results of the theoretical analysis. Figure 4-7 shows the relative amplitude of the braces to member 1 with respect to the relative stiffness of the main members to the damaged brace (member 9) at an eigenfrequency of the structure. Note that member 1 is one of the main members.

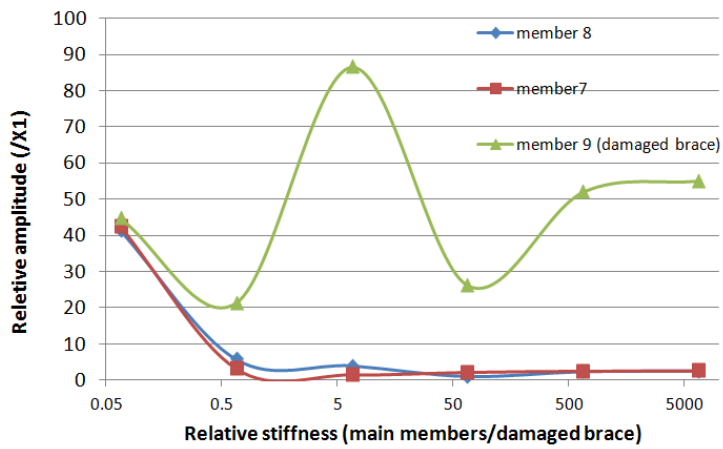

Figure 4-7 Isolated local vibration mode (ILVM)

The damaged brace locally vibrates in one eigenvalue of the whole system as the stiffness of the main members drastically increases. It means that if the main members are much stiffer than the damaged brace, there is one ILVM corresponding to the damaged brace. Figure 4-8 shows changes of the eigenvalue of ILVM and the degree of mode localization (DML), defined in chapter 3, when the stiffness of the main members is increased.

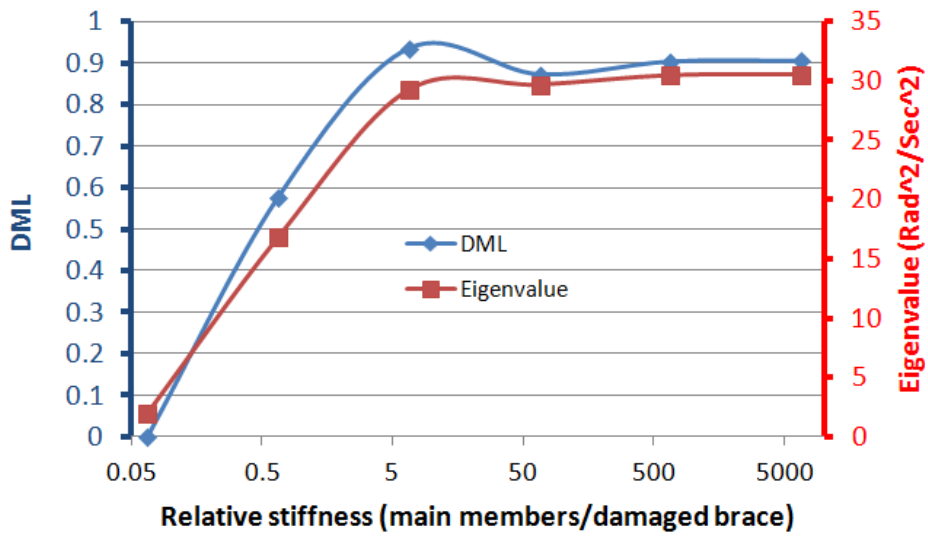

Figure 4-8 Changes of the DML and eigenvalue of the ILVM

The eigenvalue of ILVM becomes closer to 30 when the relative stiffness of the main members to the damaged brace increases. In other words, the eigenvalue of ILVM in the system almost equals to the eigenvalue of the damaged brace provided the main members are much stiffer than the damaged brace. Moreover, the DML increases as the main members become stiffer. It means that the ILVM becomes more localized when the stiffness of the main members increases. Therefore, the existence condition of ILVM with the same eigenvalue of the corresponding substructure is that the main members are much stiffer than the corresponding secondary members.

Figure 4-9 shows the relative amplitude of the braces to member 1 with respect to the relative stiffness of the main members to the undamaged braces (member 7 & 8) at another eigenfrequency of the structure.

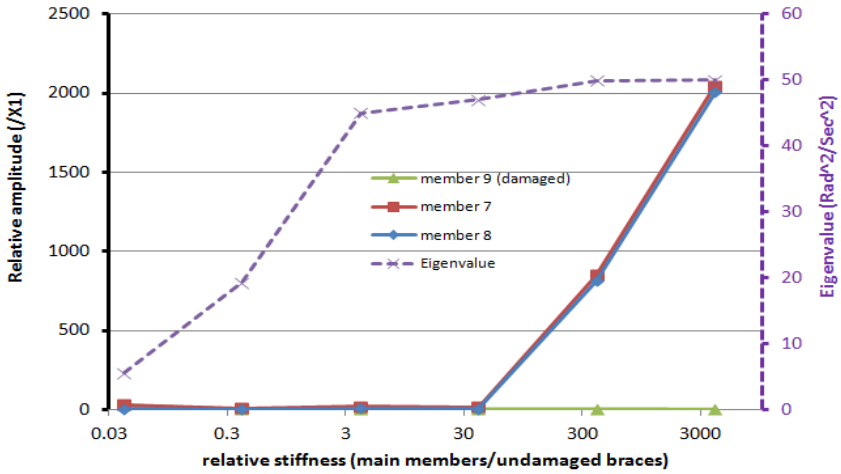

Figure 4-9 Periodic local vibration mode (PLVM)

As shown in figure 4-9, the modal displacements of the undamaged braces are much larger than the damaged brace as the main members are much stiffer than the undamaged braces and the corresponding eigenvalue of the structure is close to 50 which equals to the eigenvalue of the undamaged braces. To better judge about the existence condition of mode localization, figure 4-9 is zoomed in the low relative stiffness range and shown in figure 4-10.

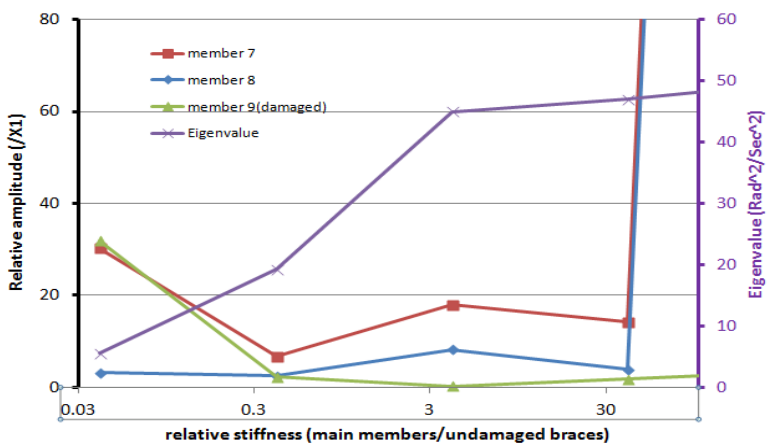

Figure 4-10 Relative amplitudes in the low relative stiffness range

The modal displacements of the undamaged and damaged braces are close to each other when the main members are not too stiff compared to the undamaged braces. Therefore, like the existence condition of ILVM, the existence condition of PLVM with the same eigenvalue of the corresponding substructure is that the main members are much stiffer than the corresponding secondary members.

It should be noted that since two identical undamaged braces exist in the system, other than the mentioned PLVM, there is another PLVM in the structure with an eigenvalue close to the eigenvalue of the undamaged braces provided the main members are much stiffer than the undamaged braces.

Figure 4-11 demonstrates comparison of the modal amplitude of the main members with respect to the relative stiffness of the main members to the undamaged braces at an eigenfrequency of the structure. As shown, when the main members are much stiffer than the braces, the modal amplitude of the main members are close to each other. To have a better comparison between the modal amplitude of the main members in the low relative stiffness range, figure 4-11 is zoomed in the low relative stiffness range and shown in figure 4-12.

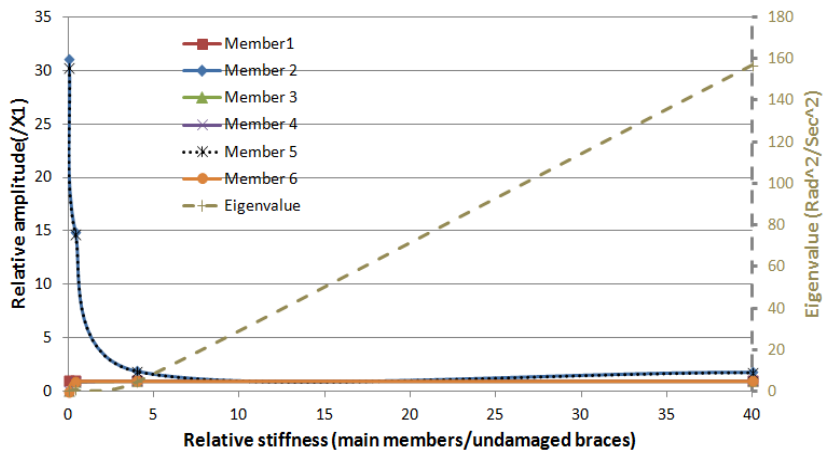

Figure 4-11 Relative amplitude of the main members

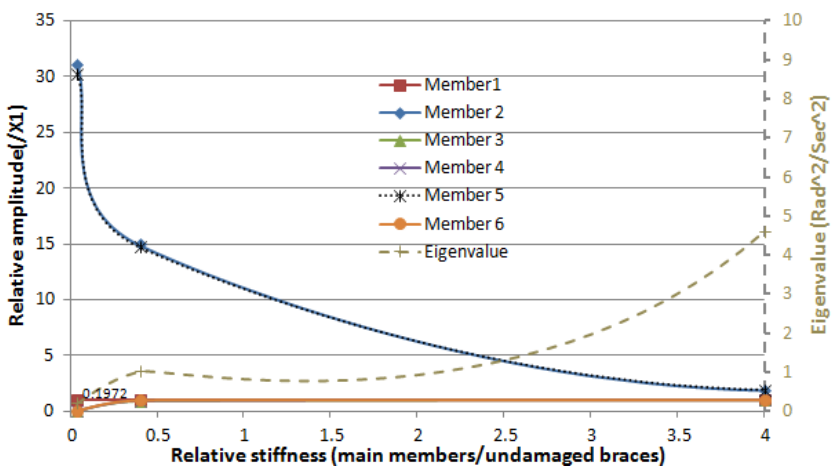

Figure 4-12 Relative amplitude of the main members in the low relative stiffness range

As shown in this figure, when the stiffness of the main members is far lower than the stiffness of the braces, the modal amplitudes of members 2 and 5 are much larger than those of the other main members and the corresponding eigenvalue is close to 0.2 which equals to the eigenvalue of the main members. It should be noted that members 2 and 5, unlike the other main members, are not connected to the external springs, as shown in figure 4-5, and accordingly not identical with the other main members and locally vibrate with an eigenvalue close to their own eigenvalue when their stiffness is much less than the secondary members.

4.3.2 Structure with continuous main members

In order to carry out a numerical eigenvalue analysis for the existence condition of local vibration modes in the structure with continuous main members, representative values of different parameters in the structure are considered like the values for the structure with separated main members except the values of K2, K3, K6, K7 (internal stiffness components between the main members) which are considered large (equal to 100000) to make the main member continuous.

The stiffness of the main members changes to find its effect on the existence of local vibration modes and confirm the results of the theoretical analysis. Figure 4-13 shows the relative amplitude of the braces to member 1 with respect to the relative stiffness of the main members to the damaged brace (member 9) in one of the eigenvalues of the structure.

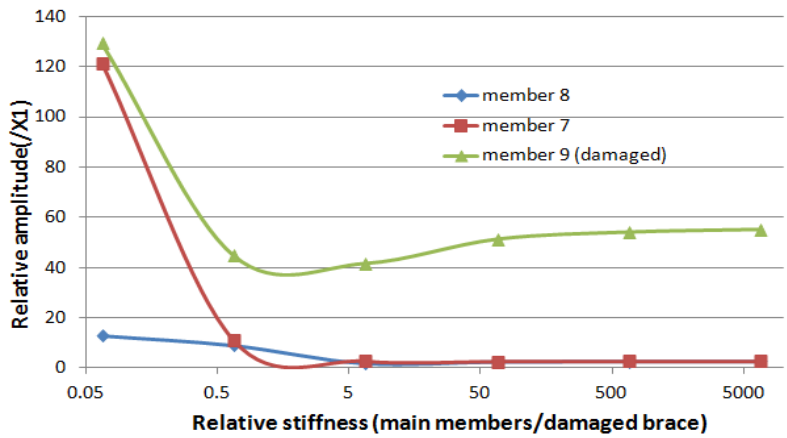

Figure 4-13 Isolated local vibration mode (ILVM)

The damaged brace locally vibrates in one eigenvalue of the system as the stiffness of the main members drastically increases. It means if the main members are much stiffer than the damaged brace, there is one ILVM in which the damaged brace locally vibrates. Figure 4-14 shows changes of the eigenvalue of ILVM and the degree of mode localization (DML), defined in chapter 3, when the stiffness of the main members increases.

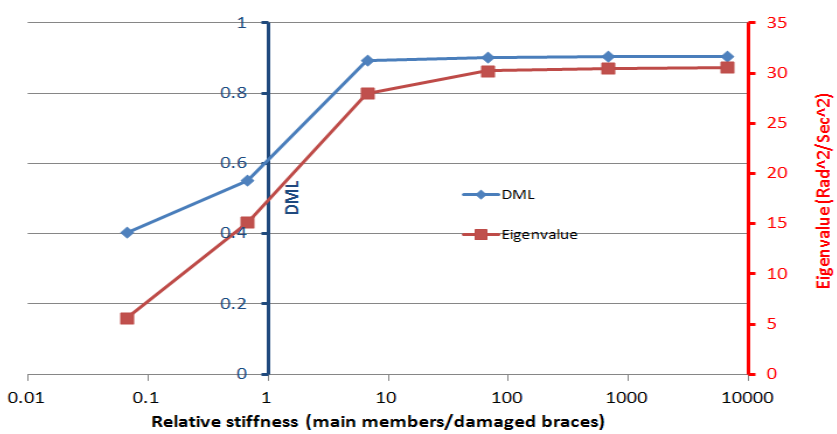

Figure 4-14 Changes of the DML and eigenvalue of the ILVM

The eigenvalue of ILVM becomes close to 30 when the relative stiffness of the main members to the damaged brace increases. It means that the eigenvalue of ILVM in the system almost equals to the eigenvalue of the damaged brace provided the main members are much stiffer than the damaged brace. Moreover as shown in the above figure, the DML increases as the main members become stiffer. It means that the ILVM becomes more localized when the stiffness of the main members increases. Therefore, the existence condition of ILVM with the same eigenvalue of the corresponding substructure is that the main members are much stiffer than the corresponding secondary members.

Figure 4-15 shows the relative amplitude of the braces to member 1 with respect to the relative stiffness of the main members to the undamaged braces (member 7 & 8) in another eigenvalue of the structure.

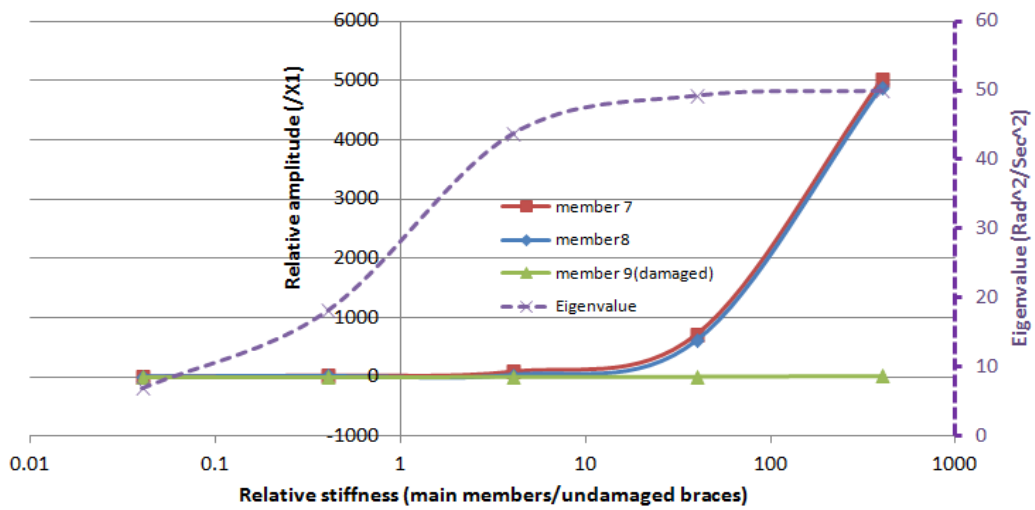

Figure 4-15 Periodic local vibration mode (PLVM)

As shown in the above figure, the modal displacements of the undamaged braces are much larger than the damaged brace as the main members are much stiffer than the undamaged braces and the corresponding eigenvalue of the structure is close to 50 which equals to the eigenvalue of the undamaged braces. Therefore, like the existence condition of ILVM, the existence condition of PLVM with the same eigenvalue of the corresponding substructure is that the main members are much stiffer than the corresponding secondary members.

Note that since two identical undamaged braces exist in the system, other than the mentioned PLVM, there is another PLVM in the structure with an eigenvalue close to 50 which equals to the eigenvalue of the undamaged braces provided the main members are much stiffer than the undamaged braces.

In order to analyze more cases, the stiffness of the damaged and undamaged braces in the system take different values and the other parameters remain same as presented in table 4-3. Table 4-4 shows the considered values of the stiffness of the damaged and undamaged braces. It should be noted that case 1 is the same as the one in table 4-3 and has been already analyzed.

Table 4-4 Properties of the braces in different cases

Properties	Case1	Case 2	Case 3	Case 4	Case 5	Case 6
Mass of the braces	10	10	10	10	10	10
Stiffness of the undamaged braces	500	600	700	800	900	1000
Stiffness of the damaged brace	300	360	420	480	540	600
Eigenvalue of the undamaged braces	50	60	70	80	90	100
Eigenvalue of the damaged brace	30	36	42	48	54	60

Same analyses as before (case 1) are done for each case. The stiffness of the main members changes to find its effect on the existence of local vibration modes. In each case, it is found that the damaged brace locally vibrates in one eigenvalue of the system as the stiffness of the main members drastically increases. It means that if the main members are much stiffer than the damaged brace, there is one ILVM corresponding to the damaged brace. Figure 4-16 shows changes of the eigenvalue of ILVM in each case when the stiffness of the main members increases.

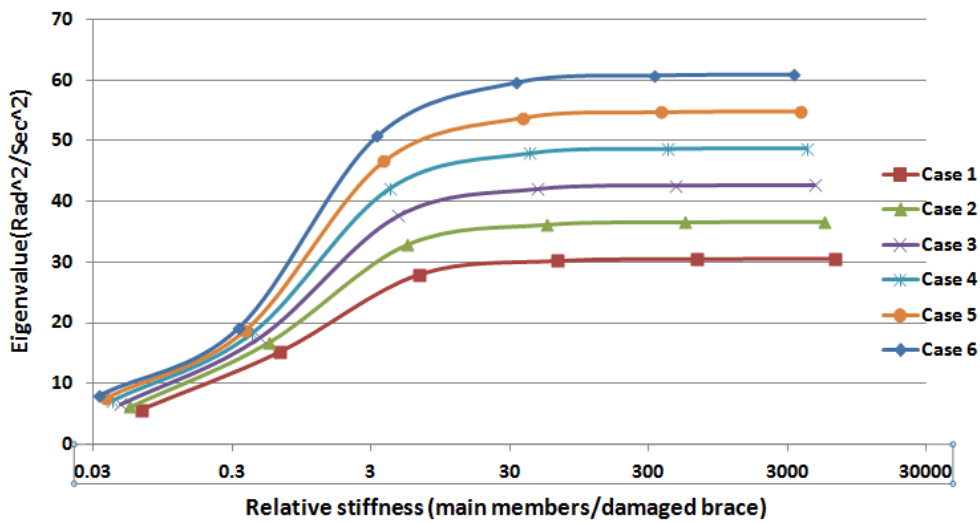

Figure 4-16 Changes of the eigenvalue of ILVM in each case

As shown in the above figure, in each case, when the main members are much stiffer than the damaged brace, the eigenvalue of ILVM is close to the eigenvalue of the damaged brace. Figure 4-17 shows changes of the degree of mode localization (DML) in each case with respect to the relative stiffness of the main members to the damaged brace.

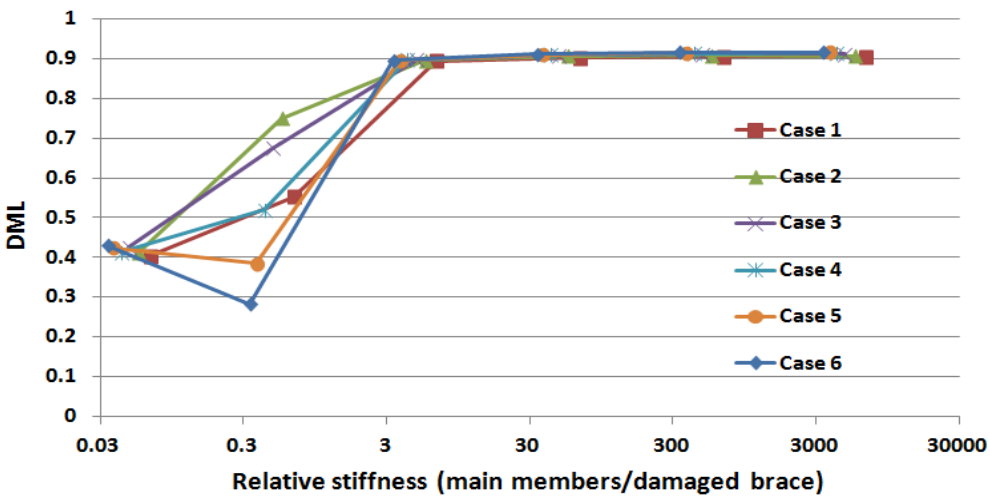

Figure 4-17 Changes of the DML in each case

The DML, generally, increases as the main members become stiffer. It means that the ILVM becomes more localized when the stiffness of the main members increases. Therefore, the existence condition of ILVM with the same eigenvalue of the corresponding substructure is that the main members are much stiffer than the corresponding secondary members.

Likewise, in each case, it is found that the modal displacements of the undamaged braces are much larger than that of the damaged brace in one eigenvalue of the structure as the main members are much stiffer than the undamaged braces. This mode is PLVM corresponding to the undamaged braces. Figure 4-18 shows changes of the eigenvalue of PLVM corresponding to the undamaged braces in each case with respect to the relative stiffness of the main members to the undamaged braces.

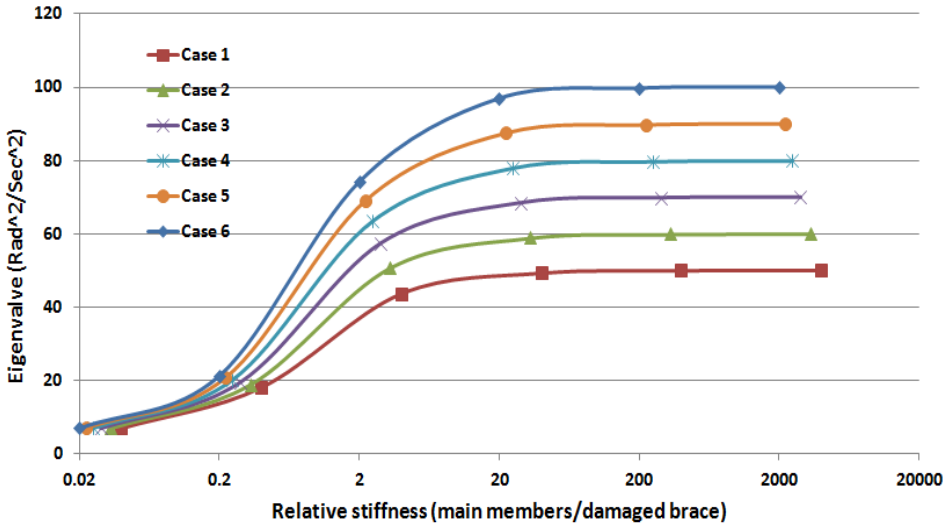

Figure 4-18 Changes of the eigenvalue of PLVM in each case

In each case, when the main members are much stiffer than the undamaged braces, the eigenvalue of PLVM is close to the eigenvalue of the undamaged braces. It should be noted that since two identical undamaged braces exist in the system, other than the mentioned PLVM, in each case, there is another

PLVM in the structure with an eigenvalue close to the eigenvalue of the undamaged braces. Therefore, the existence condition of PLVM with the same eigenvalue of the corresponding substructure is that the main members are much stiffer than the corresponding secondary members.

Unlike the system with separated main members, in these cases, there is no vibration mode in which any of the main members locally vibrate even if the stiffness of the main members is much less than the stiffness of the secondary members in the system because the main members are continuous.

4.4 Numerical analysis for the existence of ILVM in finite element models

In this part, the existence condition of isolated local vibration mode in the finite element model, shown in figure 3-3, is numerically examined and the obtained results in the previous parts are verified. Formula of the deflections of simple supported and clamped-clamped beams, shown in figure 4-19, under a known load P at the center is used to calculate the stiffness of each member of the model.

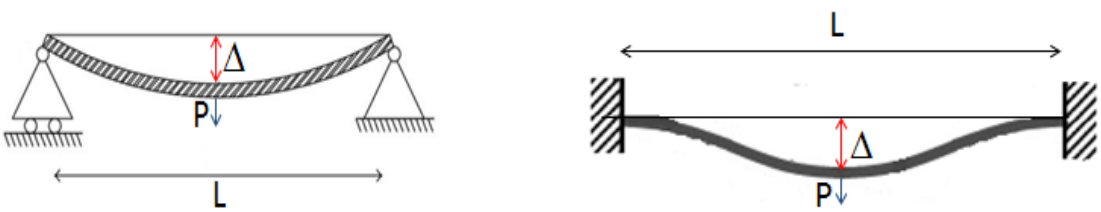

$$\Delta = \frac{PL^3}{48\,EI} \qquad \Delta = \frac{PL^3}{192\,EI}$$

Figure 4-19 Deflections of the simple supported and clamped-clamped beams

Since P = KΔ, the stiffness of simple supported and clamped-clamped beams are respectively considered as:

$$K = \frac{48EI}{L^3} \tag{4.17.a}$$

$$K = \frac{192EI}{L^3} \tag{4.17.b}$$

In this model, the longitudinal members of the main frame are considered as main members and the other members of the main frame are secondary. Since longitudinal members are continuous in the model, the formula of clamped-clamped beam is used to calculate the stiffness of the main members. As for secondary members, the formula of simple supported beam is used since soft rotational springs (500 N.m/rad) have been used at the ends of these members and accordingly they are close to a simple supported beam. Table 4-5 shows the values of the relative stiffness of different secondary members to the main members in this finite element model of the belt conveyor.

Table 4-5 Values of the relative stiffness of different secondary members to the main members

Secondary members	Value of relative stiffness
Bottom or top braces	417
Lateral members	192
Side braces	132
Vertical members	23

Figure 4-20 shows the longitudinal members in red color, and 12 identical braces at the bottom part of the structure. In this model, the stiffness of the longitudinal members is about 417 times larger than the stiffness of the 12 identical braces at the bottom part of the structure.

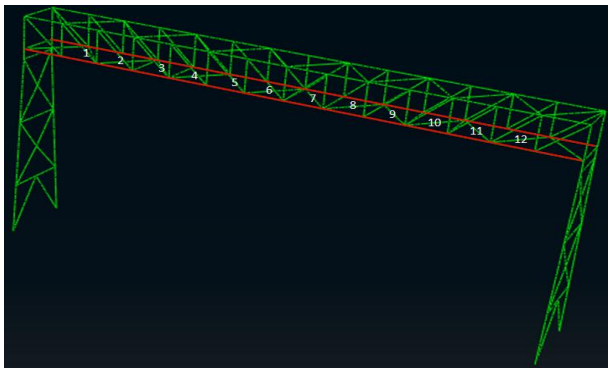

Figure 4-20 Main members and 12 identical braces at the bottom part of the structure

To confirm the results in the previous parts of this chapter, member 4 is damaged by 10% and 20% stiffness reduction. In each case, the stiffness of the main members changes. Then, the frequency of ILVM corresponding to member 4 is acquired through eigenvalue analysis in FEM and the degree of mode localization is calculated using modal amplitudes of the 12 identical braces.

First, member 4 is damaged by 10%. Figure 4-21 shows the frequency and DML changes, calculated among the 12 identical braces at the bottom part of the belt conveyor, with respect to the relative stiffness of the main members to the 12 identical braces. As shown in this figure, the DML reaches 1 as the relative stiffness increases. Moreover, the frequency of ILVM exactly equals to 40.048 Hz when the main members are much stiffer than the identical braces.

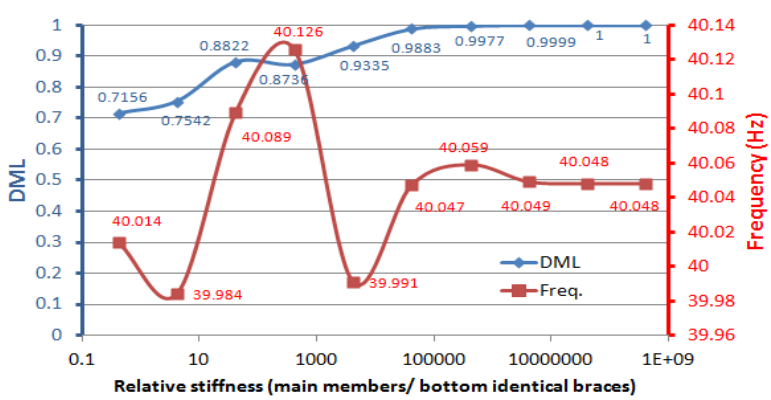

Figure 4-21 Frequency and DML changes for 10% stiffness reduction of brace 4

On the other hand, as shown in figure 4-22, brace 4 is separately modeled with the boundary conditions similar to its local boundary conditions in the structure.

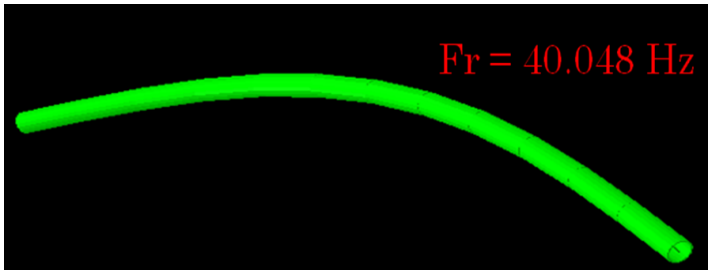

Figure 4-22 Separated brace 4 with 10% stiffness reduction

It is found that the frequency of the first bending mode of this separated brace is 40.048 Hz which equals to the frequency of ILVM in figure 4-21 when the main members are much stiffer than the identical braces. This confirms the previous result that when the main members are much stiffer than the secondary members, the eigenvalues of ILVM for the secondary members in the structure are close to the eigenvalues of the corresponding secondary members. Note that even with a low relative stiffness, the ILVM is close to the eigenvalue of brace 4. Because the structure contains other members attached to the main frame at the connections, i.e. lateral members, side braces, or vertical members, their overall stiffness at the connection points are much larger than the bottom braces.

To better understand DML changes, the ILVM is shown in figure 4-23. In this figure, the ILVM corresponds to member 4 with different stiffness ratio of the main members to the identical braces at the bottom part of the structure.

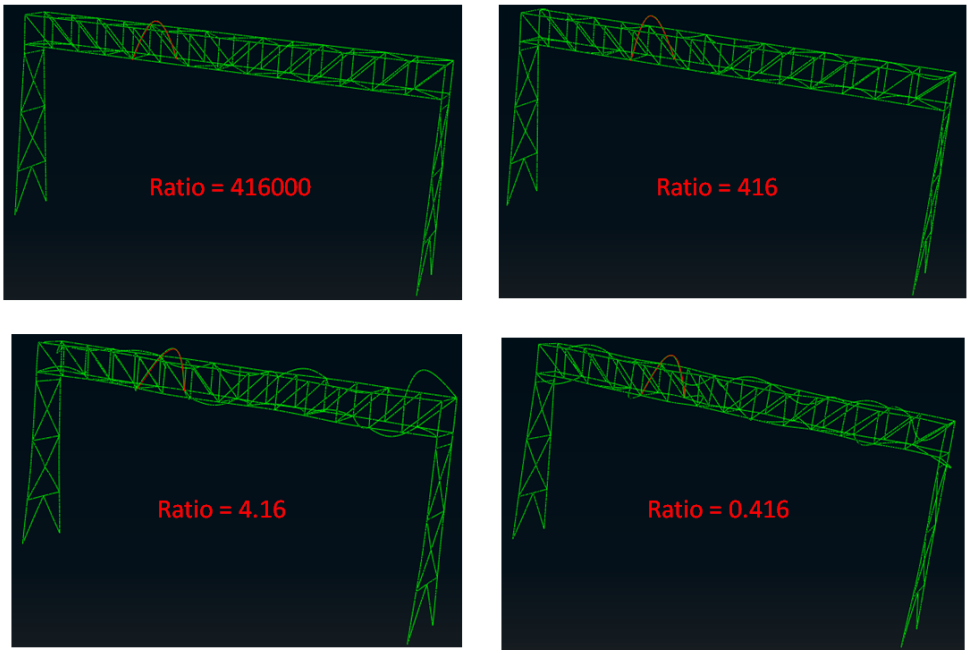

Figure 4-23 ILVM for different relative stiffness

As shown in the above figures, the relative modal amplitude of brace 4 to the other identical braces increases, in other words the DML increases, as the stiffness ratio of the main members to the identical braces is increased.

As another analysis, member 4 damages by 20%. Figure 4-24 shows the frequency and DML changes, calculated among the 12 identical braces at the bottom part of the structure, with respect to the relative stiffness of the main members to the 12 identical braces. As shown in the figure, the DML reaches 1 as the relative stiffness increases. Meanwhile, the frequency of ILVM equals to 37.776 Hz when the main members are much stiffer than the identical braces.

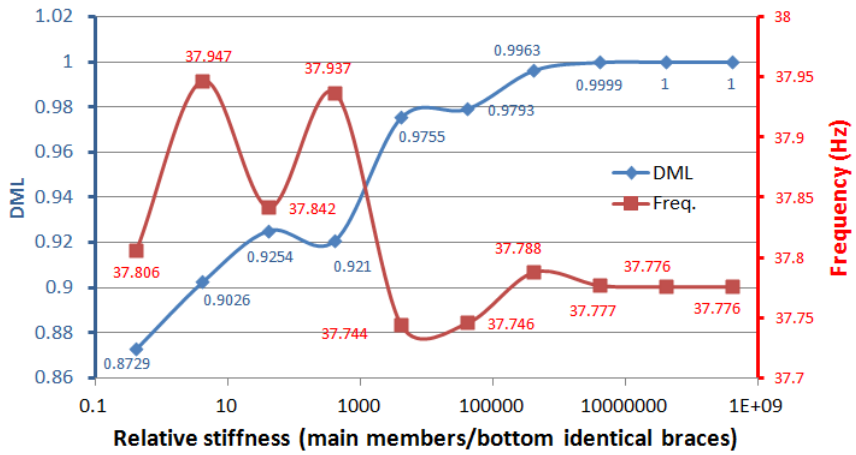

Figure 4-24 Frequency and DML changes for 20% stiffness reduction of brace 4

To compare the result of the above figure with brace 4 as a sub-structure, brace 4 is separately modeled with its local boundary conditions shown in figure 4-25.

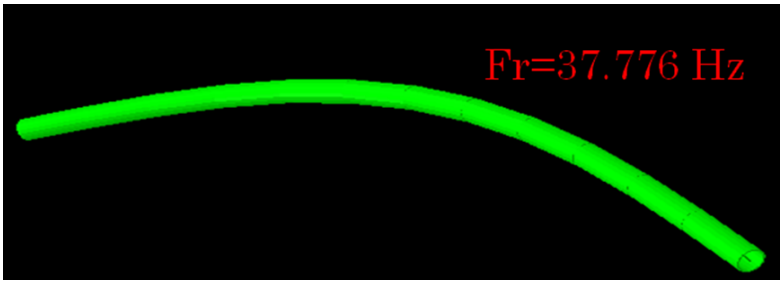

Figure 4-25 Separated brace 4 with 20% stiffness reduction

The frequency of the first bending mode of this separated brace is 37.776 Hz which equals to the frequency of ILVM in figure 4-24 when the main members are much stiffer than the identical braces.

4.5 Summary

In this chapter, the existence condition of local vibration modes in systems which consist of main and secondary members is investigated. At first a 3-DOF system including coupler, main, and secondary members are considered and mathematically prove that if main members are much stiffer than a secondary member, one of the eigenvalue of the system equals to the eigenvalue of the secondary member

in which the secondary member locally vibrates. The results are numerically verified in this system. Then a 21-DOF spring-mass system is compared with a belt conveyor model. The existence condition of PLVM and ILVM with the same eigenvalues of the corresponding substructures is that the main members are much stiffer than the corresponding secondary members. This conclusion is consistent with the theoretical result. Finally the existence condition of ILVM is examined in a finite element model and realized that the frequency of ILVM equals to the relevant frequencies of the associated sub-structures which modeled separately with their own local boundary conditions provided the main members are much stiffer than the secondary members. This conclusion is consistent with the pervious theoretical and numerical results.

Chapter 5

Damage identification using PLVM and ILVM

5.1 Introduction

In this chapter, two damage identification techniques based on PLVM and ILVM are introduced. At the beginning, the beam theory and its applicability on quantification of the damage degree are discussed based on the appropriate parameters in updating procedures. Then, a damage identification technique is proposed. The technique is applied to the finite element model. Some members of the support structure of belt conveyor damage and frequencies of PLVM, ILVM as well as mode shapes of global vibrations are acquired using simulated velocity time history data and eigenvalue analysis. Then, location of damaged members and damage degree of secondary members are identified. Next, another damage identification technique with less necessary hit points is proposed using the finite element model. One of the identical bottom and top braces in a damaged structure is hit and the velocity time history data of identical braces is simulated and damaged bottom and top braces are identified by comparing the amplitude of Fourier spectrum of the bottom and top braces in PLVM range.

5.2 Beam theory and its applicability on the quantification of damage degree

This section discusses the beam theory and its applicability on the quantification of damage degree based on properties of the member and its boundary conditions which affect significantly the frequencies of PLVM and ILVM. The vibration problems of Euler-Bernoulli beams have analytica1 solutions for various boundary conditions **[70, 71 and 72].** The fundamental natural frequencies are calculated by variation methods such as Rayleigh-Ritz or some discretized numerical methods. Additionally some innovative semi analytical approximation methods have been applied **[73, 74]**.

Consider a uniform simply supported beam with two rotational springs with linear stiffness k_{r1} and k_{r2}, shown in figure 5-1, vibrating in one of its natural frequencies. The end is hinged if $k_r = 0$ and clamped if $k_r \to \infty$.

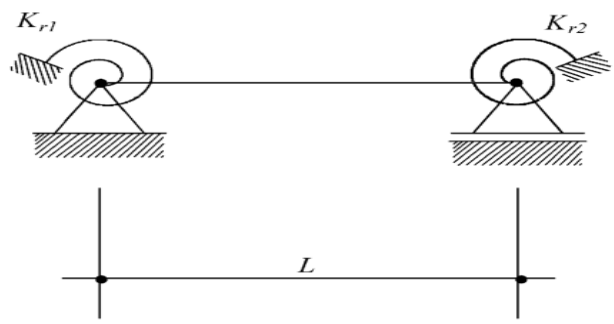

Figure 5-1 Simply supported beam with two elastic rotational springs at the ends

The exact *n*-th natural frequency ω_n of the elastically restrained beam can be shown as the square of a dimensionless coefficient λ_n multiplied by the fundamental frequency of the same hinged end beam:

$$\omega_n = \lambda_n^2 \sqrt{\frac{EI}{\rho A L^4}} \tag{5.1}$$

In which *EI* is the modulus of flexural rigidity, ρA is mass per unit length and L is the span length. λ_n is the n*th* none-zero root of the following equation:

$$2R_1R_2\phi_1(\lambda)\lambda^2 + (R_1 + R_2)\phi_6(\lambda)\lambda - \phi_4(\lambda) = 0 \tag{5.2}$$

Where:

$$R_1 = \frac{EI}{k_{r_1}L}, R_2 = \frac{EI}{k_{r_2}L}, \phi_1(\lambda) = \sin(\lambda)\sinh(\lambda), \phi_4(\lambda) = \cos(\lambda)\cosh(\lambda) - 1,$$

$$\phi_6(\lambda) = \sin(\lambda)\cosh(\lambda) - \sinh(\lambda)\cos(\lambda) \tag{5.3}$$

This general equation for restrained Euler-Bernoulli beams can be used for different combinations of boundary conditions presented by Maurizi et al. **[75, 76]** and later on by Fung **[77]**.

As explained in chapter 3, frequencies of PLVM and ILVM almost depend only on the properties of the relevant member and its local boundary conditions. Therefore, the above equations can be used in quantification of damage degree in belt conveyors. The first, second, or higher frequencies of PLVM and ILVM are estimated from measurement. Then, using the above equation, the loss of stiffness is estimated.

Another parameter that has to be considered for frequencies of PLVM and ILVM, or natural frequencies of simple supported beam with rotational springs at the ends, is axial load. In general, stiffness of a beam can be written as **[78]**:

$$[K] = [K_m] + [K_G] \tag{5.4}$$

where $[K_m]$ and $[K_G]$ are elemental and geometric stiffness matrix respectively. Geometric stiffness matrix for frame elements including shear and bending effects is a function of material properties and axial force **[79]**. In equation (5.4), this matrix is positive for tensile force and negative for compressive force. This means stiffness of an element reduces with compressive force and increases with tensile force.

Accordingly, the natural frequencies of a compressive beam are less than the natural frequencies of a similar tensile beam.

The exact n*th* natural frequency ω_n of a pinned-pinned, sliding-sliding and pined-sliding beam is **[80, 81]**:

$$\omega_n = (n\pi)^2 \sqrt{1+\frac{p}{p_{cr)n}}} \sqrt{\frac{EI}{mL^4}} \tag{5.5}$$

where P is the applied axial load and P_{cr} is the critical load. Therefore, the frequency ratio is:

$$\frac{\omega_{n\,p\neq 0}}{\omega_{n\,p=0}} = \sqrt{1+\frac{p}{p_{cr)n}}} \tag{5.6}$$

where $\omega_{np=0}$ and $\omega_{\mathrm{np}\neq 0}$ are rhe n*th* natural frequency with and without axial force, respectively.

For other boundary conditions, i.e. with rotational springs at the ends, the frequency ratio is **[82]**:

$$\frac{\omega_{n\,p\neq 0}}{\omega_{n\,p=0}} = \sqrt{1+\mu\frac{p}{p_{cr)n}}}\ ,\ \mu \leq 1 \tag{5.7}$$

P_{cr} is minimum for pined-pined beam. Therefore, the frequency ratio is maximum for pined-pined beam for a constant axial force.

The sensitivity analysis of the frequency of PLVM with respect to axial loads created by self-weight of the belt conveyor is carried out. Since the internal forces of members under self-weight of the belt conveyor are almost constant for different stiffness of internal rotational springs , the connections are considered as pined for each secondary member as the most critical case. Then, axial force of each secondary member under self-weight of the structure is numerically calculated in the finite element model. Figure 5-2 shows the deformation of the structure.

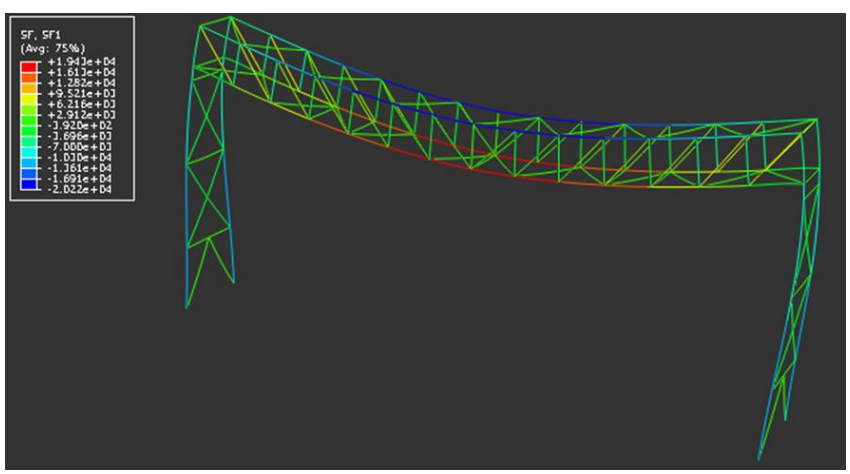

Figure 5-2 Deformation of the structure under its weight

Figure 5-3 shows the frequencies changes of PLVM for all secondary identical members of different set after considering the effect of axial forces under self-weight of the structure.

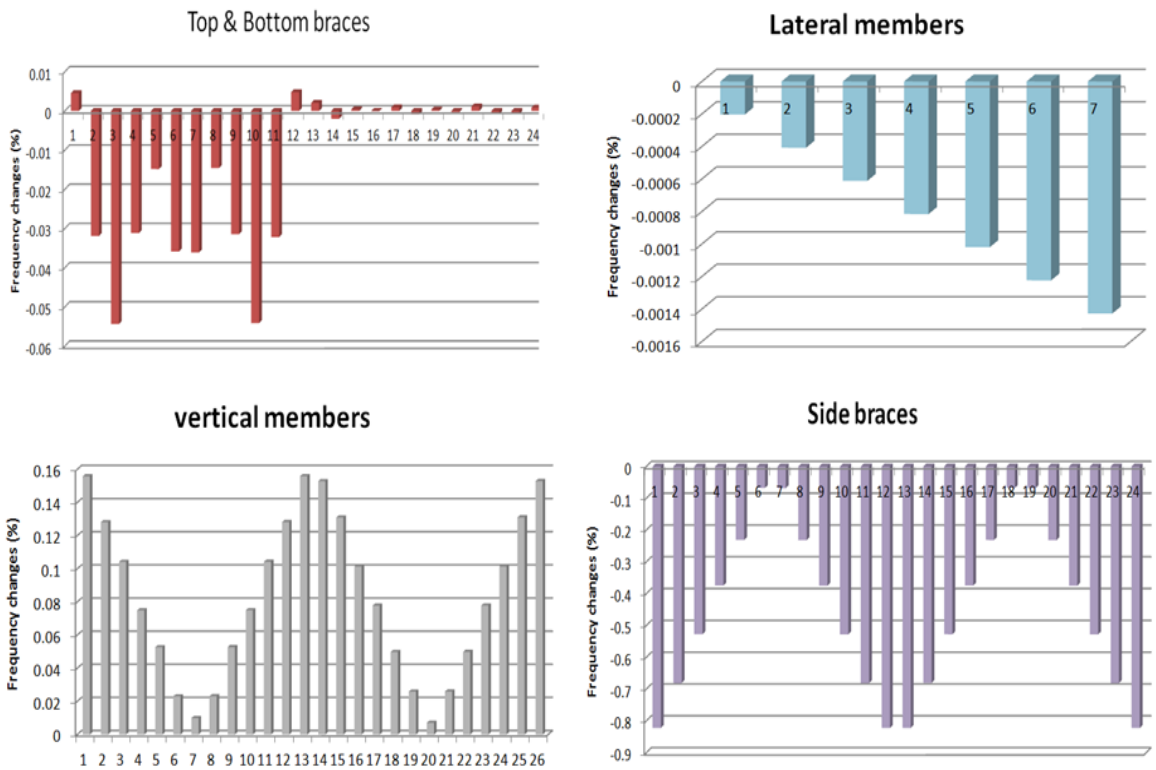

Figure 5-3 Frequencies changes of PLVM for all secondary identical members of different set

As shown, the frequencies changes of PLVM are small and at most are 0.82%. Note that this frequency changes are for pined connections. For real cases, where the connections are between pined-pined and clamped-clamped, the change is even less than 0.82%. Therefore, the effect of internal axial loads, created by self-weight of the structure, on the frequencies of PLVM of secondary members is negligible.

5.3 Damage identification technique using PLVM and ILVM frequencies comparison

To detect the locations of damaged secondary members in the support structure of belt conveyors, first, identical members are identified. Next, vibration test is carried out for many identical and non-identical members in different parts of the structure to correctly find PLVM and ILVM corresponding to each identical members set. Then, since frequencies of PLVM and ILVM of a member is almost independent of the properties of other members as well as the global shapes or boundary conditions of the structure, damage members can be readily identified due to the fact that for each identical members set, undamaged secondary members have PLVM, yet, damaged members have ILVM in which their frequencies are smaller than the PLVM.

To quantify the damage degree, formulas of the beam theory is used. First, using frequencies of PLVM, the stiffness of local boundary conditions is estimated. Then, if we assume there is no damage on the connections, using frequencies of ILVM, the damage degree of each damaged member is quantified. The method is valid even if damage happens on the connections but higher frequencies of ILVM, i.e. 2nd, 3rd

and so on, have to be utilized. The proposed damage identification method is summarized in a flow chart shown in figure 5-4.

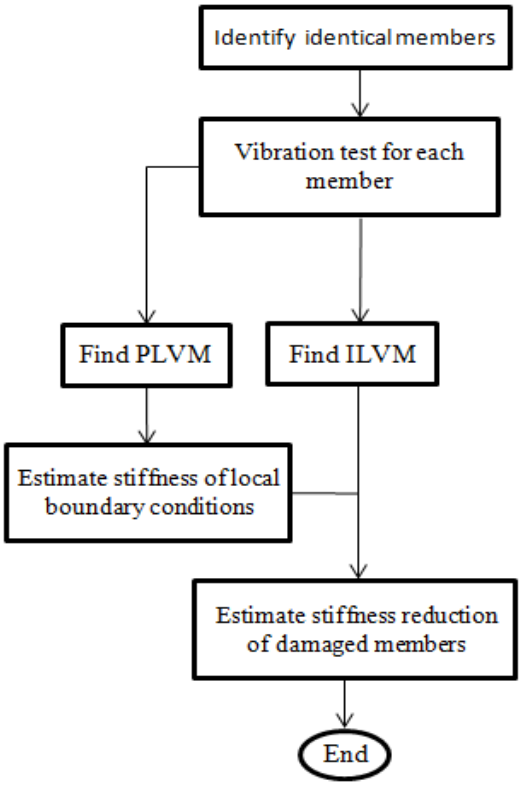

Figure 5-4 Proposed damage identification method based on PLVM and ILVM frequencies comparison

Identifying damaged secondary members together with the damage identification method based on global modes and their derivatives can be used to detect damaged main members. This is explained in the next section of this chapter.

5.4 Damage identification of a finite element model

In order to examine the applicability of damage identification of a simulated model of a belt conveyor, at first, some members of the support structure of the belt conveyor randomly damage. These members are of different members sets and shown in figure 5-5.

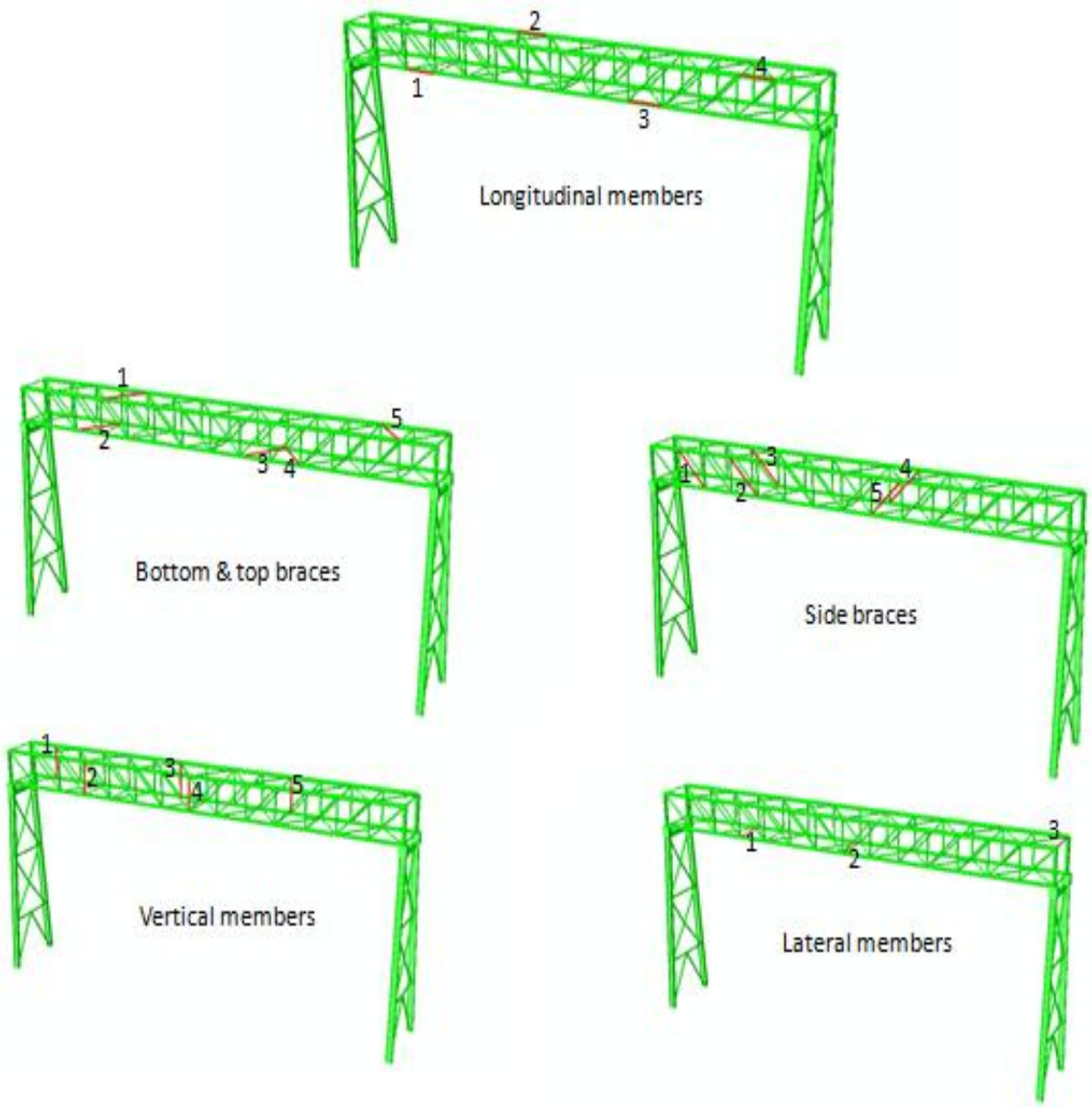

Figure 5-5 Damaged elements of different members sets

In the above figure, there are generally five member sets in the main frame of the support structure of the belt conveyor. Longitudinal elements are considered as main members and elements in the other sets are secondary members. Totally 22 members are damaged with different severities. Table 5-1 shows the percentage of stiffness reduction of the members in each set. These reductions of stiffness have been applied to the members in the simulated belt conveyor and are considered as damage in the main frame of support structure of the belt conveyor.

Table 5-1 Damage degree of the members

Member sets	Stiffness reduction of member 1	Stiffness reduction of member 2	Stiffness reduction of member 3	Stiffness reduction of member 4	Stiffness reduction of member 5
Bottom and top braces	75%	5%	10%	20%	35%
Side braces	90%	5%	65%	25%	25%
Vertical members	85%	5%	55%	15%	30%
Lateral members	5%	15%	40%	-	-
Longitudinal members	50%	10%	20%	80%	-

5.4.1 PLVM and ILVM Identification and Damage localization

The velocity time history data of many points of the main frame of support structure of the belt conveyor are requested through dynamic implicit analysis with a sampling frequency equals to 5000 Hz while the bottom of both columns are hit. The Fourier spectrum (FFT) of each data is examined to specify frequencies of PLVM and ILVM corresponding to each secondary member. Figure 5-6 shows Fourier spectrums of some of the bottom and top braces and a lateral member of the main frame of the belt conveyor. Here, the right most bottom brace and the lateral member are not identical with bottom and top braces and have been plotted to find PLVM.

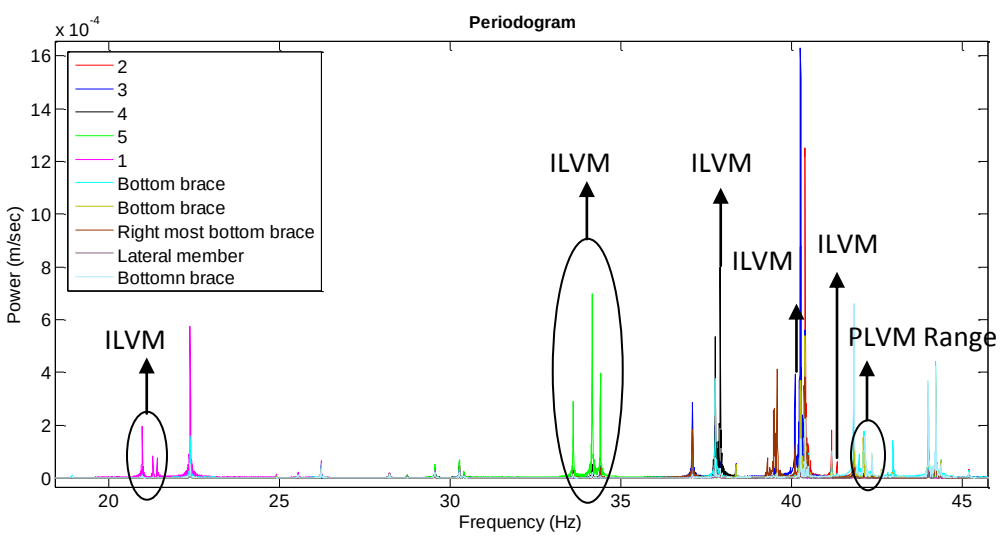

Figure 5-6 Fourier spectrums of some members (PLVM and ILVM of bottom and top braces)

As shown in the above figure, there are five ILVM corresponding to members 1 to 5 and one PLVM range in which the amplitude of bottom and top braces are much larger than members 1 to 5 and the other members. The other peaks correspond to global vibration modes or other modes in which all or some

parts of the structure disorderly vibrate. Figure 5-6 is zoomed on the PLVM range and shown in figure 5-7.

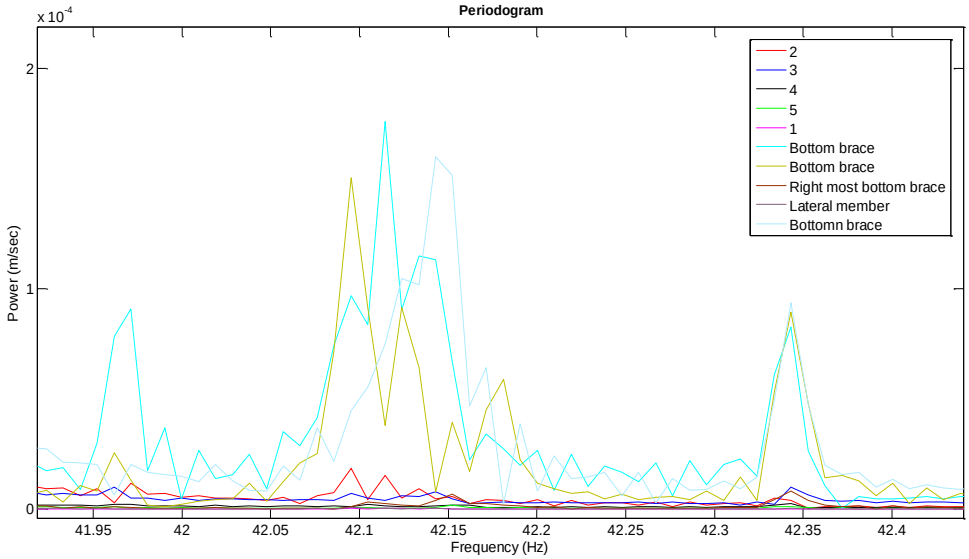

Figure 5-7 Fourier spectrums of some members (PLVM range of bottom and top braces)

Note that the other 16 identical braces in bottom and top parts of the main frame have peaks in the PLVM range but not shown in the above figure. Therefore, 19 out of 24 identical braces strongly vibrate at PLVM range and members 1 to 5 have small vibrations. It means that members 1 to 5 have been damaged. As illustrated in figure 5-6, these damaged members have their own peaks called ILVM in which the vibrations of these damaged members are much larger than the other members. Figure 5-6 is zoomed on the ILVM corresponding to member 5 and shown in figure 5-8.

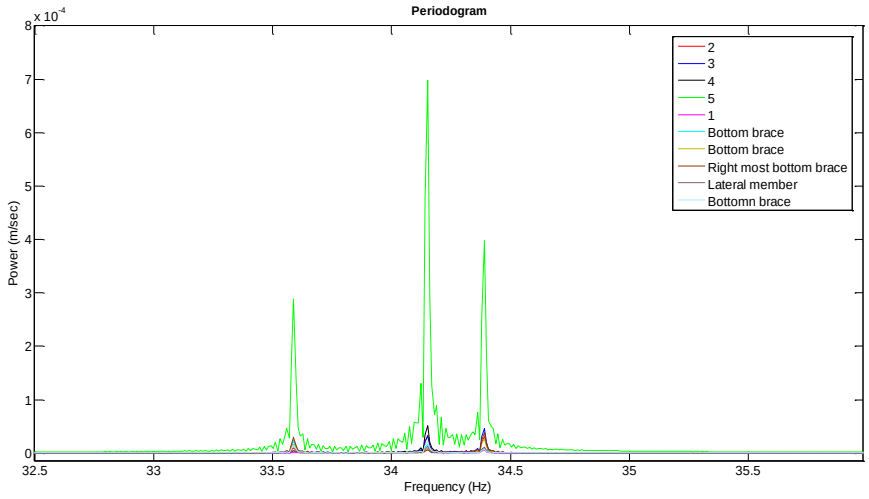

Figure 5-8 Fourier spectrums of some members (ILVM of member 5)

The amplitude of member 5 is much larger than the other members in the three peaks and this damaged member locally vibrates. In fact only one of the three peaks in the above figure corresponds to the ILVM

of member 5; however, because the frequency of ILVM is at the vicinity of the frequencies of other two modes in the structure, member 5 has much larger amplitude than the other members. Therefore, in case many peaks exist, the mean value of frequencies of these peaks is considered as frequency of ILVM since these peaks are always close to each other. As shown in figure 5-6, member 5 and 1 have three peaks while member 2, 3, 4 have only one peak which correspond to their ILVM.

Frequency of the PLVM of the identical bottom and top braces as well as frequencies of the ILVM of member 1 to 5 are presented in table 5-2. Note that the frequency of PLVM, presented in the table, is the mean value of the PLVM range. Moreover these frequencies acquired through eigenvalue analysis in ABAQUS and shown in this table.

Table 5-2 Frequencies of the PLVM and ILVM (bottom and top braces)

Mode	Frequency through Fourier spectrum (Hz)	Frequency through eigenvalue analysis (Hz)
PLVM	42.15	42.11
ILVM of member 1	21.22	21.285
ILVM of member 2	41.32	41.329
ILVM of member 3	40.09	40.09
ILVM of member 4	37.89	37.884
ILVM of member 5	34.04	34.154

As shown in the table, the results of two different methods are almost the same.

Figure 5-9 shows Fourier spectrums of identical lateral members of the main frame of the belt conveyor.

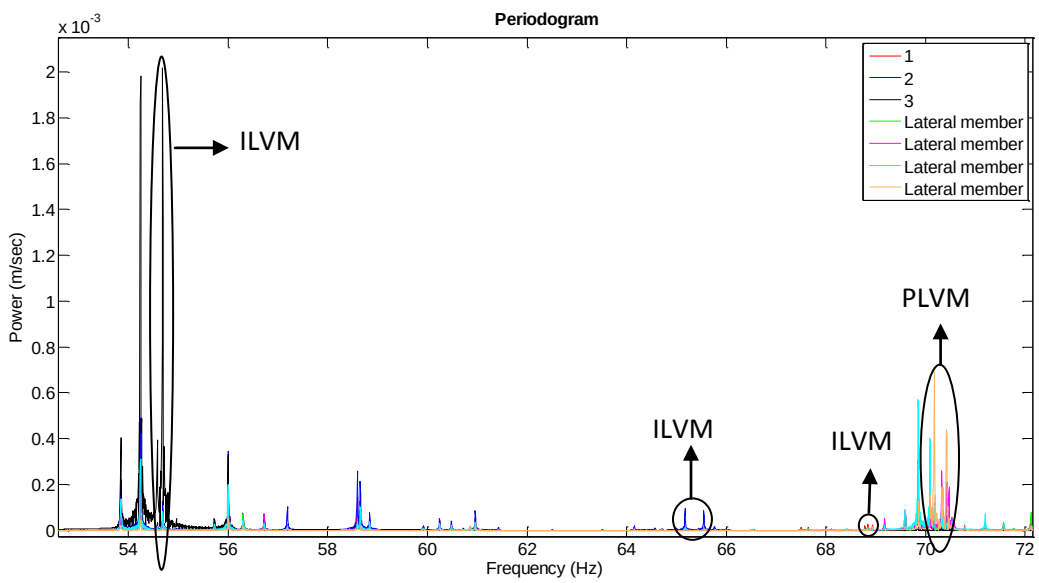

Figure 5-9 Fourier spectrums of some lateral members

In the above figure, there are three ILVM corresponding to members 1, 2 and 3 and one PLVM range in which the amplitude of other lateral members are much larger than members 1, 2 and 3. The other peaks

correspond to global vibration modes or other modes in which all or some parts of the structure disorderly vibrate. Figure 5-9 is zoomed on the PLVM range and shown in figure 5-10.

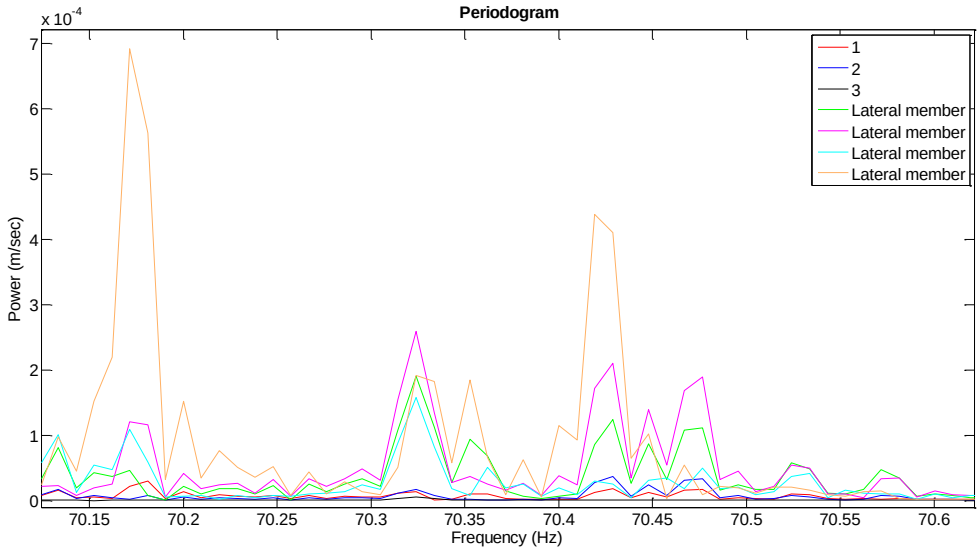

Figure 5-10 Fourier spectrums of lateral members in PLVM range

Four out of seven identical lateral members strongly vibrate at the PLVM range and members 1, 2 and 3 have small vibrations. It means that members 1, 2 and 3 have been damaged. As illustrated in figure 5-9, these damaged members have ILVM in which their vibrations are much larger than the other members. Figure 5-9 is zoomed on the ILVM corresponding to member 2 and shown in figure 5-11.

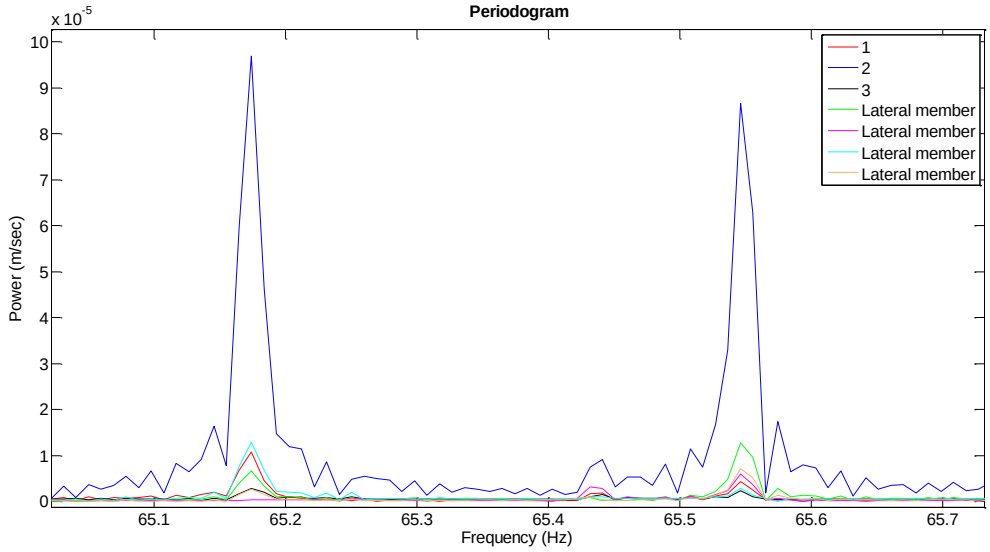

Figure 5-11 Fourier spectrums of lateral members (ILVM of member 2)

The amplitude of member 2 is much larger than the other lateral members and this damaged member locally vibrates. As already explained, in case many peaks exist, the mean value of frequencies of these peaks would be considered as frequency of ILVM.

Frequency of the PLVM of identical lateral members as well as frequencies of the ILVM of member 1, 2 and 3 are presented in table 5-3. It should be noted that frequency of the PLVM, presented in the table, is the mean value of the PLVM range. Moreover these frequencies acquired through eigenvalue analysis in ABAQUS and shown in this table.

Table 5-3 Frequencies of the PLVM and ILVM (lateral members)

Mode	Frequency through Fourier spectrum (Hz)	Frequency through eigenvalue analysis (Hz)
PLVM	70.37	70.466
ILVM of member 1	68.82	68.861
ILVM of member 2	65.21	65.075
ILVM of member 3	54.63	54.657

As shown in the table, the results of two different methods almost show the same value.

Figure 5-12 shows Fourier spectrums of some identical side braces of the main frame of the belt conveyor.

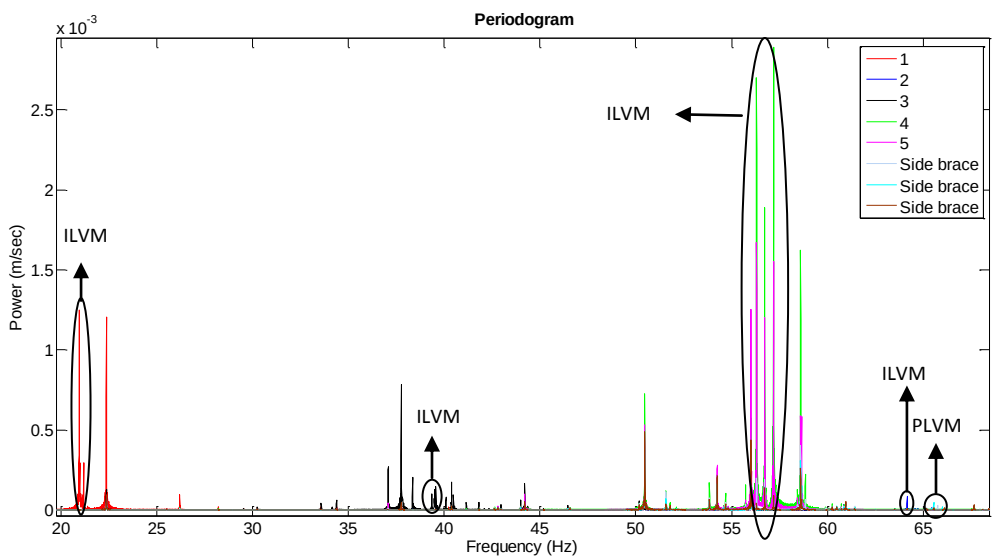

Figure 5-12 Fourier spectrums of some side braces

In the above figure, there are five ILVM corresponding to members 1 to 5 and one PLVM range in which the amplitude of side braces are much larger than members 1 to 5. The other peaks correspond to global vibration modes or other modes in which all or some parts of the structure disorderly vibrate. Figure 5-12 is zoomed on the PLVM range and shown in figure 5-13.

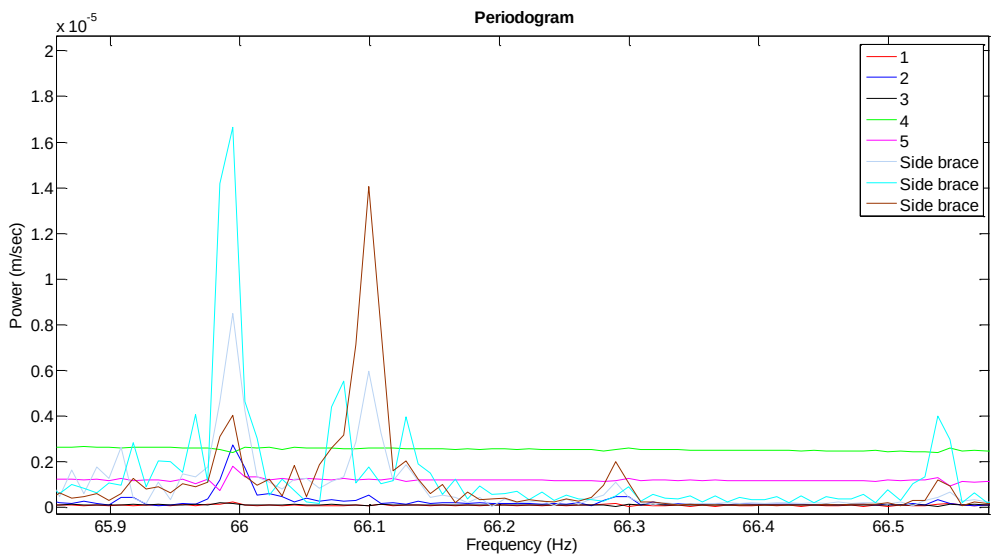

Figure 5-13 Fourier spectrums of some side braces in the PLVM range

Note that the other 16 identical side braces of the main frame have peaks in the PLVM range but not shown in the above figure. Therefore, 19 of 24 identical braces strongly vibrate at the PLVM range and members 1 to 5 have small vibrations. It means that members 1 to 5 have been damaged. As shown in figure 5-12, these damaged members have ILVM in which their vibrations are much larger than the other members. Figure 5-12 is zoomed on the ILVM corresponding to member 3 and shown in figure 5-14.

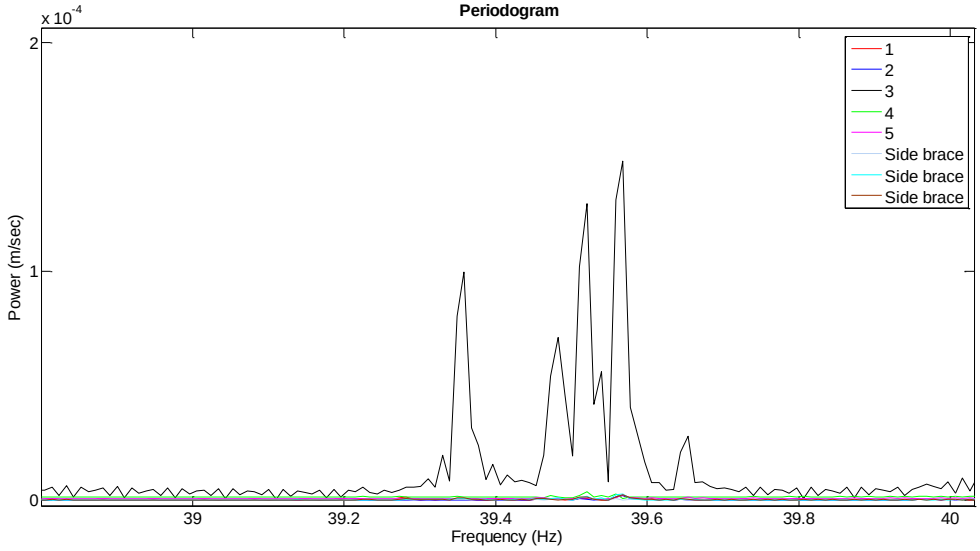

Figure 5-14 Fourier spectrums of some side braces (ILVM of member 3)

The amplitude of member 3 is much larger than the other side braces and this damaged member locally vibrates. As explained, the mean value of frequencies of these peaks would be considered as frequency of the ILVM.

Frequency of the PLVM of identical side braces and frequencies of the ILVM of member 1 to 5 are presented in table 5-4. Note that the frequency of PLVM, presented in the table, is the mean value of the PLVM range. Moreover these frequencies calculated through eigenvalue analysis in ABAQUS and shown in this table.

Table 5-4 Frequencies of the PLVM and ILVM (side braces)

Mode	Frequency through Fourier spectrum (Hz)	Frequency through eigenvalue analysis (Hz)
PLVM	66.22	65.955
ILVM of member 1	21.08	20.976
ILVM of member 2	64.48	64.609
ILVM of member 3	39.516	39.355
ILVM of member 4	56.74	57.22
ILVM of member 5	56.74	57.22

As shown in the table, the results of two different methods almost show the same value.

Figure 5-15 shows Fourier spectrums of some identical vertical members of the main frame of the belt conveyor.

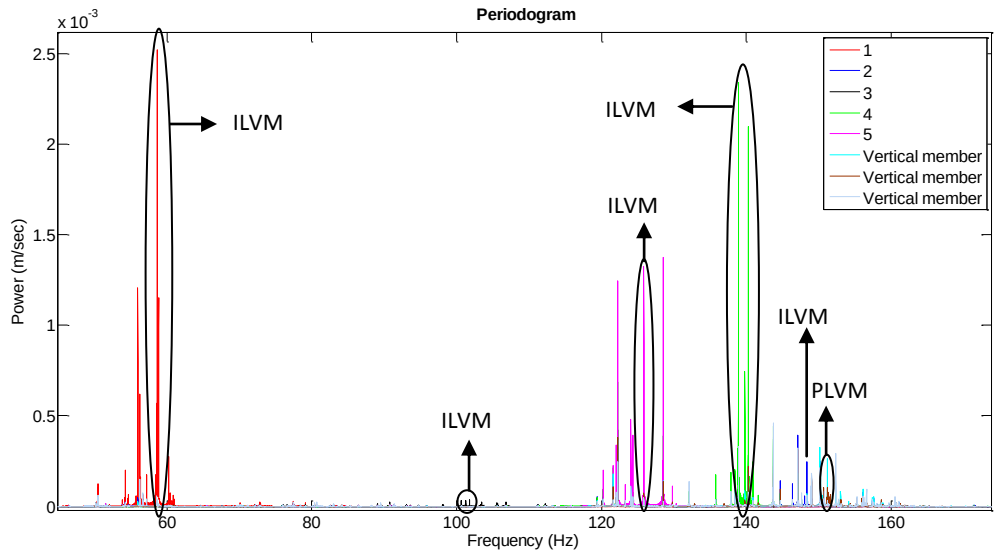

Figure 5-15 Fourier spectrums of some vertical members

In the above figure, there are five ILVM corresponding to members 1 to 5 and one PLVM range in which the amplitude of vertical members are much larger than members 1 to 5. The other peaks correspond to global vibration modes or other modes in which all or some parts of the structure disorderly vibrate. Figure 5-15 is zoomed on the PLVM range and shown in figure 5-16.

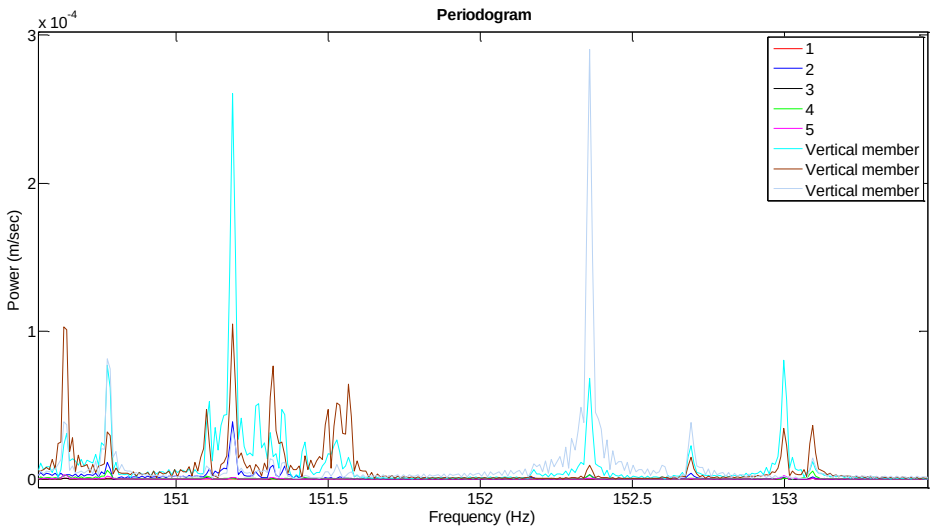

Figure 5-16 Fourier spectrums of some vertical members in the PLVM range

Note that the other 18 identical vertical members of the main frame have peaks in the PLVM range but not shown in the above figure. Therefore, 21 of 26 identical vertical members strongly vibrate at the PLVM range and members 1 to 5 have small vibrations. It means that members 1 to 5 have been damaged. As shown in figure 5-15, these damaged members have ILVM in which their vibrations are much larger than the other members. Figure 5-15 is zoomed on the ILVM corresponding to member 1 and shown in figure 5-17.

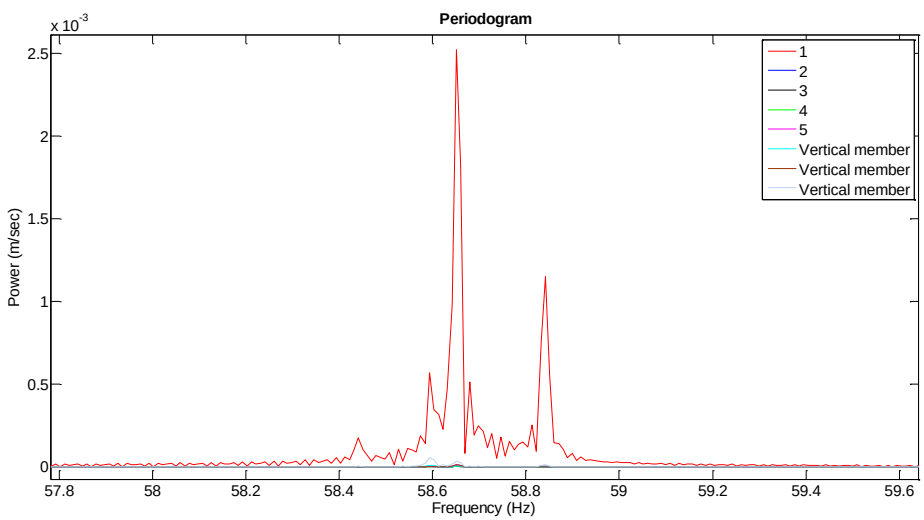

Figure 5-17 Fourier spectrums of some vertical members (ILVM of member 1)

In the above figure, the amplitude of member 1 is much larger than the other vertical members and this damaged member locally vibrates. As already explained, in case of existence many peaks in ILVM, the mean value of frequencies of these peaks is considered as frequency of ILVM.

Frequency of the PLVM of identical vertical members and frequencies of the ILVM of member 1 to 5 are presented in table 5-5. Note that the frequency of PLVM, presented in the table, is the mean value of the

PLVM range. Moreover these frequencies calculated through eigenvalue analysis in ABAQUS and shown in this table.

Table 5-5 Frequencies of the PLVM and ILVM (vertical members)

Mode	Frequency through Fourier spectrum (Hz)	Frequency through eigenvalue analysis (Hz)
PLVM	152.35	151.805
ILVM of member 1	58.75	58.879
ILVM of member 2	148.2	148.34
ILVM of member 3	101.78	101.94
ILVM of member 4	139.67	139.37
ILVM of member 5	125.8	125.99

As shown in the table, the results of two different methods almost show the same value for frequencies.

5.4.2 Damage quantification

Reduction in the young's modulus of the members is considered as damage in the simulated model. Here, based on the design drawings, the connections at the both ends of each secondary member are identical. So the stiffness of rotational springs at the both ends of each member has same value.

All undamaged members in each members set have PLVM. Therefore, from equation (5.1) λ_n is:

$$\lambda_n = \left(\frac{\omega_n}{\sqrt{\frac{EI}{\rho L^4}}}\right)^{0.5} \tag{5.8}$$

The frequency of PLVM ω_n and the properties of undamaged members are known. Therefore, λ_n is calculated from the above equation. Since the stiffness of rotational springs at the ends of each secondary member has same values, equation (5.2) is written as:

$$2R^2\phi_1(\lambda)\lambda^2 + 2R\phi_6(\lambda)\lambda - \phi_4(\lambda) = 0 \tag{5.9}$$

where $\phi_1(\lambda)$, $\phi_4(\lambda)$ and $\phi_6(\lambda)$ have been already defined and $R = \frac{EI}{KL}$ in which K is the stiffness of rotational springs at the ends of each secondary member. Therefore, the only unknown in equation (5.9) is K and can be readily calculated.

For the damaged members, the frequencies of ILVM ω_n are known. Since we have assumed that the damage have only occurred in members not on connections, the stiffness of rotational springs at the both ends of damaged identical members is the same as undamaged members. Therefore, the only unknown parameter in equation (5.8) is EI. The ratio of calculated EI to initial EI indicates the damage degree of the members. Table 5-6 shows calculated damage degree of the members using the above equations.

Table 5-6 Calculated damage degree of the members

Member sets	Stiffness reduction of member 1	Stiffness reduction of member 2	Stiffness reduction of member 3	Stiffness reduction of member 4	Stiffness reduction of member 5
Bottom and top braces	74.81%	4.50%	10.10%	19.70%	35.19%
Side braces	89.86%	5.15%	64.38%	25.39%	25.39%
Vertical members	85.11%	5.27%	55.32%	15.86%	31.74%
Lateral members	4.28%	14.06%	39.69%	-	-

Figure 5-18 shows the absolute error of damage quantification using this method.

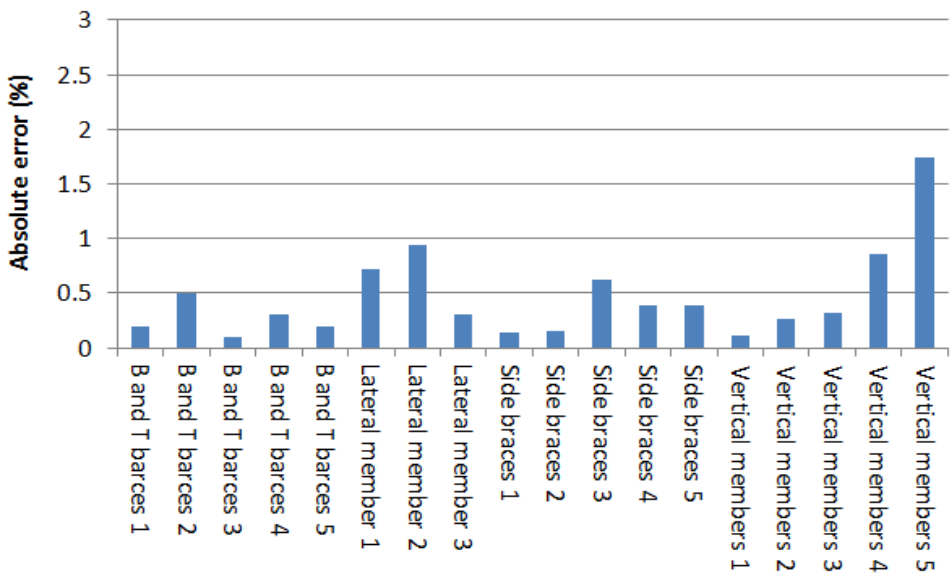

Figure 5-18 Absolute error of damage quantification

The maximum error is 1.74% which corresponds to member 5 of the vertical members. For the other damaged members, the error is less than 1%. Thus, the damage of secondary members in the main frame of the belt conveyor has been quantified with an acceptable accuracy. Using PLVM and ILVM, even small damage of secondary members is located and quantified without need of modal properties information of the undamaged structure.

5.4.3 Damage localization of the longitudinal members

As for longitudinal members, PLVM or ILVM are observed neither through eigenvalue analysis nor Fourier spectrum. The reason is that longitudinal members are continuous. Therefore, the local mode is not applicable for the longitudinal members. To detect damage locations of the main members, the 2nd derivative of the 1st lateral and vertical bending mode shapes of the main frame of the structure along line 1, 2, 3 and 4, shown in figure 3-30, are compared in the damaged and undamaged structures. Based on the

results obtained in chapter 3, locations of the damaged members are identified. Figure 5-19 and 5-20 show the 2nd derivative of 1st vertical and lateral bending modes respectively. Note that the interval between two successive points to calculate the 2nd derivative is 0.1 m for the lines 1, 2, 3 and 4.

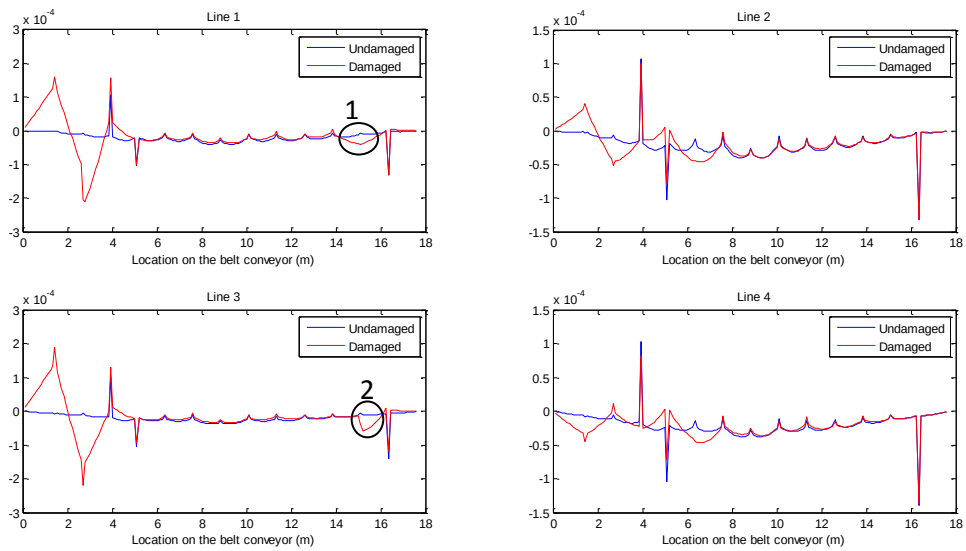

Figure 5-19 2nd derivative of the 1st vertical bending mode shape of the main frame of the damaged and undamaged structure

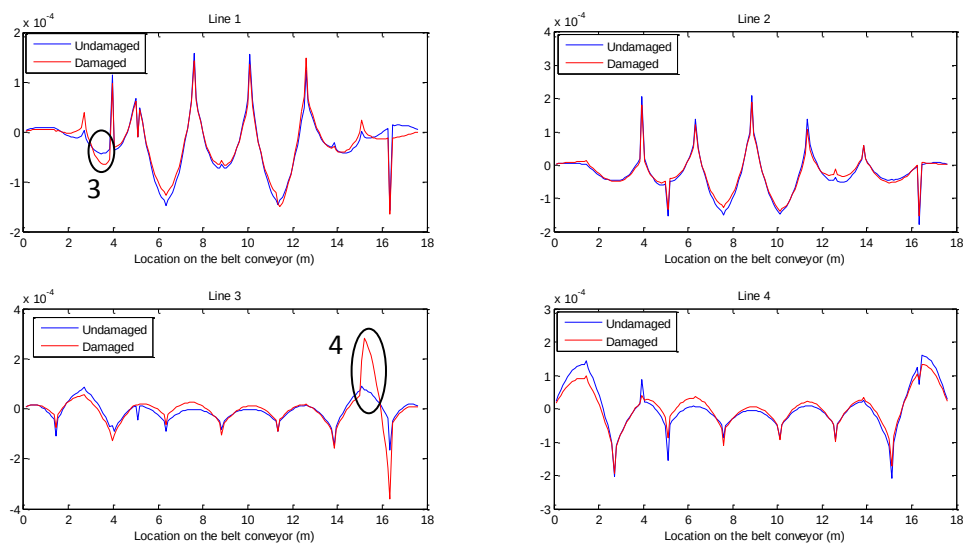

Figure 5-20 2nd derivative of the 1st lateral bending mode shape of the main frame of the damaged and undamaged structures

Based on the results in chapter 3, the 2nd derivative of the 1st lateral bending mode shapes along the 4 lines is sensitive to damage on the corresponding longitudinal members as well as the corresponding bottom or top braces. It is also a little sensitive to damage on the corresponding lateral members. Moreover it was found that the 2nd derivative of the 1st vertical bending mode shapes along the 4 lines is sensitive to damage

on the corresponding longitudinal members as well as the corresponding side braces. It is also a little sensitive to damage on the corresponding vertical members. As for damage on the longitudinal members, it should be noted that the 2nd derivative of the 1st vertical bending mode shapes along the 4 lines, not only sensitive to the damage on the corresponding longitudinal members but also the other longitudinal members connected to the corresponding longitudinal members by vertical members.

The locations and damage percentage of the secondary members have been already identified. Therefore, among the disordered mismatches between two curves in figures 5-19 and 5-20, the only mismatches which show damage locations of the longitudinal members are specified in figure 5-19 and 5-20. Mismatches 1, 2, 4 indicate the existence of damage on member 4 but mismatch 3 shows the existence of damage on member 1. Members 2 and 3 are not identified using this method. It is recalled that the damaged longitudinal members and the degree of damage have been shown in figure 5-5 and table 5-1 respectively. Note that members 1 and 4, which are correctly identified, have been damaged by 50% and 80%, respectively. However, members 2 and 3, which are not identified, have been damaged by 10% and 20%, respectively. The disadvantages of this method are:

1. Mode shapes of the undamaged structure are needed to compare with mode shapes of the damaged structure.
2. The method fails for small damage if many parts of the structure damage even for the 2nd derivative of mode shapes which is more sensitive to damage than the corresponding 1st derivative of mode shapes as well as mode shapes themselves.
3. Even though locations of large damage are identified, damage degree cannot be quantified using this method.

5.5 Damage identification Technique using PLVM amplitude comparison

PLVM corresponding to each identical secondary members set are easily observed when one of the undamaged identical members of the corresponding set is hit. Therefore, if one member damages, it is no longer identical with the other members of the set and no longer strongly vibrates at PLVM when hitting one of the undamaged identical members of the set.

Consider the damaged members of the bottom and top braces shown in figure 5-5. Brace 1, shown in figure 3-96, is hit by 500 N and the velocity time history data of all 24 bottom and top braces is simulated. Figure 5-21 shows the maximum amplitude of Fourier spectrums of 24 bottom and top braces at their PLVM range when brace No 1 is hit.

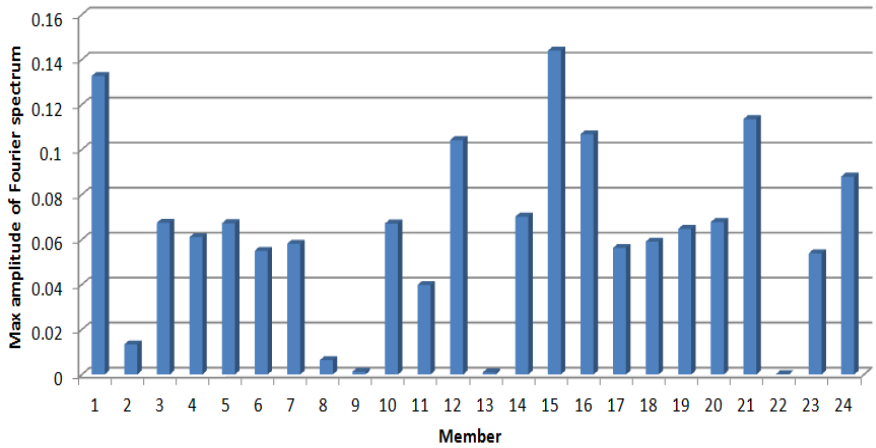

Figure 5-21 Maximum Fourier spectrums amplitude of 24 bottom and top braces at their PLVM range when brace No 1 is hit

As shown in the above figure, the maximum amplitude of Fourier spectrums for members 2, 8, 9, 13 and 22 are much smaller than the other members at their PLVM range. These are damaged members as shown in figures 5-5 and 3-96. Moreover, the relative severity of damage has inverse correlation with the value of maximum Fourier spectrums amplitude of identical members at the PLVM range. The more severe damage results in having the smaller amplitude in the PLVM range. Therefore, as shown in the above figure, the order of damage severity is estimated as member 22, 13, 9, 8 and 2 which is consistent with the introduce damage. The proposed damage identification method is summarized in a flow chart shown in figure 5-22.

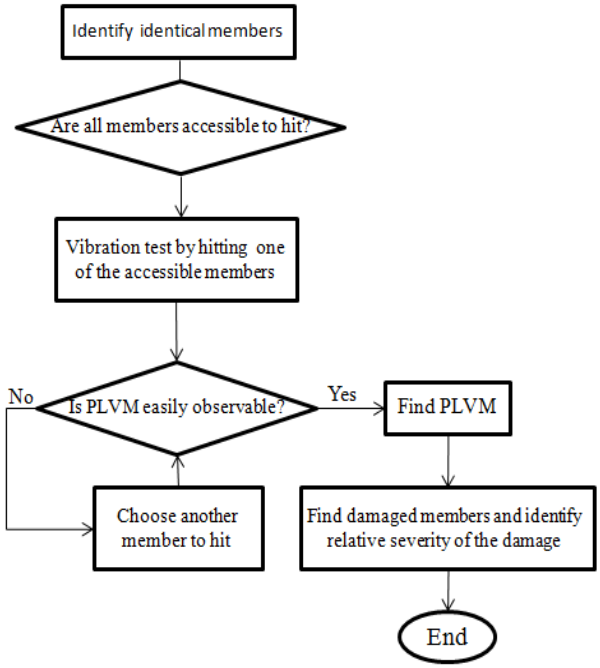

Figure 5-22 Proposed damage identification method based on PLVM amplitude comparison by hitting one of the undamaged identical members

To formulate this phenomenon, eigenvalue analysis is performed to extract all PLVM (which are obviously in the PLVM range). The modal matrix can thus be formed as:

$$[\phi] = [\{\phi\}_1, \{\phi\}_2, \dots, \{\phi\}_n] \tag{5.10}$$

where $\{\phi\}$ corresponds to each PLVM within the PLVM range and n represents the number of PLVM in the PLVM range.

It is known that the equation of motion for an undamped system in normal coordinate is written as:

$$[\widehat{M}]\{\ddot{q}\} + [\widehat{K}]\{q\} = \{\widehat{P(t)}\} \tag{5.11}$$

in which $\{q\}$ is the modal displacement vector and $[\widehat{M}]$, $[\widehat{K}]$ and $\{\widehat{P(t)}\}$ are modal mass matrix, modal stiffness matrix and modal force vector respectively. These matrices are defined as:

$$[\widehat{M}] = [\phi]^T[M][\phi] \tag{5.12.a}$$

$$[\widehat{K}] = [\phi]^T[K][\phi] \tag{5.12.b}$$

$$\{\widehat{P(t)}\} = [\phi]^T\{P(t)\} \tag{5.12.c}$$

where $[M]$, $[K]$ and $\{P(t)\}$ are mass matrix, stiffness matrix and load vector respectively. Equation (5.11) contains n independent linear equations and since for each mode $k_i = m_i\omega_i^2$ (ω_i^2 is the eigenvalue of i-th mode and m_i is the generalized mass for each mode), those equations are in the following form:

$$\ddot{q}_i + \omega_i^2 q_i = \frac{\{\phi\}_i^T}{m_i}\{P(t)\}\ ,\ i = 1,2,\dots,n \tag{5.13}$$

The maximum modal amplitude of each identical member in their PLVM range is needed to calculate due to any impact force applied to one of the identical members. The impact load vector can be presented as:

$$\{P(t)\} = P_0\{\mathbb{P}\} \tag{5.14}$$

where P_0 is the value of impact force and $\{\mathbb{P}\}$ is a unit vector whose arrays are zero except for the location where the impact load applied. Therefore, to consider the effect of the location of applied impact load, **P**articipation **F**actor (PF) for each PLVM is defined as:

$$PF = \frac{\{\phi\}_i^T}{m_i}\{\mathbb{P}\}\ ,\ i = 1,2,\dots,n \tag{5.15}$$

Therefore, the maximum amplitude of each identical member in its PLVM range, $Max\ A_{PLVM}$, (independent from the value of impact force) is the maximum value of the following matrix for each identical member:

$$[\phi]\mathrm{Diag}\{\mathrm{PF}\} \tag{5.16}$$

Figure 5-23 shows the maximum modal amplitude of each identical bottom and top brace in its PLVM range while the location of impact force is at the center of brace 1. Note that only the value of mode shapes at the center of each 24 identical bottom and top braces along the vertical direction is extracted to calculate maximum modal amplitude of the members.

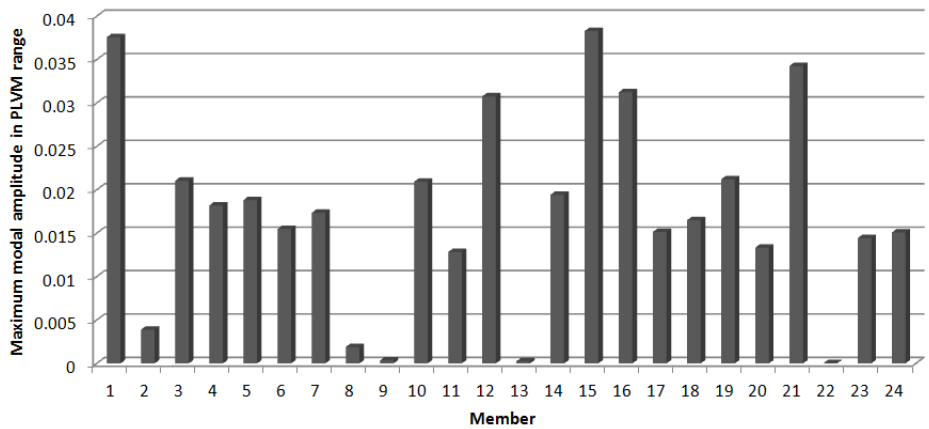

Figure 5-23 Maximum modal amplitude of each identical bottom and top brace in its PLVM range when brace 1 is hit

Comparing this figure with figure 5-21 shows that the results in two figures are nearly the same and the damaged members as well as the relative severity of the damage are identified. Possible reason for the difference is the effect of damping in the structure. The maximum modal amplitude of the damaged members in the PLVM range, calculated by the above formulas, and the relative damage severity are presented in table 5-7.

Table 5-7 Maximum modal amplitude of the damaged members in the PLVM range and the damage severity

Member	**Stiffness reduction**	**Max amplitude of PLVM ($\times 10^3$)**
2	5%	3.89
8	10%	1.89
9	20%	0.34
13	35%	0.25
22	75%	0.03

The advantage of this damage identification technique is that excitation force does not need to be provided at all of the members because only PLVM range is examined and PLVM can be excited by impact excitation at one of the undamaged secondary members. Note that combination of this technique with the damage identification method based on global modes and their derivatives can be used to detect damaged main members of the support structure of belt conveyors.

5.6 Summary

Based on the sensitivity analysis in chapter 3, a damage identification method using PLVM and ILVM frequencies comparison is proposed. The method use the fact that for each identical members set, undamaged secondary members have PLVM, yet, damaged members have ILVM in which their frequencies are smaller than the PLVM. Moreover, since frequencies of PLVM and ILVM almost depend only on the properties of the relevant member and its local boundary conditions, the formulas of natural frequencies of a simple supported beam together with rotational springs at the ends are used in the quantification of damage severity of the secondary members in belt conveyors. The method successfully identifies damaged secondary members of a finite element model of the belt conveyor support structure

with large number of damaged elements. Meanwhile, combination of this method with the damage identification method based on global vibration modes and their derivatives is used to detect damaged main members in the finite element model. The damaged main members with relatively large severity are correctly localized.

Another damage identification technique based on PLVM amplitude comparison is proposed. The method is based on the fact that PLVM corresponding to each identical secondary members set are easily observed when one of the undamaged identical members of the corresponding set is hit. Using this method, damaged secondary elements of each identical members set are identified by comparing their maximum modal amplitude at the corresponding PLVM range while hitting one of the undamaged members of the identical members set. Moreover, relative damage severity of damaged members in each identical members set is identified. Combination of this technique with the damage identification approach based on global vibration modes and their derivatives can be used to detect damaged main members of the support structure of belt conveyors.

Chapter 6

Damage identification experiment on scale-model space structures

6.1 Introduction

In this chapter, two different space structures with continuous and non-continuous main members are considered. At the beginning, existence of PLVM is checked. Next, some secondary members of the frames are damaged and the locations of damaged members are identified using frequency changes of PLVM and, accordingly, existence of ILVM. Perusing the fact found in chapter 4, the frequencies of PLVM and ILVM in the frames are compared with the natural frequencies of the corresponding simple supported beams. Finally, damage identification using PLVM amplitude comparison for the structure with continuous main member is examined and the results of the previous chapter are experimentally verified. The damage identification method based on global vibration modes and their derivatives are not examined for these laboratory models.

6.2 Damage identification using PLVM and ILVM frequencies comparison: laboratory space frame with non-continuous main members

6.2.1 Description of the laboratory model

Figure 6-1 shows a 5-bay laboratory truss frame. The model is two meters tall from its base plate and each bay is a 40 cm cube. The model contains diagonal and lateral members which are considered as secondary members and made of aluminum. The secondary members are pipes whose external and internal diameters are respectively 1 and 0.8 cm. The model has non-continuous longitudinal members, which is considered as the main members. The main members are steel solid bars whose diameter is 1.5 cm.

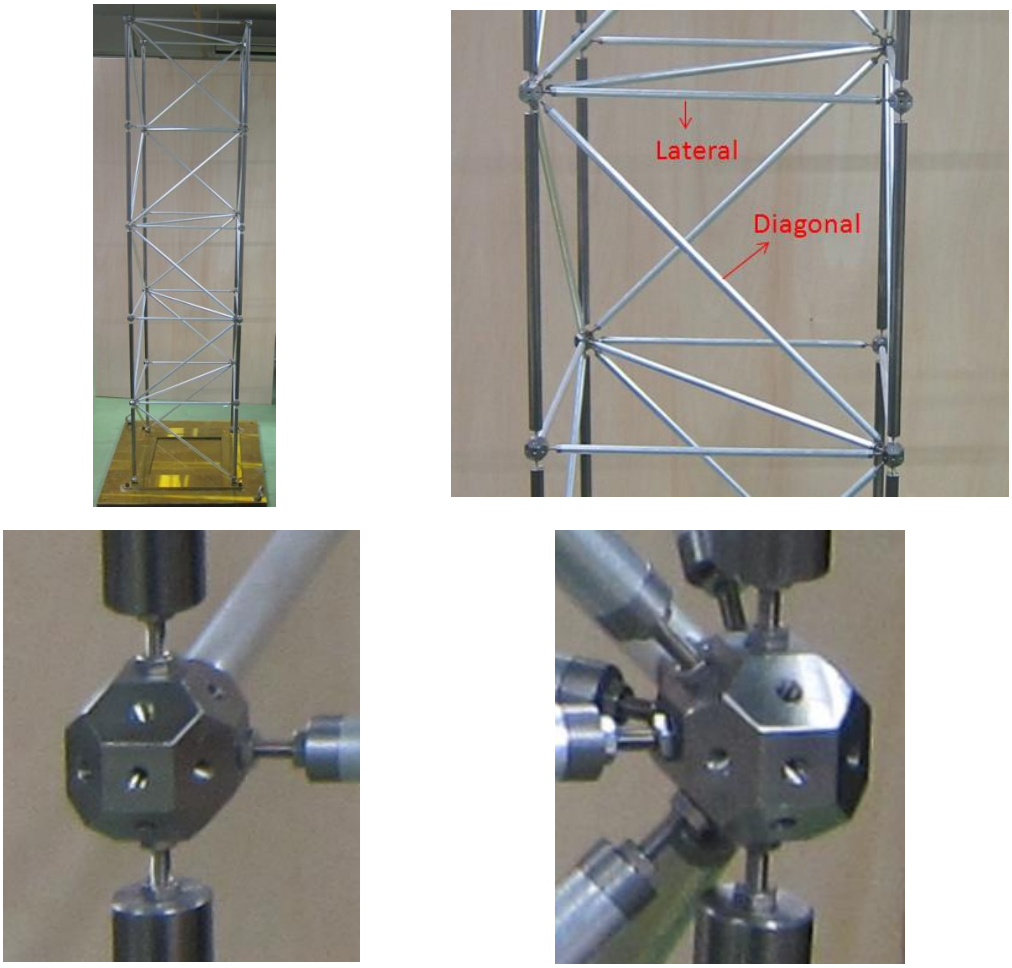

Figure 6-1 Laboratory space frame with non-continuous main members

6.2.2. Existence of PLVM for secondary members

In order to observe PLVM corresponding to the identical secondary members, the velocity time history of each secondary member is measured by Laser Doppler Vibrometer (LDV) as shown in figure 6-2 and its power spectral density (PSD) is examined. Each member is directly hit and the sampling frequency is 10000 Hz.

Figure 6-2 Measurement by Laser Doppler Vibrometer

Based on the formula of the deflections of simple supported and clamped-clamped beams presented in chapter 4, the stiffness of the main members are about 73 times larger than the diagonal members. Moreover, as shown in figure 6-1, many members are attached to the connections of diagonal members. Therefore, the relative stiffness of the diagonal members is much less than the total stiffness of the main members together with other secondary members attached to the connections and, accordingly, PLVM and ILVM are expected to exist for diagonal members and their frequencies are nearly the same as natural frequencies of the corresponding diagonal member itself. For lateral members, the stiffness of the main members is only about 26 times larger than the lateral members. Additionally, as shown in figure 6-1, there is no other secondary member attached to the connections of the lateral members at one side. Therefore, coupling of local vibration modes might happen among the lateral members. The frequencies of PLVM and ILVM are expected not necessarily nearly the same as natural frequencies of the corresponding lateral members.

As explained in the previous chapters, to find PLVM corresponding to each identical members set, the results of some identical members of the set should be compared with the other members. Figure 6-3 shows the result for four diagonal, one lateral and one longitudinal members to find the PLVM corresponding to the diagonal members.

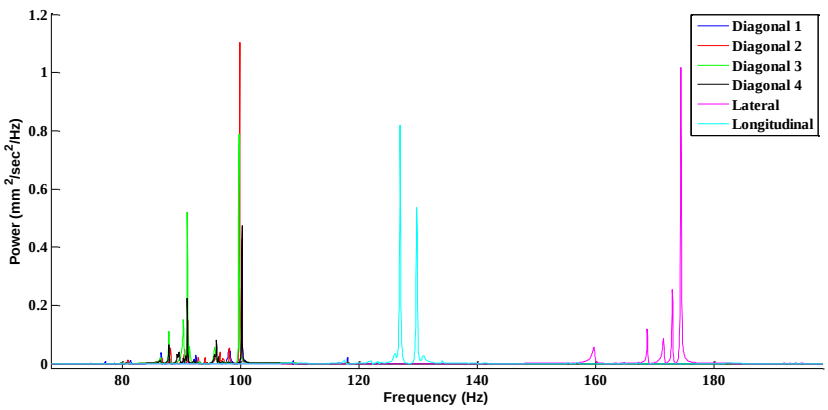

Figure 6-3 PSD diagrams of four diagonal, one lateral and one longitudinal members

As shown in the above figure, between 85 Hz to 100 Hz, the diagonal members have large amplitudes. In order to compare the amplitude of diagonal members with the lateral and longitudinal members, the figure is zoomed in the PLVM range and shown in figure 6-4.

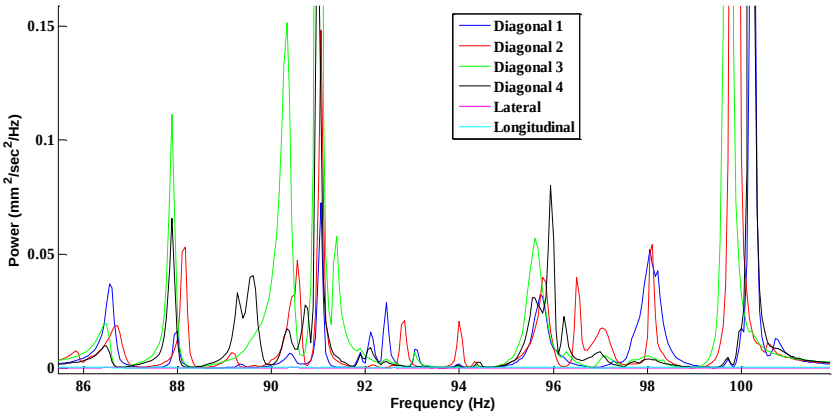

Figure 6-4 1st PLVM range of the diagonal members

In the above figure, the amplitude of the diagonal members is much larger than the lateral and longitudinal members and common for all diagonal members. Therefore these peaks are corresponding to the 1st PLVM of the diagonal members. Higher PLVM can be observed. Figure 6-5 and 6-6 respectively show the 2nd and 3rd PLVM range corresponding to the diagonal members.

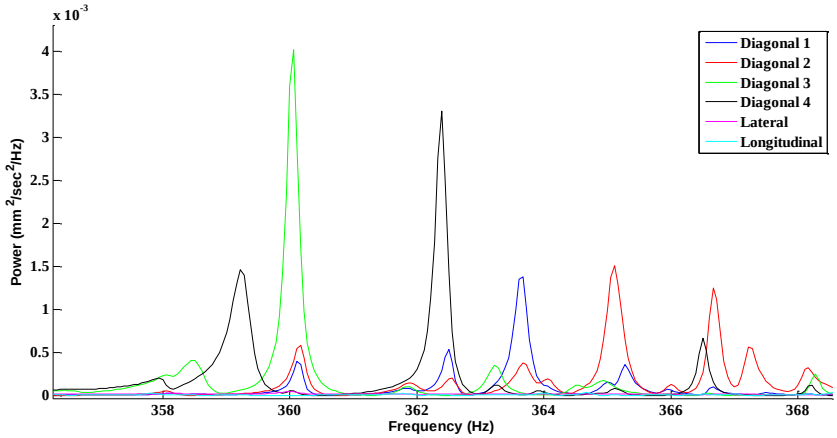

Figure 6-5 2nd PLVM range of the diagonal members

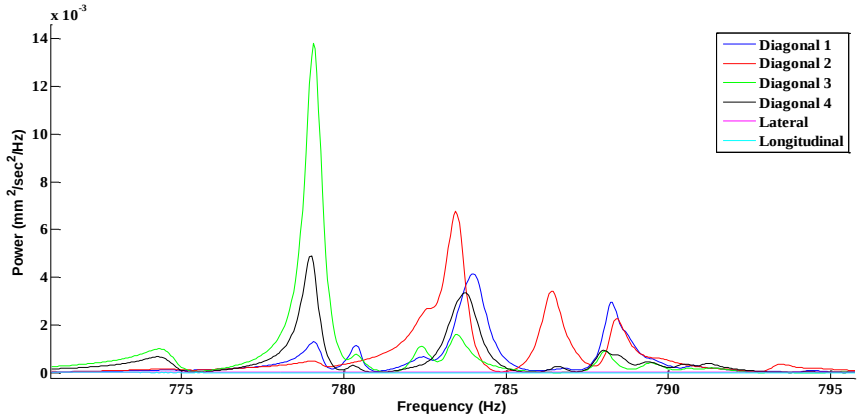

Figure 6-6 3rd PLVM range of the diagonal members

The amplitude of the diagonal members is much larger than the lateral and longitudinal members and common for all diagonal members in the above figures. Note that there is a range for PLVM because the identical diagonal members are soft and a little difference between their length, connections or their axial loads, caused by manufacturing errors, can change the frequencies of these local vibration modes.

Figure 6-7 shows the result for four lateral, one diagonal and one longitudinal members to find PLVM corresponding to the lateral members.

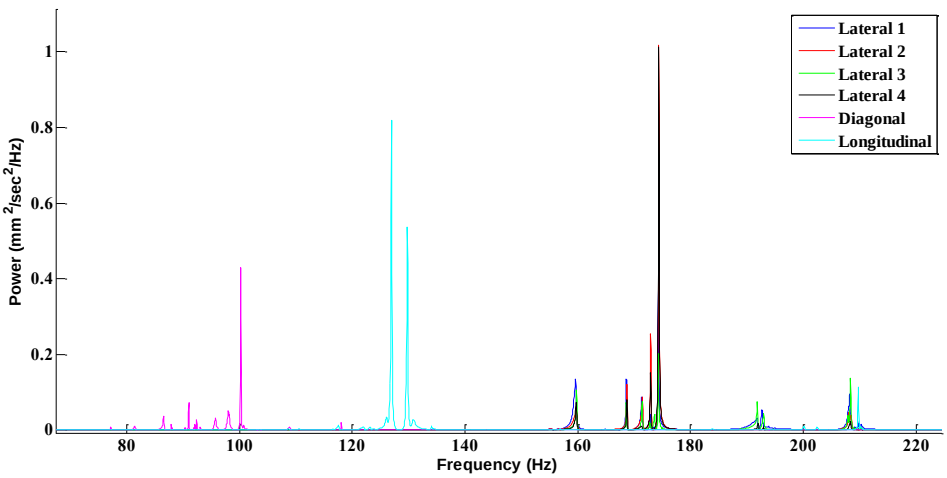

Figure 6-7 PSD diagrams of four lateral, one diagonal and one longitudinal members

In the above figure, between 160 Hz to 210 Hz, the lateral members have large amplitudes. In order to compare the amplitude of lateral members with the diagonal and longitudinal members, the figure is zoomed in this range and shown in figure 6-8.

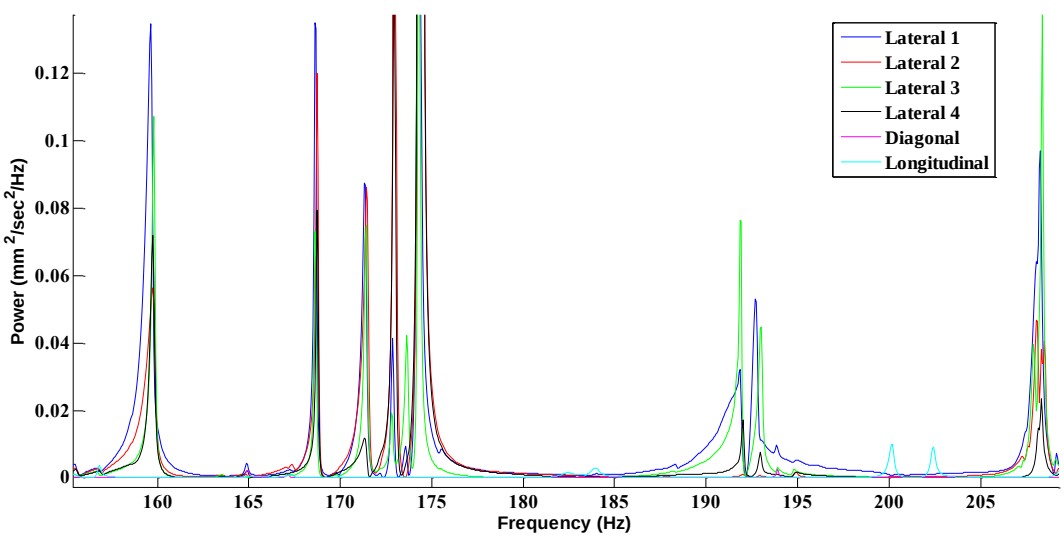

Figure 6-8 1st PLVM range of the lateral members

In the above figure, the amplitude of the lateral members is much larger than the diagonal and longitudinal members and common for all lateral members. Therefore, these peaks are considered the 1st PLVM of the lateral members. However, the range is wide and about 50 Hz. This wide frequency range might be due to the fact that the stiffness of the main members are not much larger than the lateral members and no other secondary member is attached to one of the connections of each lateral member.

6.2.3 Existence of ILVM in two damaged structures with non-continuous longitudinal members

In order to investigate the existence of ILVM, two damage cases are considered. To apply damage, several secondary members are replaced by bars with various diameters or cut by different portions of the diameter at the center. Locations of damaged secondary members in the laboratory models are shown in figure 6-9. The damaged members are listed in table 6-1. The thickness of all pipes is 1 mm.

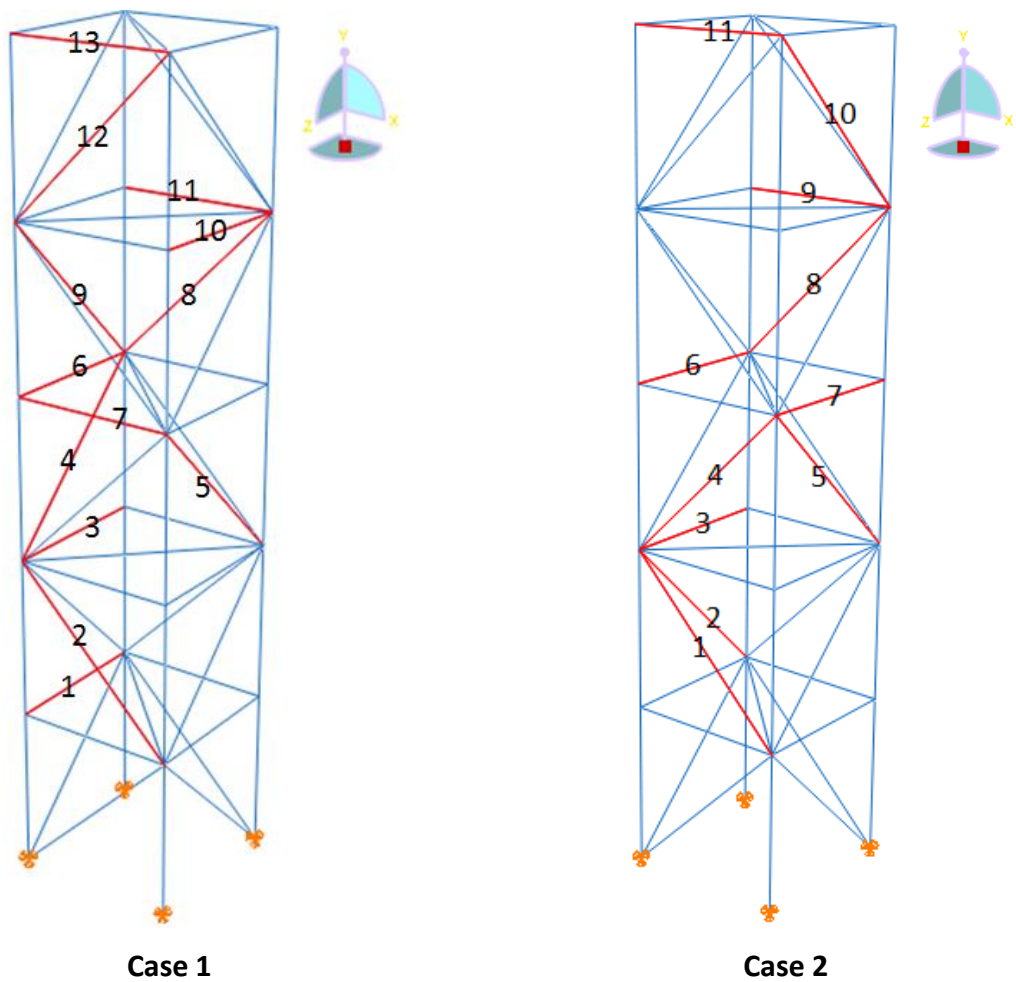

Figure 6-9 Locations of damaged members in the laboratory models with non-continuous longitudinal members

Table 6-1 Damaged members in the laboratory models with non-continuous longitudinal members

Case 1		**Case 2**	
Element No	Damage	Element No	Damage
1	Φ8×1	1	Φ8×1
2	Φ9.5×1	2	Φ13×1
3	Φ13×1	3	Φ11×1
4	Φ10×1 (1/2 cut)	4	Φ10×1 (1/3 cut)
5	Φ10×1 (2/3 cut)	5	Φ8×1
6	Φ15×1	6	Φ10×1 (1/2 cut)
7	Φ10×1 (2/3 cut)	7	Φ6×1
8	Φ6×1	8	Φ10×1 (3/4 cut)
9	Φ15×1	9	Φ6×1
10	Φ10×1 (1/3 cut)	10	Φ12×1
11	Φ9.5×1	11	Φ12×1
12	Φ11×1		
13	Φ8×1		

The velocity time history of secondary members in two damaged structures is measured. Moreover each secondary member is measured while separately connected to bearings, similar with the connections in the structure, as shown in figure 6-10.

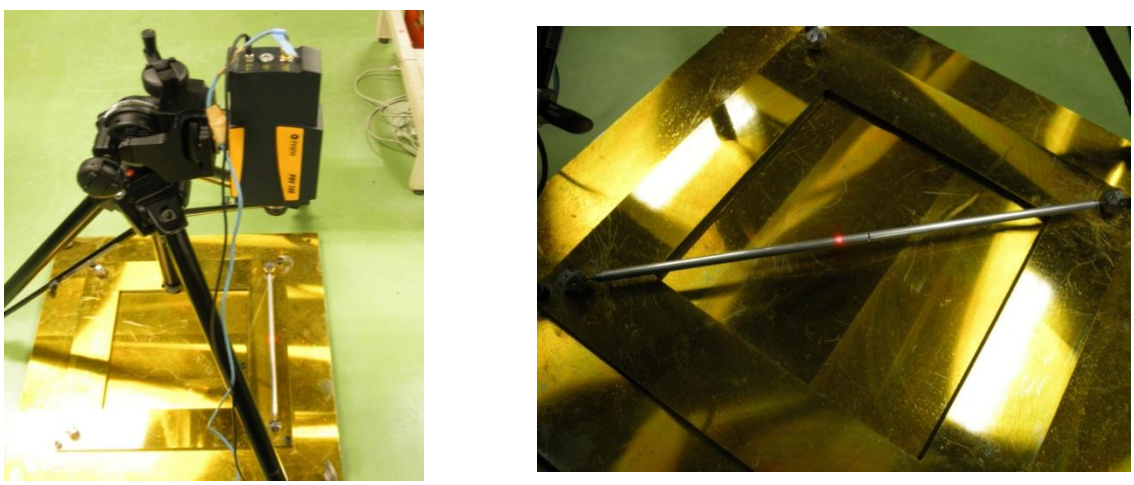

Figure 6-10 Simple beam connected to bearings

Figure 6-11 and 6-12 respectively show the power spectral density diagrams of member 4 and 8 in the first damaged structure (case 1). In addition the diagrams of the corresponding simple beam are plotted in these two figures. It is seen that these two members are vibrating in their own natural frequencies in the structure. These modes are ILVM corresponding to member 4 and 8. This is true for the other damaged diagonal members in the structure. For the undamaged diagonal members, they have PLVM with almost the same frequency range as it is for the diagonal members of the undamaged structure (85 Hz-100 Hz).

The PLVM range for some undamaged diagonal members of the damaged structure is shown in figure 6-13.

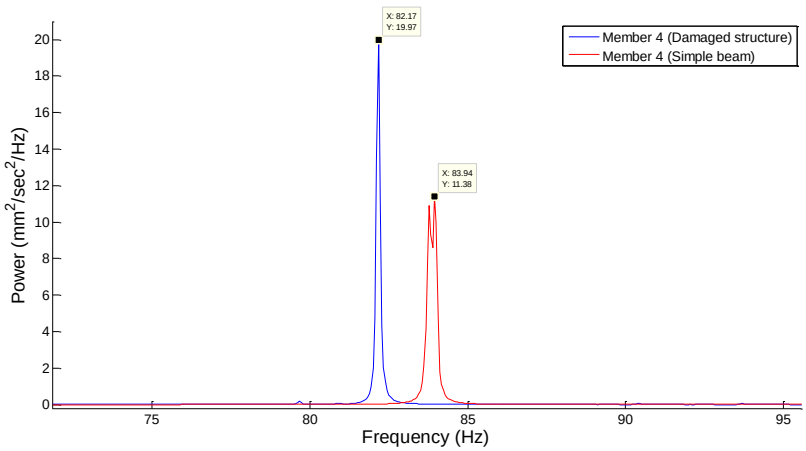

Figure 6-11 Power spectral density diagrams of member 4 (Case 1)

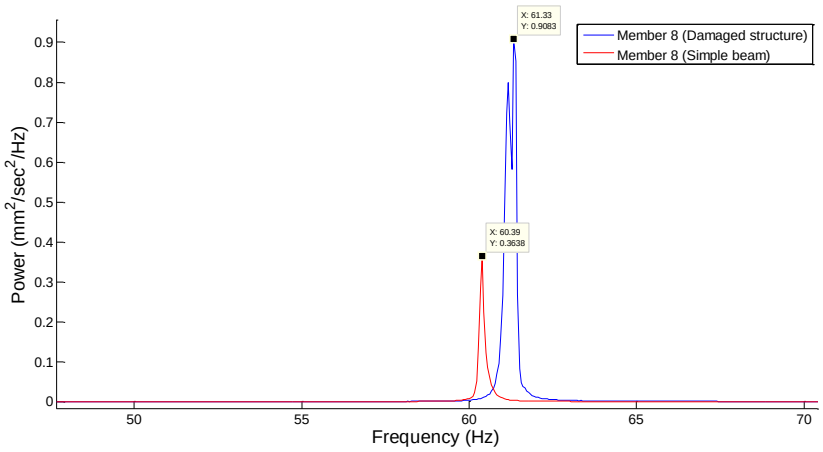

Figure 6-12 Power spectral density diagrams of member 8 (Case 1)

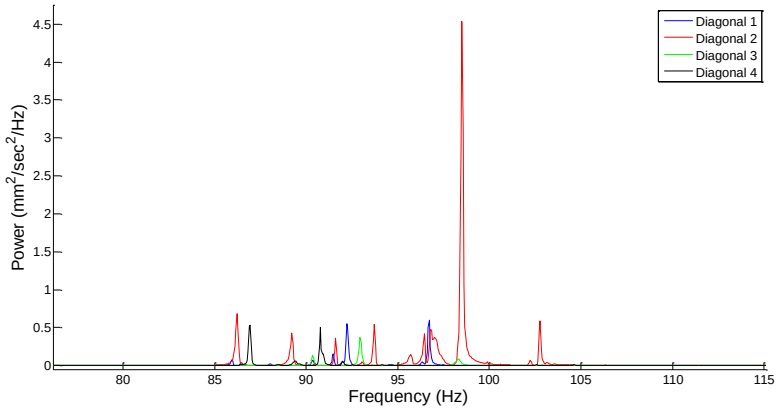

Figure 6-13 PLVM range for some undamaged diagonal members of the damaged structure (Case 1)

Figure 6-14 and 6-15 respectively show the power spectral density diagrams of member 5 and 10 in the second damaged structure (case 2). In addition the diagrams of the corresponding simple beams are plotted in these two figures.

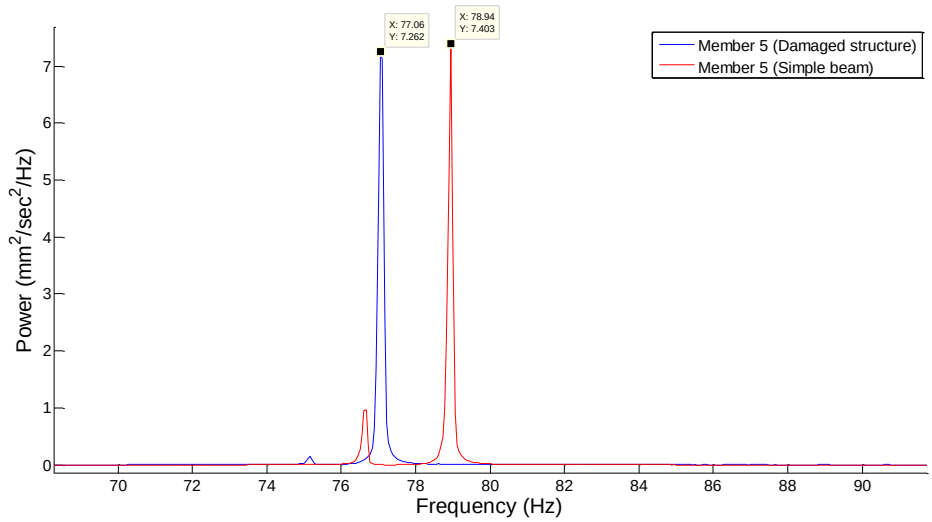

Figure 6-14 Power spectral density diagrams of member 5 (Case 2)

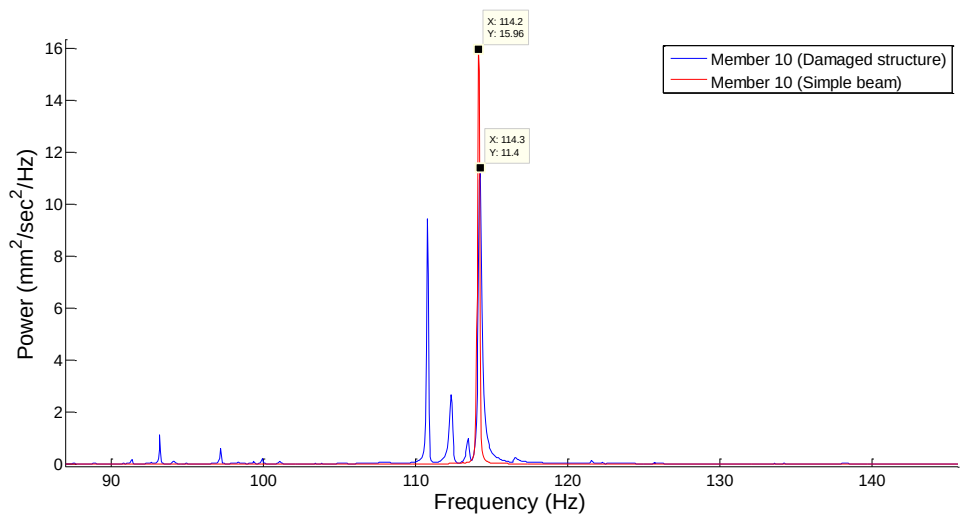

Figure 6-15 Power spectral density diagrams of member 10 (Case 2)

As shown in the above figures, these two members vibrate in their own frequencies in the structures. However as for member10, there are some peaks which are close to the first natural frequency of the member because there are some other modes near the ILVM of member 10 so that member 10 vibrates in these modes as well. Therefore in this case, the mean value of frequencies is considered as the frequency of ILVM. The other damaged diagonal members have ILVM whose frequencies are close to the natural frequencies of the corresponding diagonal members. Like the first damaged structure (case 1), for the undamaged diagonal members, they have PLVM with almost the same frequency range as it is for the diagonal members of the undamaged structure (85 Hz-100 Hz). The frequencies of the 1st PLVM and

ILVM of the diagonal members in the damaged structures and the 1st natural frequencies of the corresponding simple beams connected to bearings are shown in table 6-2.

As already mentioned, for the lateral members in the undamaged structure, the PLVM range is wide. Accordingly, the natural frequencies of the corresponding simple beam cannot be considered close to the frequencies of PLVM in the structure. Figure 6-16 and 6-17 respectively show the power spectral density diagrams of member 1 and 7 in the first damaged structure (case 1). In addition, the PSD diagrams of the corresponding simple beams are plotted in these two figures. As shown, the frequencies of ILVM of the damaged lateral members are not close to the first natural frequency of the same simple beam. The reason might be due to the fact that the stiffness of the main members are not much larger than the lateral members and no other secondary member is attached to one of the connections of each lateral member.

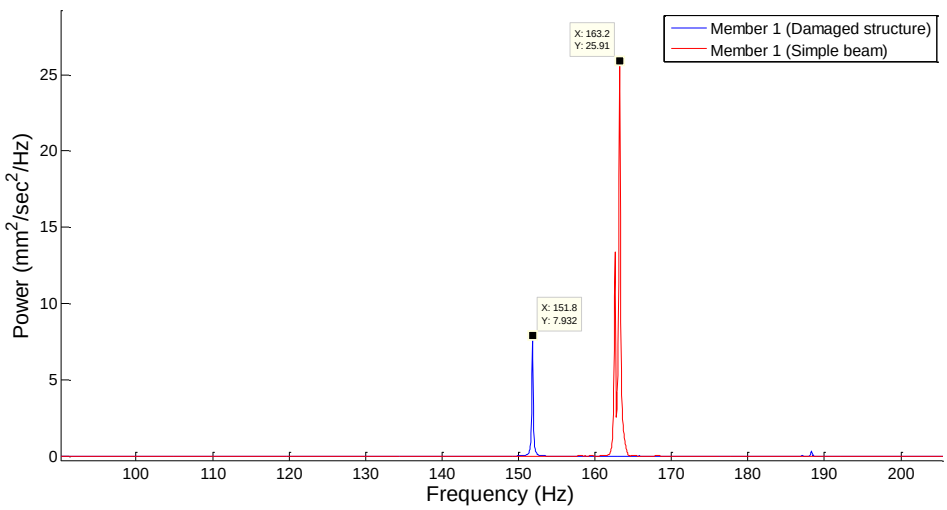

Figure 6-16 Power spectral density diagrams of member 1 (Case 1)

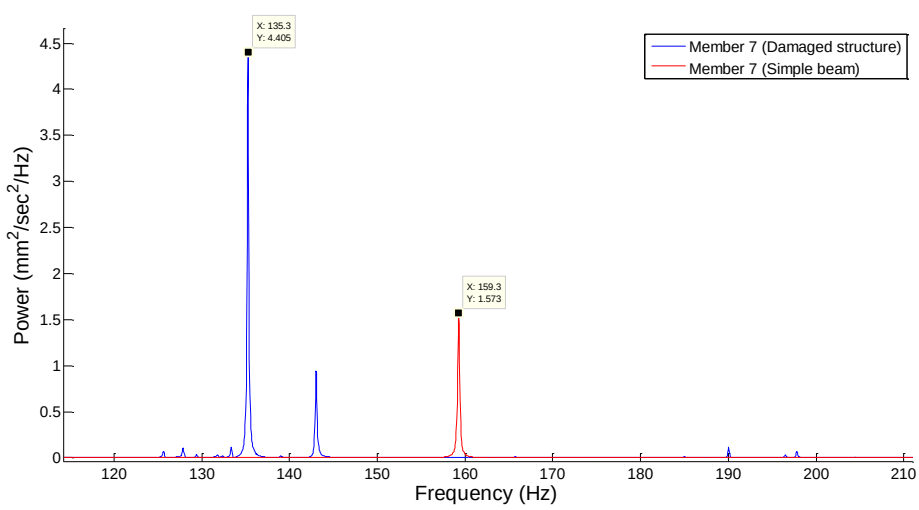

Figure 6-17 Power spectral density diagrams of member 7 (Case 1)

Figure 6-18 and 6-19 respectively show the power spectral density diagrams of member 7 and 11 in the second damaged structure (case 2). In addition, the PSD diagrams of the corresponding simple beams are plotted in these two figures. It is seen that the frequency of ILVM of member 7 is close to the natural frequency of the corresponding simple beam because member 7 is weak (ϕ6×1) and accordingly the stiffness of the main members are much larger (146 times) than this member. As explained, since two peaks appear close to each other for member 7 in the damaged structure, the mean value is considered as the frequency of ILVM of member 7.

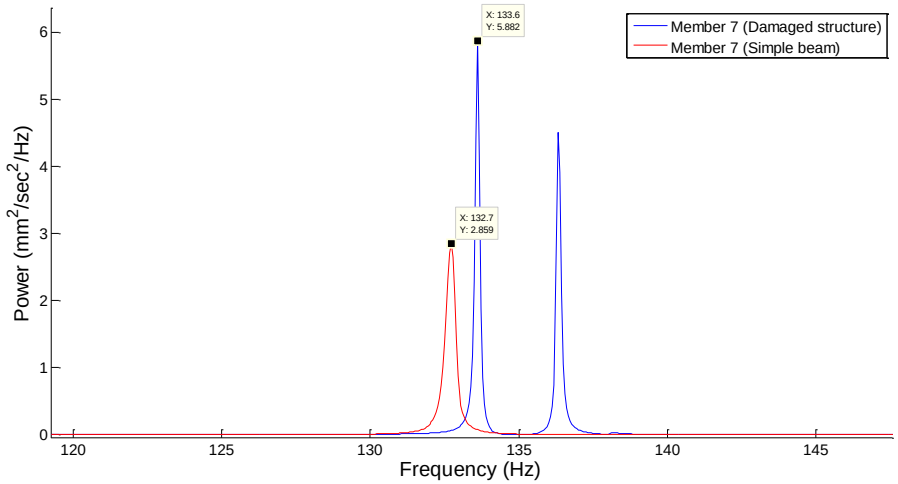

Figure 6-18 Power spectral density diagrams of member 7 (Case 2)

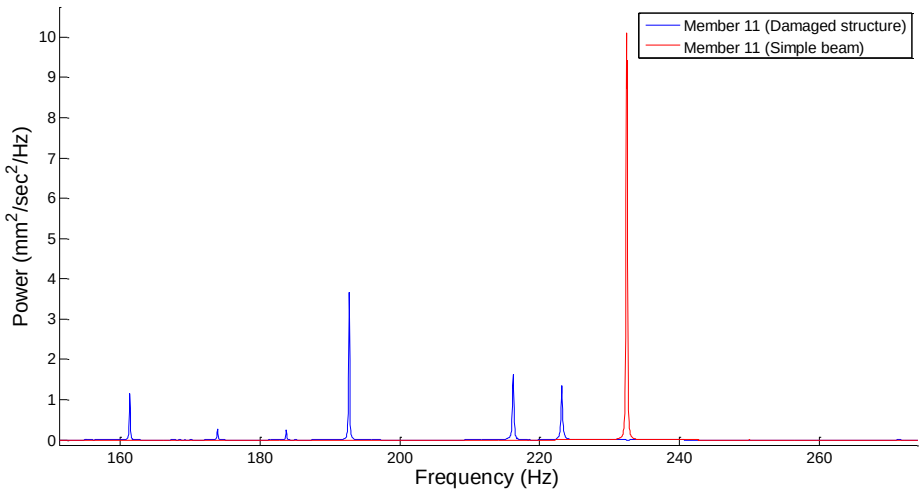

Figure 6-19 Power spectral density diagrams of member 11 (Case 2)

As expected, due to the coupling of modes, there are several peaks for member 11 in the damaged structure which are not close to each other and are not nearly close to the natural frequency of the corresponding simple supported beam. Therefore, the ILVM of member 11 cannot be identified. For the undamaged lateral members in the second damaged structure (case 2), the members have several peaks

but the frequencies are not common with each other as shown in figure 6-20. Moreover, these frequencies are not nearly the same as the frequencies of the lateral members in the undamaged structure shown in figure 6-8 due to the coupling of different modes. Therefore, the locations of damaged lateral members cannot be identified using PLVM and ILVM. This method is only applicable for the diagonal members of this laboratory structure.

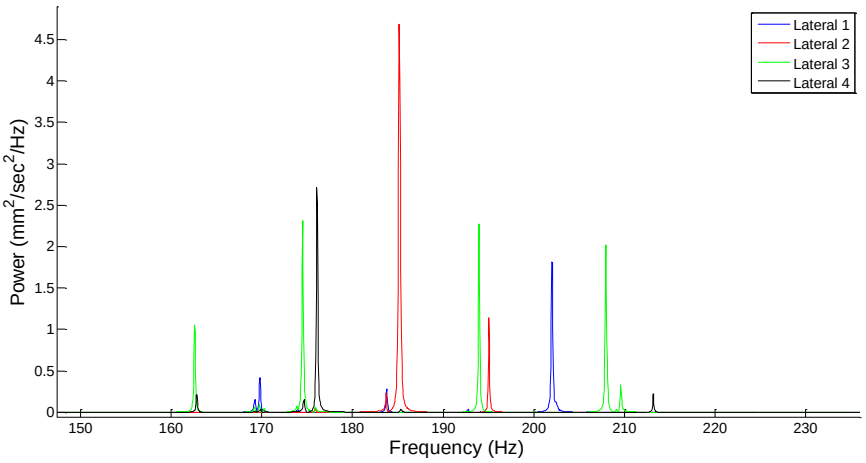

Figure 6-20 peaks correspond to some undamaged lateral members in the damaged structure (Case 2)

The frequencies of the 1st ILVM of the lateral members in the damaged structures, if available, and the 1st natural frequencies of the corresponding simple beams connected to bearings are presented in table 6-2.

Table 6-2 Frequencies of PLVM and ILVM of the secondary members and their corresponding simple beams

Case 1					Case 2				
Element No	**Cross section**	**Type**	**Freq (Hz) Structure**	**Freq (Hz) Simple Beam**	**Element No**	**Cross section**	**Type**	**Freq (Hz) Structure**	**Freq (Hz) Simple Beam**
1	Φ8	ILVM	151.8	163.2	1	Φ8	ILVM	76.72	78.94
2	Φ9.5	ILVM	86.28~94.22	90.17	2	Φ13	ILVM	110.7~123	118.7
3	Φ13	-	178.8~227.6	251.8	3	Φ11	-	175.9~212.9	224.2
4	Φ10 (1/2 cut)	ILVM	82.17	83.78	4	Φ10 (1/3 cut)	ILVM	90.06	92.67
5	Φ10 (2/3 cut)	ILVM	75.67	77.28	5	Φ8	ILVM	77.6	78.94
6	Φ15	-	177.2~245.8	288.8	6	Φ10 (1/2 cut)	ILVM	157.2	175.4
7	Φ10 (2/3 cut)	ILVM	135.3	159.3	7	Φ6	ILVM	133.6~136.3	132.7
8	Φ6	ILVM	62.39	60.39	8	Φ10 (3/4 cut)	ILVM	64.06	64
9	Φ15	ILVM	143.1	144	9	Φ6	ILVM	133.7~136.4	132.7
10	Φ10 (1/3 cut)	-	159.1~185.1	198.6	10	Φ12	ILVM	110.8~114.3	114.2
11	Φ9.5	-	159.1~185.1	196.2	11	Φ12	-	161.4~223.2	232.4
12	Φ11	ILVM	98.39~106.2	109.4	Undamaged Diagonal elements	Φ10	PLVM	86.56~100.2	97.94
13	Φ8	ILVM	147.9	163.2	Undamaged Lateral elements	Φ10	-	Not observable(in a wide range)	204.8
Undamaged Diagonal elements	Φ10	PLVM	86.56~100.2	97.94					
Undamaged Lateral elements	Φ10	-	Not observable(in a wide range)	204.8					

For diagonal members there are ILVM whose frequencies are close to the natural frequencies of the corresponding simple beams and the difference is less than 2 Hz. If the damage is not severe, there is a range for ILVM since the frequency is in or close to the PLVM range. Therefore, damaged diagonal members are identified. As for lateral members, ILVM is available for weak elements; however, the difference between frequencies of ILVM and the relevant simple beams is not small. Only for members 7 and 9 (Φ6×1) of case 2, these frequencies are close to each other since these members are much softer than the main members. Meanwhile, PLVM of the lateral members are not observable. Therefore, damaged lateral members are not detected.

6.2.4 Independency of PLVM frequencies from global shape of the structure

To confirm that the frequencies of PLVM of the diagonal member are independent from the global shape of the structure, three out of five bays of the laboratory model are disassembled and the velocity time history of each member is measured. The 2-bay laboratory structure is shown in figure 6-21.

Figure 6-21 2-bay laboratory structure

Figure 6-22 shows the result for four diagonal, one lateral and one longitudinal members to find the PLVM corresponding to the diagonal members. As shown in this figure, the frequencies of PLVM of the diagonal members are almost in the same range as it is for the 5-bay structure (85 Hz-100 Hz). This means that the frequencies of PLVM are almost independent from the global shape of the structure.

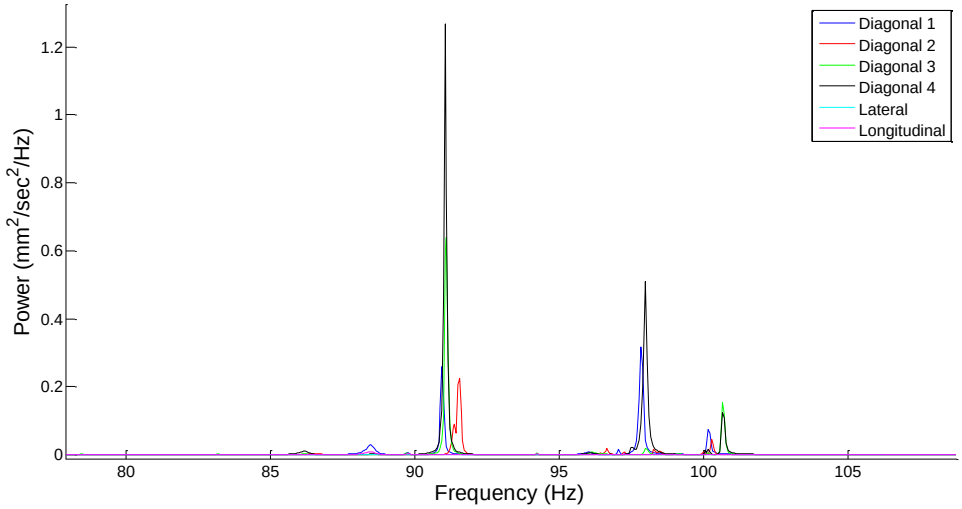

Figure 6-22 1st PLVM range of the diagonal members of the 2-bay structure

Figure 6-23 shows the result for four lateral, one diagonal and one longitudinal members. In this figure, the amplitude of the lateral members is much larger than the diagonal and longitudinal members and common for all lateral members. Therefore, these peaks correspond to the 1st PLVM of the lateral members of the 2-bay laboratory structure.

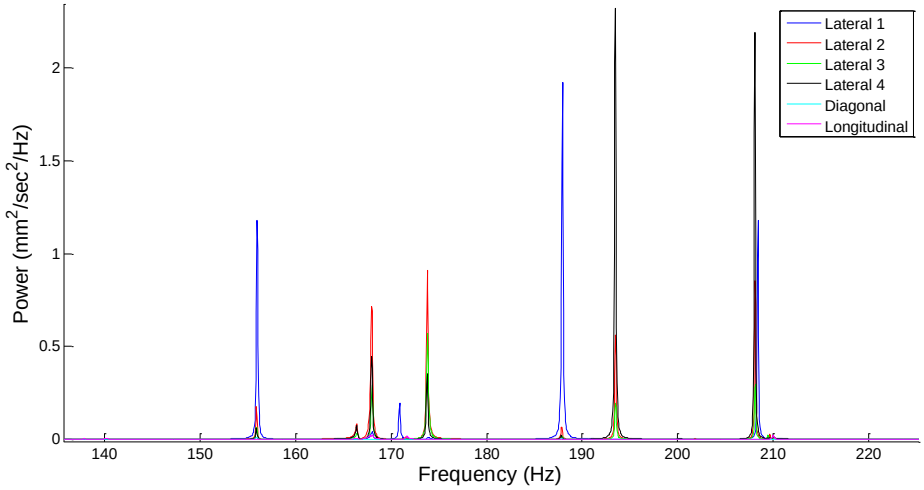

Figure 6-23 1st PLVM range of the lateral members of the 2-bay structure

The frequency range is wide (about 55 Hz) and the frequencies are not nearly the same as the frequencies of the 1st PLVM of the 5-bay structure, shown in figure 6-8.Therefore the frequencies of PLVM of the lateral members depend on the global shape of the structure.

6.3 Damage identification using PLVM and ILVM frequencies comparison: laboratory space frame with continuous main members

6.3.1 Description of the laboratory model

Figure 6-24 shows a 5-bay laboratory truss frame. The model is two meter tall from its base plate and the dimensions of each bay are 41×41×40 cm in which the height is 40 cm. The model contains diagonal and lateral members which are considered as secondary members and made of aluminum. The secondary members are pipes whose external and internal diameters are respectively 1 and 0.8 cm. The model has four continuous longitudinal members and is considered as main members. The main members are steel solid bars whose diameter is 1.5 cm.

Figure 6-24 Laboratory structure with continuous main members

6.3.2 Existence of PLVM for secondary members

In order to observe PLVM corresponding to the identical secondary members, the velocity time history of each secondary member is measured by Laser Doppler Vibrometer (LDV) as shown in figure 6-25 and its power spectral density (PSD) is examined. The sampling frequency is 10000 Hz and each member is directly hit.

Figure 6-25 Laser Doppler Vibrometer

Based on the formula of the deflections of simple supported and clamped-clamped beams presented in chapter 4, the stiffness of the main members are about 291 times larger than the diagonal members. Moreover, as shown in figure 6-24, many members attached to connections of the diagonal members. Therefore, the relative stiffness of the diagonal members is much less than the total stiffness of the main members together with other secondary members attached to the connections. Accordingly PLVM and ILVM exist for the diagonal members and their frequencies are nearly the same as natural frequencies of the corresponding diagonal member. As for lateral members, the stiffness of the main members is about 103 times larger than the lateral members. Therefore, coupling of local vibration modes might not happen among the lateral members. Accordingly the frequencies of PLVM and ILVM are nearly the same as natural frequencies of the corresponding lateral members themselves.

As explained in the previous chapters, in order to find PLVM corresponding to each identical members set, the results of some identical members of the set should be compared with the other members. Figure 6-26 shows the result for four diagonal, one lateral and one longitudinal members to find the PLVM corresponding to the diagonal members.

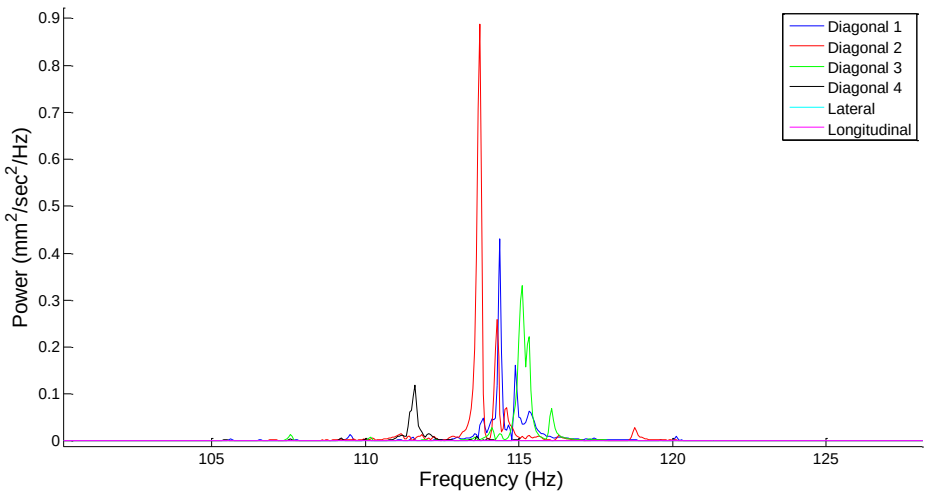

Figure 6-26 PSD diagrams of four diagonal, one lateral and one longitudinal members

As shown in the above figure, the diagonal members have large amplitudes between 106 Hz to 116 Hz. In order to compare the amplitude of diagonal members with the lateral and longitudinal members, this figure is zoomed in the PLVM range and illustrated in figure 6-27.

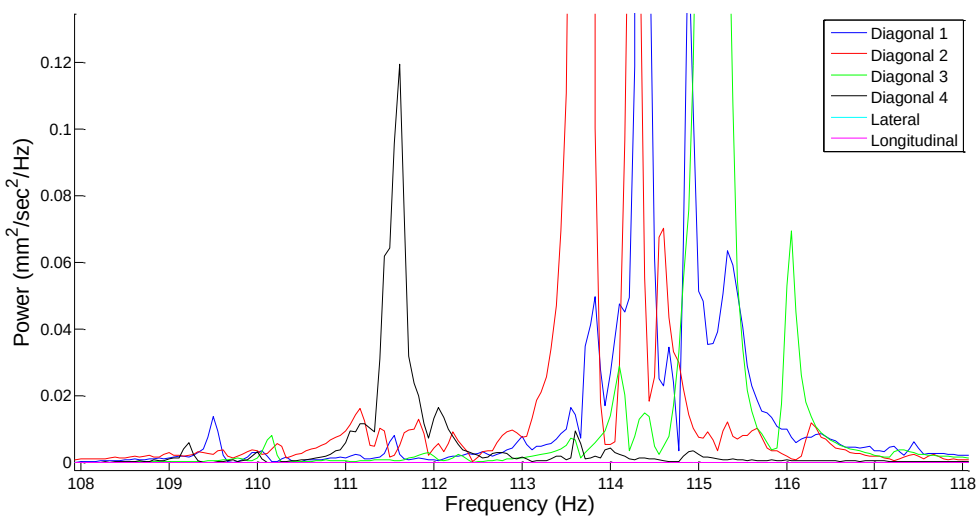

Figure 6-27 1st PLVM range of the diagonal members

In the above figure, the amplitudes of the diagonal members are much larger than the lateral and longitudinal members and common for all diagonal members. Therefore these peaks correspond to the 1st PLVM of the diagonal members. Higher PLVM of the diagonal members are observed. Figure 6-28 and 6-29 show the 2nd and 3rd PLVM range of the diagonal members respectively.

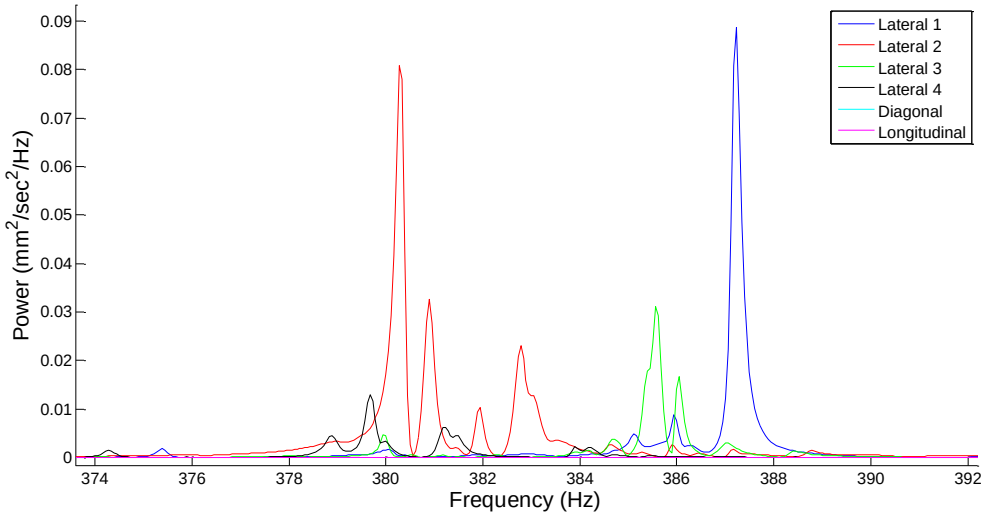

Figure 6-28 2nd PLVM range of the diagonal members

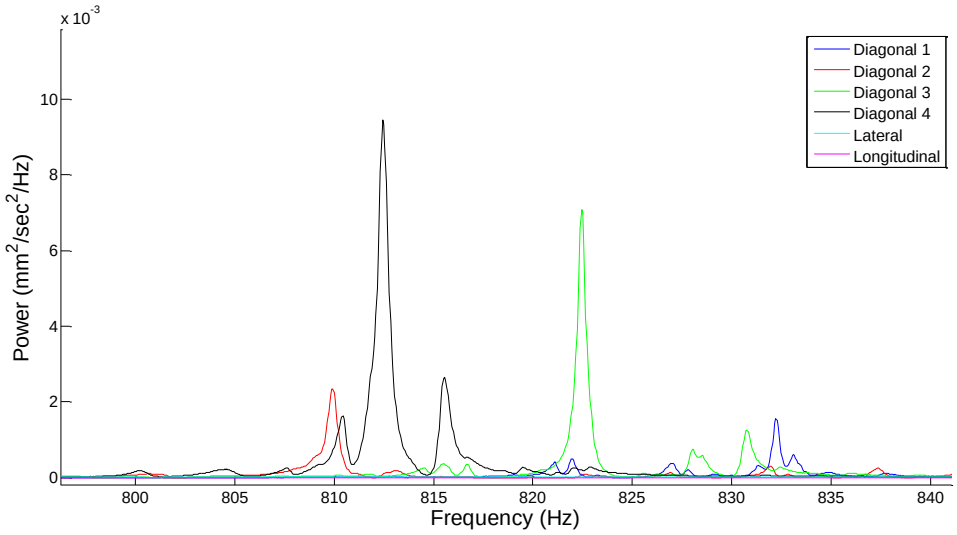

Figure 6-29 3rd PLVM range of the diagonal members

The amplitudes of the diagonal members are much larger than the lateral and longitudinal members in the above figures. Note that there is a range for PLVM because the identical diagonal members are soft and a little difference between their length, connections or their axial loads, caused by manufacturing errors, can change the frequencies of these local vibration modes.

Figure 6-30 shows the result for four lateral, one diagonal and one longitudinal members to find PLVM of the lateral members.

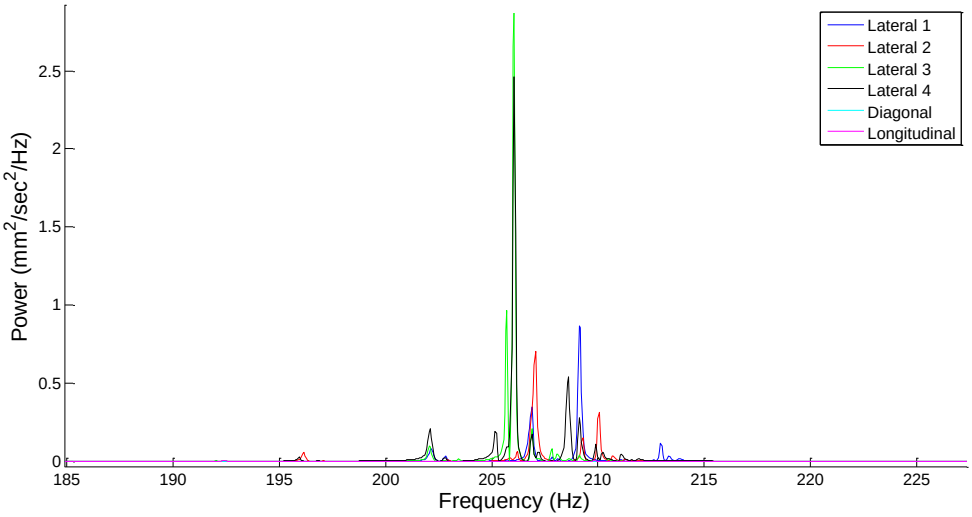

Figure 6-30 PSD diagrams of four lateral, one diagonal and one longitudinal members

As shown in the above figure, the lateral members have large amplitudes between 202 Hz to 212 Hz. To compare the amplitude of lateral members with the diagonal and longitudinal members, this figure is zoomed in this range and shown in figure 6-31.

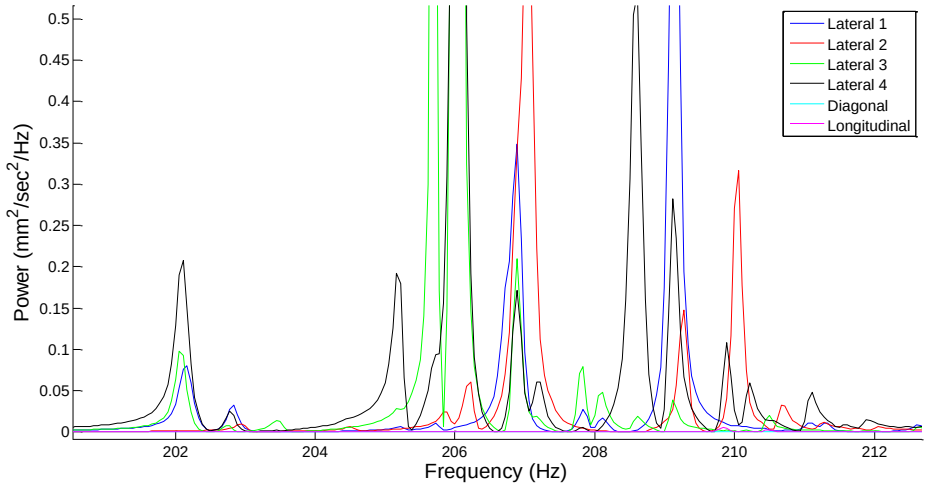

Figure 6-31 1st PLVM range of the lateral members

In the above figure, the amplitudes of the lateral members are much larger than the diagonal and longitudinal members. Therefore these peaks correspond to the 1st PLVM of the lateral members. Higher PLVM of the lateral members are observed. Figure 6-32 shows the 2nd PLVM range of the lateral members.

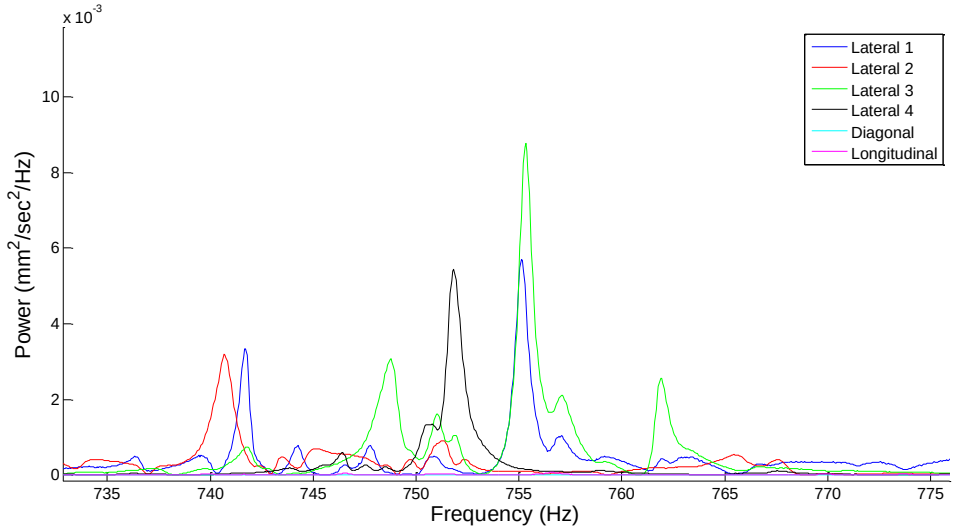

Figure 6-32 2nd PLVM range of the lateral members

The amplitudes of the lateral members are much larger than the diagonal and longitudinal members in the above figure. Therefore, these peaks correspond to the 2nd PLVM of the lateral members. Once again, note that there is a range for PLVM because the identical lateral members are soft and a little difference between their length, connections or axial load can remarkably change the frequencies of these local vibration modes.

6.3.3 Existence of ILVM in two damaged structures with continuous longitudinal members

In order to investigate about the existence of ILVM, two damage cases are considered. To apply damage, several secondary members are replaced by bars with various diameters or cut by different portions of the diameter at the center. Locations of damaged secondary members in the laboratory models with continuous main members are shown in figure 6-33. The damaged members are listed in table 6-3. The thickness of all pipes is 1 mm.

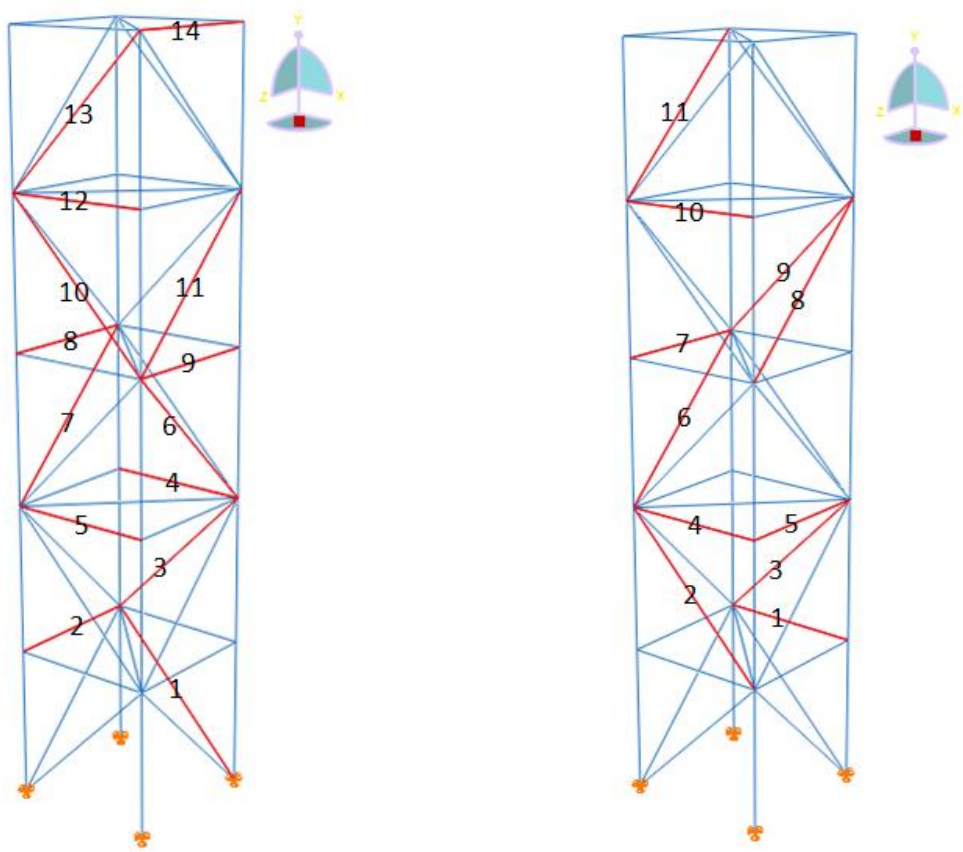

Case 1 **Case 2**

Figure 6-33 Locations of damaged members in the laboratory model with continuous longitudinal members

Table 6-3 Damaged members in the laboratory model with continuous longitudinal members

Case 1		**Case 2**	
Element No	Damage	Element No	Damage
1	Φ13×1	1	Φ15×1
2	Φ12×1	2	Φ6×1
3	Φ11×1	3	Φ12×1
4	Φ10×1 (1/2 cut)	4	Φ10×1 (2/3 cut)
5	Φ12×1	5	Φ11×1
6	Φ13×1	6	Φ10×1 (3/4 cut)
7	Φ10×1 (2/3 cut)	7	Φ9.5×1
8	Φ8×1	8	Φ10×1 (1/3 cut)
9	Φ10×1 (1/3 cut)	9	Φ15×1
10	Φ10×1 (1/2 cut)	10	Φ6×1
11	Φ9.5×1	11	Φ12×1
12	Φ13×1		
13	Φ8×1		
14	Φ12×1		

The velocity time history of the secondary members in two damaged structures is measured and each secondary member is measured while separately connected to the bearings which are similar to its connections in the structures, as shown in figure 6-10. Figure 6-34, 6-35 and 6-36 respectively show the power spectral density diagrams of members 4, 12 and 13 in the first damaged structure (case 1). Moreover, the PSD diagrams of the corresponding simple beams are plotted. As shown, these three members vibrate in their own natural frequencies in the structure. These modes are ILVM of members 4, 12 and 13. This is true for the other damaged diagonal and lateral members in the structure. For the undamaged diagonal and lateral members, there are PLVM with almost the same frequency ranges as they are for the diagonal and lateral members of the undamaged structure. Figure 6-37 and 6-38 respectively show the PLVM range of some undamaged diagonal and lateral members in the damaged structure (case1).

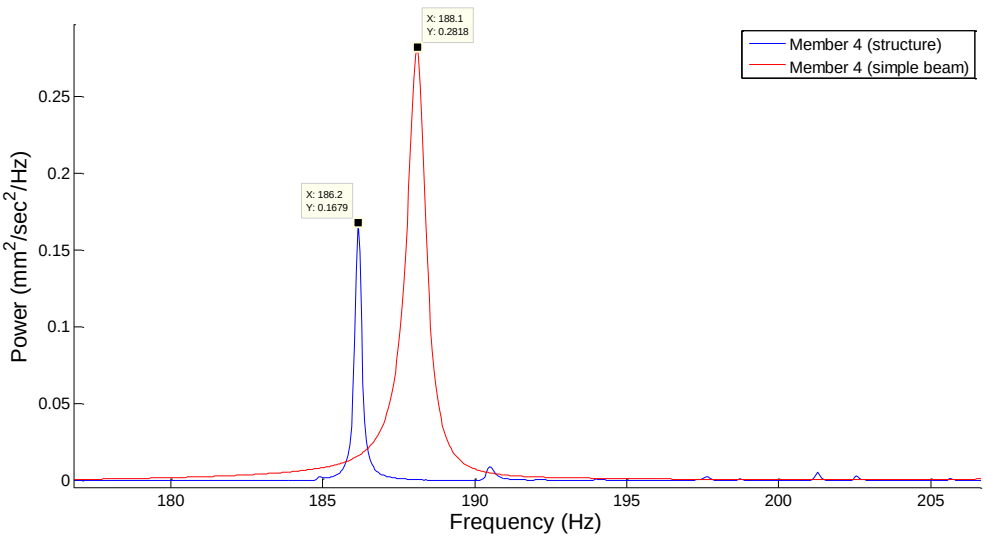

Figure 6-34 Power spectral density diagrams of member 4 (Case 1)

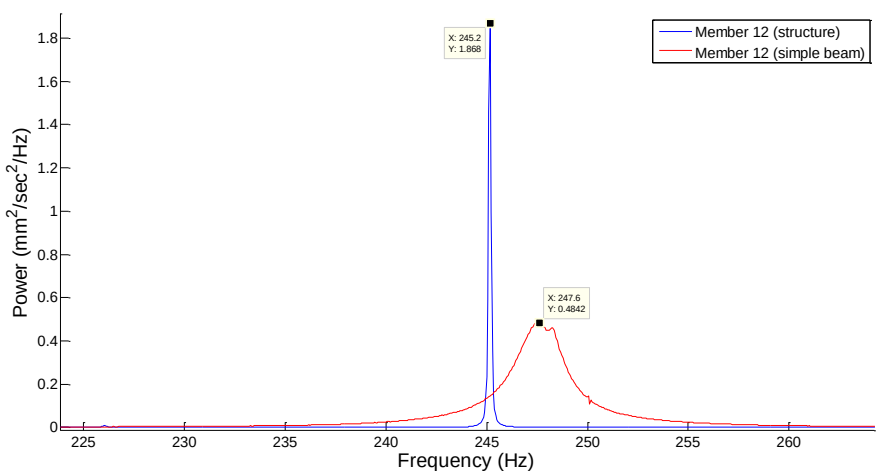

Figure 6-35 Power spectral density diagrams of member 12 (Case 1)

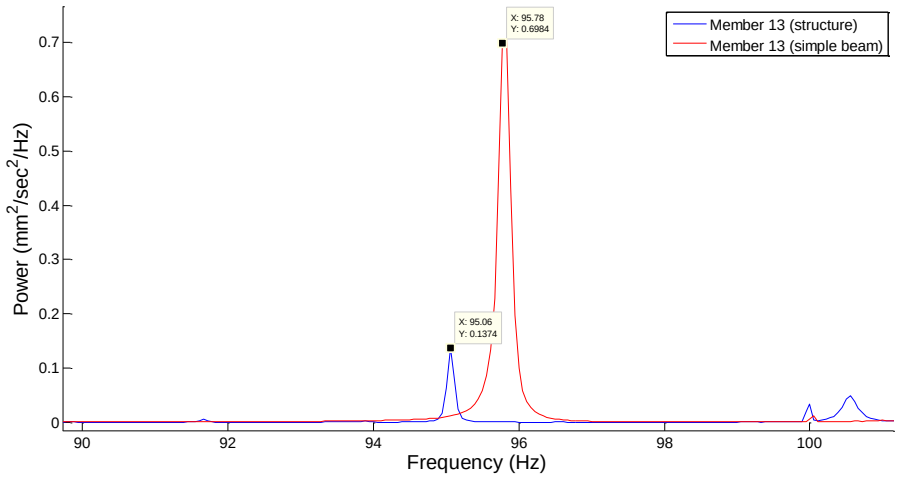

Figure 6-36 Power spectral density diagrams of member 13 (Case 1)

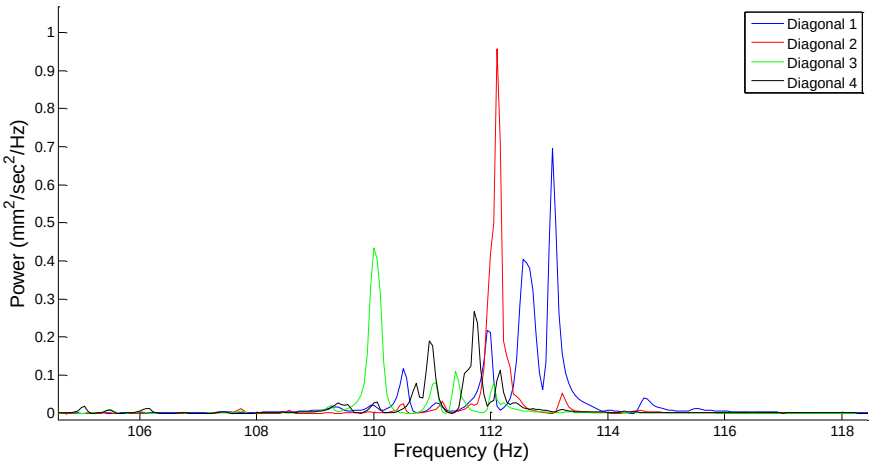

Figure 6-37 PLVM range of some undamaged diagonal members in the damaged structure (Case 1)

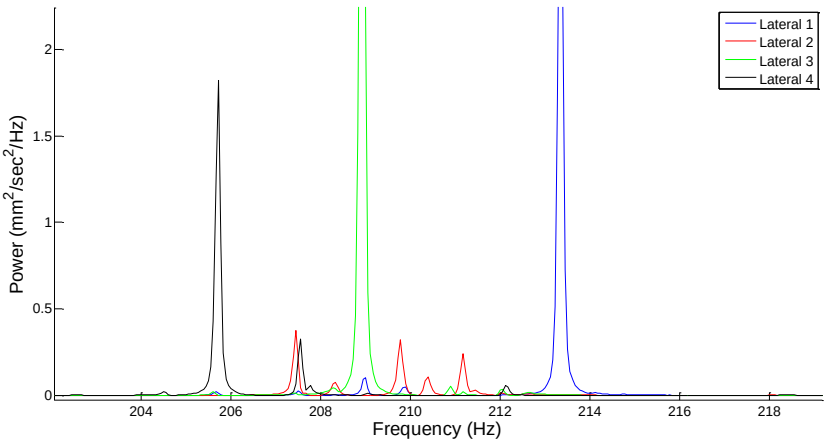

Figure 6-38 PLVM range of some undamaged lateral members in the damaged structure (Case 1)

As shown in the above figures, the frequencies of ILVM and PLVM in the damaged structure are almost the same as the natural frequencies of the corresponding members when separately connected to bearings.

Figure 6-39, 6-40 and 6-41 respectively show the power spectral density diagrams of members 5, 9 and 10 in the second damaged structure (case 2). In addition the PSD diagrams of the corresponding simple beams are plotted in these three figures. It is shown that these three members almost vibrate in their own natural frequencies in the structure. These modes are ILVM of members 5, 9 and 10. This is true for the other damaged members in the structure. For the undamaged diagonal and lateral members, there are PLVM with almost the same frequency ranges as they are for the diagonal and lateral members of the undamaged structure. Figure 6-42 and 6-43 respectively show the PLVM range of some undamaged diagonal and lateral members in the damaged structure (case2).

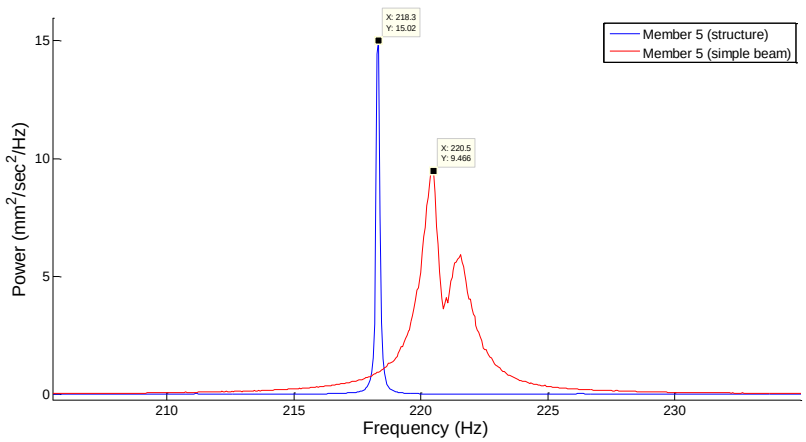

Figure 6-39 Power spectral density diagram of member 5 (Case 2)

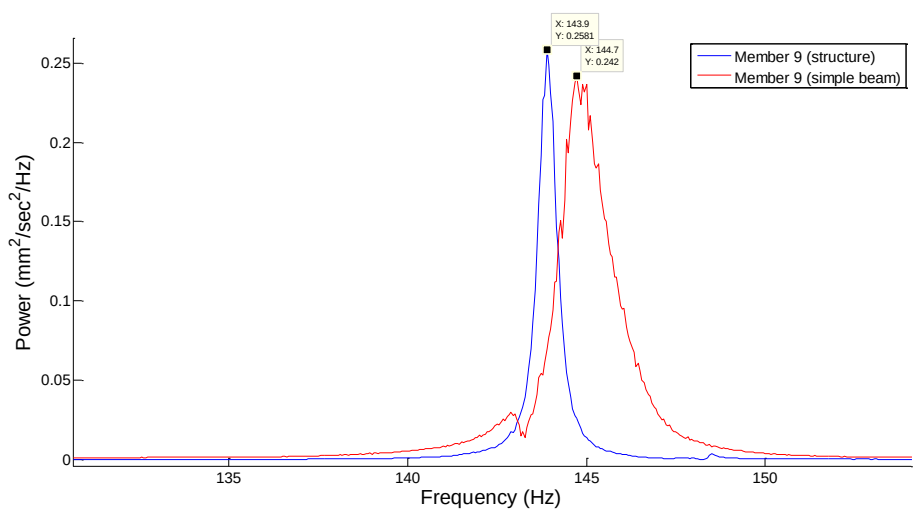

Figure 6-40 Power spectral density diagrams of member 9 (Case 2)

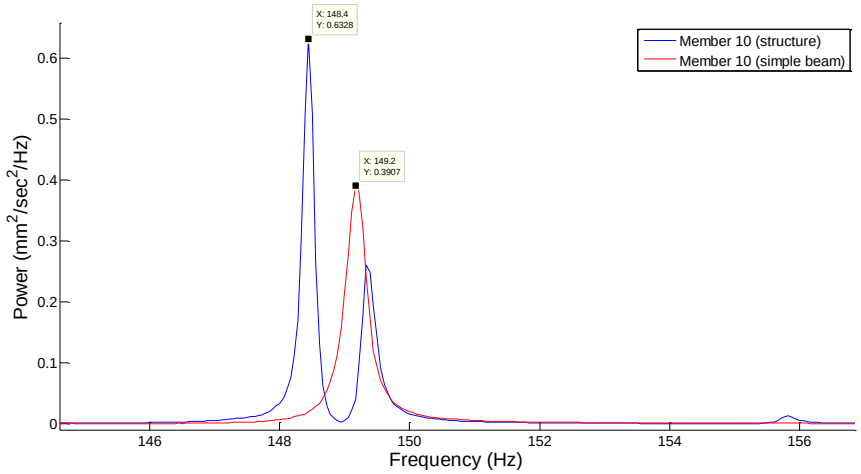

Figure 6-41 Power spectral density diagrams of member 10 (Case 2)

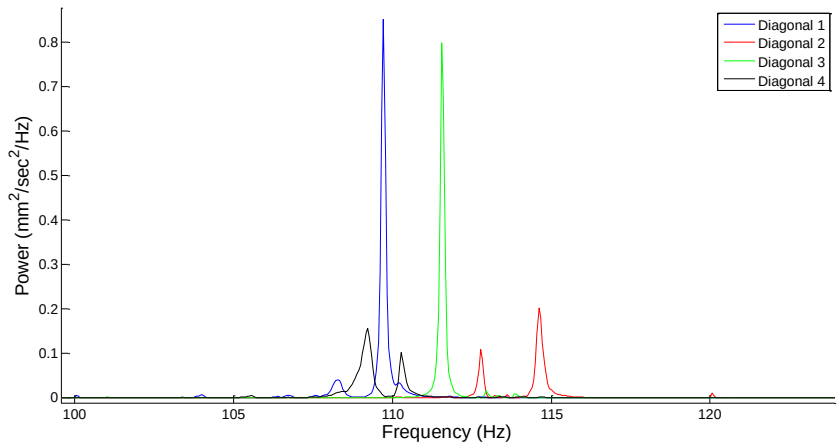

Figure 6-42 PLVM range of some undamaged diagonal members in the damaged structure (Case 2)

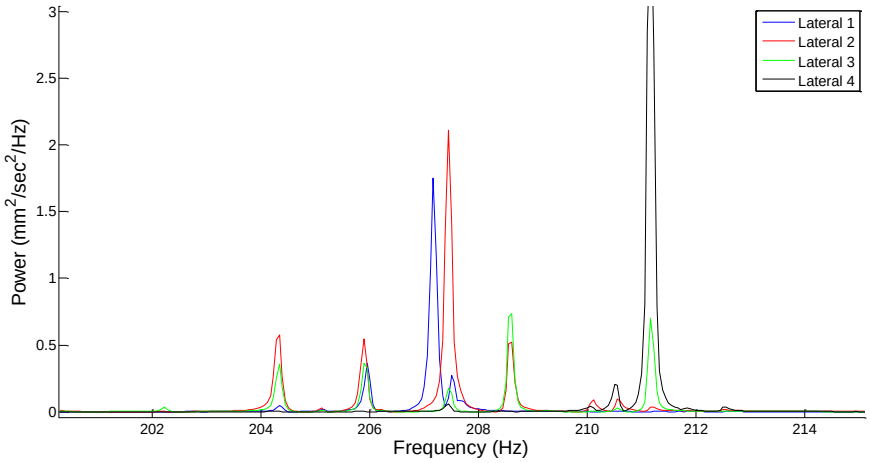

Figure 6-43 PLVM range of some undamaged lateral members in the damaged structure (Case 2)

In the above figures, the frequencies of ILVM and PLVM in the damaged structure are almost the same as the natural frequencies of the corresponding simple beams when separately connected to bearings.

The frequencies of the 1st PLVM and ILVM of the secondary members in the damaged structures and the 1st natural frequencies of the corresponding simple beams connected to bearings are shown in table 6-4.

Table 6-4 Frequencies of ILVM of the secondary members and their corresponding simple beams

Case 1					Case 2				
Element No	**Cross section**	**Type**	**Freq (Hz) Structure**	**Freq (Hz) Simple Beam**	**Element No**	**Cross section**	**Type**	**Freq (Hz) Structure**	**Freq (Hz) Simple Beam**
1	Φ13×1	ILVM	132.2	130.8	1	Φ15×1	ILVM	295.7	292.1
2	Φ12×1	ILVM	230.82	233.6	2	Φ6×1	ILVM	85.06	84.17
3	Φ11×1	ILVM	115.5	114.1	3	Φ12×1	ILVM	120.1	121.1
4	Φ10×1 (1/2 cut)	ILVM	186.2	188.1	4	Φ10×1 (2/3 cut)	ILVM	141.3	144.2
5	Φ12×1	ILVM	228.4	233.6	5	Φ11×1	ILVM	218.3	220.4
6	Φ13×1	ILVM	127.4	126	6	Φ10×1 (3/4 cut)	ILVM	53.5	53.56
7	Φ10×1 (2/3 cut)	ILVM	89.61	90.06	7	Φ9.5×1	ILVM	198	196.8
8	Φ8×1	ILVM	167	167.1	8	Φ10×1 (1/3 cut)	ILVM	101.4	103
9	Φ10×1 (1/3 cut)	ILVM	201	198.6	9	Φ15×1	ILVM	143.9	144.7
10	Φ10×1 (1/2 cut)	ILVM	92.22	93.44	10	Φ6×1	ILVM	148.4	149.2
11	Φ9.5×1	ILVM	109.3	107.7	11	Φ12×1	ILVM	118.6	118.6
12	Φ13×1	ILVM	245.2	247.6	Undamaged Diagonal elements	Φ10	PLVM	104~116	112.1
13	Φ8×1	ILVM	95.06	95.83	Undamaged Lateral elements	Φ10	PLVM	204~213	207.6
14	Φ12×1	ILVM	216.9	233.6					
Undamaged Diagonal elements	Φ10	PLVM	104~116	112.1					
Undamaged Lateral elements	Φ10	PLVM	204~213	207.6					

There are ILVM of the damaged members whose frequencies are close to the natural frequencies of the corresponding simple beams. The exception is member 14 in the 1st damaged structure in which the ILVM is not close to the natural frequency of the corresponding beam. A possible reason is that the main members have been connected to the external connection balls with thin screw bars, as shown in figure 6-44, and accordingly their stiffness has significantly reduces. Therefore, coupling of different modes have occurred involving top lateral members.

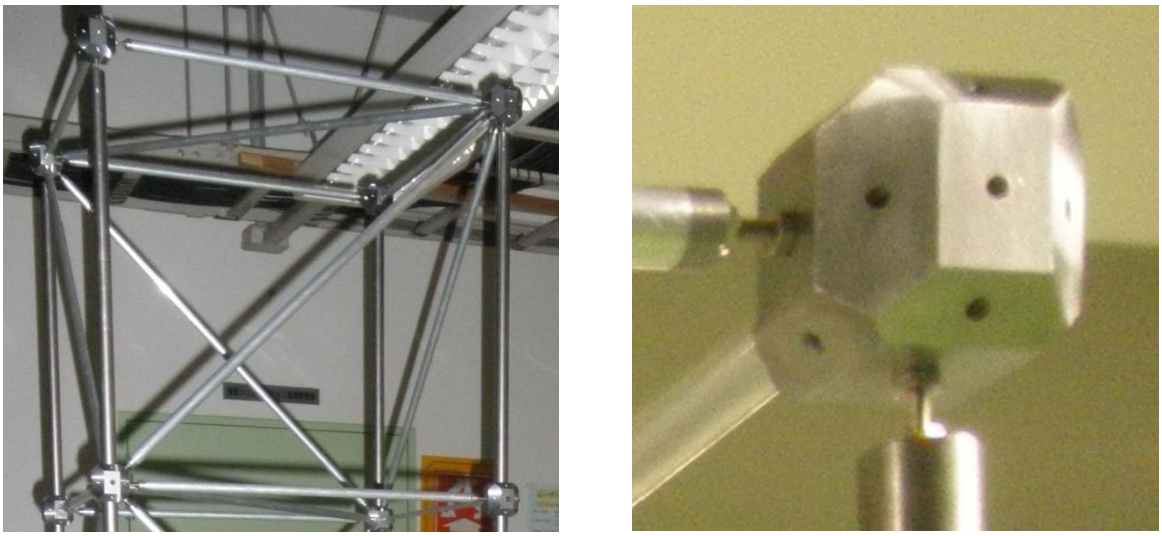

Figure 6-44 The most top bay of the structure

Moreover, for the undamaged diagonal and lateral members, there are PLVM ranges in which these members vibrate in frequencies close to the natural frequencies of the corresponding undamaged diagonal and lateral members. Therefore, the damaged members are identified. Note that, unlike the structure with non-continuous main members, the lateral members have ILVM and PLVM with nearly the same frequencies as the natural frequencies of the corresponding simple beams.

6.4 Damage identification using PLVM amplitude comparison

PLVM corresponding to each secondary members set are easily observed when one of the identical members of the corresponding set is hit. Therefore, if one member damages, it is no longer identical with the other members of the set and no longer strongly vibrates at PLVM when hitting one of the undamaged identical members of the set.

Consider the damaged structure and hit members shown in figure 6-45. This structure is the same as the damaged structure with continuous longitudinal members (case 1). Figure 6-46 shows the power spectral density diagrams of four undamaged diagonal members and members 1 and 7, which are damaged diagonal members, when the undamaged diagonal member, shown in figure 6-45, is hit. Note that these diagrams are shown in the PLVM range of the diagonal members.

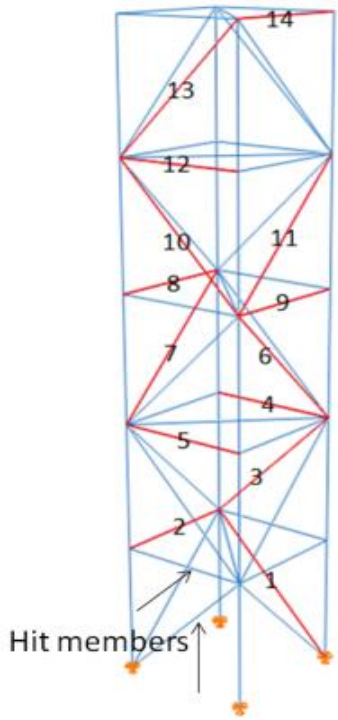

Figure 6-45 Location of hit members

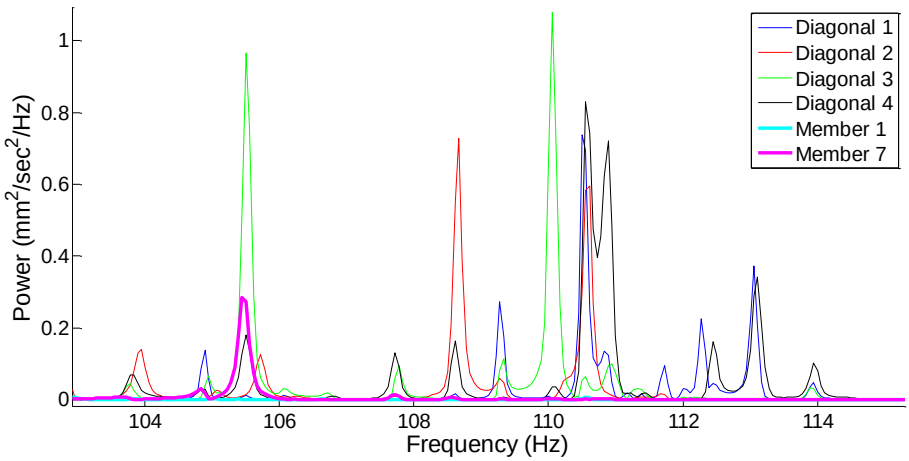

Figure 6-46 PSD diagrams of some diagonal members in their PLVM range

Maximum amplitude of PSD for the damaged diagonal members in the PLVM range of the diagonal members is smaller than the undamaged diagonal members when the undamaged diagonal member, shown in figure 6-45, is hit. Figure 6-47 shows the values of maximum amplitudes of PSD for the intact and damaged diagonal members in their PLVM range when the undamaged diagonal member, shown in figure 6-45, is hit.

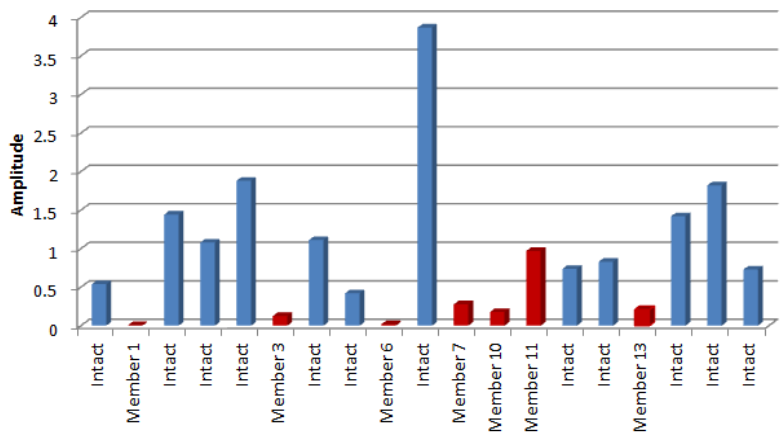

Figure 6-47 Maximum PSD amplitudes of the diagonal members in their PLVM range

The maximum PSD amplitudes of the damaged diagonal members in the PLVM range is smaller than the intact diagonal members when the undamaged diagonal member, shown in figure 6-45, is hit. The exception is member 11 because the damage severity is small, as presented in table 6-4, and its frequency of ILVM is in the PLVM range. Therefore, damaged diagonal members are detected by comparing PLVM amplitude.

Figure 6-48 shows the power spectral density diagerams of four undamaged lateral members, members 2 and 4, when the undamaged lateral member, shown in figure 6-45, is hit. Note that these diagrams are shown in the PLVM range of the lateral members.

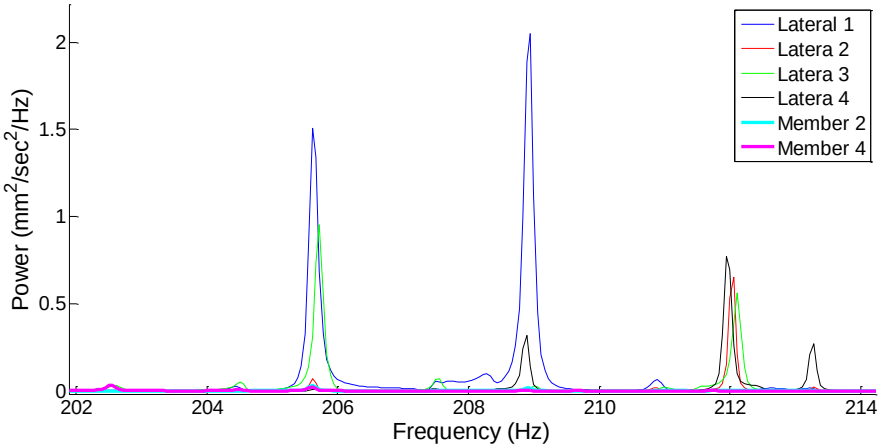

Figure 6-48 PSD diagrams of some lateral members in their PLVM range

As shown, the maximum PSD amplitude of the damaged lateral members in the PLVM range of the lateral members is smaller than the undamaged lateral members when the undamaged lateral member, shown in figure 6-45, is hit. Figure 6-49 shows the values of maximum amplitudes of PSD for the undamaged and damaged lateral members in their PLVM range when the undamaged lateral member, shown in figure 6-45, is hit.

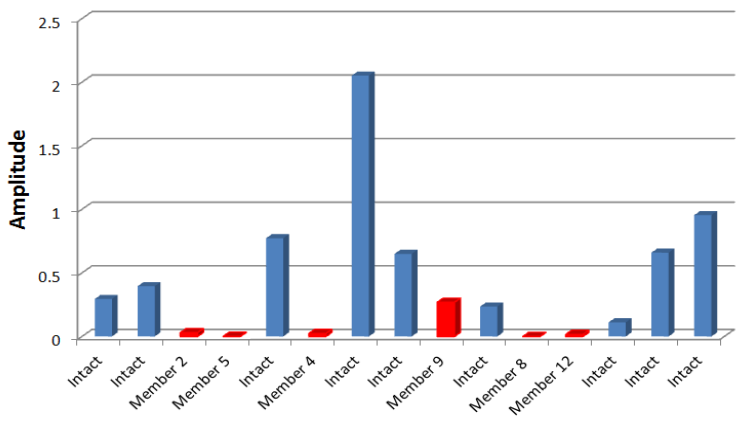

Figure 6-49 Maximum PSD amplitudes of the lateral members in their PLVM range

The maximum PSD amplitudes of the damaged lateral members in PLVM range is relatively smaller than the undamaged lateral members when the undamaged lateral member, shown in figure 6-45, is hit. The exception is member 9 because the damage severity is small, as presented in table 6-4, and its frequency of ILVM is close to the PLVM range. Therefore, damaged lateral members are identified by hitting one of the undamaged lateral members. It should be mentioned that the input force has not been measured through this analysis. By measuring the input force and tuning the output data, clearer results would be obtained.

6.5 Summary

In this chapter, the proposed damaged identification techniques, based on frequencies of PLVM and ILVM comparison as well as PLVM amplitude comparison, are experimentally examined for two scale-model space structures and the frequencies of PLVM and ILVM are compared with the natural frequencies of the corresponding simple supported beam.

The identification method using PLVM and ILVM frequencies comparison is successfully performed for diagonal members of the scale-model space structure with non-continuous main members. Yet, this technique cannot be successfully performed for all lateral members of this model because the stiffness of the main members are not much larger than the lateral members and no other secondary member is attached to one of the connections of each lateral member. The two identification techniques are successfully performed for both lateral and diagonal members of the scale-model space structure with continuous main members.

Chapter 7

Damage identification experiment on a planar full-scale model of a belt conveyor and a real belt conveyor

7.1 Introduction

In this chapter, the existence of Periodic Local Vibration Modes (PLVM) and Isolated Local Vibration Mode (ILVM) in braces and lateral members of a planar full-scale model of a belt conveyor are examined. In order to find PLVM, the undamaged structure is tested by Laser Doppler Vibrometer (LDV) in some points of members. Then, to simulate damage, two 1kg masses are added to members and the structure is tested to find PLVM and ILVM. Next, the measurement results of a real undamaged belt conveyor are shown and the existence of PLVM is investigated and the results are compared with the corresponding finite element model. Finally, damaged secondary members of a real damaged belt conveyor are localized and the degree of damage is identified using PLVM and ILVM frequency comparison. Moreover, damage identification using PLVM amplitude comparison is experimentally verified for the lateral members of the structure. In this chapter, the damage identification method based on global vibration modes and their derivatives are not examined

7.2 Identification of PLVM and ILVM of a full-scale model

A four-panel planar-full scale model of a belt conveyor, shown in figure 7-1, is tested using LDV.

Figure 7-1 A full-scale model of a belt conveyor

The design drawing of this structure is shown in figure 7-2. Based on the formula of the deflections of simple supported and clamped-clamped beams, the relative stiffness of the main members to the secondary members are estimated as in table 7-1.

Table 7-1 Values of relative stiffness of the main members to the secondary members

Secondary members	Condition of the secondary members	Value of the relative stiffness
Diagonal members	Pined-Pined	415
Diagonal members	Clamped-Clamped	104
Lateral members	Pined-Pined	173
Lateral members	Clamped-Clamped	43

The actual relative stiffness for diagonal members is between 104 and 415 and for lateral members is between 43 and 173. Even with clamped-clamped secondary members, the main members are much stiffer than the secondary members. Moreover, some secondary members are attached to the main members at the same connections. Therefore, the stiffness of diagonal and lateral members is much less than the overall stiffness of adjacent members. Therefore, the frequencies of PLVM and ILVM are close to the natural frequencies of the corresponding secondary members.

To identify PLVM and ILVM of the braces around the axis in the plane of the structure perpendicular to the direction of members, first, the velocity time history of the points shown in figure 7-2 is measured along vertical direction using LDV while each member is directly hit and its power spectral density is examined. The sampling frequency is 10000 Hz. To simulate damage, two 1kg masses are added to member 2 as shown in figure 7-3 and the structure is tested again.

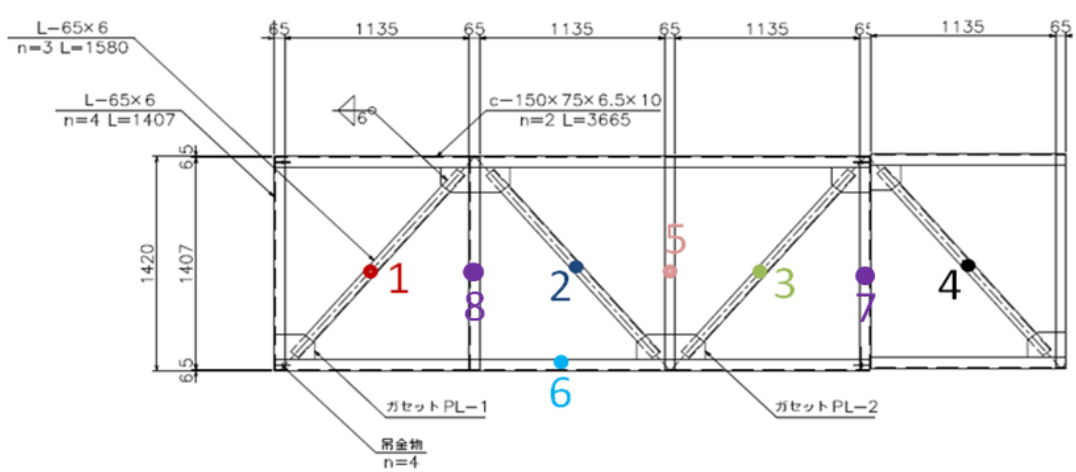

Figure 7-2 measurement points to identify PLVM of the braces

Figure 7-3 Added mass to member 2

Several peaks can be observed. Some of them correspond to the global vibration modes as all braces, lateral, and longitudinal members strongly vibrate at the same frequency. Figure 7-4 shows one of the global vibration modes.

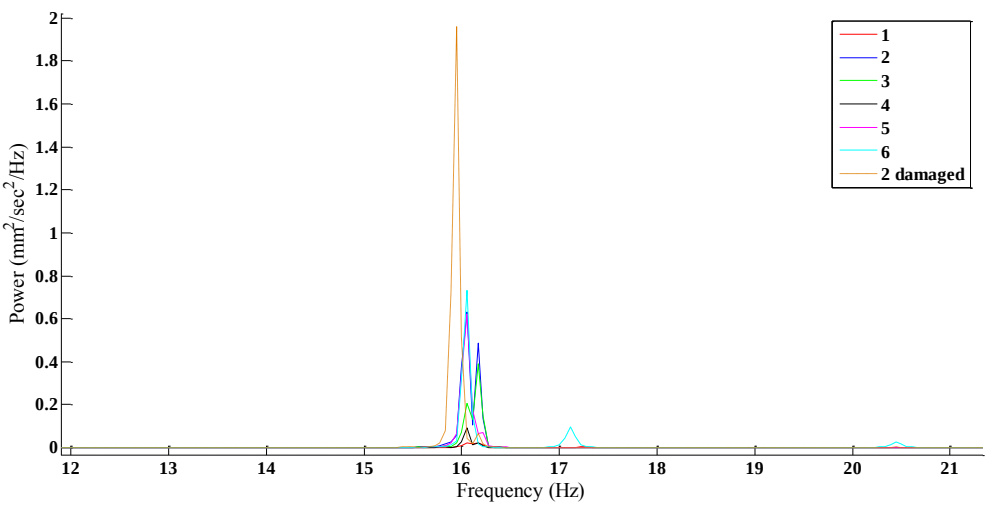

Figure 7-4 Peaks corresponds to one of the global modes (vertical)

As shown in the above figure, the frequency of the global mode reduces about 0.1 Hz as two masses are added to member 2.

Some other modes are neither global nor PLVM. In these modes only some members, which all of them are not necessarily identical, strongly vibrate. Figure 7-5 shows one of these modes. As shown, member 5 vibrates together with all the braces; however, this member is not identical with the braces. Therefore this mode is not PLVM. This mode cannot be considered as a global mode since some members such as member 6 have no peak.

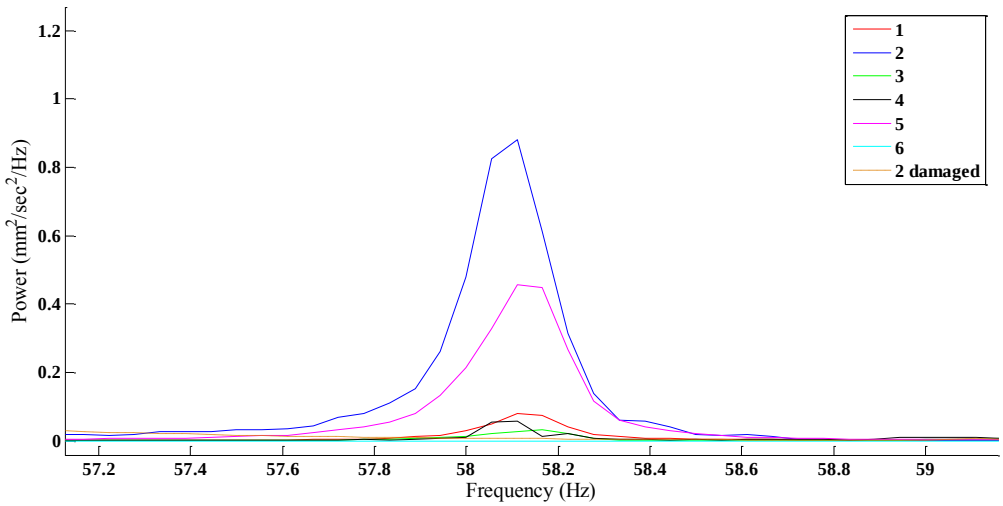

Figure 7-5 A mode that cannot be considered as PLVM or global mode (vertical)

There are peaks in which only the braces strongly vibrate. These modes are PLVM of the braces. Figure 7-6 and 7-7 show the 1st and 2nd PLVM of the braces respectively.

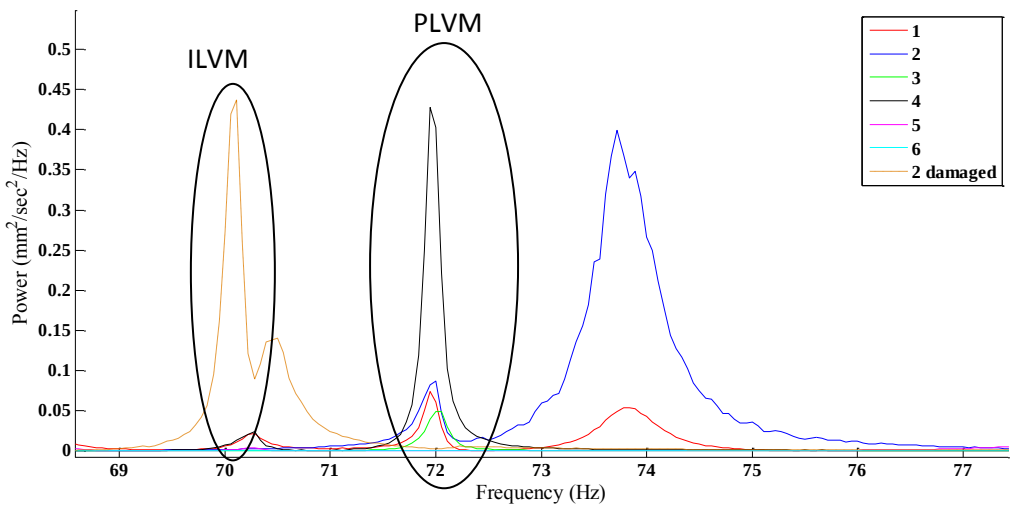

Figure 7-6 1st PLVM of the braces (vertical)

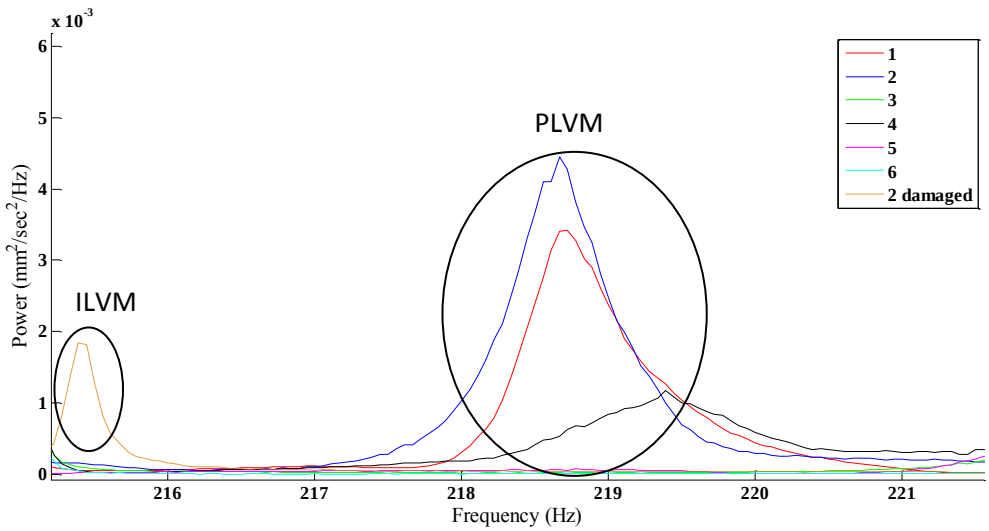

Figure 7-7 2nd PLVM of the braces (vertical)

The 1st and 2nd PLVM of the braces have frequencies equal to about 72 and 219 Hz respectively. As shown in the above figures, after adding mass to member 2, the property of this member changes and this member no longer vibrates in the PLVM. Instead, there are ILVM corresponding to this member. The 1st and 2nd ILVM of member 2 after adding mass have frequencies equal to 70.11 and 215.4 Hz respectively. Note that due to adding mass, the frequencies changes of the PLVM are much larger than global modes. In other words, PLVM are much more sensitive than global modes with respect to properties changes of members.

Note that after adding mass to member 2, the frequency of PLVM corresponding to the other members are almost the same as before adding mass. Figure 7-8 shows the 1st PLVM of the braces with and without adding mass to member 2.

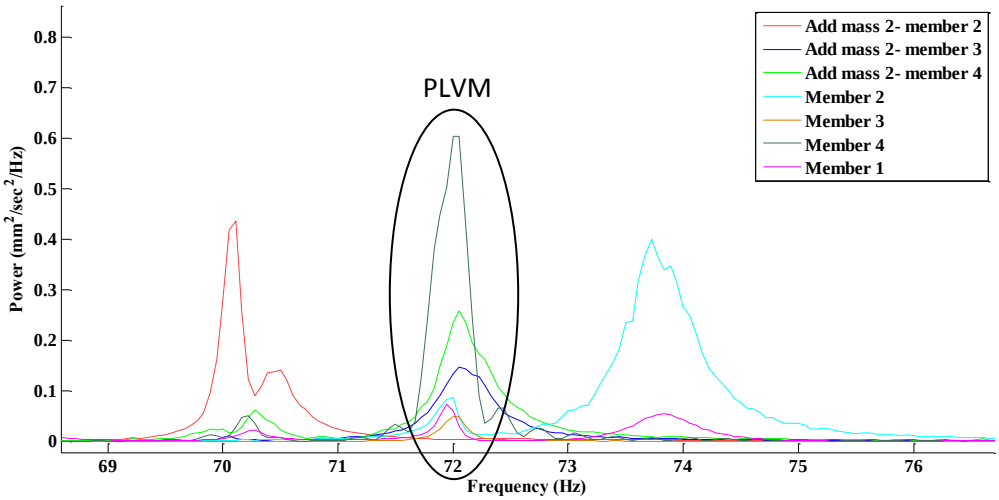

Figure 7-8 1st PLVM of the braces with and without adding mass to member 2 (vertical)

To identify PLVM and ILVM of the braces around the axis perpendicular to the plane of the structure, the velocity time history of the points shown in figure 7-2 is measured along the direction in the plane of the structure perpendicular to the direction of members using LDV while each member is directly hit and its power spectral density is examined. The sampling frequency is 10000 Hz. To simulate damage, two 1kg masses are added to member 2 and the structure is tested again. There are peaks in which only the braces strongly vibrate. These modes are PLVM of the braces. Figure 7-9 shows the 1st PLVM of the braces.

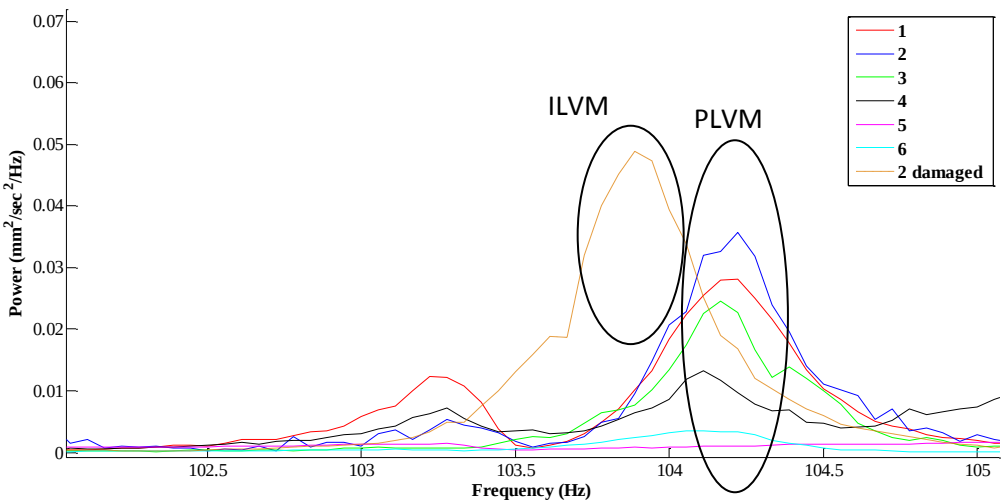

Figure 7-9 1st PLVM of the braces (Horizontal)

As shown in the above figure, after adding mass to member 2, the property of this member changes and this member no longer vibrates in the PLVM. Instead there is ILVM corresponding to this member which has lower frequency than the PLVM.

In order to identify PLVM and ILVM of the lateral members around the axis perpendicular to the plane of the structure, the velocity time history of the points shown in figure 7-10 is measured along the direction in the plane of the structure perpendicular to the direction of members using LDV while each member is directly hit and its power spectral density is examined. The sampling frequency is 10000 Hz. To simulate damage, two 1kg masses are added to member 2 and the structure is tested again.

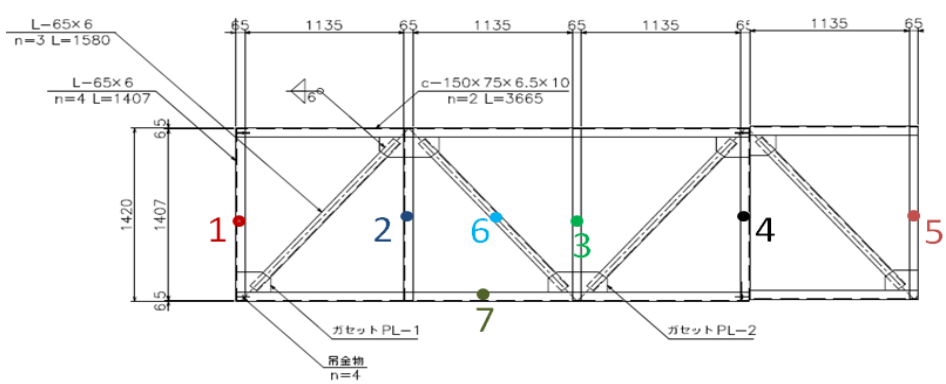

Figure 7-10 measurement points to identify PLVM of the lateral members

There are peaks in which only the lateral members strongly vibrate. These modes are PLVM of the lateral members. Figure 7-11 and 7-12 show the 1st and 2nd PLVM of the lateral members respectively.

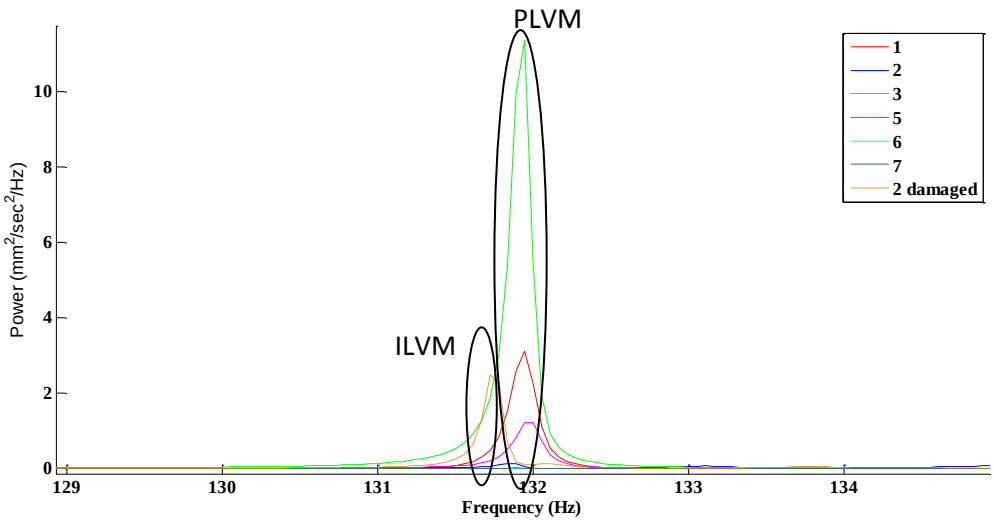

Figure 7-11 1st PLVM of the lateral members (Horizontal)

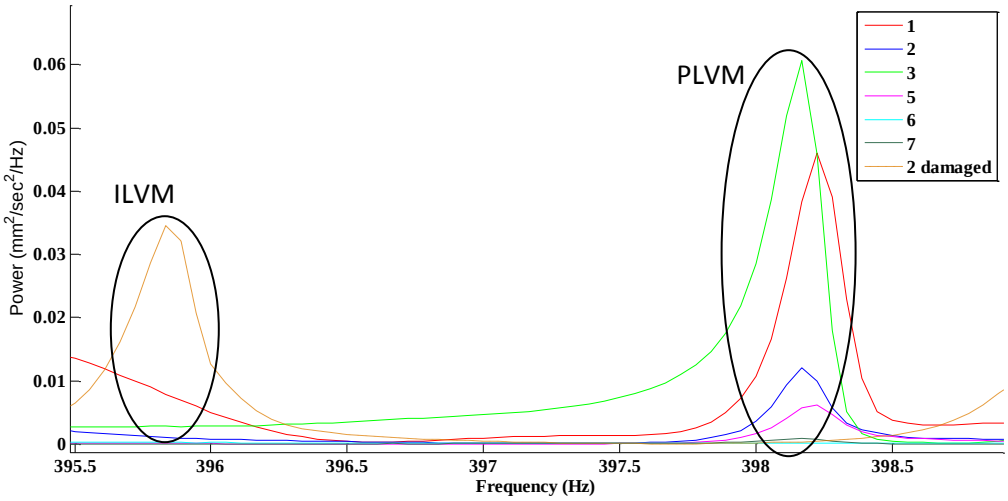

Figure 7-12 2nd PLVM of the lateral members (Horizontal)

The 1st and 2nd PLVM of the lateral members have frequencies equal to 132 and 398.2 Hz respectively. As shown in the above figures, after adding mass to member 2, the property of this member changes and this member no longer vibrates in the PLVM. Instead, there are ILVM corresponding to this member. The 1st and 2nd ILVM of member 2, after adding mass, have frequencies equal to 131.7 and 395.8 Hz respectively.

To identify PLVM and ILVM of the lateral members around the axis in the plane of the structure perpendicular to the direction of members, the velocity time history of the points shown in figure 7-10 is measured along vertical direction using LDV while each member is directly hit and its power spectral

density is examined. The sampling frequency is 10000 Hz. To simulate damage, two 1kg masses are added to member 2 and the structure is tested again. There are peaks in which only the lateral members strongly vibrate. These modes are PLVM of the lateral members. Figure 7-13 shows the 1st PLVM of the lateral members.

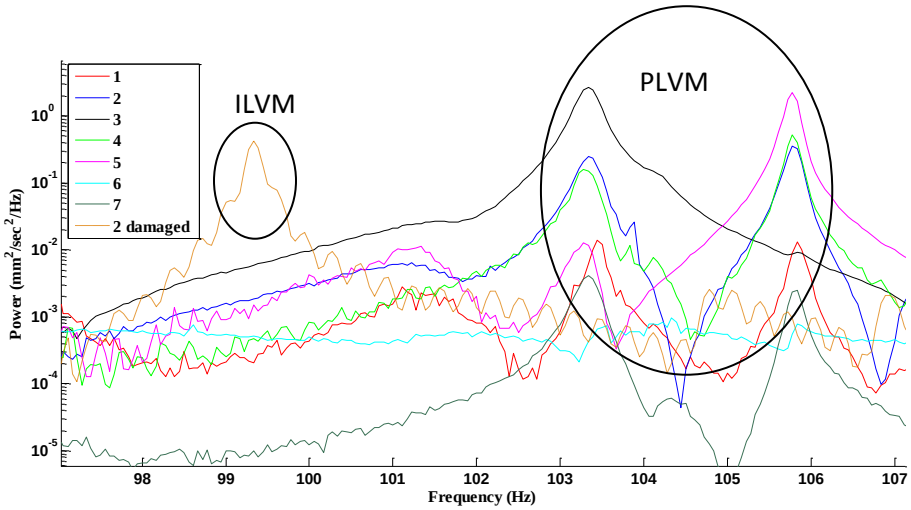

Figure 7-13 1st PLVM of the lateral members (vertical)

The 1st PLVM of the lateral members has frequency about 104.5 Hz. As shown in the above figure, after adding mass to member 2, the property of this member changes and this member no longer vibrates in the PLVM. Instead, there is ILVM corresponding to this member. The 1st ILVM of member 2, after adding mass, has a frequency equals to 99.4 Hz. Meanwhile the frequency of the 2nd PLVM of the lateral members is about 375 Hz and the frequency of the 2nd ILVM of member 2 equals to 360.2 Hz.

7.3 Existence of PLVM in a real belt conveyor

Figure 7-14 shows a bottom part of an undamaged belt conveyor. Different members at the bottom part of the belt conveyor, shown in figure 7-15, are measured by LDV through ambient vibration test. Member 1, 8, 12 and 16 are not identical with the other members. The sampling frequency is 10000 Hz.

Figure 7-14 Bottom part of an undamaged belt conveyor

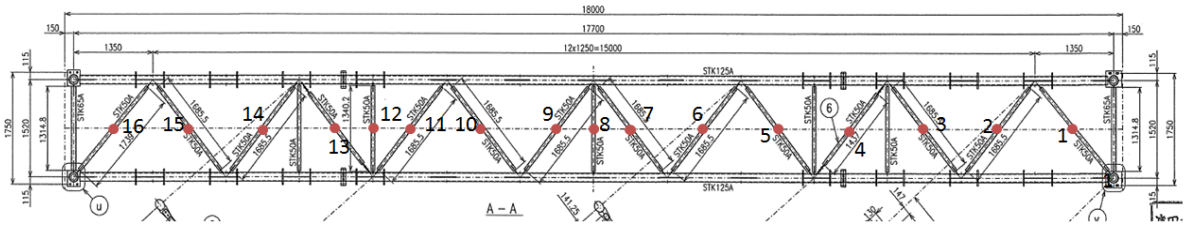

Figure 7-15 Measurement points

Figure 7-16 shows the PSD diagrams of the measurement points. All members vibrate in some frequencies. These frequencies correspond to global vibration modes and mostly happen in low frequency range. Moreover there are other modes in which some non-identical members or some parts of the structure vibrate together. These modes can be disordered or coupled local modes. Yet, there is one mode in which only identical bottom braces strongly vibrate. This mode is possibly a PLVM of the identical bottom braces. In this figure, members 8 and 12 have small amplitudes in the PLVM because they are not identical with the others.

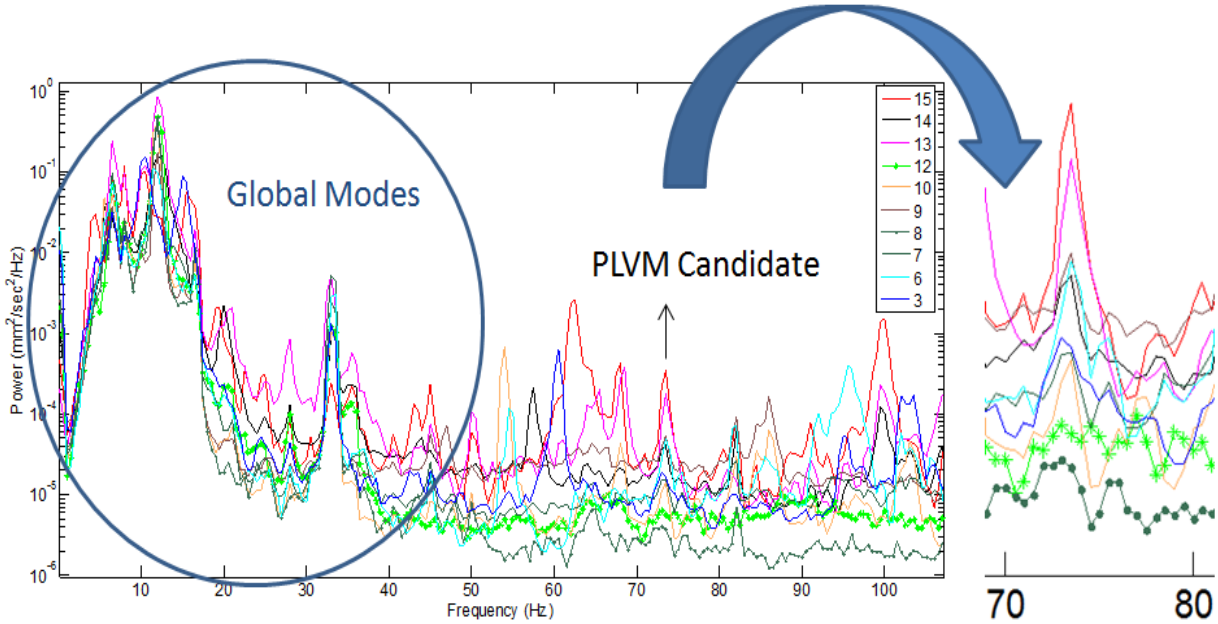

Figure 7-16 PSD diagrams of the measurement points

The finite element model of this structure shows that PLVM of identical bottom braces varies between 42 Hz and 96 Hz as the connections of these members change from hinged-hinged to clamped-clamped. Therefore, the measured PLVM is in the range. Figure 7-17 shows PSD diagrams of the members in the finite element model after updating the internal connections of the members based on the measurement results.

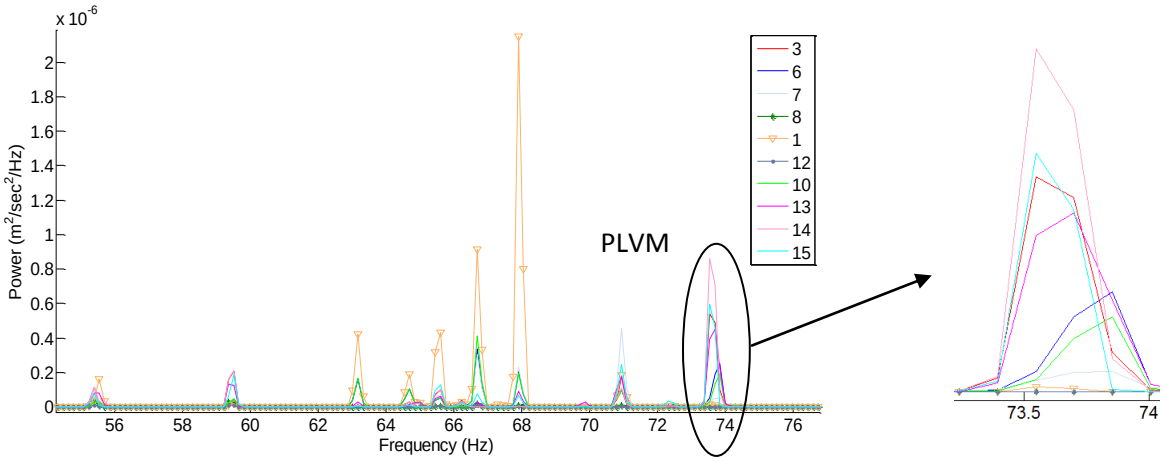

Figure 7-17 PSD diagrams of the members in the finite element model

After updating, the frequency of PLVM corresponding to the identical bottom braces in the finite element model is the same as it is for the real belt conveyor.

7.4 Damage identification of a real belt conveyor using PLVM and ILVM frequencies comparison

Figure 7-18 shows a real belt conveyor. This structure contains a support structure of the belt conveyor, walkways, machinery parts and some non-structural segments to protect the machinery parts.

Figure 7-18 A real belt conveyor

One representative span which is 10 m long is chosen. The drawing of this span is shown in figure 7-19. All members are L50×50×6 made of SS400. Lateral members are 1.3 m long while side braces are 1.06 m long. Regarding the relative stiffness of main members to secondary members for real belt conveyors, even with low relative stiffness, the frequencies of PLVM and ILVM are close to the natural frequencies of the corresponding secondary members since many secondary members are attached to the main members at the same connestions. Therefore, the relative stiffness of the corresponding secondary member is usually much less than the total stiffness of the main members and other secondary members. Moreover, in the real belt conveyors, many non-structural parts such as walkways, machinery parts or additional elements have been attached to the main frame which causes the overall stiffness of the main frames is much larger than each secondary member.

To identify PLVM and ILVM of secondary members, i.e. lateral members and side braces, the velocity time history of the points shown in figure 7-19 is measured using LDV while each member is directly hit and their power spectral density is examined. The sampling frequency is 10000 Hz. Note that the lateral members are measured along vertical direction and the longitudinal members, side braces and vertical members are measured along transversal direction.

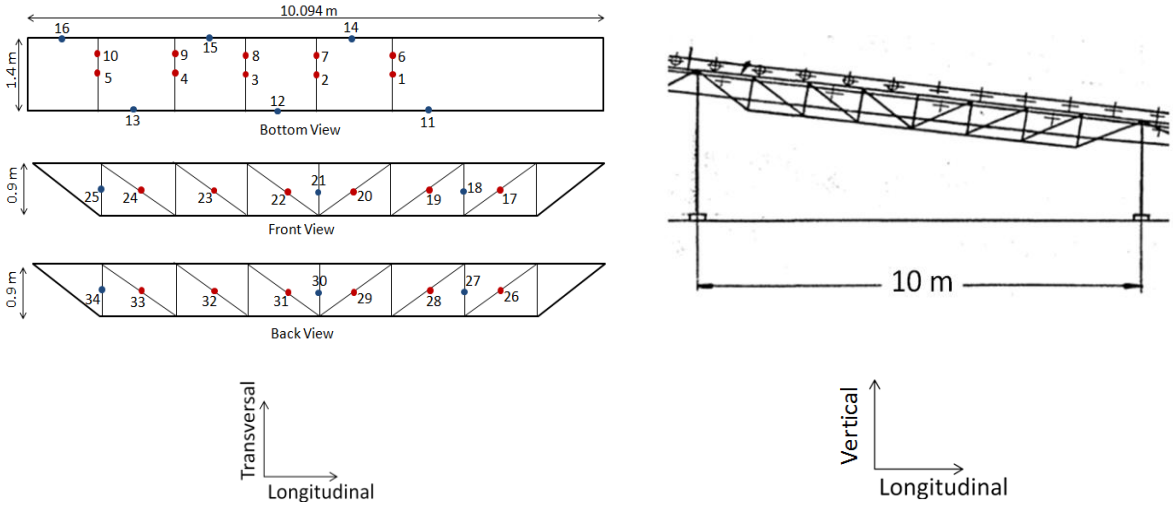

Figure 7-19 Measurement point of the belt conveyor

7.4.1 Damage identification of lateral members using PLVM and ILVM frequencies comparison by direct hit of each member

Figure 7-20 shows the power spectral density diagrams of the lateral members together with some of the non-identical members to identify PLVM and ILVM of the lateral members. Note that the results in this figure are for hammer test in which each member is directly hit.

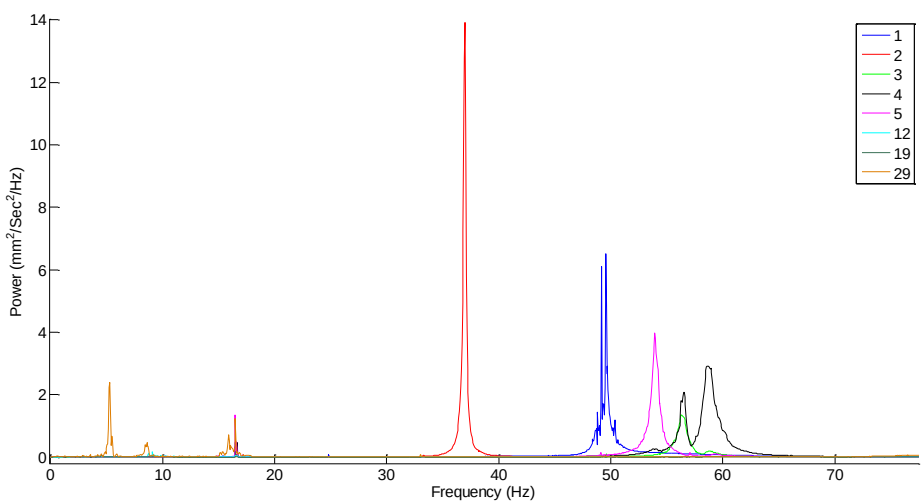

Figure 7-20 PSD diagrams of the lateral members together with some other members (1st PLVM and ILVM)

There is a range in which only members 3 and 4 strongly vibrate. This range corresponds to the 1st PLVM of the undamaged lateral members which are members 3 and 4. Moreover, there are three 1st ILVM corresponding to members 1, 2 and 5. These members are damaged and since the frequency of the 1st ILVM of member 2 is less than member 1; and the frequency of the 1st ILVM of member 1 is less than member 5, the order of damage severity is member 2, 1 and 5 respectively. Photos of the lateral members are shown in figure 7-21. As shown in this figure, member 2 has been severely corroded.

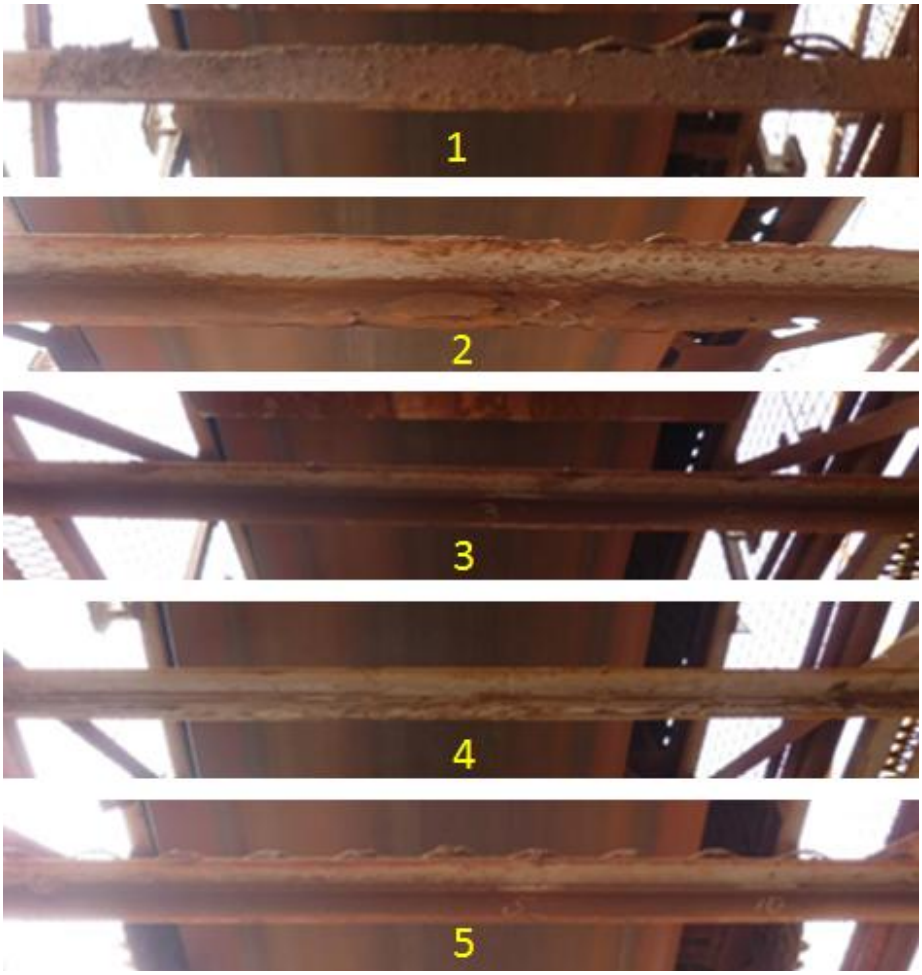

Figure 7-21 Lateral members

In order to confirm that the amplitudes of the undamaged lateral members are much larger than the amplitudes of the other members at the PLVM range, the corresponding part of figure 7-20 is zoomed in and shown in figure 7-22.

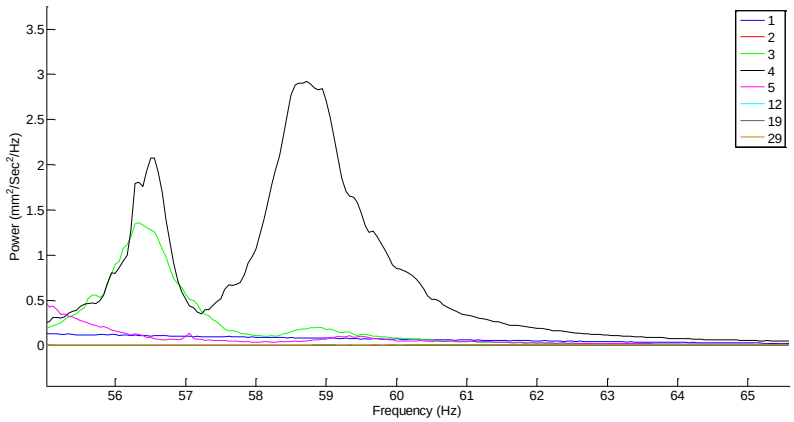

Figure 7-22 PSD diagrams of the lateral members together with some other members at the 1st PLVM range

Note that other than the 1st PLVM and ILVM of the lateral members, the higher PLVM and ILVM are observed when each lateral members is directly hit. Some of the higher PLVM and ILVM of the lateral members are shown in figure 7-23.

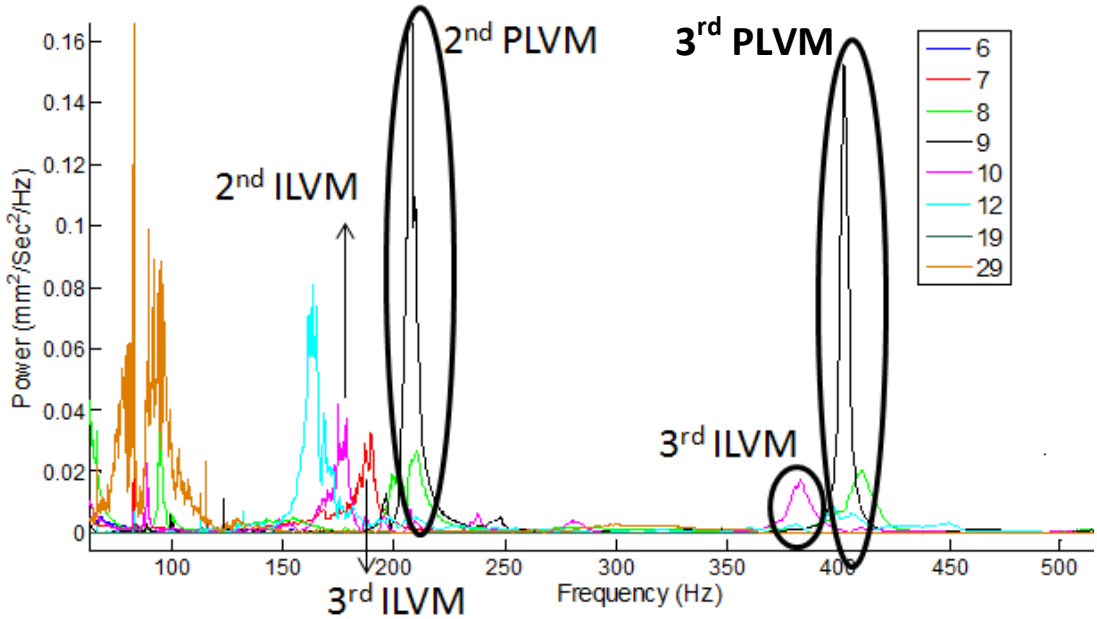

Figure 7-23 Higher PLVM and ILVM of some lateral members

In the above figure, the measurement data of the points at the quarter of the members length is used to examine PSD since at the middle of the members, the 2nd PLVM and ILVM cannot be observed. Table 7-2 and 7-3 respectively show the frequencies ranges of PLVM corresponding to the undamaged lateral members and the frequencies of ILVM corresponding to the damaged lateral members.

Table 7-2 Frequencies ranges of PLVM (Hz) corresponding to the undamaged lateral members

Member	1st PLVM	2nd PLVM	3rd PLVM	Condition
3 , 4	56.33 - 58.94	199.2 – 207.4	402.4 – 411.4	Undamaged

Table 7-3 Frequencies of ILVM (Hz) corresponding to the damaged lateral members

Member	1st ILVM	2nd ILVM	3rd ILVM	Condition
1	49.37	154.3	353.5	Damaged
2	37	116.1	188.3	Damaged
5	53.94	176.7	381.7	Damaged

From the values shown in the above tables and based on the fact that the frequencies of PLVM and ILVM are nearly the same as natural frequencies of the corresponding beams with the same boundary conditions of the relevant secondary members in the structure, the absolute severity of the damage is evaluated assuming the connections are undamaged. First the frequencies of PLVM for the undamaged members are utilized to find the stiffness of six springs (three rotational and three translational at each side) at the ends of the undamaged members. Abaqus software is used to estimate the best values of the stiffness of springs so that the corresponding natural frequencies of the single beam are as close as possible to the frequencies

of PLVM. Table 7-4 shows the estimated values of the stiffness of springs at the ends of the lateral members.

Table 7-4 Estimated values of the stiffness of springs at the ends of the lateral members

Spring	Direction	Value of stiffness
Rotational	Transversal	$15000\ N.m/rad$
Rotational	Vertical	$15000\ N.m/rad$
Rotational	Longitudinal	$10^4\ N.m/rad$
Extensional	Transversal	$10^5\ N/m$
Extensional	Vertical	$10^9\ N/m$
Extensional	Longitudinal	$10^{14}\ N/m$

Figure 7-24 shows natural frequencies and mode shapes of the corresponding beam with the springs at the ends. It is seen that the natural frequencies are close to the corresponding frequencies of PLVM.

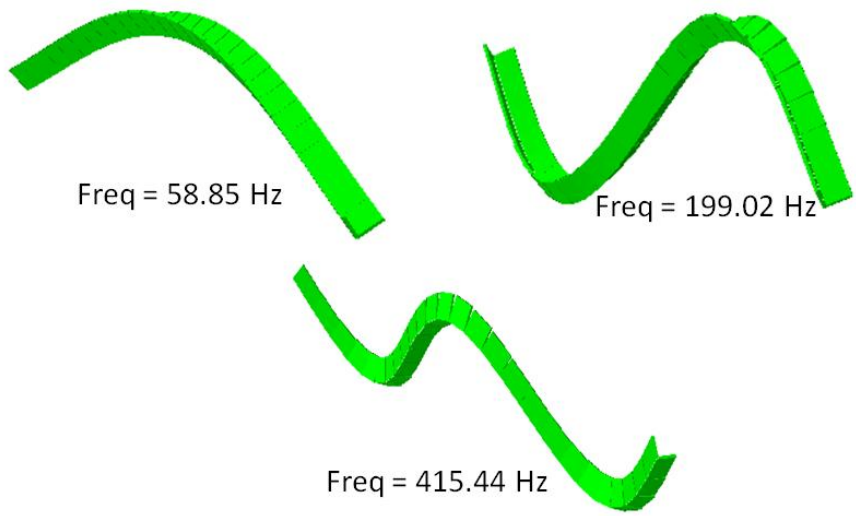

Figure 7-24 Natural frequencies and mode shapes of the corresponding beam with the springs at the ends

Then, the equivalent stiffness reduction of the damaged members (reduction of EI) is estimated using the finite element model and the measured frequencies of ILVM for each damaged lateral member. The equivalent stiffness reduction of each damaged member and the corresponding calculated natural frequencies of the damaged members are shown in table 7-5.

Table 7-5 Equivalent stiffness reduction of each damaged member and the corresponding calculated natural frequencies of the damaged members

Member	Stiffness reduction (%)	1st Freq. (Hz)	2nd Freq.(Hz)	3rd Freq.(Hz)
1	42%	49.37	157.76	324.48
2	77%	37.12	108.98	209.67
5	23%	53.99	177.75	369.44

The corresponding calculated natural frequencies of each damaged member are close to the frequencies of ILVM. One of the reasons of difference is the assumption of uniform damage (stiffness reduction) of the members.

7.4.2 Damage identification of lateral members using PLVM and ILVM frequencies comparison in ambient vibration test

As explained in chapter 3, PLVM and ILVM are more clearly observed when the corresponding members are directly hit compared to the ambient vibration test. To confirm this fact, the velocity time history of the points shown in figure 7-19 is measured using LDV in the ambient vibration test and their power spectral density is examined. Figure 7-25 shows PSD diagrams of the lateral members together with some non-identical members in the ambient vibration test.

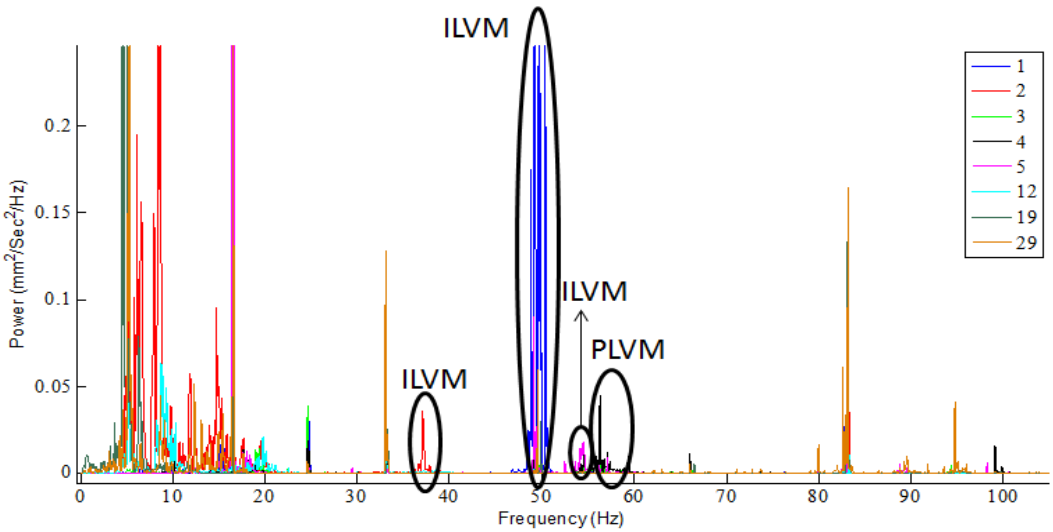

Figure 7-25 PSD diagrams of the lateral members together with some non-identical members in the ambient vibration test

Comparing this figure and figure 7-20 confirms that directly hitting each secondary member strongly excites PLVM and ILVM as compared to the other modes. As shown in the above figure, the amplitudes of PLVM and ILVM are much less or nearly the same level as many other modes and it causes the differentiation problems of different vibration modes. As an example, consider figure 7-26 and 7-27. Figure 7-25 is zoomed in the PLVM range and ILVM of member 5 and shown in figure 7-26. Figure 7-27 shows a mode which is not neither PLVM (nor ILVM) nor global vibration mode since members 2 and 19 (and some other members not shown here) do not vibrate with the other members. This mode can be another kind of local vibration mode introduced in chapter 3.

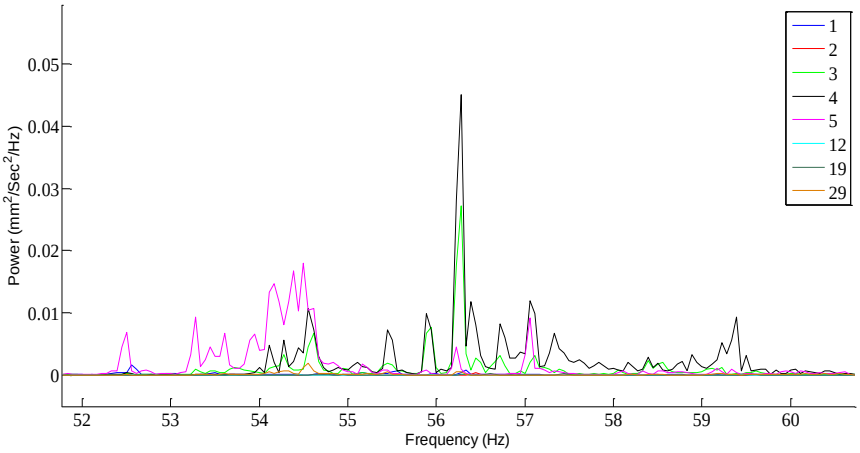

Figure 7-26 PSD diagrams of the lateral members together with some non-identical members at the 1st PLVM range and the 1st ILVM of member 5

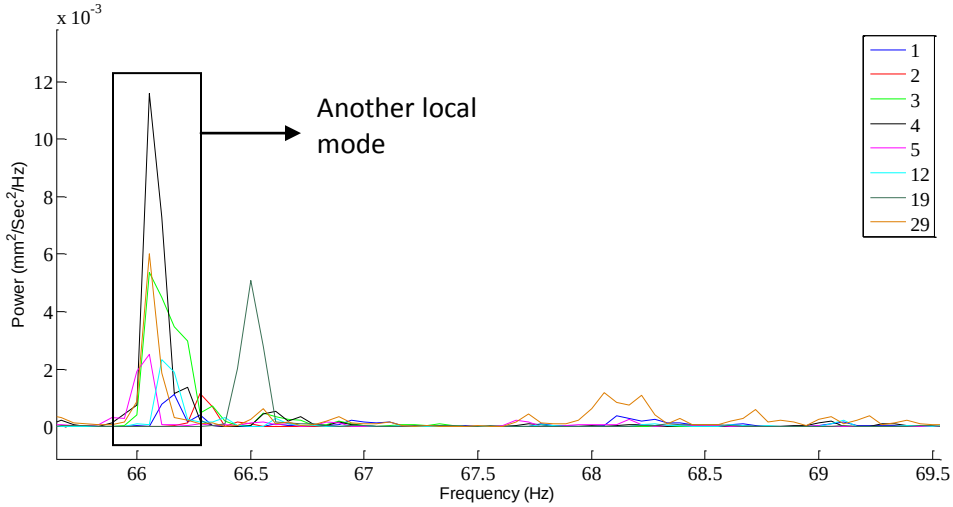

Figure 7-27 kind of local vibration mode (neither PLVM nor ILVM)

As shown, the amplitude of this local mode is nearly the same as the amplitudes of the 1st PLVM and the 1st ILVM of member 5.

7.4.3 Damage identification of side braces using PLVM and ILVM frequencies comparison by direct hit of each member

Figure 7-28 and 7-29 show the power spectral density diagrams of the side braces together with some non-identical members in PLVM range of the side braces. Note that the results in these figures are for hammer test while each member is directly hit.

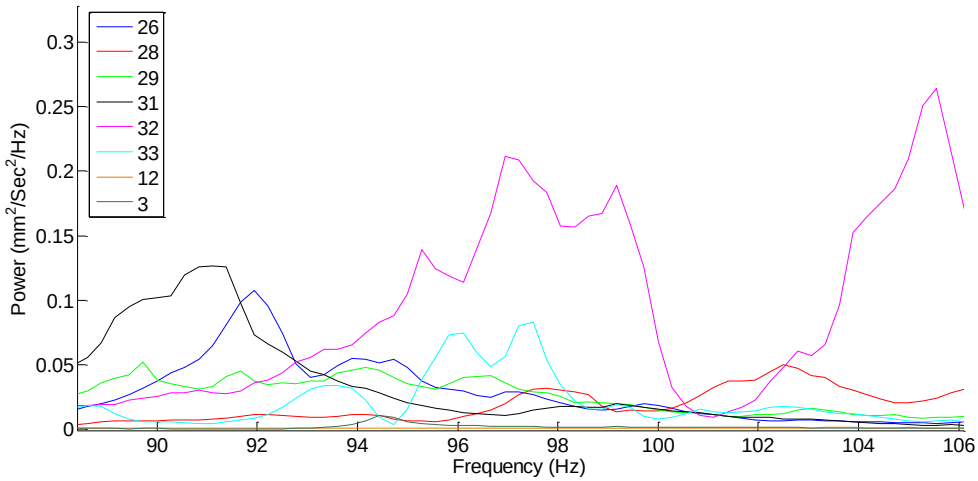

Figure 7-28 PSD diagrams of the back side braces together with some members at the PLVM range

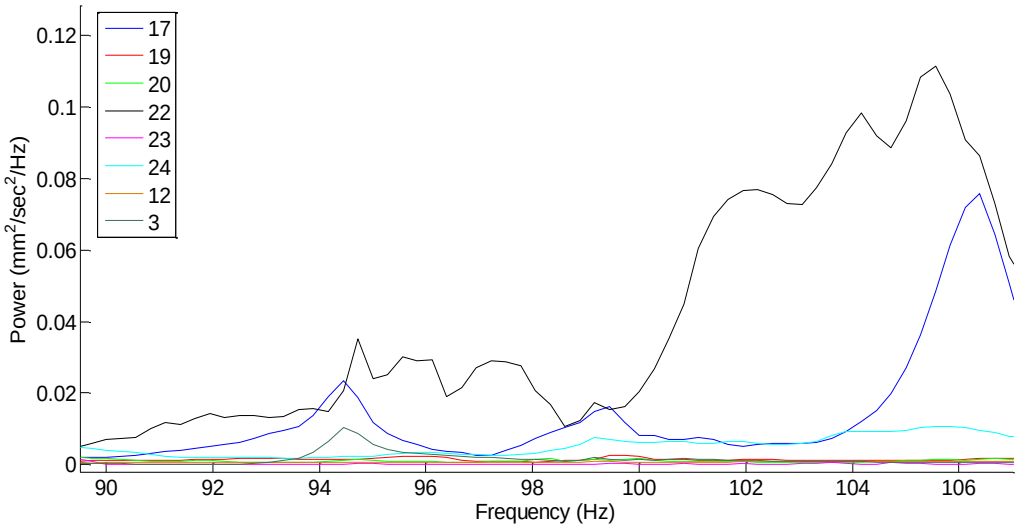

Figure 7-29 PSD diagrams of the front side braces together with some members at the PLVM range

As shown in the above figures, the amplitudes of all braces at the back side of the belt conveyor, which defined in figure 7-19, and brace 17 and 22 at the front side of the structure, are much larger than the other braces as well as other non-identical members. The PLVM range is 16 Hz wide. For braces 19, 20, 23 and 24, which do not strongly vibrate in the PLVM range, no ILVM can be observed. This means that these braces are not damaged. They do not strongly vibrate in the PLVM range because they are attached to the other parts of the belt conveyor and accordingly they are no longer identical with the other braces which strongly vibrate at their PLVM range. Figure 7-30 shows member 23 which is attached to the walkway of the belt conveyor.

Figure 7-30 A brace attached to the walkway

7.5 Damage identification of lateral members using PLVM amplitude comparison

PLVM of each identical members set are strongly excited when one of the undamaged identical members of the corresponding set is directly hit. Moreover the relative severity of damage can be determined by comparing the maximum amplitude of Fourier spectrum of identical members at their PLVM range. The more severe damage results in the smaller amplitude in their PLVM range. Based on the results of the previous part, members 3 and 4 are undamaged among the lateral members. Therefore member 4, as an undamaged lateral member, is hit and the velocity time history of the other members is measured by LDV and their Fourier spectrums are examined. To calculate and accordingly tune the input force to have the same force for each measurement, a smart hammer (model 086C03) is used. This hammer is shown in figure 7-31.

Figure 7-31 Smart hammer (model 086C03)

After tuning the velocity time history of members based on the tuned input force, the Fourier spectrum corresponding to each lateral member and some other members is examined. Figure 7-32 shows the Fourier spectrum diagrams of some members in the PLVM range of the lateral members.

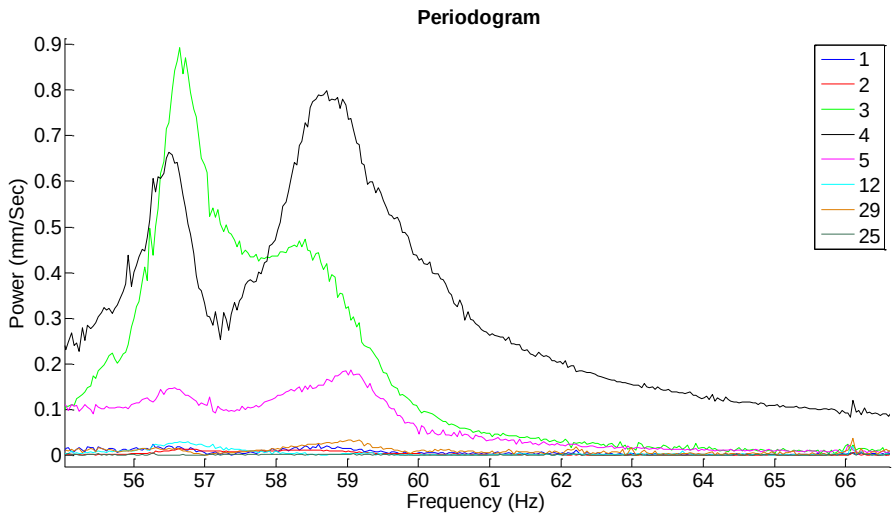

Figure 7-32 Fourier spectrums of some members in the PLVM range of the lateral members

As shown in the above figure, the maximum amplitudes of Fourier spectrum for members 3 and 4 are much larger than the other members while hitting member 4 because these members are undamaged. Figure 7-33 shows maximum amplitudes of Fourier spectrum of the lateral members in their PLVM range while hitting member 4.

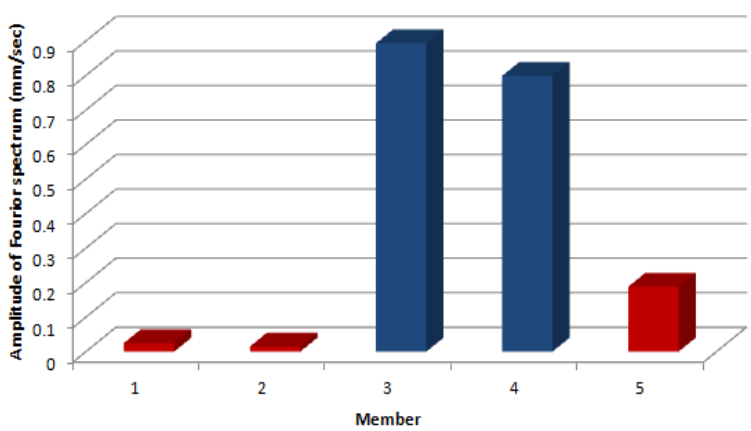

Member	Amplitude
1	0.024
2	0.015
3	0.893
4	0.799
5	0.188

Figure 7-33 Maximum amplitudes of Fourier spectrum of the lateral members at their PLVM range

The maximum Fourier spectrum amplitudes of members 1, 2 and 5 are much smaller than the undamaged members (members 3 and 4). Moreover, among the damaged lateral members, the smallest amplitude is for member 2 which has the most severe damage and the largest is for member 5 which has the less severe damage. Therefore, the damaged members as well as relative severity of damage are identified and the results of the previous chapters are experimentally verified.

7.6 Summary

Periodic local vibration modes (PLVM) and isolated local vibration modes (ILVM) of braces and lateral members of a planar full scale model of a belt conveyor are observed by using Laser Doppler Vibrometer (LDV). Comparing the frequencies of these two modes between identical members, the damaged elements are identified.

As for the real damaged belt conveyor, damaged members are correctly detected using PLVM and ILVM frequencies comparison and the equivalent damage degree is identified for each damaged member while each member is directly hit. As another method for damage identification of secondary members, which is based on PLVM amplitude comparison, one of the undamaged lateral members is hit with a amart hammer and by comparing the maximum amplitudes of Fourier spectrum of the lateral members in their PLVM range, the damaged lateral members and relative severity of the damage are correctly identified and the proposed damage identification methods in the previous chapters are experimentally verified.

Chapter 8

Conclusions and recommendations for future research

8.1 General conclusions

In this dissertation, damage identification of belt conveyors are investigated using properties of global and local vibration modes. The methods based on global vibration modes need to compare frequencies, mode shapes, and their derivatives before and after damage. By employing two specific local vibration modes, called PLVM and ILVM, two damage identification techniques using PLVM and ILVM frequencies comparison and PLVM amplitude comparison are introduced, and the damage location and severity are identified even when multiple damages exist. Existence condition of these local modes is first theoretically and numerically investigated for lumped mass-spring systems and numerically verified for a finite element model. The damage identification methods are examined on a finite element model of a typical belt conveyor, and then, experimentally verified for two laboratory models and a planar full scale model as well as a real belt conveyor. The general conclusions of this thesis are listed below:

- Before-and-after comparison is needed for global mode-based damage localization of the main frame of belt conveyors using frequencies, mode shapes and their derivatives even without considering the effects of non-structural elements. Moreover, damage localization would be difficult, if not impossible, when the number of damage element is large.

- Among different types of local vibration modes, there are **P**eriodic **L**ocal **V**ibration **M**odes (PLVM) in which vibrations of one set of the identical secondary members sets are much larger than the other members. If one of the identical members of the set damages, this member no longer vibrates in the PLVM. Instead, the member vibrates in the **I**solated **L**ocal **V**ibration **M**ode (ILVM).

- Frequencies of PLVM and ILVM of a secondary member are nearly the same as natural frequencies of the corresponding secondary member if the main members are much stiffer than the secondary member or the total stiffness of the adjacent members are much larger than the secondary member.

- Using frequencies of PLVM and ILVM in damage identification of the support structure of belt conveyors, damaged secondary members are localized and damage degree are identified without the need of before-and-after comparison even with large number of damaged elements. Meanwhile, effects of non-structural elements are negligible in this method.
- PLVM and ILVM are easily observed when each secondary member is directly hit. As an alternative method to easily observe PLVM, instead of direct impact, only one of the undamaged secondary members of a set can be hit to properly observe the corresponding PLVM. Comparing the PLVM amplitude, damaged members of the set as well as relative severity of the damage are identified.

The proposed damage identification methods of secondary members using PLVM and ILVM are summarized and depicted in a flow chart shown in figure 8-1.

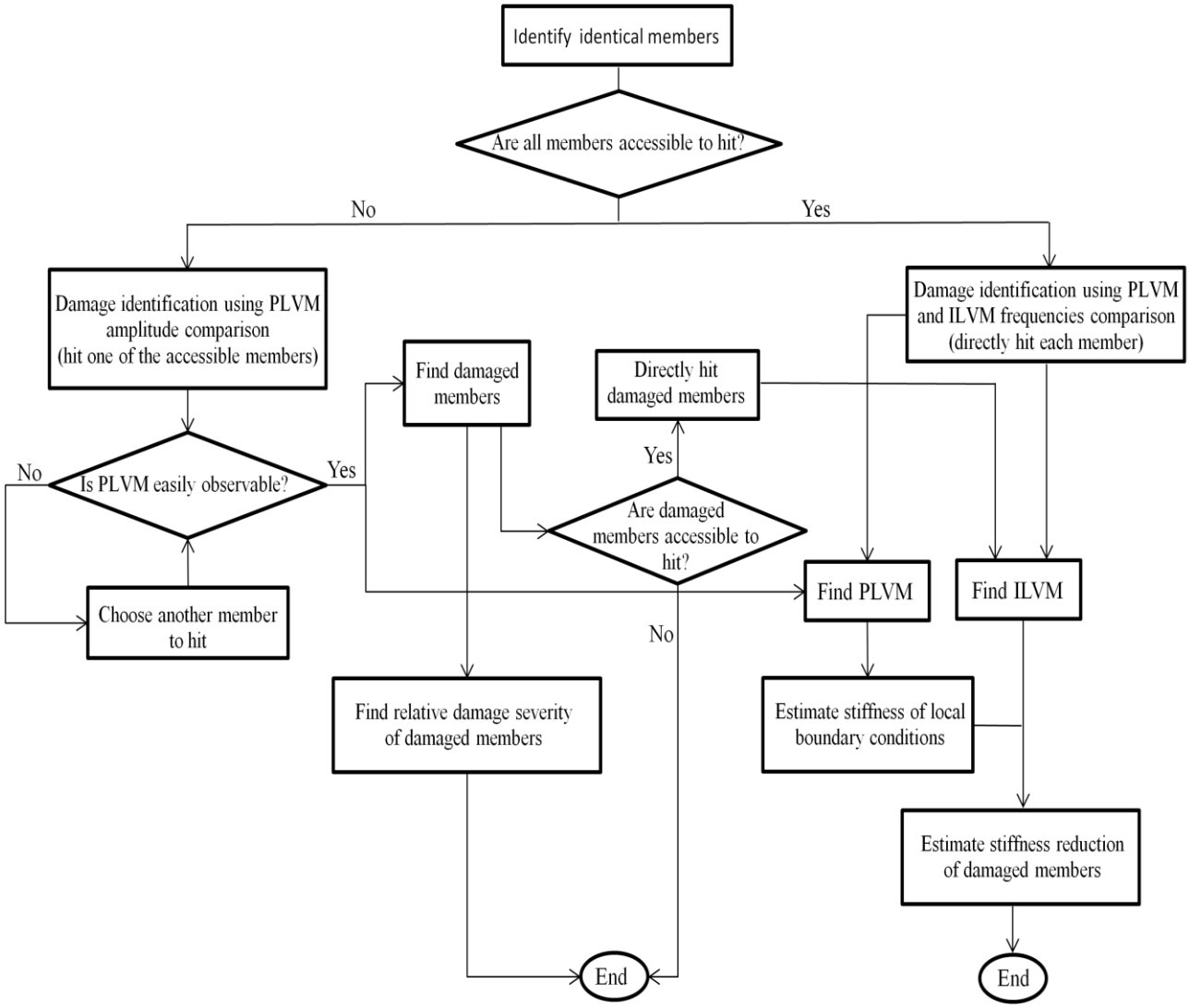

Figure 8-1 Proposed damage identification methods using PLVM and ILVM

8.2 Future works and recommendations

In this thesis the applicability of two damage identification methods based on PLVM and ILVM on the support structure of belt conveyors is investigated. The recommendations for the future works are as follows:

- Investigate about damage identification of main members in the support structure of belt conveyors. Main members of belt conveyors carry most of the loads and do not have PLVM because they are continuous. Therefore, another damage identification method should be proposed for these members. Among the secondary members of the belt conveyor support structure, damage identification of the members close to the columns are given priority because they carry more loads compared to the other secondary members.
- Find statistical criteria to automatically choose peaks corresponding to PLVM and ILVM from the output data. Current analyses and experiments in this research show each members set in each structures has their own threshold. Table 8-1 shows the modal amplitude ratio between the smallest amplitude of PLVM in each identical members set and the largest amplitude of the non-identical members set in the PLVM range.
- Investigate the existence of PLVM and ILVM in other space structures such as bridges, towers, domes and antennas, and examine the applicability of the damage identification methods using PLVM and ILVM frequency comparison as well as PLVM amplitude comparison in the health monitoring of these structures.

Table 8-1 Modal amplitude ratio for the PLVM of different structures

Structure	Members set	Ratio
Finite element model	Bottom and top braces	19
Finite element model	Lateral members	14
Finite element model	Side braces	6
Finite element model	Vertical members	37
Laboratory model with continuous main members	Lateral members	21
Laboratory model with continuous main members	Diagonal members	1219
Full-scale model	Lateral members	4
Full-scale model	Braces	101
Real belt conveyor	Lateral members	79
Real belt conveyor	Side braces	6

Bibliography

[1] WWW.Precisionautomationinc.com/cs/conveyor-systems.

[2] Harrison, A., 1985, “A magnetic transducer for testing steel-cord deterioration in high-tensile strength conveyor belts,” NDT International, Volume 18, Issue 3, 133‑138.

[3] Bozma H.I and H. Yalcin, 2002, “Visual processing and classification of items on a moving conveyor: a selective perception approach,” Robotics and Computer Integrated Manufacturing 18, 125–133.

[4] Mazurkiewicz, D., 2008, “Analysis of the ageing impact on the strength of the adhesive sealed joints of conveyor belts,” Journal of Materials Processing Technology.

[5] Farrar C.R. and K. Worden, 2006, “An introduction to structural health monitoring,”.

[6] Migliori, A., T.M. Bell, R.D. Dixon, R. Strong, 1993, “Resonant ultrasound non-destructive inspection,” Los Alamos National Laboratory report LA-UR-93-225.

[7] Farrar, C.R., W.E. Baker, T.M. Bell, K.M. Cone, T.W. Darling,T.A. Duffey, A. Eklund,and A. Migliori, 1994, “Dynamic characterization and damage detection in the I-40 Bridge over the Rio Grande,” Los Alamos National Laboratory report LA-12767-MS.

[8] Yoshioka, T., H. Yamaguchi, Y. Matsumoto, 2010, “Structural Health Monitoring of Steel Truss Bridges Based on Modal Damping Changes in Local and Global Modes,” 5th World Conference on Structural Control and Monitoring (5WCSCM), PP 167-179.

[9] Cawley, P. and R. D. Adams, 1979, “The locations of defects in structures from measurements of natural frequencies,” Journal of Strain Analysis, 14 (2), 49–57.

[10] Richardson, M.H. and M.A. Mannan, 1992, “Remote Detection and Location of Structural Faults Using Modal Parameters,” in Proc. of the 10th International Modal Analysis Conference, 502–507.

[11] Srinivasan, M.G. and C.A. Kot, 1992, “Effects of Damage on the Modal Parameters of a Cylindrical Shell,” in Proc. of the 10th International Modal Analysis Conference, 529–535.

[12] Kim, J.-H., H.-S. Jeon, and C.-W. Lee, 1992, “Application of the Modal Assurance Criteria for Detecting and Locating Structural Faults,” in Proc. 10th International Modal Analysis Conference, 536–540.

[13] Ko, J. M., C. W. Wong, and H. F. Lam, 1994, “Damage Detection in Steel Framed Structures by Vibration Measurement Approach,” in Proc. of 12th International Modal Analysis Conference, 280–286.

[14] Lim, T.W. and T.A.-L. Kashangaki, 1994, “Structural Damage Detection of Space Truss Structure Using Best Achievable Eigenvectors,” AIAA Journal, 32(5), 1049–1057.

[15] Ricci, S., 2000, “best achievable Modal Eigenvectors in Structural Damage Detection,” Journal of experimental mechanics, vol. 40, No. 4.

[16] Kashangaki, T.A-L., S.W. Smith, and T.W. Lim, 1992, “Underlying Modal Data Issues for Detecting Damage in Truss Structures,” in Proc. of 33rd AIAA/ASME/ ASCE/AHS/ ASC Structures, Structural Dynamics and Materials Conf.,1437–1446, AIAA-922264-CP.

[17] Friswell, M.I. and Penny, J.E.T., 1997, "The Practical Limits of Damage Detection and Location Using 18bration Data," 11th VPI&SU Symposium on Structural Dynamics and Control, Blacksburg, VA.

[18] Carrasco, C.J., Osegueda, R.A., and Ferregut, C.M., 1996, “Modal Tests of a Space Truss Model and Damage Localization Using Modal Strain Energy,” Report No. Fast 96-01, University of Texas at El Paso, El Paso, Texas.

[19] Park, S, and Y.B. Kim, 2002, “Nondestructive damage detection in large structures via vibration monitoring,” Electronic Journal of Structural Engineering (EJSE, 2), PP 59-75.

[20] Anil K. Jain, Fellow, IEEE, Robert P.W. Duin, and Jianchang Mao, 2000, “Statistical pattern recognition: a review”, IEEE Transactions on Pattern Analysis and Machine Intelligence, Vol 22, No. 1.

[21] Pandey, A.K., M. Biswas, and M.M. Samman, 1991, “Damage Detection from Changes in Curvature Mode Shapes,” Journal of Sound and Vibration, 145(2), 321–332.

[22] Salawu, O.S. and C. Williams, 1994, “Damage Location Using Vibration Mode Shapes,” in Proc. of 12th International Modal Analysis Conference, 933–939.

[23] Chance, J., G.R. Tomlinson, and K. Worden, 1994, "A Simplified Approach to the Numerical and Experimental Modeling of the Dynamics of a Cracked Beam," in Proc. of the 12th International Modal Analysis Conference 778–785.

[24] Ojalvo, I.U. and D. Pilon, 1988, "Diagnostics for Geometrically Locating Structural Math Model Errors from Modal Test Data," in Proc. of 29th AIAA/ASME/ASCE/AHS/ ASC Structures, Structural Dynamics, and Materials Conference, 1174–1186.

[25] Friswell, M.I. and J.E. Mottershead, 1995, "Finite Element Model Updating in Structural Dynamics," Kluwer Academic Publishers, 286 pp., ISBN 0-7923-3431-0.

[26] Hemez, F.M., 1993, "Theoretical and Experimental Correlation Between Finite Element Models and Modal Tests in the Context of Large Flexible Space Structures," Ph. D. Dissertation, Dept. of Aerospace Engineering Sciences, University of Colorado, Boulder, CO.

[27] Smith Kaouk, M., 1993, Finite Element Model Adjustment and Damage Detection Using Measured Test Data, Ph. D. Dissertation, Dept. of Aerospace Engineering Mechanics and Engineering Science, Univ. of Florida, Gainesville, FL.

[28] Zimmerman, D.C. and S.W. Smith, 1992, "Model Refinement and Damage Location for Intelligent Structures," from Intelligent Structural Systems, H.S. Tzou and G.L. Anderson, Eds., Kluwer Academic Publishers, 403–452.

[29] Liu, P.-L., 1995, "Identification and Damage Detection of Trusses using Modal Data," Journal of Structural Engineering, 121(4), 599–608.

[30] Berman, A. and E.J. Nagy, 1983, "Improvement of Large Analytical Model Using Test Data," AIAA Journal, 21(8) 1168–1173.

[31] Kabe, A.M., 1985, "Stiffness Matrix Adjustment Using Mode Data," AIAA Journal, 23(9), 1431–1436.

[32] Yang H., Z. Wu and Y. Yan, 2009," A Study on Structural Damage Identification Method Based on Model Updating," IEEE.

[33] Zimmerman, D.C. and M. Kaouk, 1994, "Structural Damage Detection Using a Minimum Rank Update Theory," Journal of Vibration and Acoustics, 116, 222–230.

[34] Kaouk, M. and D.C. Zimmerman, 1994, "Assessment of Damage Affecting All Structural Properties," in Proc. of the 9th VPI&SU Symposium on Dynamics and Control of Large Structures, 445–455.

[35] Zimmerman, D.C., M. Kaouk, and T. Simmermacher, 1995, "Structural Damage Detection Using Frequency Response Functions," in Proc. of the 13th International Modal Analysis Conf., 179–184.

[36] Doebling, S.W., 1996, "Damage Detection and Model Refinement Using Elemental Stiffness Perturbations with Constrained Connectivity," in Proc. of the AIAA/ASME/AHS Adaptive Structures Forum, 360–370, AIAA-96-1307.

[37] Caesar, B. 1987. "Updating System Matrices Using Modal Test Data," 5th International Modal Analysis Conference, London, England, April 1987, 453-459.

[38]Link, M., M. Weiland, and J.M. Barragan, 1987. "Direct physical Matrix Identification as Compared to Phase Resonance Testing: An Assessment Based on Practical Application," 5th International Modal Analysis Conference, London, England, April 1987, 804-811.

[39] Lim, T.W., 1995, "Structural Damage Detection Using Constrained Eigen Structure Assignment," Journal of Guidance, Control, and Dynamics, 18(3), 411–418.

[40] Hemez, F.M., 1993, Theoretical and Experimental Correlation Between Finite Element Models and Modal Tests in the Context of Large Flexible Space Structures, Ph. D. Dissertation, Dept. of Aerospace Engineering Sciences, University of Colorado, Boulder, CO.

[41] Dinh, H.M., T. Nagayama, Y. Fujino, 2012, "Structural parameter identification by use of additional known masses and its experimental application", Structural Control and Monitoring, Volume 19, Issue 3, 436-450.

[42] Nalitolela, N., J.E.T. Penny and M.I. Friswell, 1993," Updating Modal Parameters By Adding an Imagined Stiffness to the Structure", Journal of Mechanical System and Signal Processing, 7(2), 161-172.

[43] Nalitolela, N., J.E.T. Penny and M.I. Friswell, 1990," Updating Structural Parameters of a Finite Element Model by Adding Mass or Stiffness to the System." 8th International Modal Analysis Conference, Kissimmee, Florida, February 1990, 836-842.

[44] Nalitolela, N., J.E.T. Penny and M.I. Friswell, 1992," A Mass or Stiffness Addition Technique for Structural Parameter Updating." International Journal of Analytical and Experimental Modal Analysis, 7(3), 157-168.

[45] Li, S., H. Vold and D.L. Brown, 1993," Application of UMPA to PBC Testing," 11th International Modal Analysis Conference, Kissimmee, Florida, February 1993, 223-231.

[46] Dinh, H.M., 2011, "Structural Condition Evaluation by Model Updating under System Perturbation and its Application to Girder Bridges", Ph. D. dissertation, The University of Tokyo.

[47] Jung, D.-S., C.Y. Kim and J.H. Kang, 2007, "Hybrid Optimization Technique Based on GA-NMS for FE Model Updating", Conference: IMAC-XXV.

[48] Li, C. and S.W. Smith, 1994, "A Hybrid Approach for Damage Detection in Flexible Structures," in Proc. of 35th AIAA/ASME/ASCE/AHS/ASC Structures, Structural Dynamics, and Materials Conference, 285–295.

[49] Li, C. and S.W. Smith, 1995, "Hybrid Approach for Damage Detection in Flexible Structures," Journal of Guidance, Control, and Dynamics, 18(3), 419–425.

[50] Kim, H.M. and T.J. Bartkowicz, 1993, "Damage Detection and Health Monitoring of Large Space Structures, Sound and Vibration, 27(6), 12–17.

[51] Kim, H.M. and T.J. Bartkowicz, 1994, "A Two-Step Structural Damage Detection Using a Hexagonal Truss Structure," in Proc. of 35th AIAA/ASME/ASCE/AHS/ASC Structures, Structural Dynamics and Materials Conf., 318–324, AIAA-94-1713-CP.

[52] Toksoy, T. and A.E. Aktan, 1994, "Bridge-condition Assessment by Modal Flexibility," Experimental Mechanics, 34, 271–278.

[53] Lin, C.S., 1994, "Unity Check Method for Structural Damage Detection," in Proc. of 35th AIAA/ASME/ASCE/AHS/ASC Structures, Structural Dynamics and Materials Conference, 347–354, AIAA-94-1717-CP.

[54] He, J. and D.J. Ewins, 1986, "Analytical Stiffness Matrix Correction Using Measured Vibration Modes," Modal Analysis: The International Journal of Analytical and Experimental Modal Analysis, 1(3), 9–14.

[55] Bernal, D., 2002. "Load vectors for damage localization," Journal of Engineering Mechanics, 128(1), 7-14.

[56] Gao, Y., B.F. Spencer, 2005, "Structural health monitoring strategies for smart sensor networks," Ph. D. dissertation, University of Illinois at Urbana-Champaign.

[57] Bernal, D., 2006, "Flexibility-based damage localization from stochastic realization results," Journal of Engineering Mechanics, 132(6), 651-658.

[58] Nagayama, T., B.F. Spencer, 2007, "Structural Health Monitoring Using Smart Sensors," Ph. D. dissertation, University of Illinois at Urbana-Champaign.

[59] Moser P., B. Moaveni, 2011, "Environmental Effects on the identified natural frequencies of the Dowling Hall footbridge," Mech Syst and Signal Process, 25 (7): 2336-2357.

[60] Alampalli S., 2000, "Effects of testing, analysis, damage, and environment on modal parameters," Mech Syst and Signal Process, 14 (1): 63-74.

[61] Sohn H., 2003, "Effects of environmental and operational variability on structural health monitoring," Philosophical Transactions of the Royal Society A 365(1851), 539–560.

[62] Doebling, S. W., C. R. Farrar, 1997, "Using statistical analysis to enhance modal-based damage identification" In Proc. DAMAS 97: structural damage assessment using advanced signal processing procedures, University of Sheffield, UK, 199–210.

[63] Wood, M. G., 1992, "Damage analysis of bridge structures using vibrational techniques," Ph.D. thesis, University of Aston, Birmingham, UK.

[64] Dong C., P.Q. Zhang, W.Q. Feng, and T.C. Huang, 1994, "The Sensitivity Study of the Modal Parameters of a Cracked Beam," in Proc. of the 12th International Modal Analysis Conference, 98–104.

[65] Nwosu, D.I., A.S.J. Swamidas, J.Y. Guigne, and D.O. Olowokere, 1995, "Studies on Influence of Cracks on the Dynamic Response of Tubular T-Joints for Nondestructive Evaluation," in Proc. of the 13th International Modal Analysis Conference, 1122–1128.

[66] Kim, D.-O and I.-W Lee, 1998, "Mode Localization in Structures Consisting of Substructures and Couplers," Journal of Engineering Structures 22, 39-48.

[67] Pierre, C. and P.D. Cha, 1989, "Strong Mode Localization in Nearly Periodic Disordered Structures," AIAA Journal, Vol. 27, No 2, 227-241.

[68] Bendiksen, O.O., 1987, "Mode Localization Phenomena in Large Space Structures," AIAA Journal, Vol. 25, No 2, 1241-1248.

[69] Pierre, C., 1988, “Mode Localization and Eigenvalue Loci Veering Phenomena in Disordered structures,” Journal of Soung and Vibration, Vol. 126, No 2.

[70] Dimarogonas, A, 1996, ”Vibration for Engineers,” 2nd ed., Prentice-Hall, Inc.

[71] Rao, S.S., 1995, ”Mechanical Vibrations,” 3rd ed. Addison-Wesley Publishing Company.

[72] Weaver, W., S.P. Timoshenko and D.H. Young, 1990, “Vibration Problems in Engineering,” 5th ed., John Wiley & Sons, Inc.

[73] Lai, H.-L., J.-C. Hsu, C.-K. Chen, 2008, ”An innovative eigenvalue problem solver for free vibration of Euler-Bernoulli beam by using the Adomian Decomposition Method,” Computers and Mathematics with Applications 56, 3204-3220.

[74] Liu, Y. and C. S. Gurram, 2009, “The use of He’s variational iteration method for obtaining the free vibration of an Euler-Bernoulli beam,” Mathematical and Computer Modelling, 50, 1545-1552.

[75] Maurizi, M.J., R.E. Rossi, J.A. Reyes, 2003, “Comments on a note on vibrations of generally restrained beams,” Journal of Sound and Vibration 147, 167–171.

[76] Maurizi, M.J., P.M. Belles, H.D. Martin, 2003, “An almost semicentennial formula for a simple approximation of thenatural frequencies of Bernoulli–Euler beams,” Journal of Sound and Vibration 260,191–194.

[77] Fung, T.C., 2004, “Improved approximate formulas for the natural frequencies of simply supported Bernoulli–Euler beams with rotational restrains at the ends,” Journal of Sound and Vibration 273, 451-455.

[78] Humar, J.L., 2002, “Dynamics of structures,” 2nd ed., Swets & Zeitlinger B.V., Lisse.

[79] Gavin, H., 2011, “Geometric Stiffness Effects in 2D and 3D Frames,” CE 131L. Matrix Structural Analysis, Duke University.

[80] Timoshenko, S.P., Revised by W. Weaver, 1990, “Vibration problems in Engineering,” 5th ed., John Wiley & Sons Inc.

[81] Shaker, F.J., 1975, “Effect of Axial Load on Mode Shapes and frequencies of Beams,” Nasa Technical Note, D-8109.

[82] Bokaian, A., 1988, “Natural Frequencies of Beams under Compressive Axial Loads,” Journal of sound and vibration, 126(1), 49-65.